UNIVERSITÀ DEGLI STUDI DI TORINO

DIPARTIMENTO DI SCIENZE DELLA TERRA

DOTTORATO DI RICERCA IN SCIENZE DELLA TERRA – XXXII CICLO

THE UPPER MIOCENE MARINE DIATOMITES OF THE MEDITERRANEAN BASIN AND THEIR PALEOBIOLOGICAL CONTENT: SEDIMENTOLOGICAL AND PALEOCEANOGRAPHIC SIGNIFICANCE

CANDIDATO

LUCA PELLEGRINO

SUPERVISORE

PROF. GIORGIO CARNEVALE

COMMISSIONE VALUTATRICE

PROF.SSA ELISA MALINVERNO (UNIVERSITÀ DEGLI STUDI DI MILANO-BICOCCA)

PROF. RICHARD W. JORDAN (YAMAGATA UNIVERSITY)

PROF. FRANCESCO DELA PIERRE (UNIVERSITÀ DEGLI STUDI DI TORINO)

COORDINATRICE DEL CORSO DI DOTTORATO
PROF.SSA ANNA MARIA FERRERO

ANNO ACCADEMICO 2019-2020

SETTORE SCIENTIFICO-DISCIPLINARE DI AFFERENZA: GEO/01

SUMMARY

INTRODUCTION

Diatom-rich deposits represent an intriguing issue for multidisciplinary researches. Their sedimentological and paleontological analysis may shed light on past climate conditions and oceanographic circulation patterns, as well as on spatial and temporal variations of the nutrient supply to oceanic and lacustrine basins (e.g., Kemp, 1996; Jordan and Stickley, 2010). Their paleobiological content, often exquisitely preserved, provides a unique opportunity to reconstruct the ancient marine biocoenoses (e.g., Bradley and Landini, 1984; Gaudant et al., 1996, 2010; Carnevale, 2004a, b, c; 2006a, b, 2007; Carnevale and Bannikov, 2006; Carnevale and Pietsch, 2006). Moreover, diatomaceous earths have been investigated for commercial purposes and oil production (Shukla and Mohan, 2012; Cermeño, 2016).

Thick successions of marine diatomaceous sediments were deposited in the Mediterranean region during the late Neogene, especially during the early Messinian (~7-6 Ma). These diatom-rich deposits are usually alternated with organic-rich layers and marls, forming cyclical successions reflecting orbitally-controlled (precession) climatic changes (e.g., Hilgen and Krijgsman, 1999; Pérez-Folgado et al., 2003). Their deposition has been classically linked to the progressive closure of the connection between the Atlantic Ocean and the Mediterranean Sea (Selli, 1954; Krijgsman, 2002) at about 7.2 Ma (Kouwenhoven et al., 1999; Kouwenhoven and van der Zwaan, 2007), which culminated in the extensive deposition of evaporites

(carbonate minerals, gypsum and halite) between 5.97 and 5.33 Ma, during the so-called Messinian salinity crisis (Krijgsman et al., 1999; Manzi et al., 2013).

However, many aspects of this extensive biosiliceous event are still poorly understood. Among them, micropaleontology, sedimentology and (silica) biogeochemistry represent three research fields that have been only marginally treated. As far as the micropaleontological aspects are concerned, it is worth noting that in the central Mediterranean, the study of the microfossil content of the upper Miocene diatomaceous deposits has been mainly focused on the well-exposed and continuous Sicilian sections of the Caltanissetta basin, in order to define cyclostratigraphic correlations with other circum-mediterranean localities, especially in Spain (Sorbas Basin) and Greece (island of Gavdos; e.g., Hilgen and Krijgsman, 1999; Pérez-Folgado et al., 2003). Conversely, the scattered sections outcropping along the Italian Peninsula have received less attention. Moreover, very few works attempted to compare both the siliceous and calcareous microfossils recorded in these sediments (e.g., Bonci et al., 1991; Gaudant et al., 2010), mostly focusing on the calcareous assemblages. Paradoxically, this resulted in a general overlooking of the role of silicifiers during an event of significant increase in the opaline deposition.

As far as regards the sedimentology, until now macroscale descriptions have prevailed over high-resolution approaches, limiting the interpretation of the different facies, especially the laminated one, that characterizes the diatomaceous deposits of the circum-mediterranean area. In light of these considerations, and taking into

account the importance of diatom-rich sediments for a comprehensive interpretion of the paleoceanographic processes in the Mediterranean basin during a critical phase of its geodynamic evolution, detailed lamina-scale investigations are urgently needed.

Finally, many aspects concerning the sources of the silica exploited by diatoms are still poorly understood. In this context, it is interesting to note that a global enhancement of biosiliceous productivity occurred during the so-called late Miocene-early Pliocene biogenic bloom (Cortese et al., 2004). This suggests that the Mediterranean diatomaceous deposition was possibly controlled by the synergistic effect of regional and supra-regional processes, although the latter have been overlooked or just briefly discussed (e.g. Ogniben, 1955, 1957; Moissette and Saint Martin, 1992; El Ouahabi et al., 2007).

Following this perspective, the research herein presented is aimed at addressing the following points: i) the micropaleontological content of the Messinian diatomaceous deposits and its paleoceanographic significance, with special emphasis on the biosiliceous assemblages and their relationships with the calcareous ones; ii) the sedimentological features of these deposits and the mechanisms responsible for the formation of different microfacies and, especially, lamina-types; iii) the possible relationships between the Mediterranean and the global opal deposition during the late Miocene, under the perspective of the silica biogeochemical cycle.

In order to address the first and second points, this research combines the analysis of siliceous and calcareous microfossil assemblages and provides the first detailed sedimentological investigation of the upper Miocene diatom-bearing section of Pecetto di Valenza, located in the Monferrato Arc structural high (Piedmont Basin, NW Italy), i.e. the northernmost offshoot of the Mediterranean basin during the late Miocene.

The third point has been addressed throughout the review of the current state of knowledge about the lower Messinian Mediterranean diatomites, with particular focus on the possible terrestrial sources of silica and the processes that may have promoted their seaward export. Moreover, the paleoclimatic and paleoceanographic significance of the precessionally-controlled lithological cycles observed in the Mediterranean diatomaceous successions is proposed, highlighting potential relationships with the silica biogeochemical cycle.

CHAPTER 1 - INTEGRATED MICROPALEONTOLOGICAL STUDY OF THE MESSINIAN DIATOMACEOUS DEPOSITS OF THE MONFERRATO ARC (PIEDMONT BASIN, NW ITALY): NEW INSIGHTS INTO THE PALEOCEANOGRAPHIC EVOLUTION OF THE NORTHERNMOST MEDITERRANEAN REGION[*]

The upper Miocene diatom-bearing section of Pecetto di Valenza (Piedmont, NW Italy) represents a unique site for studying the paleoceanographic processes that occurred before the onset of the Messinian salinity crisis in the northernmost sector of the Mediterranean basin. The first micropaleontological investigation of the Pecetto di Valenza section was carried out by Sturani and Sampò (1973), mainly aimed at characterizing the foraminifer assemblage. Subsequently, Fourtanier et al. (1991) investigated the matrix embedding a single fish specimen recovered during the controlled excavations conducted in the Pecetto di Valenza area in the 1980s (Pavia, 1989), providing a first list of the siliceous microfossils of Pecetto di Valenza. Finally, Gaudant et al. (2010) reported the first cursory analysis of the microfossil assemblage of the Pecetto di Valenza section, including diatoms, foraminifers and calcareous nannofossils. This chapter presents an expanded and integrated analysis

[*] This chapter is based on Pellegrino, L., Abe, K., Dela Pierre, F., Gennari, R., Lozar, F., Natalicchio, M., Mikami, Y., Jordan, R.W. and Carnevale, G. (in review). Integrated micropaleontological study of the Messinian diatomaceous deposits of the Monferrato Arc (Piedmont Basin, NW Italy): new insights into the paleoceanographic evolution of the northernmost Mediterranean region. Marine Micropaleontology.

of foraminifers, calcareous nannofossils, diatoms and other siliceous microfossils, aimed at better defininig the evolution of the biogenic sedimentation at Pecetto di Valenza.

1. Geological and stratigraphic settings

The Pecetto di Valenza section is located in the Monferrato Arc, the northernmost tectono-sedimentary domain of the Piedmont Basin (e.g., Piana, 2000; **Fig. 1A**). The Piedmont Basin corresponds to a large wedge-top basin filled with upper Eocene to Messinian sediments that developed in the Alpine retroforeland and eventually became involved in the Apennine orogeny (Mosca et al., 2010; Rossi and Craig, 2016; Rossi, 2017). The sedimentary succession of the Monferrato Arc begins with the Cretaceous-Eocene Ligurian units ('Argille Varicolori') that are unconformably overlain by Oligo-Miocene terrigenous sediments recording the main evolutionary phases of the Apennine fold and thrust belt (e.g., Piana, 2000). Since the early Miocene the Monferrato Arc became a structural high separating the Alessandria Basin from the Po foreland basin (e.g., Frigerio et al., 2017). The diatomaceous accumulation occurred in the Monferrato Arc for the first time during the early Miocene (e.g., Bonci et al., 1990); a second stage of increased opaline deposition, involving other sectors of the Piedmont Basin, took place in the late Miocene, both before and after the onset of the Messinian salinity crisis (Sturani and

Sampò, 1973; Bonci et al., 1991; Fourtanier et al., 1991; Bonci et al., 1995; Irace, 2004).

In the Pecetto di Valenza area (**Fig. 1B**), the upper Miocene sedimentary succession consists of the Sant'Agata Fossili Marls (Tortonian-lower Messinian) and of the Cassano Spinola Conglomerates (upper Messinian). The Sant'Agata Fossili Marls are tectonically juxtaposed against the Cretaceous-Eocene Ligurian units and consist of cyclically bedded hemipelagites (marls and silty clays) with lens-shaped, coarse-grained bodies (sandstones and conglomerates) emplaced by gravity flows (**Fig. 1C**). The upper part of the Sant'Agata Fossili Marls is locally characterized by organic-rich shales (**Fig. 1C**) and by carbonate and biosiliceous sediments (e.g., Frigerio et al., 2017); the latter are described herein. The Cassano Spinola Conglomerates unconformably overlie the Sant'Agata Fossili Marls (**Fig. 1C**) and consist of fluvio-deltaic and lacustrine deposits with brackish water faunal assemblages typical of the Lago Mare biofacies. These sediments were deposited during the final stage of the Messinian salinity crisis (Sturani, 1976; Dela Pierre et al., 2011, 2016; Frigerio et al., 2017).

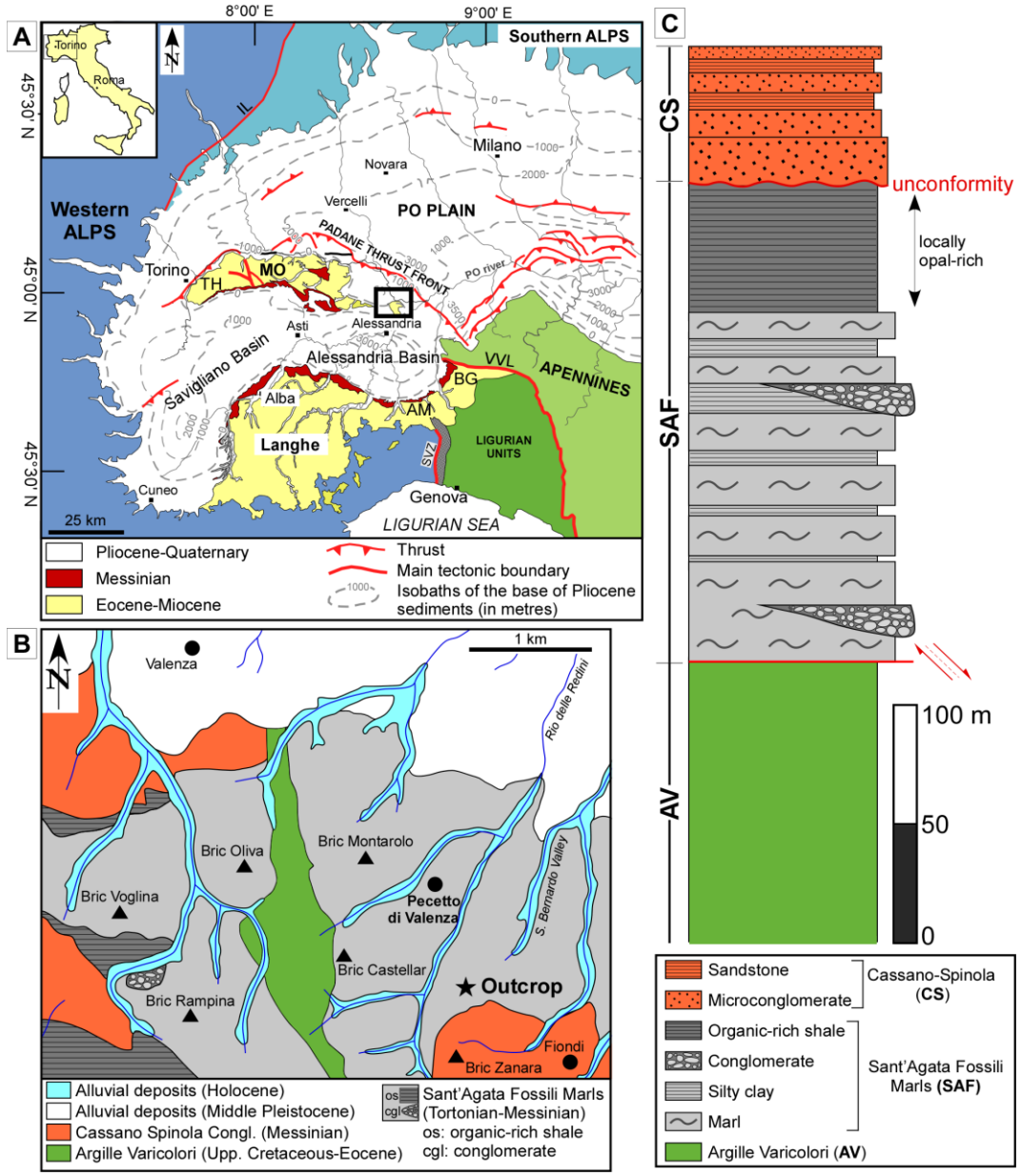

Figure 1. Geological and stratigraphic setting of the Monferrato Arc and Pecetto di Valenza area. A) Structural sketch map of NW Italy and location of the study area (rectangle). TH – Torino Hill; MO – Monferrato; AM – Alto Monferrato; BG – Borbera Grue; SVZ – Sestri Voltaggio fault zone; VVL – Villavernia-Varzi line; IL – Insubric line. B) Geological sketch map of the Pecetto di Valenza area. C) Sedimentary succession of the Pecetto di Valenza area. Panel A modified from Bigi et al. (1990); panels B and C modified from Frigerio et al. (2017).

The studied section belongs to the upper part of the Sant'Agata Fossili Marls (**Fig. 1C**). Four lithological units have been distinguished from bottom to top (**Fig. 2**), including: 1) grayish-greenish homogenous marls (~60 cm-thick; **Fig. 2A**) containing plant remains, pteropods, rare bivalves and echinoids; 2) a dark brown Mn-rich laminated layer (~90 cm-thick; **Fig. 2B**) typified by rare nuculid bivalves and fish remains; 3) white-to-pale-brown or yellowish laminated diatomites (~195 cm-thick; **Fig. 2C**) that yielded a remarkable fossil assemblage (Sturani and Sampò, 1973; Pavia, 1989; Carnevale and Tyler, 2010; Gaudant et al., 2010), mostly represented by pelagic fishes (mainly myctophids, followed by *Alosa elongata*, *Lepidopus* sp., *Syngnathus albyi*, *Maurolicus muelleri*, Scombrid indet., *Merluccius merluccius*, *Sarda* sp., *Trachurus trachurus*, *Archaeotetraodon bannikovi*, and small specimens of *Arnoglossus sauvagei* and *Solea* cf. *solea*), rare crustaceans (represented by the decapod *Necronectes* sp. and the cirriped *Lepas* sp.), abundant plant remains (e.g., wood fragments encrusted by the small oyster *Ostrea* cf. *neglecta*), and rare seagrasses (Zosteraceae); 4) grayish-greenish homogenous marly sediments (~120 cm-thick) barren in macrofossils.

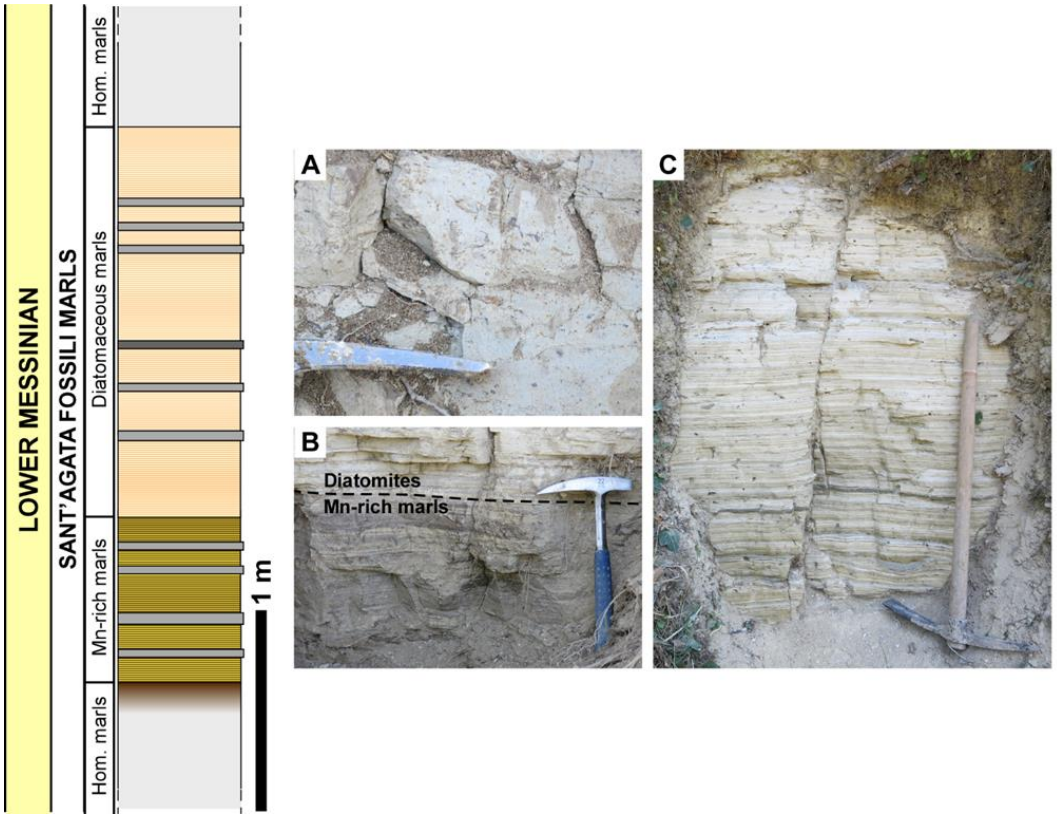

Figure 2. Stratigraphic column of the Pecetto di Valenza section (left) and images of the outcrop (right). A) Homogeneous grayish marls. B) Transition from Mn-rich brownish laminated marls (below) to diatomites (above). C) The diatomaceous interval.

1.1. Age of the section

The age of the Pecetto di Valenza section is controversial. While some nannofossil and diatom biozonal markers seem to suggest a late Tortonian age (Fourtanier et al., 1991; Gaudant et al., 2010), the planktonic foraminifer assemblage indicates an early Messinian age (Sturani and Sampò, 1973; Violanti, 1996; Gaudant et al., 2010). In this regard, three points are worth noting: i) the main lower Messinian

nannofossil biozonal markers, that are mostly oligotrophic taxa (*Amaurolithus* spp., *Discoaster* spp.), can be underrepresented or even absent in the biosiliceous sediments, due to the abundance of silica-secreting primary producers which outcompete the non-siliceous phytoplankton in silica-rich waters (e.g., Egge and Aksnes, 1992; García-Bernal et al., 2017); ii) the diatom biostratigraphy for the Mediterranean Neogene has been rarely used and is not updated; moreover, it is based on the comparison of the circum-mediterranean diatom zonal markers with those of the Pacific Ocean deposits (e.g., Burckle, 1978; Gersonde and Schrader, 1984), assuming their synchronic occurrence in very different paleogeographic and paleoceanographic settings; this assumption makes the Mediterranean zonation scheme highly questionable; and iii) conversely, the planktonic foraminiferal biostratigraphy for the Mediterranean Neogene is very well-constrained, widely applied and updated (e.g., Lirer et al., 2019). Indeed, in the sediments underlying the diatom-rich unit Sturani and Sampò (1973) observed the presence of *Globorotalia acostaensis*, *G. continuosa*, *G. scitula*, *G. incompta*, *G. humerosa*, *Orbulina universa* and *O. suturalis*, whereas in the diatom-rich unit, they identified *G. acostaensis*, *G. humerosa*, *Turborotalita multiloba*, *G. dutertei*, *O. universa* and *O. suturalis*. Gaudant et al. (2010) also identified *Globigerinoides eamesi*, *G. conomiozea* and *G. praemargaritae*. The presence of *T. multiloba*, an undisputable lower Messinian planktonic marker whose first common occurrence is dated at 6.415 Ma (e.g., Sierro et al., 2001), strongly supports the attribution of the studied section to the early Messinian (e.g., Gennari et al., 2019). This conclusion is also confirmed by the

occurrence of the Messinian calcareous nannofossil *Reticulofenestra rotaria* (Young, 1990; Raffi et al. 2003) and by the pteropod *Cavolinia gypsorum* (Sturani and Sampò, 1973; see also Zorn, 1997; Merle et al., 2002).

2. Material and methods

The sampling campaign for micropaleontological investigations was conducted on the section outcropping along the crossroad called 'Strada Molina' (44°58'50.2''N, 8°40'30.8''E), next to the village of Pecetto di Valenza. The upper homogenous marly layer originally reported by Sturani and Sampò (1973) and Pavia (1989) was not recorded during the fieldwork, because of the extensive vegetation and soil cover. The section was systematically sampled every ~15 cm, obtaining four samples from the lower homogeneous marls, six samples from the laminated Mn-rich layer, and 11 samples from the diatomaceous layer. The samples were collected using horizontally-oriented C-shaped metal boxes of ~15x4x4 cm, in order to obtain small sediment cores of equal thicknesses.

Each sample was then separated in two aliquots: one half was removed for the study of the foraminifers, while the remaining portion was smeared all along its thickness for the study of calcareous nannofossils and siliceous microfossils.

For the investigation of foraminifer assemblages, about 150 g of dry sediment were treated with hydrogen peroxide for 12 hours, gently washed, sieved into grain

fractions greater than 125 μm and 63–125 μm and weighed. Quantitative analyses were carried out on the residue greater than 125 μm and every sample was split into two aliquots containing approximately 300 planktonic and benthic foraminifer tests, respectively. Foraminifers were picked and classified at the species or genus level. *Globigerina bulloides* and *G. falconensis* were grouped in the *G. bulloides* gr. and all the neogloboquadrinids were lumped into the *Neogloboquadrina* gr. The *Rectuvigerina* specimens either occur with only triserial, triserial then biserial and triserial, biserial and then uniserial enrollments; these three types are more easily recognizable according to their test lengths, which varies from 200 to >550 μm and are accordingly distinguished in the plots. The taxonomy of this group is rather complicated (see Thomas, 1980); apart from the relatively short, only-triserial morphotypes, in the samples analyzed it is possible to recognize both thick (*R. cylindrica gaudrynoides*), thin (*R. cylindrica cylindrica*) and compressed (*R. bononiensis*) tests, which are generally prevalent. To avoid a taxonomic bias, the three taxa were lumped together in the *Rectuvigerina* gr. Another noteworthy group is represented by the epiphytic taxa, including *Elphidium* spp., *Rosalina* spp., *Discorbis* spp., *Cibicides refulgens*, *Cibicides labatulus*, *Neoconorbina* spp. and *Astigerinata* spp. (Langer, 1993). Despite its overall low frequency, this group is considered herein since it includes species requiring a substratum (mostly represented by macrophytes), thereby living within the euphotic zone in an inner shelf environment.

For the investigation of calcareous nannofossils, samples were prepared as simple smear slides (Bown and Young, 1998), scratching the surface (about 6.25 cm^2) of each cored sample onto a cover-slide, then adding a drop of distilled water to the powder. The suspension was dried on a hot plate, smeared with a toothpick on the cover-slide, and permanently mounted with Norland Optical Adhesive 61. Counting of at least 500 specimens was performed to obtain relative abundances at the species level; the raw data were later transformed as percentages of the total assemblage. The search for rare but biostratigraphically useful taxa (*Discoaster* spp., *Amaurolithus* spp.) was also performed on a given area of the slide (4.5 cm^2), but is not reported due to the rare occurrence of such taxa. *Reticulofenestra minuta* and *R. haqii* (small reticulofenestrid taxa, with open central area) have been clustered into the *Reticulofenestra* < 5 μm group, and *R. perplexa* and *R. producta* (reticulofenestrid < 8 μm, with closed central area) into the *R. antarctica* group.

For the investigation of siliceous microfossils, each subsample (~2 g) was first transferred into a beaker. Then, hydrogen peroxide and hydrochloric acid were added, in order to remove the organic matter and the carbonate fraction, respectively. A few grams of sodium pyrophosphate were also added in order to remove the clay particles attached to the surface of microfossils. The beaker was then placed on a hot plate (~70°C), until the effervescence vanished. Then, pure water was added and the solution decanted at room temperature. After at least 8 hours, the supernatant was aspirated with a vacuum pump, paying attention not to remove the sediment settled on the bottom of the beaker. Various cycles of washing, decantation and supernatant

aspiration were repeated, until the pH of the solution was raised to ~7. Around 100 µL of each solution was pipetted onto a coverslip and dried on a hot plate (~70°C). The coverslip was then fixed onto a slide glass with mounting media. Permanent slides were observed at 500x, using a light microscope. A minimum of 250 diatoms were counted for each subsample, as well as all the associated siliceous microfossils encountered. In order to improve the identifications, further observations were carried out using a scanning electron microscope (JEOL JSM 6510 LV). A few drops of each solution were pipetted into a filter holder with ~200-250 mL of distilled water and filtered onto a HA-type nitrocellulose Millipore filter (47 mm diameter, 0.45 µm porosity) that was then air-dried and stored in a plastic Petri dish. A 5x5 mm piece of each filter was then cut, glued onto an aluminum stub and sputter coated with gold in an Eiko IB-3 ion coater, then observed in the SEM.

3. Results

Well-preserved planktonic and benthic foraminifers (**Figs. 3, 4A-F**) and calcareous nannofossils (**Figs. 3, 4G-O**) have been identified all along the section. Among the planktonic foraminifers, it is worth to mention the occurrence of *Turborotalita multiloba*, a biozonal marker that supports the attribution of the Pecetto di Valenza section to the early Messinian (e.g., Lirer et al., 2019; **Figs. 4A-B**). Conversely, well-preserved siliceous microfossils have been identified only in the diatomaceous interval (**Figs. 3, 5-8**). However, it is worth to mention that strongly

etched centric diatoms and sponge spicules have been observed in the Mn-rich level during preliminary SEM observations (see below).

3.1. Foraminifers

3.1.1. Planktonic foraminifers

The lower part of the homogeneous marls (samples 1 and 2) is characterized by a high abundance of planktonic foraminifers. This group is dominated by the *Globigerina bulloides* gr. and by *Turborotalita quinqueloba*, showing opposed abundance trends (**Fig. 3**); the *Globoturborotalita* gr. records its maximum abundance (>15%) own to the common *G. druryi*. The neogloboquadrinids are subordinated and show a shift from prevalent left-coiled to right-coiled specimens (ca. 75%), a ratio that is maintained up to the top of the Mn-rich interval (**Fig. 3**). The *Globigerinoides* gr. is rare (<2%). The upper part of the homogeneous marls (samples 3 and 4) records a reduction of both planktonic and benthic abundance but the composition of the assemblage is transitional to that of the Mn-rich laminated marls, as right-coiled neogloboquadrinids became gradually prevalent among planktonic at the expense of the *Globoturborotalita* gr. and of *T. quinqueloba* (**Fig. 3**). At the same time the *Globigerina bulloides* gr. retains common occurrences and the *Globigerinoides* gr. records the maximum abundance (5-7%). Along the Mn-rich

interval a clear upward trend of increasing relative abundance (45 to >60%) of the *Neogloboquadrina* gr. is recorded, which culminates at the base of the diatomaceous marls; neogloboquadrinids are still prevalently right-coiled (ca. 75%), but the coiling ratio starts to decrease at the base of the diatomaceous marls (**Fig. 3**). The *G. bulloides* gr. describes an opposite trend decreasing from 33% down to ca. 20% at the Mn-rich/diatomaceous marls transition (**Fig. 3**). The other taxa are relatively uncommon, each accounting for 5 to 10%. From the middle part of the diatomaceous marls to the top of the section the only evident trend is the increase of *T. quinqueloba* and the decrease of the *Globoturborotalita* gr., while the dominant taxa, the *G. bulloides* gr. and the neogloboquadrinids show fluctuations in the range of 20 to 30% and 40 to 50%, respectively (**Fig. 3**). Short-living excursion of increased left-coiled neogloboquadrinids are recorded in the diatomaceous marls; the most pronounced of which show values as high as ca. 70% (**Fig. 3**).

3.1.2. Benthic foraminifers

Benthic foraminifers are characterized by low abundances in the lowermost homogeneous marls (**Fig. 3**), where their diversity is relatively high; however, a marked prevalence of *Cibicidoides pseudoungerianus* and *Hanzawaia boueana*, which together reach ca. 30%, is recorded. Other common to rare taxa are *Bolivina scalprata* var. *miocenica*, *Cibicidoides ungerianus*, *Globocassidulina oblunga*, *Melonis padanum*, *Pullenia* spp., *Siphonina reticulata*, *Uvigerina peregrina*.

As also observed for the planktonic counterpart, the transition from the homogenous to the Mn-rich marls records a gradual change of the benthic foraminifer assemblages (**Fig. 3**). Sample 3 is characterized by a high percentage of bolivinids (*B. dentellata*, *B. dilatata* and *B. spathulata*), which are upward replaced by the *Rectuvigerina bononiensis* gr. (up to ca. 90%), becoming prevalent along the Mn-rich interval despite an upward decreasing trend. This interval also records an increase in overall benthic foraminifer abundance (**Fig. 3**). Along with the rectuvigerinids, the occurrence of *Globobulimina affinis*, *Gyroidina parva*, *Cancris auricula* and *G. oblunga* it is noteworthy. Instead, the transition to the diatomaceous marls is sharp in term of benthic foraminifers (**Fig. 3**); abundance drops and, apart from the persistence of rare *G. oblonga*, all the taxa observed in the Mn-rich interval temporary disappear and are replaced by *C. pseudoungerianus*, *H. boueana*, *C. refulgens*, *C. lobatulus*, *Elphidium* sp. (and other scattered epiphytic taxa; see Langer, 1993) and rare bolivinids (among which, *B. scalprata* var. *miocenica* is dominant). This assemblage is recorded up to sample 17 and then gradually decrease (**Fig. 3**); above this level, the abundance increases and the assemblage is the same observed in the Mn-rich interval (**Fig. 3**), except that *R. bononiensis* gr. is less abundant and shows an upward decreasing trend, opposite to that of the *Bolivina* gr., here dominated by *B. spathulata* and *B. dilatata*. Another difference is the variable occurrence from 5 to 15% occurrence of *Stainforthia* sp., which is absent in the Mn-rich interval (**Fig. 3**).

3.2. Calcareous nannofossils

The calcareous nannofossil assemblage is dominated by placolith taxa, although nicely-preserved coccospheres have been occasionally recorded throughout the section (**Figs. 3G-O**). From bottom to top, placoliths exhibit remarkably different relative abundances that are often correlated with lithological changes (**Fig. 3**). The most abundant taxa are *Reticulofenestra* < 5 µm gr., *Reticulofenestra antarctica* gr., *Coccolithus pelagicus*, *Umbilicosphaera jafari*, *R. pseudoumbilicus* < 7 µm and *Helicosphaera carteri* (**Fig. 3**). *U. jafari* dominates the assemblage at the base of the section (up to 46% in the lower homogenous marls) and decreases in abundance below 20% from the base of the Mn-rich marls upward (**Fig. 3**). *R. antarctica* gr., *C. pelagicus*, and *H. carteri* abundances increase from bottom to top of the homogeneous marls and show their highest abundance just below (*R. antarctica*) or at the base of the Mn-rich bed (*C. pelagicus*, 23%; *H. carteri*, 9%), where *U. jafari* decreases below 15% (**Fig. 3**). The highest abundance of *C. pelagicus* occurs just at the base of the Mn-rich laminated marls, and steadily decreases toward the top of this layer; its abundance drops below 10% and remains low in the diatomaceous interval towards the top of the section, where a small increase occurs (13%; **Fig. 3**). *H. carteri* decreases slowly from the base of the Mn-rich laminated marls to the top of the section (**Fig. 3**). *Reticulofenestra* < 5 µm is common in the homogeneous marls and in the Mn-rich marls (20 to 33%) and dramatically increases (up to 64%) in the

lower half of the diatomaceous interval; it shows a fluctuating and decreasing abundance trend towards the top of the layer, despite its overall abundance remains above 28% (**Fig. 3**). *R. pseudoumbilicus* < 7 µm shows a positive abundance trend from bottom to top of the section, although characterized by marked fluctuations (between 4% and 12%) from the lower half of the diatomaceous interval to the top (**Fig. 3**). In this interval *R. antarctica* gr. shows an opposite fluctuation trend (between 16% and 29%; **Fig. 3**). At the base of the diatomaceous interval very rare *Sphenolithus abies* and *S. moriformis* are recorded, their total abundance never exceeding 3% of the assemblage. *Pontosphaera multipora*, *P. discopora*, and *Rhabdosphaera clavigera* also occur discontinuously.

Besides sphenoliths, the entire section is characterized by the scattered presence of deep photic zone dwellers (such as the discoasterids); amaurolithids, commonly used as biostratigraphic markers in upper Miocene sediments, are absent. The Messinian marker species *R. rotaria* is discontinuously present along the section.

3.3. Diatoms

Diatoms mostly occur as well-preserved single valves, with the exception of the larger (especially discoid) specimens, which are often fragmentary or partly dissolved. The diatom assemblage is composed by fully marine taxa that, according to their present-day ecology (e.g., Round et al., 1990; Hasle and Syvertsen, 1997),

can be separated into five sub-assemblages (**Tab. 1**), listed herein based on their decreasing abundance: i) an opportunistic, monospecific sub-assemblage, represented by the planktonic pennate diatom *Thalassionema nitzschioides* (**Fig. 5A-C**); ii) a resting stage sub-assemblage, composed by *Chaetoceros* resting spores (**Fig. 5D-I**); iii) an open ocean sub-assemblage, mainly composed by the planktonic pennate diatom *Denticulopsis* (**Fig. 5J-K**); iv) a neritic sub-assemblage, composed of a wide variety of benthic and epiphytic genera associated to a scarcely diversified but more abundant meroplanktonic component, mainly represented by *Actinoptychus senarius* (**Fig. 5L-U**); v) a deep chlorophyll maximum (hereafter: DCM) sub-assemblage, mostly characterized by large and heavily silicified discoid diatoms, especially *Coscinodiscus* spp. (**Fig. 6**).

Diatom sub-assemblage	**Main components**	**LA**	**HA**	**µA**
Opportunistic	*Thalassionema nitzschioides*	~65%	~39%	~50%
Resting stage	*Chaetoceros* resting spores	~9%	~37.5%	~20%
Open ocean	*Denticulopsis* spp. (mostly *D. simonsenii*)	~0.5%	~15%	~5%
Neritic	Benthic-epiphytic: *Biddulphia* spp., *Climacosphenia* sp., *Cocconeis* spp., *Grammatophora* spp., *Haslea* sp. (?), *Isthmia* sp., *Lithodesmium* sp., *Navicula* spp., *Rhaphoneis* spp., *Synedra* sp. Meroplanktonic: *Actinoptychus* spp. (mostly *A. senarius*), *Paralia sulcata*	~4%	~16%	~9%
DCM	*Coscinodiscus* spp. (mostly *C. marginatus* and *C. radiatus*), *Hemiaulus* spp., *Hemidiscus cuneiformis*, *Stephanopyxis turris*, *Thalassiosira leptopus*, *Rhizosolenia* spp. (mostly *R. miocenica* and *R. styliformis*)	~3%	~13%	~6.5%

Table 1. Diatom sub-assemblages observed in the diatomaceous interval, with their main components and relative abundances. LA: lowest abundance; HA: highest abundance; µA: mean abundance.

An ecologically uncertain sub-assemblage, is mostly represented by planktonic diatoms of the genus *Thalassiosira*. The opportunistic group exhibits a fluctuating trend around 50%, increasing in the upper part of the diatomaceous interval, opposite to that of the resting stage sub-assemblage, which is more abundant in the lower part; indeed, these two sub-assemblages show an opposing trend (**Fig. 3**). The open ocean sub-assemblage tends to decrease toward the upper part of the diatomaceous interval (**Fig. 3**). The neritic and DCM sub-assemblages show a rather similar, fluctuating trend; the neritic sub-assemblage shows a significant increase in the uppermost part of the diatomaceous interval (**Fig. 3**).

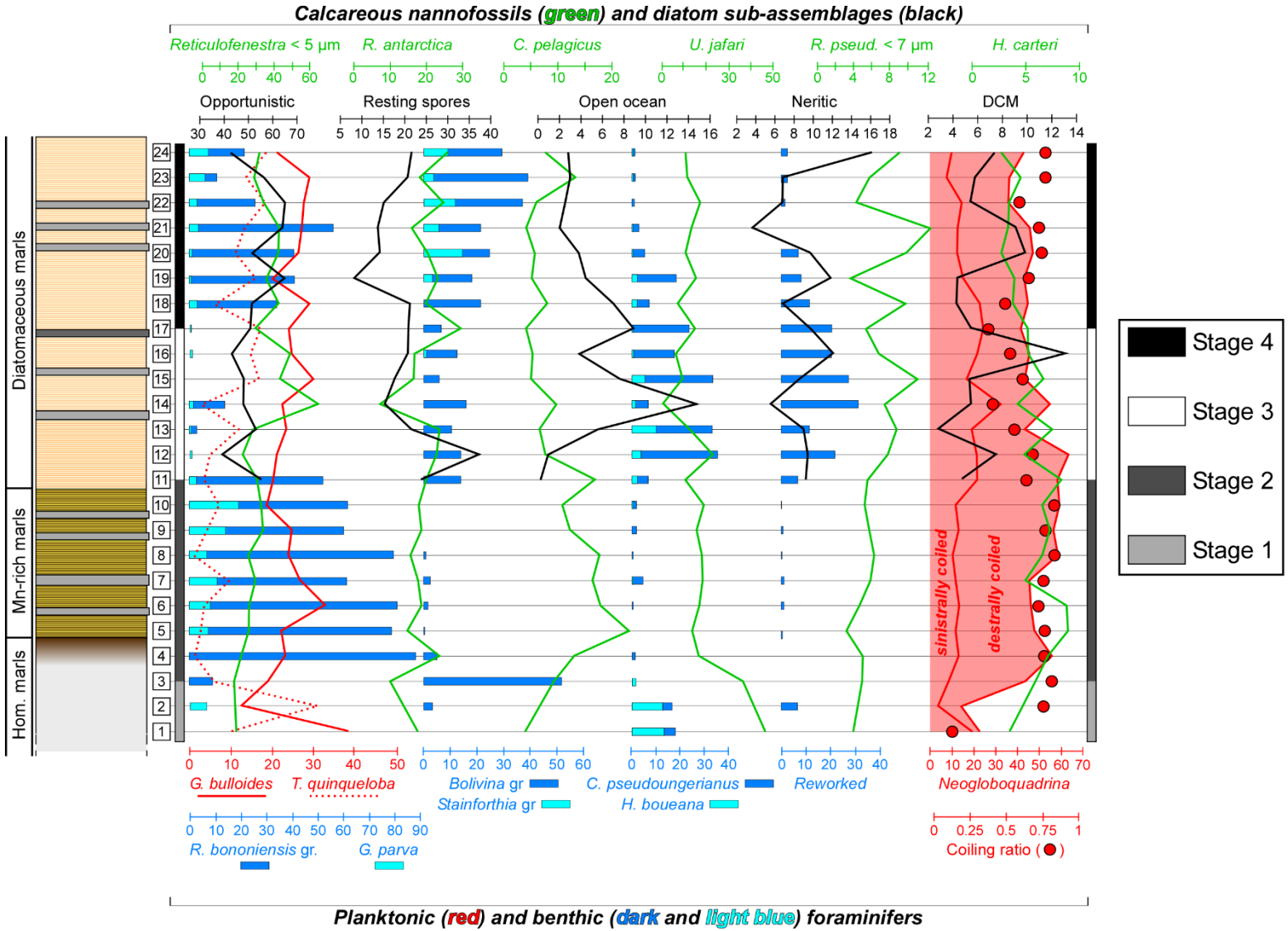

Figure 3. Relative abundances (%) of the most relevant foraminifers, calcareous nannofossils and diatoms. Sample numbers are reported on the right of the stratigraphic column.

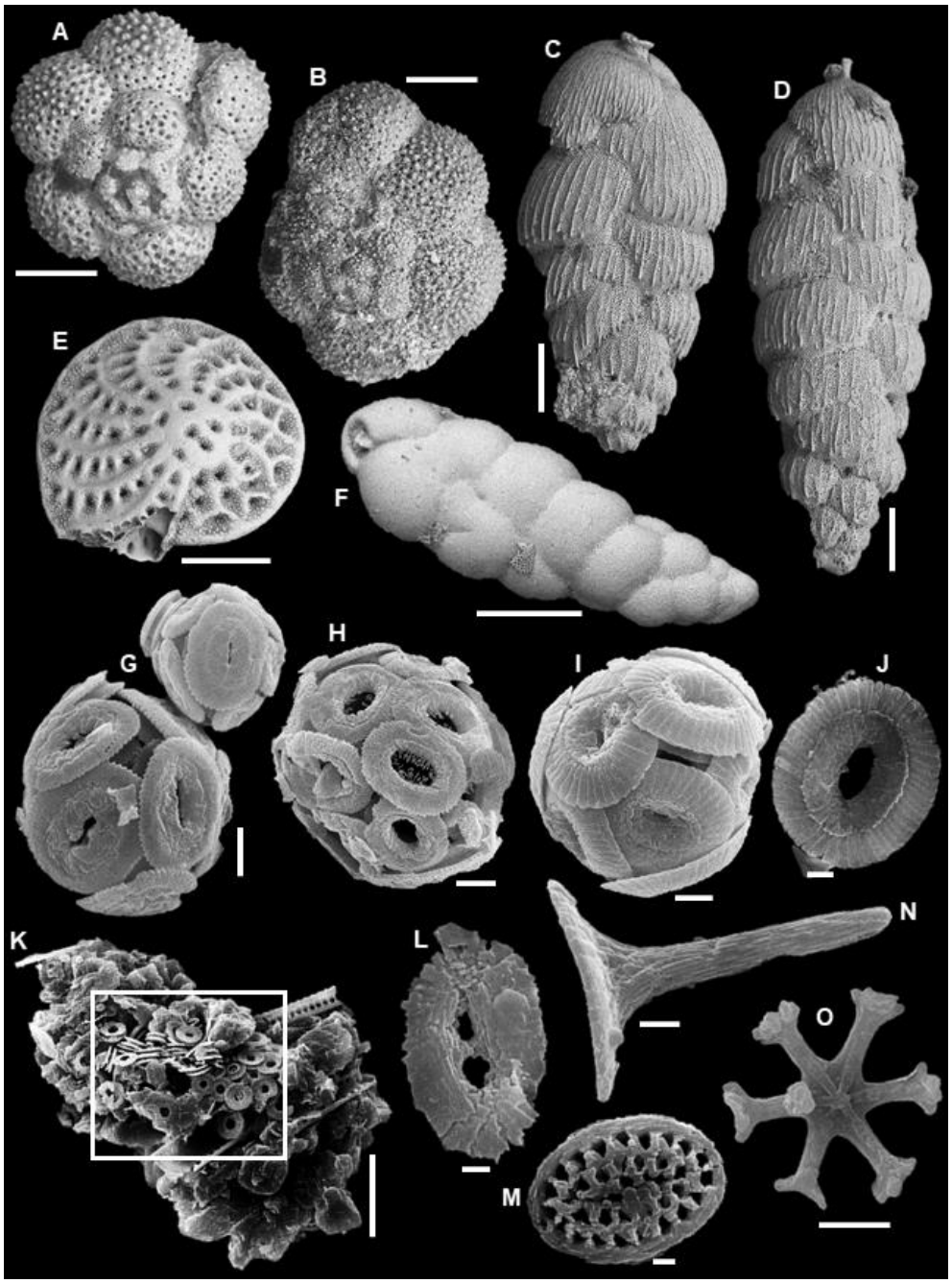

Figure 4. Selected foraminifers and calcareous nannofossils (SEM micrographs). Planktonic foraminifers: A-B) *Turborotalita multiloba*. Benthic foraminifers: C-D) (Recto)*Uvigerina bononiensis*; E) *Elphidium macellum*. F) *Stainforthia* cf. *fusiformis*. Calcareous nannofossils: G) coccospheres of *Reticulofenestra perplexa* (bigger) and *R. producta* (smaller); H) coccosphere of *Reticulofenestra haqii*; I) coccosphere of *Coccolithus pelagicus*; J) placolith of *C. pelagicus*; K) placoliths of *Umbilicosphaera jafari* (white rectangle) in a fecal pellet; L) placolith of *Helicosphaera carteri*; M) placolith of *Pontosphaera* sp.; N) *Rhabdosphaera claviger*; O) *Discoaster* sp. Scale bars: A-B = 50 µm; C-F = 100 µm; G-J = 2 µm; K = 10 µm; L-N = 1 µm; O = 5 µm.

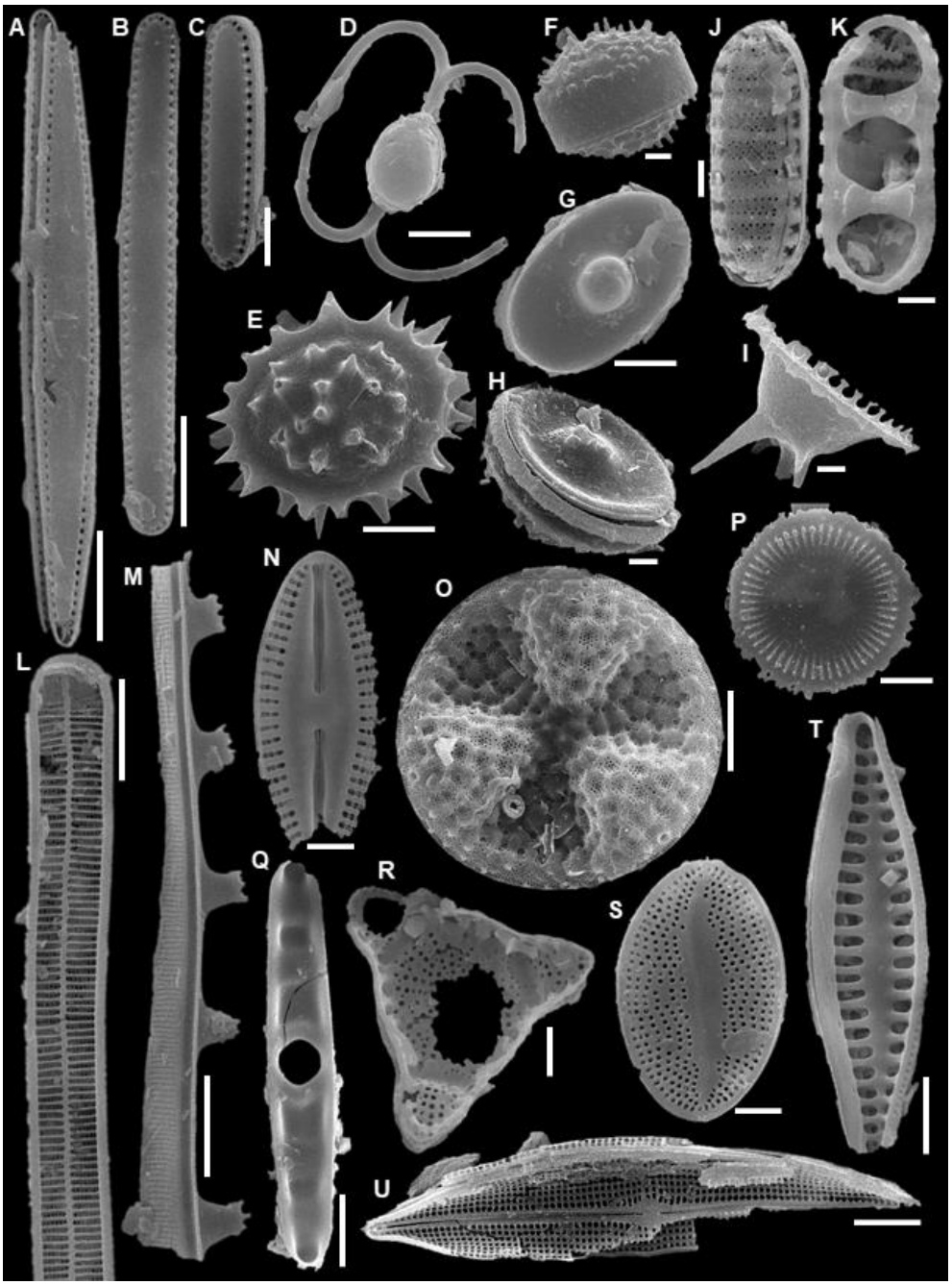

Figure 5. Diatoms (SEM micrographs). Opportunistic sub-assemblage: A-C) *Thalassionema nitzschioides*. Resting stage sub-assemblage: D-I) *Chaetoceros* resting spores. Open-ocean sub-assemblage: J-K) *Denticulopsis* sp.. Neritic sub-assemblage: L) *Synedra* sp.; M) *Climacosphenia* sp. (fragment); N) *Diploneis* sp.; O) *Actinoptychus senarius*; P) *Paralia sulcata;* Q) *Grammatophora* sp.; R) *Triceratium* sp.; S) *Cocconeis* sp.; T) *Rhaphoneis* sp.; U) *Haslea* sp. (?). Scale bars: A-B, O, Q, T = 10 µm; C-E, G, N, P, R-S, U = 5 µm; F, H-K = 2 µm; L-M = 20 µm.

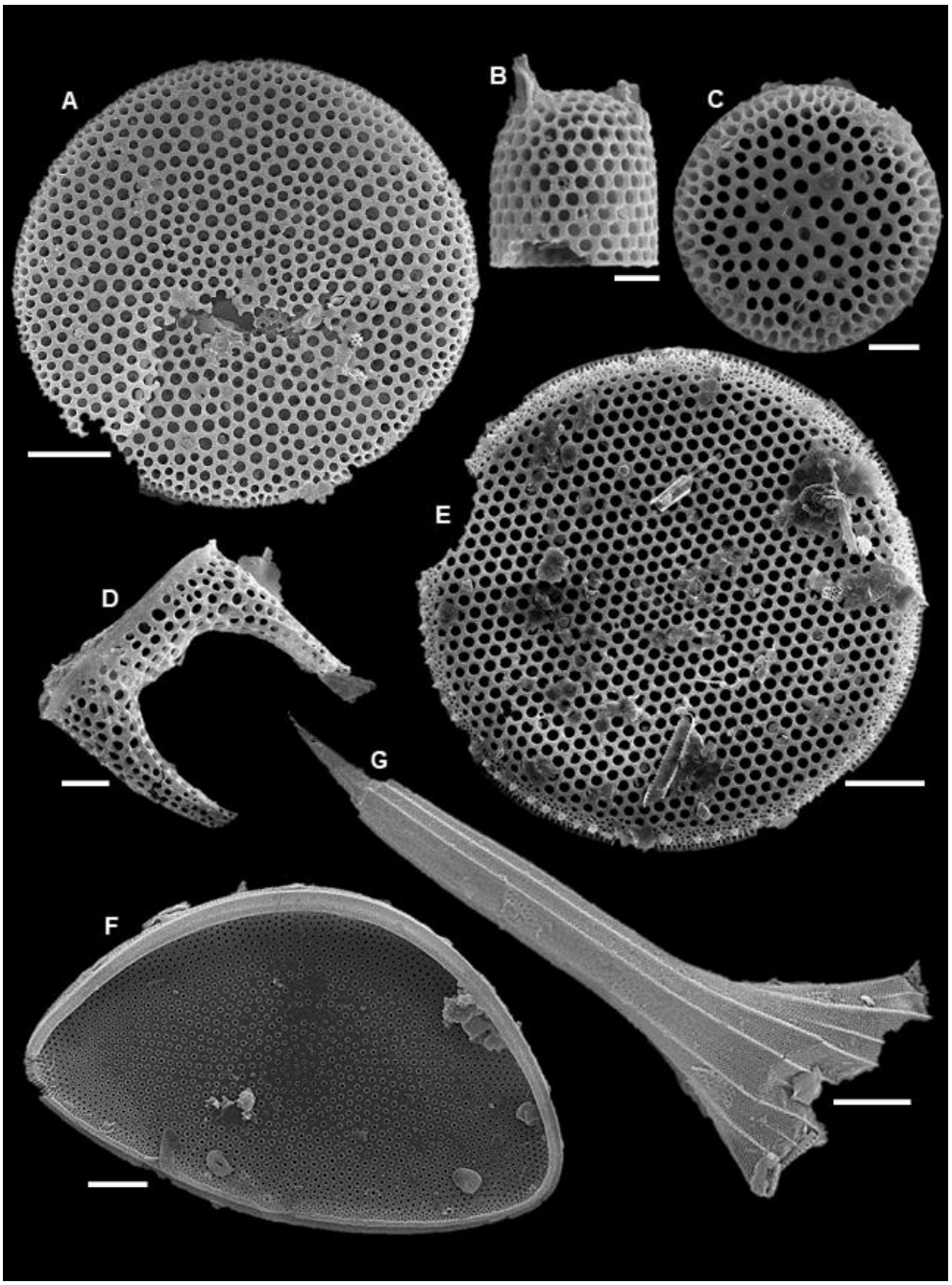

Figure 6. Diatoms (SEM micrographs). DCM sub-assemblage: A) *Coscinodiscus radiatus*; B) *Stephanopyxis turris*; C) *Coscinodiscus marginatus*; D) *Hemiaulus* sp.; E) *Thalassiosira leptopus*; F) *Hemidiscus cuneiformis*; G) *Rhizosolenia miocenica*. Scale bars: A, E = 20 µm; B, D = 5 µm; C, F-G = 10 µm.

3.4. Non-diatomaceous siliceous microfossils

Beside diatoms, six subordinated groups of siliceous microfossils (**Tab. 2; Figs. 7-8**), whose contents show a rather fluctuating trend, have been recognized in the diatomaceous interval. In order of their mean relative abundance, they are: sponge spicules, silicoflagellates, ebridians, endoskeletal dinoflagellates, radiolarians and chrysophytes.

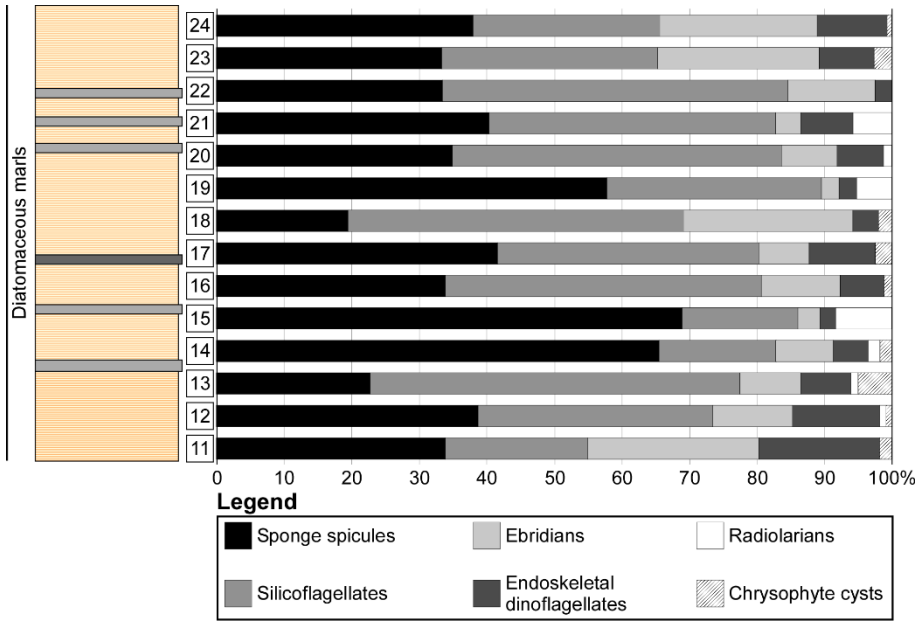

Figure 7. Relative abundances of non-diatomaceous siliceous microfossils. Sample numbers are reported on the right of the stratigraphic column.

The spongolitic assemblage **(Figs. 7, 8A-P)** comprises both macro- and microscleres, the former occasionally broken but almost lacking any sign of dissolution. The assemblage is marine, characterized by two dominant morphotypes

of macroscleres, i.e. oxeas and styles, associated to a subordinated and well-diversified component. Their trend roughly mimic that of the neritic and DCM diatom sub-assemblage.

The silicoflagellate assemblage **(Figs. 7, 8Q-U)** is generally well-preserved and includes the genera *Distephanopsis* (e.g., *D. crux*), *Dyctiocha* (e.g., *D. aspera*, *D. fibula*), *Mesocena*, *Paramesocena* and *Stephanocha* (e.g., *S. speculum*). The latter taxon is the most common in the assemblage, that is characterized by a (*Dictyocha*+*Distephanopsis*)/*Stephanocha* mean ratio of about 0.6. Aberrant morphologies have been only rarely observed. The relative abundance trend of the silicoflagellates is highly fluctuating, especially in the lower part of the diatomaceous interval.

The ebridian assemblage (**Figs. 7, 8V-X**) is poorly preserved, however the better preserved specimens can be attributed to the genera *Haplohermesinum*, *Ammodochium* and *Parathranium*. Triangular remains (triodes) deriving from the fragmentation of *Haplohermesinum*-like ebridians are rather common. The ebridians reach the highest abundances at the base (e.g., sample 11), at the middle (e.g., sample 18) and at the top (e.g., samples 23-24) of the diatomaceous interval.

The endoskeletal dinoflagellates (**Figs. 7, 8Y-A***) are mostly represented by well-preserved specimens of the genus *Actiniscus* (especially *A. pentasterias* and *A. tetrasterias*). Like the ebridians, they reach the highest abundances in the lower (samples 11 and 12), middle (sample 17) and upper part (sample 24) of the diatomaceous interval.

The radiolarian assemblage (**Figs. 7, 8B***) is mostly composed by fragmented specimens that cannot be confidentially identified. Nassellarians seems to be more abundant and generally better preserved than Spumellarians. Only episodic, weak increases of their abundance are recorded along the diatomaceous interval.

Chrysophytes (**Figs. 7, 8C*-E***) are represented by well-preserved and variously ornamented stomatocysts. Their abundance is extremely low, with just a small increase in the lower part of the diatomaceous interval.

Other siliceous microfossils	**Main components**	**LA**	**HA**	**µA**
Sponge spicules	Oxeas and styles dominant, associated to acanthostrongyles, acanthostyles, acanthosubtylostyles, acanthotriaenes, achantoxeas, diancistrons, hexactines, isocheles, microstrongyles, microxeas, oxyasters, plagiotriaenes, sigmas, spherasters, spirasters, sterrasters (*Geodia* sp.), strongyles, toxas, triaenes (calthrops), tylostyles, tylotes.	~19%	~69%	~40%
Silicoflagellates	*Distephanopsis crux, Dictiocha aspera, D. fibula, Mesocena* sp., *Paramesocena* sp., *Stephanocha speculum*	~17%	~55%	~37%
Ebridians	*Haplohermesinum* sp., *Ammodochium rectangulare, Parathranium*	~3%	~25%	~13%
Endoskeletal dinoflagellates	*Actiniscus pentasterias, A. tetrasterias*	~2.5%	~18%	~7.5%
Radiolarians	Nassellarians (better preserved) and Spumellarians (fragmentary) unidentified	-	~8.2%	2%
Chrysophytes	Stomatocysts indet.	-	~5%	1%

Table 2. Non-diatomaceous siliceous microfossil groups, with their main components and relative abundances. LA: lowest abundance; HA: highest abundance; µA: mean abundance.

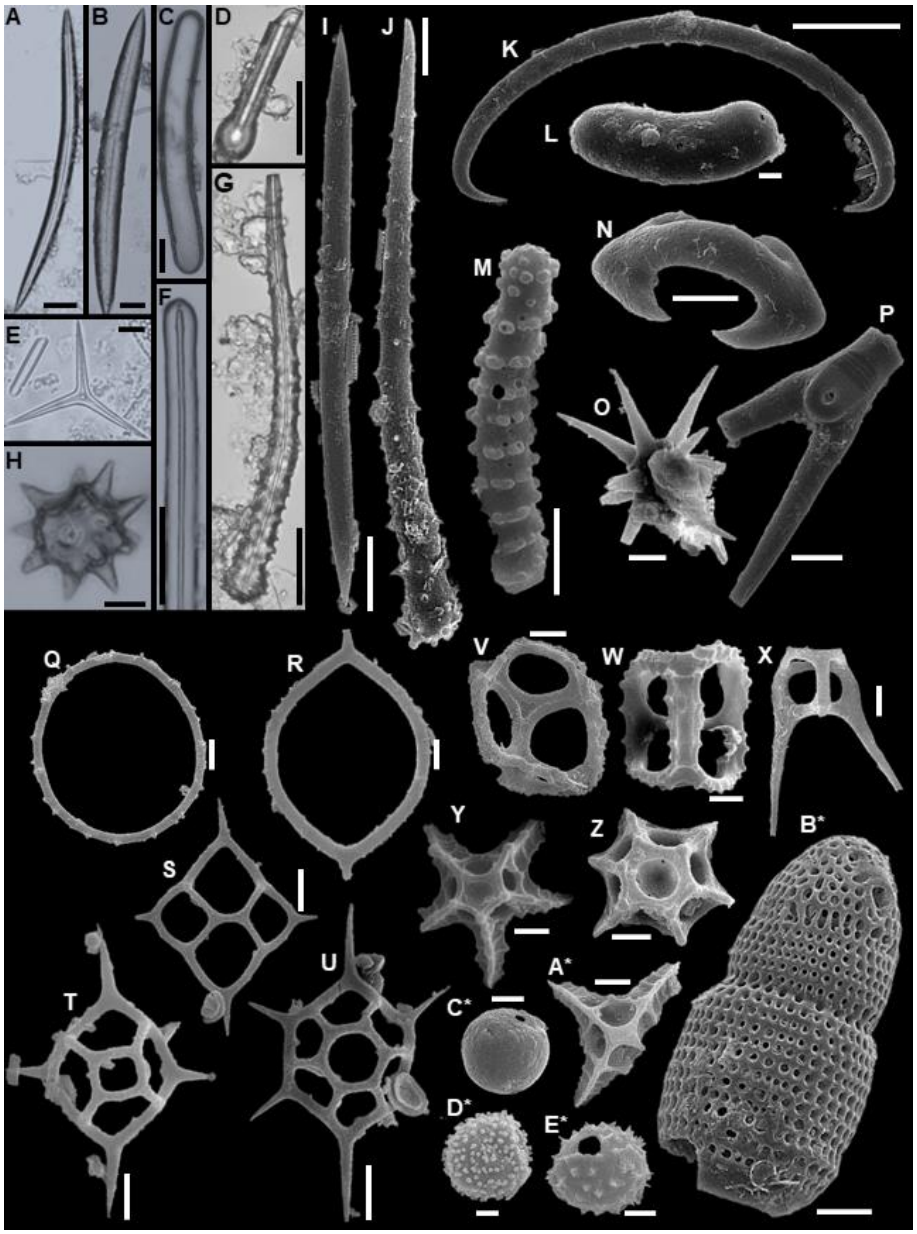

Figure 8. Non-diatomaceous, siliceous microfossils (LM and SEM micrographs). Sponge spicules: A-B, I) oxeas; C) strongyle; D) tylote (fragment); E) triaene; F) style; G, J) acanthosubtylostyle; K) sigma; L) microstrongyle; M) spicule indet.; N) isochela; H, O) oxyaster; P) plagiotriaene? (fragment). Silicoflagellates: Q) *Paramesocena* sp.; R) *Mesocena* sp.; S) *Dictyocha fibula*; T) *Distephanopsis crux*; U) *Stephanocha speculum*. Ebridians: V) *Haplohermesinum* sp.; W) *Ammodochium rectangulare*; X) *Parathranium* sp.. Endoskeletal dinoflagellates: Y-Z) *Actiniscus pentasterias*; A*) *Actiniscus tetrasterias*. Radiolarians: B*) Nasselarian indet. Chrysophytes: C*-E*) stomatocysts indet. Scale bars: A-D, F-G = 25 µm; E, J, M, P-U = 10 µm; H, L, N-O, V-A*, D*-E* = 5 µm; I, B* = 20 µm; C* = 1 µm.

4. Discussion

4.1. Foraminifers

According to the variations documented by foraminifer assemblages recorded along the section, four intervals can be recognized, which are not coincident with the lithologic changes. These intervals are defined by sudden changes in benthic assemblages, while planktonic ones show more gradual variation across the interval boundaries.

Benthic foraminifers primarily reflect changes in nutrient and oxygen content on the sea floor (Murray, 2006); in the lower part of the homogeneous marls (lowermost 2 samples) the moderate diversification and low abundance of benthic foraminifers, together with the relatively common *C. pseudoungerianus* and *H. boueana* point to a (outer) shelf environment characterized by oligo- to mesotrophic conditions and good oxygenation (Jorissen et al., 1995; Altenbach et al. 1999), where indeed these epifaunal taxa may find a suitable habitat. Planktonic foraminifers suggest that these conditions are associated with cold and productive surface waters (Kallel et al., 2000; Incarbona et al., 2019). The surface to sea-floor nutrient gradient could be explained by the remineralization process or other processes leading to inefficient export. From sample 3, a series of gradual, but rapid changes are recorded: a) decrease of *T. quinqueloba*, which suggests a slight increase of sea surface

temperature (SST); b) concomitant increase of neogloboquadrinids, which points to a shift from a prevalently surface productivity to a deeper one, possibly related to the onset of a DCM (Rigual-Hernández et al., 2012). The temperature trend may also be inferred from the shift from prevalently left to right coiled neogloboquadrinids from samples 1 to 3. Overall, the SST increase likely resulted in the stratification of the water column. In fact, towards the top of the homogeneous marls, a sudden drop of the benthic foraminifer diversity and an increase in abundance occurs, first related to the *Bolivina* gr., and then, from sample 4, to the *R. bononiensis* gr. (Thomas, 1980). These changes towards the dominance of shallow to deep infaunal taxa are related to the onset of eutrophic environments and/or low oxygen levels (see the trox model of Jorissen et al., 1995). In particular, the *Bolivina* gr. is an opportunistic taxon well-adapted to low oxygen conditions (Jorissen et al., 1992; Melki et al., 2010), while the *R. bononiensis* gr., being morphologically similar to the uvigerinids, can be associated with a high availability of organic matter (Nomaki et al., 2005, 2006). Actually, in the Pliocene successions of the Eastern Mediterranean, *R. bononiensis* is a common component of the sapropel assemblages (Jonkers, 1984).

In the Mn-rich laminated marls the trends of the *R. bononiensis* gr. and of right coiled neogloboquadrinids are opposite; however, they both constantly prevail among the benthic and planktonic foraminifer assemblages, respectively, suggesting rather constant paleoceanographic conditions. At the base of the diatomite, the former group suddenly disappears, while the second persists and reaches its maximum slightly above the Mn-rich/diatomite boundary (samples 12). Then, the *R.*

bononiensis gr. is replaced by both the epifaunal and epiphytic groups, pointing to the re-establishment of oligo/mesotrophic conditions on the sea floor. In the late Miocene to Pliocene deposits of the Eastern Mediterranean the increase of inner shelf epiphytic taxa in the diatomites is often attributed to downslope transport (Jonkers, 1984; Kouwenhoven, 2000). Another outstanding change at the Mn-rich/diatomite transition is the increase of siliceous productivity leading to silica preservation in the sediment. Recent observations highlight how the shift from calcareous to siliceous primary producers in the water column may led to a decrease of benthic productivity (Takata et al., 2018, 2019), because of the reduced ballast effect of siliceous particles respect to the calcareous ones. This mechanism may have had the same effect in the Piedmont Basin, supressing the proliferation of infaunal benthic foraminifers, thus favoring epifaunal taxa. This interval is also characterized by a slight increase of left-coiled neogloboquadrinids, which, rather than being temperature-related (indeed, no concomitant *T. quinqueloba* increases are observed), could be linked to changes in the productivity or water column structure, possibly in relation to an increase of silica-secreting biota. This feature requires detailed investigation of the different morphotypes that compose the *Neogloboquadrina* gr. (e.g., Eynaud et al., 2009).

Within the diatomaceous interval, a clear difference can be drawn between the lower and upper parts. Again, the change among the benthic foraminifers is more abrupt, while the planktonic foraminifers show a more gradual change.

On the sea floor, meso- to oligotrophic conditions can be inferred up to sample 17; from sample 18 up to the top of the section a sudden increase of the *R.*

bononiensis and *Bolivina* groups testifies to the establishment of eutrophic and probably less oxygenated conditions. Some differences can be identified comparing this interval with the Mn-rich one, where *R. bononiensis* gr. alone is prevailing. Up to sample 21 the overall abundance of benthic foraminifers is scarce (like in the lower part of the diatomite), with *R. bononiensis* gr. being dominant and minor percentages of epifaunal taxa still present; above sample 21 the *Bolivina* gr. increases, associated with *Stainforthia* sp. The latter taxon may tolerate very low oxygen conditions (Melki et al., 2010) and has an opportunistic habit, being very efficient in recolonizing the substratum after pollution episodes (Alve, 1994). Moreover, these changes are coupled with a drastic reduction of epifaunal taxa.

To better understand the benthic foraminifer trends, it is useful to consider the gradual changes recorded by the planktonic foraminifers. These show a slight reduction in the neogloboquadrinids (i.e., deep dwellers) and a concomitant increase of the cold water and eutrophic surface dweller *T. quinqueloba*. This pattern suggests a decrease of SST and a marked annual seasonality, with a possible analog in the glacial Pleistocene Tyrrhenian Sea periods (MIS 4 and 6, see Kallel, et al., 2000). The combination of calcareous surface and DCM production in the water column can explain the increasing export of organic matter to the sea floor and the proliferation of infaunal taxa, including those better adapted to low oxygen conditions.

Overall, the data confirm the previous interpretations of the diatomaceous sediments of Pecetto di Valenza as deposited in an outer shelf to upper slope

environment, ranging between 200 and 500 m (Sturani and Sampò, 1973; Violanti, 1996).

4.2. Calcareous nannofossils

The assemblage is dominated by *U. jafari*, *Reticulofenestra* < 5 μm, *R. antarctica* gr., *C. pelagicus*, and *H. carteri*, and is similar to those of other Messinian successions of the Mediterranean region (e.g., Pollenzo section, Italy: Lozar et al., 2010; Dela Pierre et al., 2011; Monte del Casino section, Italy: Negri et al., 1999; Perales section, Spain: Flores et al. 2005; Faneromeni section, Greece: Negri and Villa, 2000; Kalamaki section, Greece: Karakitsios et al., 2017; Polemi section, Cyprus: Wade and Bown, 2006; Tokhni section, Cyprus: Gennari et al., 2019). The scattered occurrence of *R. rotaria* demonstrates the Messinian age of the section. Changes in the relative abundance of selected taxa correlate with environmental and lithological changes. At Perales *U. jafari* shows high abundances in the upper marls; it has been suggested that this correlates to silica depleted surface water, immediately after diatomite deposition (Flores et al., 2005). At Pollenzo (Lozar et al., 2018) *U. jafari* peaks in carbonate beds just below or at the base of sapropels, testifying a to a well-mixed water column and arid/cool climate. The high abundance of *U. jafari* at the base of the section may indicate well remixed mesotrophic surface waters at the

time of homogeneous marl deposition, where efficient nutrient recycling occurred in the upper and middle photic zones and the water column was silica depleted.

C. pelagicus is an extant taxon mainly distributed in the northern high latitudes, where it prefers cool-temperate waters and mesotrophic to eutrophic conditions (Negri et al., 1999; Cachão and Moita, 2000; Ziveri et al., 2004) being able to proliferate in a wide range of salinities (from 26.9 to 36‰) (Silva et al., 2008). The abundance record of *C. pelagicus* is high at the base of the Mn-rich laminated marls (23%) and decreases towards the top of the bed. Similar trends have been reported in Pleistocene sapropels, where the base is marked by a sharp peak of *C. pelagicus*, followed by a sharp decrease in abundance (Negri et al., 2003); this is also recorded in Miocene sapropels (Monte del Casino, Negri et al., 1999) and suggests that the Mn-rich laminated marls could represent a sapropel-like layer, as also suggested by the increased abundance of *H. carteri*. The latter is an extant middle photic zone dweller (Crudeli et al., 2006) that lives in meso- to eutrophic, low salinity, and turbid biotopes (Bukry, 1974; Giraudeau et al., 1992; Colmenero-Hidalgo et al., 2004; Ziveri et al., 2004), especially in warm waters (Brand 1994). It is not abundant in the samples, but its presence (up to 9%) at the top of the homogeneous marls and at the base of the Mn-rich marls suggests a further trend towards warmer (and humid) conditions and an increase in surface water productivity that could be attributed to increased fresh water supply, leading in turn to enhanced stratification of the water column and possible onset of the DCM.

In the diatomaceous interval the *Reticulofenestra* gr. dominates the calcareous nannofossil assemblages. These opportunistic taxa are surface water dwellers adapted to changing environmental conditions. *R. pseudoumbilicus* is a common constituent of the calcareous nannofossil assemblage in the diatomite of the Sorbas basin (Flores et al., 2005); *Reticulofenestra* < 5 µm (often reported as small *Reticulofenestra),* has been interpreted as eutrophic surface water dwellers in other Messinian sections (Negri and Villa, 2000; Lozar et al., 2010), and *R antarctica* is regarded as a cool water species, due to its remarkable abundance in the Southern Ocean (Wei and Wise, 1990). The high abundance of *Reticulofenestra* < 5 µm in the lower half of the interval suggests a sharp increase in nutrient availability in the upper photic zone. The high abundance fluctuation of *Reticulofenestra* < 5 µm and *R. pseudoumbilicus*, with an opposite trend with respect to *R. antarctica*, suggests high seasonality and an overall eutrophic surface water with available dissolved silica (Flores et al., 2005; Negri and Villa, 2000). The decreasing trend of *Reticulofenestra* < 5 µm towards the top of the level and the opposite increasing trend of *R. antarctica* and *R. pseudoumbilicus* could suggest a shift towards cooler surface waters or a high-frequency alternation between cool and warm phases. Low abundances of the middle photic zone dwellers (*C. pelagicus*, *H. carteri*, *U. jafari*) furthermore suggest that, during diatomite deposition, calcareous nannofossils exploiting high nutrient level were mainly confined to the upper photic zone, possibly outcompeted by diatoms in the middle photic zone, where taxa able to flourish in low(er) light are more successful (Balch, 2004).

The calcareous nannofossil assemblage contain rare deep dwellers irregularly present along the section; the only weak evidence they provide to support the development of the DCM is the very low abundances of *Sphenolithus* gr. (up to 3%) in the lower part of the diatomaceous interval. This pattern is somehow unusual, since deep photic zone dwellers are usually abundant at DCM and commonly associated with warm surface waters (discoasters, sphenoliths) and common in the Pliocene and Pleistocene sapropels (e.g. Negri et al., 1999; Gibbs et al., 2004). Their low abundances at Pecetto di Valenza could be related to cooler waters linked to the latitude of the section (Lozar et al., 2010). On the other hand, their very low relative abundances (< 3%) in the lower part of the diatomaceous interval could testify to the development of the DCM. Their low abundances could also be related to high trophic level, as suggested by diatom assemblages and by the high abundance of placolith taxa along the section; eutrophic surface waters could have prevented the blooming of calcareous nannofossil DCM taxa, mainly adapted to oligotrophic warm water (Gibbs et al. 2004; Flores et al. 2005; Violanti et al., 2013; Gennari et al. 2019).

4.3. Diatoms

As far as concerns the diatom assemblage, three striking features deserve particular attention: i) the overall opposing trend of the opportunistic sub-assemblage dominated by *T. nitzschioides* and the resting stage sub-assemblage represented by *Chaetoceros* resting spores; ii) the rough similarities between the fluctuating trends

of the neritic and DCM sub-assemblages; iii) the general decline of the open ocean sub-assemblage toward the upper part of the diatomaceous interval.

The opposing trend of the opportunistic and resting-stage sub-assemblages is suggestive of marked fluctuations of the water column configuration and nutrient availability. *T. nitzschioides* is a cosmopolitan diatom, particularly abundant in nutrient-rich, neritic to oceanic surface waters influenced by a wide variety of oceanographic processes (e.g., Hasle and Syvertsen, 1997). On the other hand, *Chaetoceros* resting spores are produced in response to the nutrient depletion of the upper water column (e.g., Rigual-Hernández et al., 2013; Bosak et al., 2016). It is worth to note that the ratio between the abundances of *T. nitzschioides* and *Chaetoceros* resting spores is often considered as a reliable tracer of the occurrence and strength of upwelling (e.g., Gaudant et al., 1996; Lopes et al., 2006), with the lower values (i.e., *T. nitzschioides* << *Chaetoceros* resting spores) indicative of stronger coastal upwelling regime and upper values (i.e., *T. nitzschioides* >> *Chaetoceros* resting spores) of weaker coastal upwelling. On the other hand, other authors suggested how *Chaetoceros* resting spores may be related to shelf reworking (e.g., Pestrea et al., 2002; Pestrea and Saint Martin, 2002) or even to water column stratification (e.g., Crosta et al., 1997). Therefore, it is difficult to assess the triggering factors responsible for the proliferation of *T. nitzschioides* and the significance of *Chaetoceros* resting spores at Pecetto di Valenza. In any case, according to the traditional interpretations, a direct link with a vigorous upwelling regime can be ruled out, since *Chaetoceros* resting spores are always subordinated

to *T. nitzschioides*, similarly to other upper Miocene circum-mediterranean diatom-bearing sediments (e.g., Gaudant et al., 1996; Pestrea et al., 2002; El Ouahabi et al., 2007; Mansour et al., 2008). In agreement with Gaudant et al. (2010), the possible intensification of upwelling along the Monferrato Arc could be just inferred in the lower part of the diatomaceous interval, where *Chaetoceros* resting spores reach their maximum abundance. However, this interpretation can be challenged by the slight increase of neritic diatoms and by the peak of DCM-forming diatoms at the same stratigraphic level, hinting at a possible link with shelf sediment reworking and/or water column stratification (see below).

Shelf reworking and water column stratification could explain also the second main feature observed in the diatom assemblage of Pecetto di Valenza, i.e. the similar fluctuating trend of neritic and DCM-forming diatoms. Indeed, if the reworking of the shelf environment responsible for the displacement of neritic diatoms was triggered by riverine runoff, the input of freshwater combined to the thermal stratification of the water column may have fostered the DCM-forming diatoms. These latter are representative of a modality of primary production and sedimentation, consisting in the slow proliferation of diatoms in the deeper part of a stratified water column and their rapid sink linked to the breakdown of the stratification (fall dump *sensu* Kemp et al., 2000), which could have significantly contributed to the diatomaceous accumulation during the late Miocene in the Mediterranean area (e.g., Pestrea and Saint Martin, 2002). It is worth to note that, even if quantitatively lower than other sub-assemblages, this group is composed by

large and heavily silicified diatoms, each of them representing the equivalent biomass of a number of smaller individuals of the other sub-assemblages. Moreover, their poor state of preservation may have led to their underestimation, a problem that has been already documented in the other Messinian diatomaceous sediments (see El Ouahabi et al., 2007). The ongoing decrease of the sub-assemblage typified by *Denticulopsis* spp. may indicate a progressive deterioration of the connection with the open ocean, that agrees with the increasing inshore diatom influence in the uppermost part of the diatomaceous interval.

Summarizing (**Tab. 3**), it is possible to state that the abundance peaks of *T. nitzschioides* correspond to periods characterized by the enhanced availability of nutrients in the upper part of the water column; the eutrophication was unlikely related to the occurrence of a vigorous coastal upwelling, but can be explained with the convective remixing that normally exerts the major controls on the phytoplankton productivity in the Mediterranean area (e.g., Estrada, 1996; Siokou-Frangou et al., 2010). *Chaetoceros* resting spores reflect periods characterized by the establishment of surface oligotrophy. This condition was possibly associated with the stratification of the water column, favoring the proliferation of DCM-forming diatoms in the sub-surface layers. Runoff of diluted waters of continental origin, beside displacing the neritic diatoms, fertilized the water column and contributed to its stratification.

Diatom sub-assemblages	Interpretation
Opportunistic	Eutrophication of surface waters
Resting stage	Oligotrophy of surface waters
Open ocean	Improved oceanic circulation
Neritic	Downslope transport
DCM	Establishment of water column stratification

Table 3. Interpretation of the diatom sub-assemblages observed in the diatomaceous interval.

4.4. Non-diatomaceous siliceous microfossils

Caution is needed in interpreting the other biosiliceous microfossils (**Tab. 4**) observed in the Pecetto di Valenza section, because of the paucity of comparative studies that addressed the paleoecological significance of this overlooked component of the marine biosiliceous sediments, especially in the Mediterranean area.

As far as regards the silicoflagellates, the mean ratio of (*Distephanopsis*+*Dictyocha*)/*Stephanocha* is shifted toward *Stephanocha*. Assuming this genus as a reliable indicator of low sea surface temperatures, such result is in line with the geographical location of the Piedmont Basin in the Mediterranean. Today, significant concentrations of *S. speculum* have been observed in the Mediterranean only in the northernmost regions influenced by cold water masses (e.g., Rigual-Hernández et al., 2010; Malinverno et al., 2019). On the other hand, the high abundance of *Stephanocha* is consistent with the observations of the silicoflagellate assemblages from other upper Miocene circum-mediterranean sections (e.g., Frydas and Keupp, 2015) located in different latitudinal contexts. This

may indicate that the deep triggers of the widespread distribution of *Stephanocha* in the Mediterranean during the late Miocene were not (only) related to low sea surface temperatures, but to other processes. Indeed, Malinverno et al. (2019) suggested that, beside the linkage with cold water masses, the occurrence of *S. speculum* is strongly influenced by nutrient availability and low salinities. The very rare occurrence of aberrant morphologies in the observed samples excludes stressing conditions during the diatomaceous accumulation.

The abundant and well-diversified sponge spicule assemblage all along the diatomaceous interval is in line with the general feature of the biosiliceous accumulation in the Piedmont Basin during the late Miocene. Indeed, also the deposits of the Cappella Montei section, located few tens of kilometres south of Pecetto di Valenza and whose accumulation occurred in an inner shelf environment, record a remarkable spongolitic component (Bonci et al., 1991; Bonci, 1995; Bonci et al., 1996). In agreement with Sturani and Sampò (1973), the sponge spicules observed in the Pecetto di Valenza section were likely sourced from the shallower area of the basin, likely in response to riverine runoff. This is confirmed by SEM observations (see **Chapter 2**), that highlighted the systematic association of the spongolitic components to fine-grained terrigenous grains at lamina-scale. Such observation is also in line with the constant presence of ebridians, commonly used as an evidence of brackish water influences (Korhola and Smol, 2001).

Endoskeletal dinoflagellates represent a neglected component of the upper Miocene circum-mediterranean and global diatomaceous deposits (e.g., Bonci et al.,

1991; Rai et al., 2006; Gaudant et al., 2015). Moreover, studies concerning their present-day ecology are scarce (Takahashi, 1991; Onodera et al., 2015), thereby limiting the paleoecological interpretations. However, it is worth to note that while in the Pecetto di Valenza section the endoskeletal dinoflagellates are much rarer than the silicoflagellates, at Cappella Montei they may reach similar abundances (Bonci et al., 1991), suggesting a possible affinity with marginal settings.

For what concerns the radiolarians, any sort of speculation is precluded due to the overall poorly-preserved and inadequate record.

The rare occurrence of chrysophyte cysts, often interpreted as indicative of freshwater inputs (e.g., Kato, 2019), does not necessarily exclude the role of rivers, but may support the distal location of the Pecetto di Valenza depositional environment, shielded by the influx of freshwater biogenic particles. This interpretation is in line with that provided by Bonci et al. (1991) from the inner shelf deposits of Cappella Montei, where chrysophyte cysts may reach the same abundances of the silicoflagellates.

Other siliceous microfossils	**Interpretation**
Sponge spicules	Riverine-influenced reworking of the shelf
Silicoflagellates	Temperate to cold sea surface temperatures and/or nutrient availability
Ebridians	Brackish influence
Endoskeletal dinoflagellates	Unclear
Radiolarians	Unclear
Chrysophytes	Brackish influence

Table 4. Interpretation of the non-diatomaceous siliceous microfossils.

4.5. An integrated perspective about the evolution of the biogenic sedimentation

The integrated analysis of the foraminifers, calcareous nannofossils, diatoms and associated siliceous microfossils recorded in the Pecetto di Valenza section, allowed to recognize four main evolutionary stages of biogenic sedimentation (**Fig. 9**) that occurred in an upper slope environment and can be tentatively correlatable with specific precession/insolation phases (**Fig. 10**).

The first stage (**Fig. 9**) was characterized by a silica depleted but productive, cold and well-remixed water column. The remineralization process was very efficient, and likely occurred before the accumulation of the organic matter at the seafloor. This stage might correspond to the transition from precession maxima/insolation minima toward precession minima/insolation maxima (**Fig. 10**).

The second stage (**Fig. 9**) of the biogenic accumulation corresponds to the deposition of the Mn-rich laminated marls and was marked by a considerable productivity in both the upper and deeper water column, with the establishment of a DCM in response to the stratification of the water body, probably under a warmer and humid climate attributable to a phase of precession minima/insolation maxima (**Fig. 10**). The persistence of high productivity conditions both in the upper and deeper waters may have boosted the accumulation of organic matter at the seafloor, in turn favoring the establishment of a dense benthic population. No straightforward evidence of anoxia can be inferred

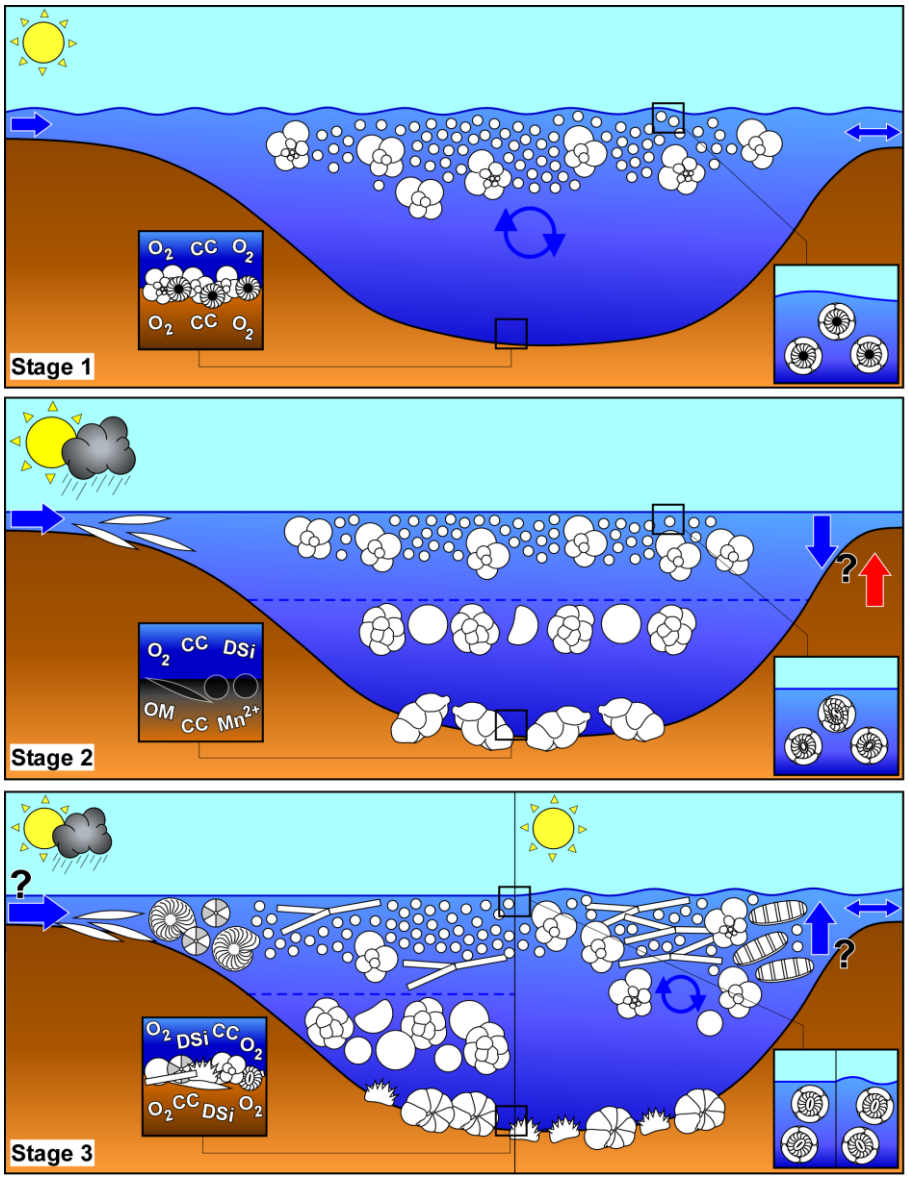
Stage 1
O_2 CC O_2
O_2 CC O_2
Stage 2
O_2 CC DSi
OM CC Mn^{2+}
?
Stage 3
?
?
O_2 DSi CC O_2
O_2 CC DSi O_2

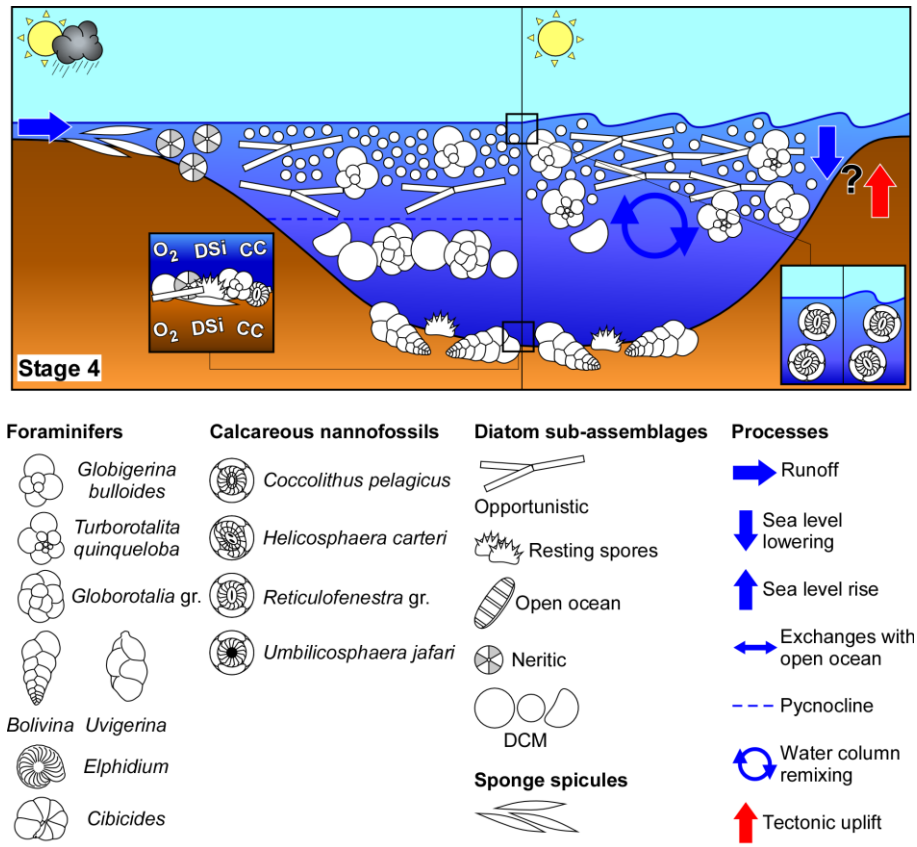

◄▲**Figure 9.** Sketch resuming the four main stages of biogenic sedimentation in the Pecetto di Valenza section. See text for detailed explanations. The black color of the sponge spicules and diatoms in stage 2 indicates their dissolution under conditions of increasing accumulation of organic matter; the different size of the symbol of water column remixing indicates the variable intensity of water column remixing, weaker in stage 3 and stronger in stage 4. For simplicity, among the non-diatomaceous biosiliceous assemblage only the sponge spicules are reported. CC: calcium carbonate. DCM: deep chlorophyll maximum. DSi: dissolved silica. OM: organic matter.

based on of the micropaleontological observations, although the accumulation of Mn oxides suggests a conspicuous build-up of Mn^{2+}, in response to the establishment of reducing conditions in the sediment pore waters during water column stratification (e.g., Robertson et al., 2019). It is possible to hypothesize that once the water column remixing occurred, oxygen repletion favored the precipitation of Mn-oxides. However, it is unclear whether the interplay between stratification/remixing of the

water column and reducing/oxidizing conditions at the seafloor occurred on seasonal scale or pluri-annually, possibly on precessional scale (e.g., Robertson et al., 2019; see also Filippelli et al., 2003, in regard of phosphorus recycling during sapropel deposition). In any case, this may point to a weak restriction of the communications between the basin and the main Mediterranean waters, likely driven by tectonics or eustatic lowering, resulting in the possible enhancement of the climatic forcing of oceanic circulation (e.g., Robertson et al., 2019). The possible role of DCM-forming diatoms in shuttling the organic matter to the seafloor during this stage can be tentatively proposed based on some evidences, but deserves future investigations.

The third stage (**Fig. 9**) represents the onset of the diatomaceous deposition, that probably occurred under an ongoing cooling trend. Remixing and stratification of the water column, respectively favorable to the proliferation of opportunistic and DCM-forming diatoms, became much more frequent, likely in response to the climatic deterioration during the transition from precession minima/insolation maxima to precession maxima/insolation minima (**Fig. 10**). A moderate productivity in the upper water column, probably associated with a good ventilation of the seafloor in turn linked to the still good connection with the Mediterranean water body, prevented a significant accumulation of organic matter and the establishment of a dense benthic population. Hypoxia was probably a very localized and transient phenomenon. It is unclear whether the displacement of epiphytic foraminifers from the shelf area corresponds to a more proximal depositional setting, or a possible increase of downslope transport likely associated with riverine runoff.

The fourth evolutionary stage (**Fig. 9**) of the biogenic sedimentation recognized in the Pecetto di Valenza led to the deposition of the second part of the diatomaceous interval, which reflects an increasing rate of primary productivity, especially in the upper water column; this was likely associated to a cooler climate triggered by the incipient onset of the precession maxima/insolation minima (**Fig. 10**), which in turn favored a more vigorous remixing of the water column. The accumulation of organic matter at the seafloor was probably fostered, favoring the establishment of benthic populations adapted to exploit nutrient-rich and probably less oxygenated environments. Nevertheless, the establishment of extensive and prolonged anoxic conditions can be ruled out, as already suggested by Violanti (1996).

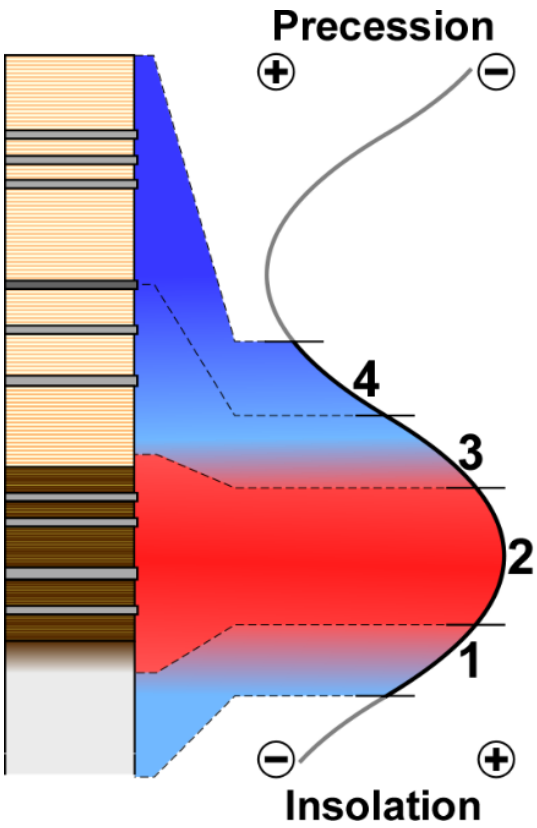

Figure 10. Possible correlation of the Pecetto di Valenza lithological cycle with the precession/insolation curve.

A reduction of the coarser biogenic fraction (epiphytic foraminifers) reworked from the neritic area may suggest both a deepening of the basin or a decrease of downslope transport attributable to runoff. In any case, the continuous occurrence of the finer biogenic fraction with neritic affinity (diatoms and associated siliceous microfossils) suggests the persistence of shelf reworking

during the whole diatomaceous deposition, likely associated to riverine plumes. A possible reduction of the communication with the Mediterranean water body, even in this case potentially linked to tectonic uplift of seaward basin margin or to eustatic lowering, can also be inferred during this stage.

4.6. Comparisons with other Messinian diatomaceous deposits of the circum-mediterranean area

In the overall context of the diatomaceous deposition that took place in the circum-mediterranean area during the Messinian, the Pecetto di Valenza section represents a very peculiar case study.

Considering the Mn-rich laminated marls of Pecetto di Valenza as analogs of sapropelitic sediments, the lithological succession studied herein is similar to that typically recorded in the Central and Eastern Mediterranean, typified by the Metochia section (Gavdos) tripartite cycles consisting of the alternation of a homogenous marl, a thin sapropel and a prominent diatomaceous layer (Pérez-Folgado et al., 2003). For what concerns the diatomaceous assemblage, the dominance of *T. nitzschioides* is a feature shared both by the Pecetto di Valenza and Gavdos diatomites, and indeed by all the other marine diatom-bearing sediments deposited in the Mediterranean area during the late Miocene. However, while at Gavdos the diatomites are characterized by a remarkable accumulation of

Rhizosolenia spp., the Pecetto di Valenza section does not record such a feature. Moreover, the *Chaetoceros* resting spores reach their highest abundances at the top of the Gavdos diatomaceous layers, while they are much more abundant at the base of the Pecetto di Valenza diatomite. In addition, conversely to the diatomaceous deposits of Gavdos, those from Pecetto di Valenza section does not record the establishment of seafloor anoxia (see Pérez-Folgado et al., 2003), as demonstrated by the continuous occurrence of benthic foraminifers. Under this perspective, the Pecetto di Valenza diatomites can be more easily assimilated than those of Sorbas, which according to Pérez-Folgado et al. (2003) accumulated under oxygenated conditions. However, the Sorbas diatomites occur within a quadripartite cycle composed by a thick sapropel, an intermediate marl, a thin diatomaceous layer and an upper marl (Pérez-Folgado et al., 2003). Therefore, it seems that the Pecetto di Valenza diatomaceous sediments occupy an intermediate "position" between those from Gavdos and Sorbas. Moreover, the planktonic foraminifer dataset confirms that a temperature gradient was present between the Piedmont and southern Mediterranean, where the pre-evaporitic successions record considerably higher percentages of warm water taxa, although concentrated in levels correlated to insolation maxima (Blanc-Valleron et al., 2002, Sierro et al. 2003). Indeed, the planktonic foraminifer assemblages of the Pecetto di Valenza section find a better analog in the present-day Atlantic Ocean rather than in the Mediterranean (Kallel et al., 2000).

5. Conclusions

The four main stages of biogenic sedimentation that occurred during the late Miocene in certain sectors of the Monferrato Arc structural high were characterized by a wide variability of both water column and seafloor conditions. The water column configuration evolved from well-remixed to periodically stratified, and the seafloor from well-oxygenated to slightly oxygen-depleted, but definitely not anoxic. Even if no data are available from the upper homogeneous marls, it is possible to hypothesize that upper marls witness water column and seafloor conditions in line with their lower analogue, i.e. a well-remixed water column and an oxygenated seafloor.

Caution is needed in attributing the onset of the diatomaceous deposition to the intensification of upwelling or to the establishment of oxygen-depleted conditions at the seafloor. Indeed, the lower part of the diatomaceous layer does not point to similar conditions. A more complex scenario, characterized by the interplay between riverine-induced fertilization, stratification and overturn of the water column, with this latter hardly controlled by a vigorous coastal upwelling, can be proposed.

Beside the use of foraminifers, calcareous nannofossils and diatoms, other siliceous microfossils constitute a promising tool for the reconstructions of the Mediterranean paleoceanographic dynamics during the late Miocene. Comparative

studies from other coeval, circum-mediterranean diatom-bearing localities are urgently needed.

Finally, it is worth to note that the bulk approach to micropaleontological investigation herein proposed has intrinsic limits, related to the main sedimentological feature of the studied material, especially their laminated fabric. Indeed, if each lamina reflects peculiar sub-annual paleoceanographic conditions (**Fig. 11;** see in particular **Chapter 2**), sediment homogenization may easily lead to biased results; the non-uniform scraping of the surface of the investigated samples during smear slide preparation, may add further biases, by intensifying or weakening the signal provided by some clusters of laminae; for example, as noted above the occurrence of poorly preserved specimens may be underestimated (**Fig. 11**). These aspects may account for the observed incongruences between the different signals, both within the same group of microfossils and especially between them. Therefore, in order to better address the paleoceanographic significance of the marine laminated sediments, it is useful to couple the bulk analysis with in-situ observations.

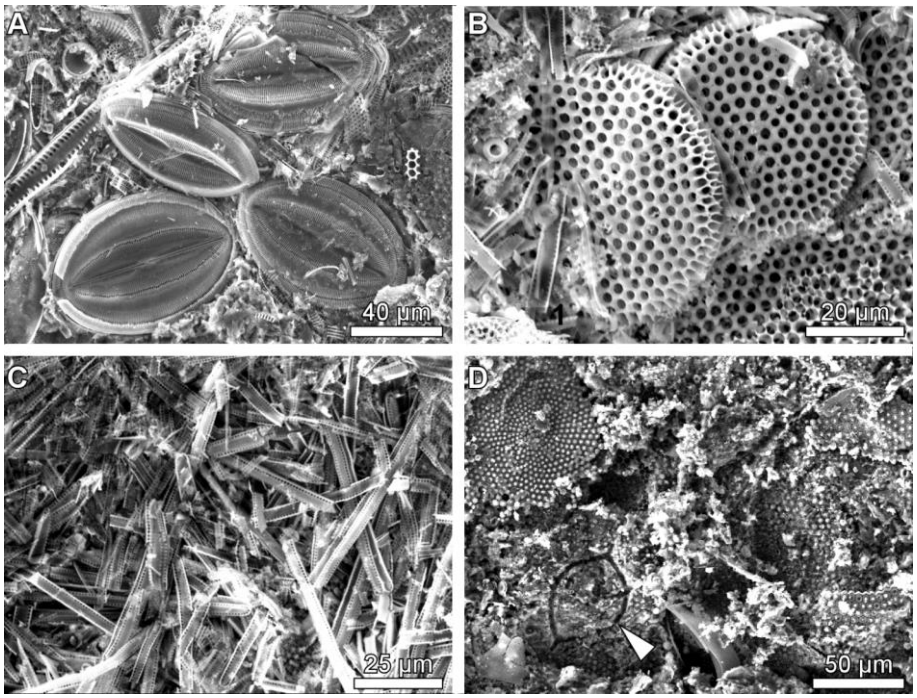

Figure 11. SEM observation of the Pecetto di Valenza laminated sediments, potentially recording sub-annual paleoceanographic signals. Diatomaceous interval: A) accumulation of benthic diatoms; B) concentration of specimens of *Coscinodiscus*; C) needle-like meshwork of *Thalassionema nitzschioides*; Mn-rich interval: D) diagenetically-altered centric diatoms; arrowhead points to a mold of the silicoflagellate *Mesocena* left on a diatom valve.

CHAPTER 2 - THE UPPER MIOCENE DIATOMACEOUS SEDIMENTS OF THE NORTHERNMOST MEDITERRANEAN REGION: A LAMINA-SCALE INVESTIGATION OF AN OVERLOOKED PALEOCEANOGRAPHIC ARCHIVE[†]

The studies concerning the diatomaceous sediments deposited in the Mediterranean area during the late Miocene essentially addressed the well-preserved macrofossil (e.g., Carnevale, 2004c, 2006; Carnevale and Bannikov, 2006; Carnevale and Pietsch, 2006; Gaudant, 2008) and microfossil contents (e.g., Jurkschat et al., 2000; Blanc-Valleron et al., 2002; El Ouahabi et al., 2007; Mansour et al., 2008) or the tuning of the cyclical stacking pattern to the astronomical periodicities, assuming that cyclicity was controlled by astronomically forced climate changes (e.g., Hilgen and Krijgsman, 1999; Pérez-Folgado et al., 2003; Sierro et al., 2003). Notably, intensified upwelling currents, increased salinity prior to the onset of the Messinian salinity crisis, and extensive build-up of bottom water anoxia have been proposed to explain the onset of the enhanced proliferation of diatoms across the entire Mediterranean basin and the laminated fabric of the diatomaceous sediments (e.g., Selli, 1954; Parea and Ricci-Lucchi, 1972; Sturani and Sampò, 1973). However, recent investigations of diatomaceous sediments from extra-mediterranean basins cast doubt upon the unequivocal model for the

[†] This chapter is based on Pellegrino, L., Dela Pierre, F., Jordan, R.W., Abe, K., Mikami, Y., Natalicchio, M., Gennari, R., Lozar, F. and Carnevale, G. (2020). The upper Miocene diatomaceous sediments of the northernmost Mediterranean region: A lamina-scale investigation of an overlooked paleoceanographic archive. Sedimentology (doi:10.1111/sed.12748).

depositional interpretation of laminated diatomites, which are not consistently related to upwelling, hypersalinity or the establishment of deep anoxic conditions (e.g., White et al., 1992; Kemp and Baldauf, 1993; King et al., 1995; Pike and Kemp, 1999; Pilskaln and Pike, 2001; Gariboldi, 2015; Kemp and Villareal, 2018; Koizumi and Yamamoto, 2018).

A significant improvement of the depositional models of the late Miocene diatomaceous event that occurred in the Mediterranean may be achieved using an SEM-based, non-destructive morphological approach. This type of approach has been successful in interpreting the paleoceanographic significance of many diatom-bearing laminated sediments of different ages worldwide, allowing for the identification of single, geologically instantaneous (annual to sub-annual) depositional processes (for an exhaustive review see Schimmelmann et al., 2016). The main advantages of this method are: i) to investigate the paleoceanographic signal recorded in each lamina, without introducing biases potentially derived from sediment homogenization and manipulation (e.g., acid cleaning), and hence avoiding the alteration of the original taphocoenosis; and ii) to discriminate small-scale but significant processes affecting the fine-grained sediments (e.g., grading and microbioturbation; O'Brien, 1996, Pike et al., 2001).

The present chapter provides the first lamina-scale, SEM-based study of the upper Miocene diatomaceous sediments from the Pecetto di Valenza section, in order to: i) describe the micro-nannofacies and taphocoenosis preserved in their lower

portion, so that the processes responsible for the onset of diatomaceous deposition can be unraveled; ii) propose an interpretative model for their annual accumulation; and iii) shed light on the mechanisms underlying the biosiliceous sedimentation at the northernmost offshoot of the Mediterranean basin during the late Miocene.

1. The Pecetto di Valenza diatom-rich unit

The diatom-rich unit studied herein (**Fig. 12**) is characterized by a fine alternation of whitish and pale- to dark-brown laminae (**Figs. 13**), frequently interrupted by cm-thick, silty-to-sandy grayish layers (**Figs. 12A** and **13C**). The latter display sharp lower contacts, convoluted bedding, soft sediment deformation structures and ripples, and are typically overlain by thicker, pale-brownish, fine-grained layers (**Fig. 13C**) that are locally characterized by plane-parallel, whitish, mm-long strings interpreted as clasts of cohesive diatom-rich sediments (Chang and Grimm, 1999).

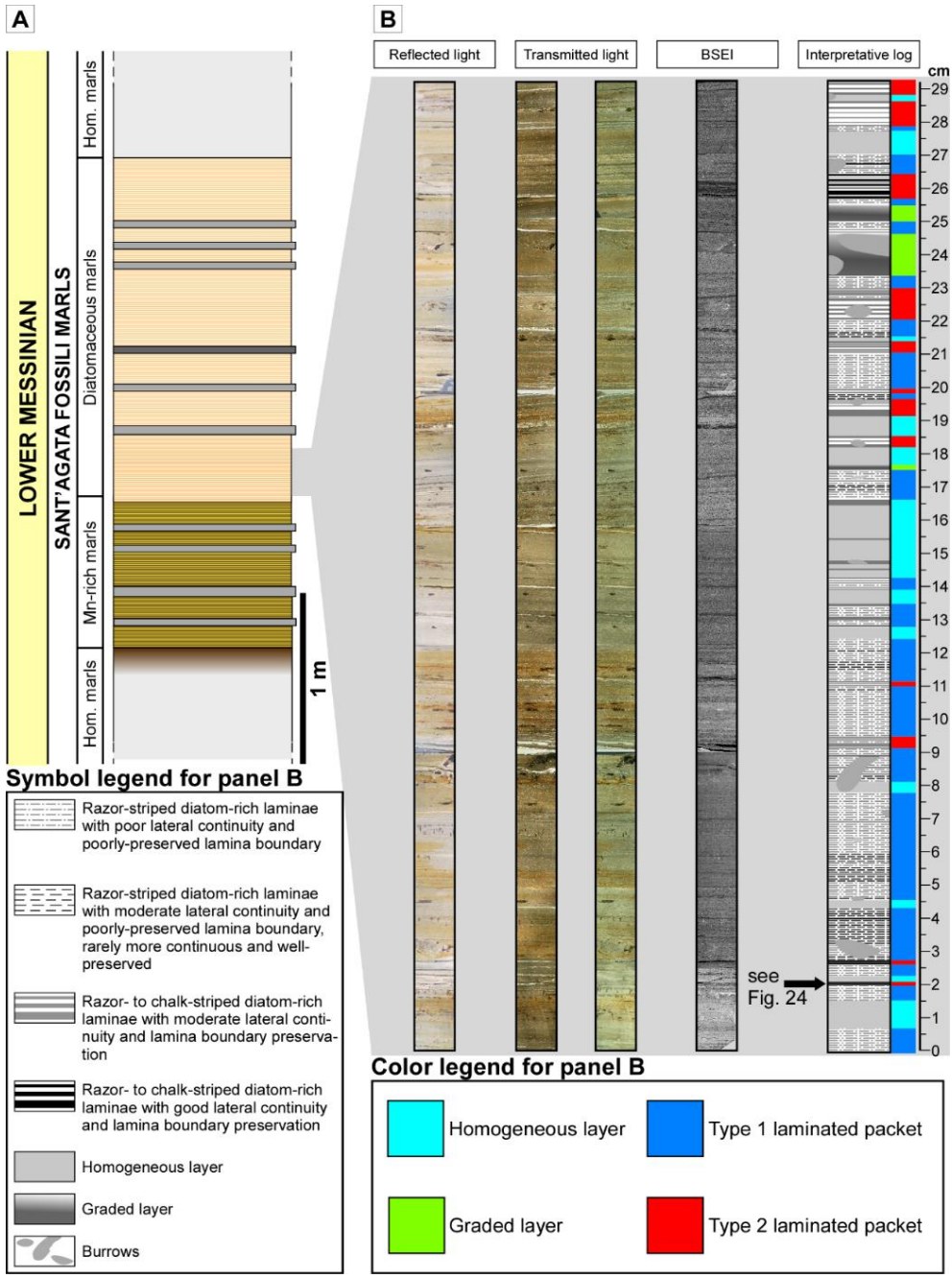

Figure 12. The Pecetto di Valenza section. A) Simplified stratigraphic column. Note the transitional contact between the lower homogeneous marls and the Mn-rich marls. Sandy layers interbedded with Mn-rich and diatomaceous marls are shaded in pale gray, while the massive layer in the diatomaceous marls is reported in dark gray. B) Photomosaic of the studied section (lower portion of the diatomaceous marls) in reflected and transmitted light (left: parallel nicols; right: crossed nicols) and backscattered electron imaging (BSEI). Note that the homogeneous layers may contain isolated diatom-rich laminae. The terminology used to describe laminae and facies is reported in Tables 5 and 7.

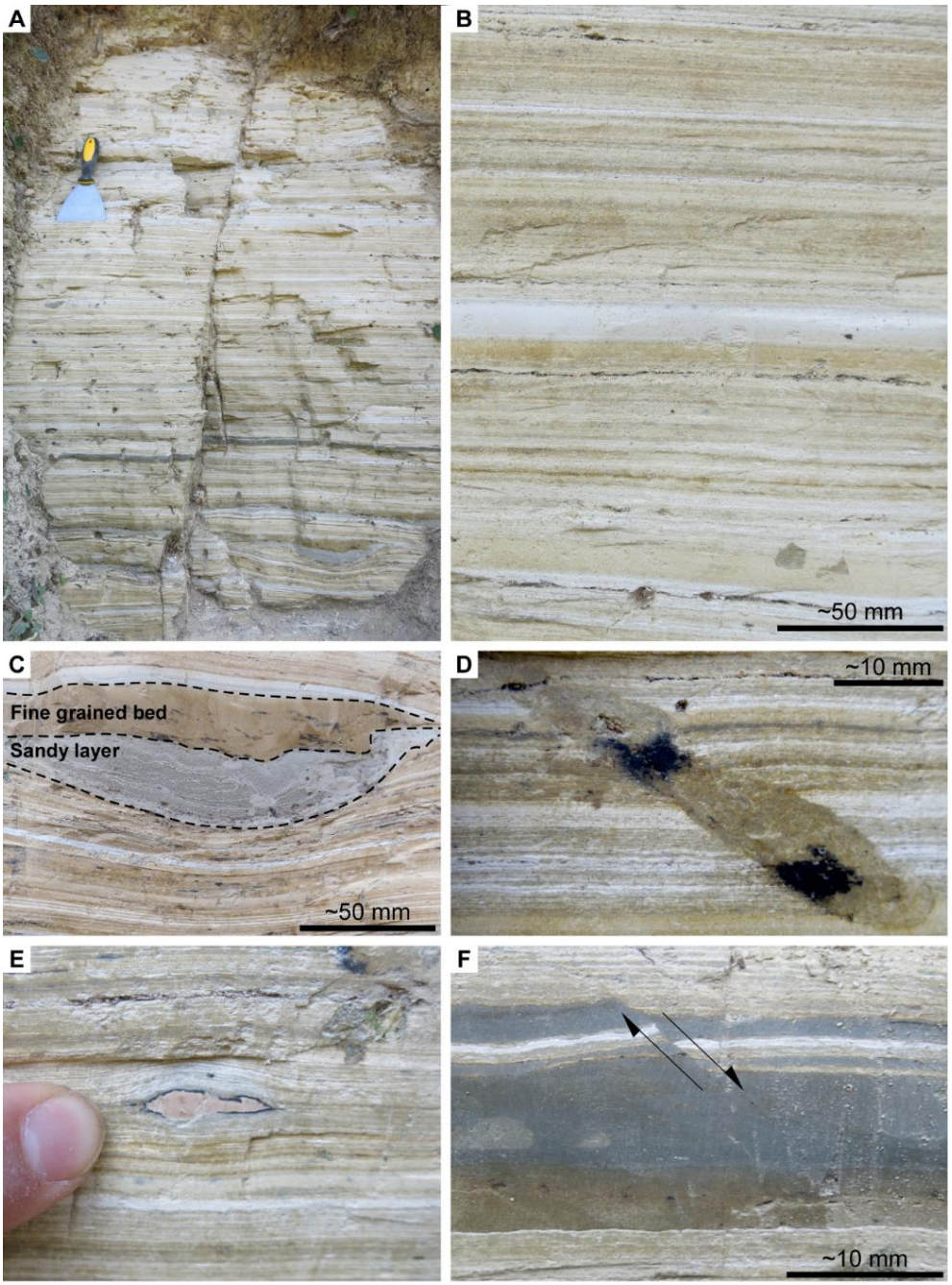

Figure 13. Outcrop-scale images of the Pecetto di Valenza diatom-rich unit. A) Overview of the diatom-rich unit. B) Detail, showing the alternation of pale and dark laminae. C) Sandy layer overlain by a fine-grained layer; note the convoluted laminae in the sandy layer. D) Burrow in the laminated layers; note the blackish spots. E) Pinkish phosphatic nodule embedded within a laminated layer; note the presence of a blackish rim. F) Normal fault in the massive muddy layer.

Transversal, oblique and plane-parallel burrows belonging to the ichnogenera *Planolites* and *Thalassinoides* are present in both the diatomaceous and sand-rich layers (**Fig. 13D**). Scattered pinkish ellipsoidal phosphatic nodules, ranging in size from some mm to a few cm, were also observed (**Fig. 13E**). At about 75 cm from the base of the diatomaceous unit, the laminae are abruptly interrupted by a ~1.5 cm-thick, dark massive muddy layer (**Fig. 13F**), characterized by an erosive lower contact with cut and fill and flame structures. Both normal and inverse synsedimentary faults locally affect the interval (**Figs. 13F**).

2. Material and methods

Before sampling, the outcrop was carefully cleaned and scraped with a spatula. Then, using a "U" shaped steel box, a ~30 cm-thick section was sampled from the lower part of the diatomaceous interval exposed along the crossroad 'Strada Molina' (44°58'50.2''N, 8°40'30.8''E), close to the village of Pecetto di Valenza (**Fig. 12**).

Half of the sample was vacuum resin-embedded and slabbed perpendicularly to the bedding plane in order to obtain 9 polished thin sections representing a continuous record of the studied interval. The thin sections were subsequently studied both with reflected and transmitted light, for comparison with the

backscattered electron imagery (BSEI). The polished thin sections were then carbon-coated and BSEI observations were performed with a JEOL JSM IT300LV scanning electron microscope (SEM) at an operating voltage of 15kV. Diatom-rich laminae, composed of highly porous frustules filled with carbon-based resin, are characterized by an average low atomic number and therefore by a low backscatter coefficient, resulting in a dark signal; less porous laminae enriched in terrigenous particles have an average high atomic number and therefore a high backscatter co-efficient, resulting in a bright signal (see Krinsley et al., 1998).

A low magnification (50x) photomosaic of each polished thin section was automatically acquired using the software AZtec (Oxford Instruments) and used as a general map for the identification of the major faciological components. These components were manually investigated in detail at higher magnification. Using a dissecting microscope, the non-consolidated counterpart of the sample was carefully split parallel to the bedding plane using a scalpel along selected intervals. The resulting sub-samples were mounted on aluminum stubs for topographic investigations. The sub-samples were first investigated under reflected light for subsequent comparison with electron imagery. Secondly, they were carbon coated and observed in secondary electron (SE) or backscattered modality. Occasionally, qualitative energy dispersive spectroscopy (EDS) was performed on both thin sections and stubs.

Laminated diatomaceous sediments in thin section were described using terminology proposed by Chang et al. (1998) that was partially modified **(Tab. 5)**. A detailed description of each micro-nannofacies, from the single lamina types to their arrangement in the laminated packets, is reported below and summarized in the **Tabs 6** and **7**. Diatom abundance was roughly estimated, following the approach used by Brodie and Kemp (1994), Bull and Kemp (1995) and Pike and Kemp (1996).

3. Results

Under reflected light, the section can be distinguished into mm- to cm-thick, whitish-grayish to reddish laminated packets that are interrupted by brownish to pale-gray non-laminated intervals (**Fig. 12B**). Laminated packets comprise alternating mixed terrigenous-biogenic laminae and diatom-rich laminae. Additional components include burrows (**Fig. 12B**), μm- to mm-thick opal-rich aggregates and mixed pelletal structures.

Category	Descriptor	Specifications
Thickness	Razor-striped	<0.2 mm
	Pin-striped	0.2-1.0 mm
	Chalk-striped	1.0-1.5 mm
Spacing	Closely-spaced	>10 laminae/cm
	Moderately-spaced	5-10 laminae/cm
	Widely-spaced	<5 laminae/cm
Bimodality	High bimodality	Marked contrast in grayscale (BSEI observation)
	Moderate bimodality	Moderate contrast in grayscale (BSEI observation)
	Low bimodality	Small contrast in grayscale (BSEI observation)
Domination	Mud-dominated	>1.5:1 mud or detritus
	Diatom-dominated	>1.5:1 biosilica
	Subequal	~1:1
Cyclicity	Couplet	Single pair of dark (mixed terrigenous-biogenic) and light (diatomaceous mud or diatom ooze) lamina.
	Triplet	Sequence of three lamina types (mixed terrigenous-biogenic, diatomaceous mud and diatom ooze).
	Packet	Suite of couplets situated between non-laminated intervals. Triplet observed in one case (Fig. 24)
Continuity	Good	Laterally continuous lamina
	Moderate	Few interruptions occurring along the lamina
	Poor	Many interruptions occurring along the lamina
Lamina boundary preservation	Good	Well-defined lamina boundaries
	Moderate	Moderately-defined boundaries
	Poor	Poorly-defined lamina boundaries

Table 5. Terminology adopted for description of single lamina types and their arrangement in laminated packets. Modified from Chang et al. (1998).

3.1. Mixed terrigenous-biogenic laminae

These laminae (**Figs 14** and **15; Tab. 6**) range in thickness from razor- to chalk-striped. They do not show clear erosional bases or grading. Under reflected light, these laminae are darker than their diatom-rich counterparts, ranging in color from grayish to pale-brown and yellowish (**Fig. 14A**). With transmitted light (**Figs. 14B** to **D**) and under BSE (e.g., **Figs. 14E-F**) the mixed terrigenous-biogenic laminae appear bright. The high birefringence observed with crossed nicols points to an enrichment in calcite and clays, confirmed by BSEI observations and EDS analysis. The matrix consists of abundant calcareous nannofossils, mostly occurring as single coccoliths and more rarely as complete coccospheres, mixed with clayey particles. Such biogenic-detrital 'mud' embeds a heterogeneous, coarse component represented by: i) silt-sized terrigenous grains (**Figs. 14E** to **G**); ii) isolated or clustered hexactinellid and demosponge spicules (mostly monoaxons) and rarer microscleres (**Figs. 14G-H**); iii) aggregates composed of silty particles, foraminifers and sponge spicules, aligned parallel to the bedding plane (**Figs. 14H** to **J**); iv) abundant and variably preserved planktonic (globigerinids; **Figs. 14D, I** and **15A**) and benthic-epiphytic foraminifers (e.g., Cibicididae, Uvigerinidae, Bolivinidae; **Figs. 14E, 15B** and **C**); v) scattered, randomly oriented centric diatoms (**Figs. 14E-F**); and vi) radiolarians (mainly polycistine spumellarians; **Fig. 15D**). The topographic observation of these laminae confirms the low abundance of well preserved diatoms

(**Fig. 15E**). However, the frustules of inshore taxa can be recognized, mostly represented by the robust planktonic genus *Actinoptychus* (*A. senarius* and rarer *A. splendens*) and by the epiphytic genera *Arachnoidiscus* and *Isthmia* (**Figs. 15A, D, F** to **I**). *Isthmia* specimens occur as valves and girdle bands still joined together, and in exceptional cases as vestiges of larger colonies (Round, 1984). The inshore diatom assemblage consists of taxa belonging to the genera *Cocconeis*, *Grammatophora* (notably *G. oceanica*), *Navicula*, *Rhabdonema* (notably *R. adriaticum*), *Synedra*, *Surirella* and *Biddulphia* (**Fig. 15J**). The planktonic, oceanic component is mostly represented by the genera *Asterolampra* (particularly *A. acutiloba*, with only the inner, star-shaped hyaline area preserved), *Chaetoceros* (resting spores), *Coscinodiscus*, *Hemidiscus* (notably *H. cuneiformis*) and *Thalassiosira*. Very rare specimens of the genus *Hemiaulus* have been also observed. Relatively well-preserved rafts or larger aggregates (discussed below) of the planktonic pennate diatom *Thalassionema nitzschioides* have been observed, but this taxon commonly occurs as etched fragments unevenly distributed on the lamina surface.

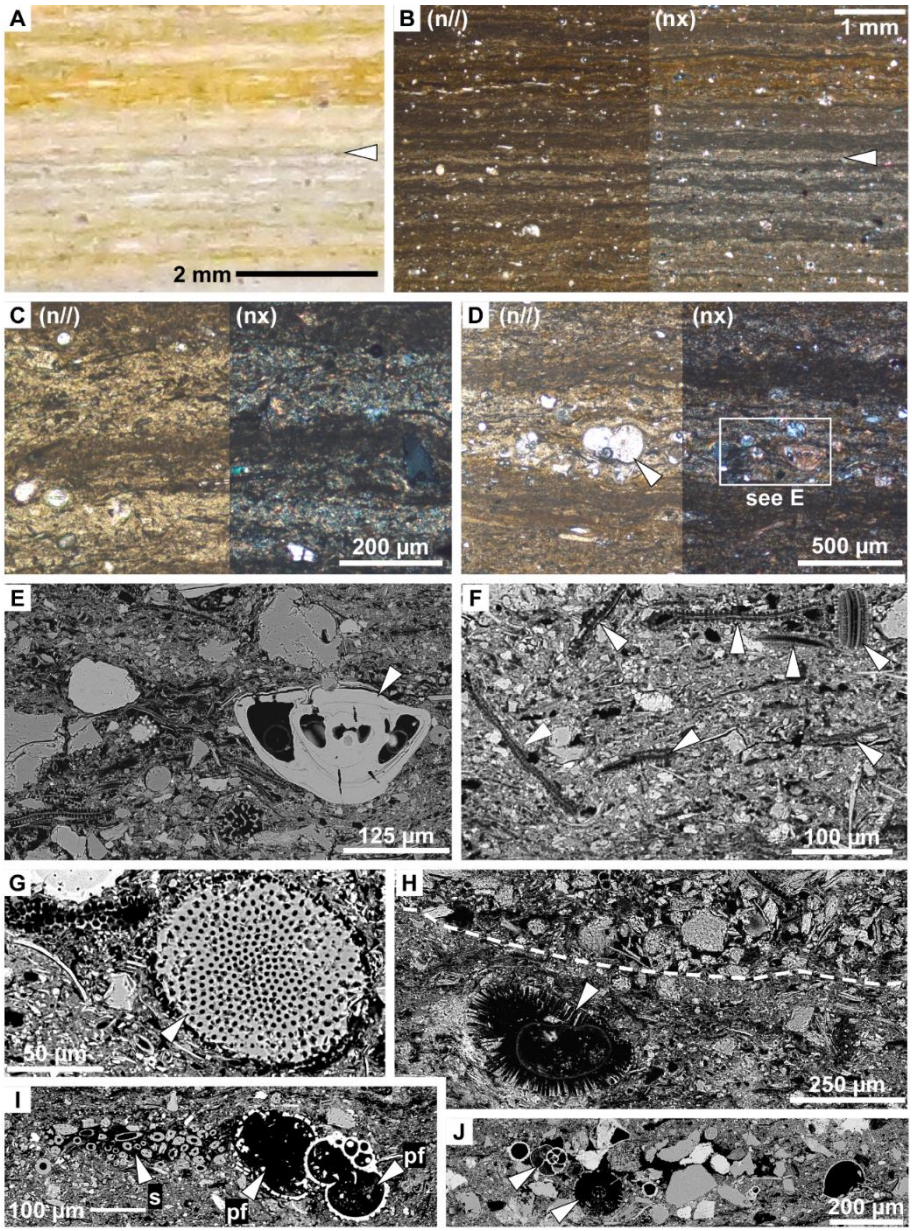

Figure 14. Mixed terrigenous-biogenic laminae in polished thin section. A) RL micrograph. Alternation of mixed terrigenous-biogenic (dark) and diatom-rich (pale) laminae; arrowhead points to a mixed terrigenous-biogenic lamina. B) TL micrograph. Same area shown in A; note the high birefringence of the mixed terrigenous-biogenic laminae; arrowhead points to the same mixed terrigenous-biogenic lamina highlighted in A. C and D) TL micrographs. Alternation of mixed terrigenous-biogenic and diatom-rich laminae; in D, the arrow points to a planktonic foraminifer (globigerinid). E) BSEI micrograph. Detail of D: specimen of *Cibicidoides* sp. (arrowhead) associated with terrigenous grains and scattered diatom frustules. F) BSEI micrograph. Randomly oriented centric diatom frustules (arrowheads), dispersed in a fine-grained, bright matrix. G and H) BSEI micrographs. Sponge microscleres (arrowheads); in H, an aggregate of terrigenous grains is highlighted (above the white dotted line). I) BSEI micrograph. Aggregate of sponge ►►

spicules (s) and planktonic foraminifers (pf). J) BSEI micrograph. Aggregate of terrigenous and skeletal grains (arrowheads). RL: reflected light. TL: transmitted light. n//: parallel nicols; nx: crossed nicols.

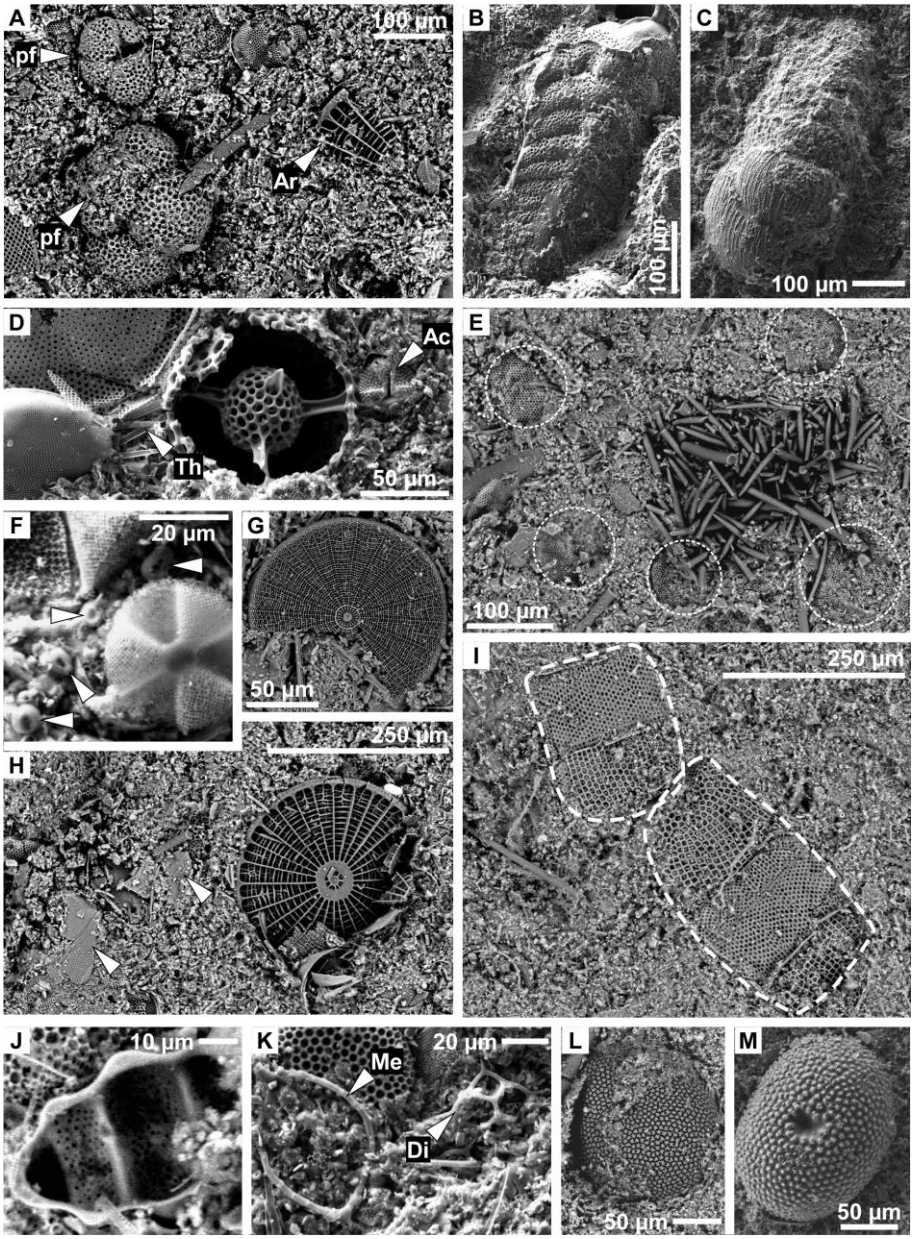

Figure 15. SEM topographic observation of mixed terrigenous-biogenic laminae. A) Planktonic foraminifers (pf) and fragments of the epiphytic diatom *Arachnoidiscus* sp. (Ar). B-C) Benthic foraminifers (*Bolivina* sp. and *Uvigerina* sp., respectively). D) Polycistine radiolarian (center); note a small specimen of *Actinoptychus senarius* (Ac) and scattered specimens of *Thalassionema nitzschioides* (Th). E) Etched diatom valves (white dotted circles) and a dense aggregate of ►►

sponge spicules. F) Meroplanktonic diatom *A. senarius* (arrowheads point to coccoliths). G to I) Epiphytic diatoms (*Arachnoidiscus* sp. in G and H; *Isthmia* sp. in I, highlighted by white dotted lines); note in H the fine-grained matrix including calcareous nannofossils and terrigenous grains (arrowheads). D) Epiphytic diatoms (*Isthmia* sp.; white dotted lines). J) Fragment of a benthic diatom (*Biddulphia* sp.). K) Warm-water silicoflagellates (*Mesocena* sp., Me; *Dictyocha* sp., Di). L-M) Sponge sterrasters.

Topographic observations included silicoflagellates, namely *Dictyocha* spp., *Distephanopsis* spp. and *Mesocena* sp., *Paramesocena* sp. and generally less common *Stephanocha speculum* (**Fig. 15K**). Additional components included endoskeletal dinoflagellates (e.g., *Actiniscus pentasterias*), ebridians and chrysophycean stomatocysts. Among the spongolitic component, besides the dominant robust monoaxons (**Fig. 15E**), well-preserved geodiid sterrasters are present (**Figs. 15L-M**).

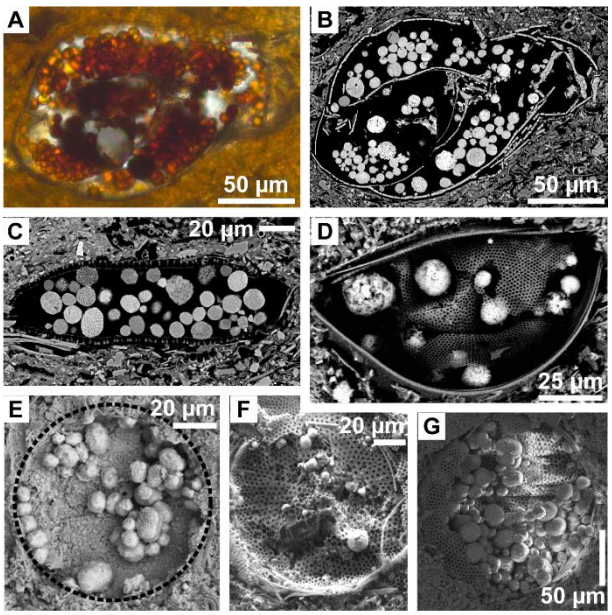

Figure 16. Biogenic remains filled with framboidal pyrite from mixed terrigenous-biogenic laminae, in polished thin section and observed parallel to the bedding plane. A) TL micrograph. Foraminifer. B) BSEI micrograph. Same foraminifer reported in A. C to G) SEI micrographs. Variously preserved centric diatoms; in E the frustule is completely dissolved (black dotted line indicates the mold). TL: transmitted light.

Framboidal pyrite mostly infills the chambers of foraminifer tests (**Figs. 16A-B**) and the frustules of some centric diatoms (**Figs. 16C** to **G)**.

3.2. Diatom-rich laminae

Under reflected light, the white color of the best-preserved, more continuous diatom-rich laminae distinguishes them from the mixed terrigenous-biogenic laminae. However, the identification of the diatom-rich laminae is not always obvious, especially if they are razor-striped and poorly continuous. In such cases, these laminae can be more confidently identified with transmitted light and BSEI; due to their opal content and high porosity, these laminae appear darker than the mixed terrigenous-biogenic laminae. According to their taxonomic composition, two main subtypes can be distinguished (**Tab. 6**): i) diatomaceous mud laminae (**Figs. 17-18**) and ii) diatom ooze laminae (**Figs. 19-20**).

3.2.1. Diatomaceous mud laminae

These are razor-striped laminae, with a few exceptions characterized by moderate to poor lateral continuity and poor preservation of the lamina boundaries (**Figs. 17A** to **G**). In thin section, these laminae are characterized by valves of centric taxa (**Figs. 17H-I**) intermingled with pennate diatoms that do not form continuous and well-defined mats. When observed parallel to the bedding plane, the assemblage appears dominated by *Coscinodiscus* spp. (notably *C. marginatus*, *C. radiatus*, *C.*

oculus-iridis; e.g., **Figs. 18A** to **D**), commonly associated with *Hemidiscus cuneiformis* (**Figs. 18C-D**) and large thalassiosiroids (e.g., *Thalassiosira leptopus*; **Fig. 18C**). In some cases, the valves of *Coscinodiscus* spp. cover the entire surface of the lamina (**Fig. 18A**). Valve preservation is poor, and evidence of maceration and partial or complete opal dissolution are often observed. In many cases the original presence of the valves can be inferred by the molds in the matrix, which is characterized by abundant calcareous nannofossils (**Fig. 18E**). In this regard, very large centric valves likely of the genus *Coscinodiscus* (likely *C. asteromphalus* or *C. wailesii*) often show evidence of dissolution resulting in a characteristic 'crescent moon' shape (**Fig. 18D**). The occurrence of *T. nitzschioides* is patchy (**Fig. 18E**), rarely abundant enough to cover significant portions of the lamina surface. The ancillary biogenic component is represented by inshore or oceanic diatoms (e.g., *Asterolampra acutiloba*; **Fig. 18F**), aggregates of *Chaetoceros* resting spores (**Fig. 18G**), sponge spicules, scattered foraminifers, radiolarians and silicoflagellates (**Fig. 18H**), as already observed in the mixed terrigenous-biogenic laminae.

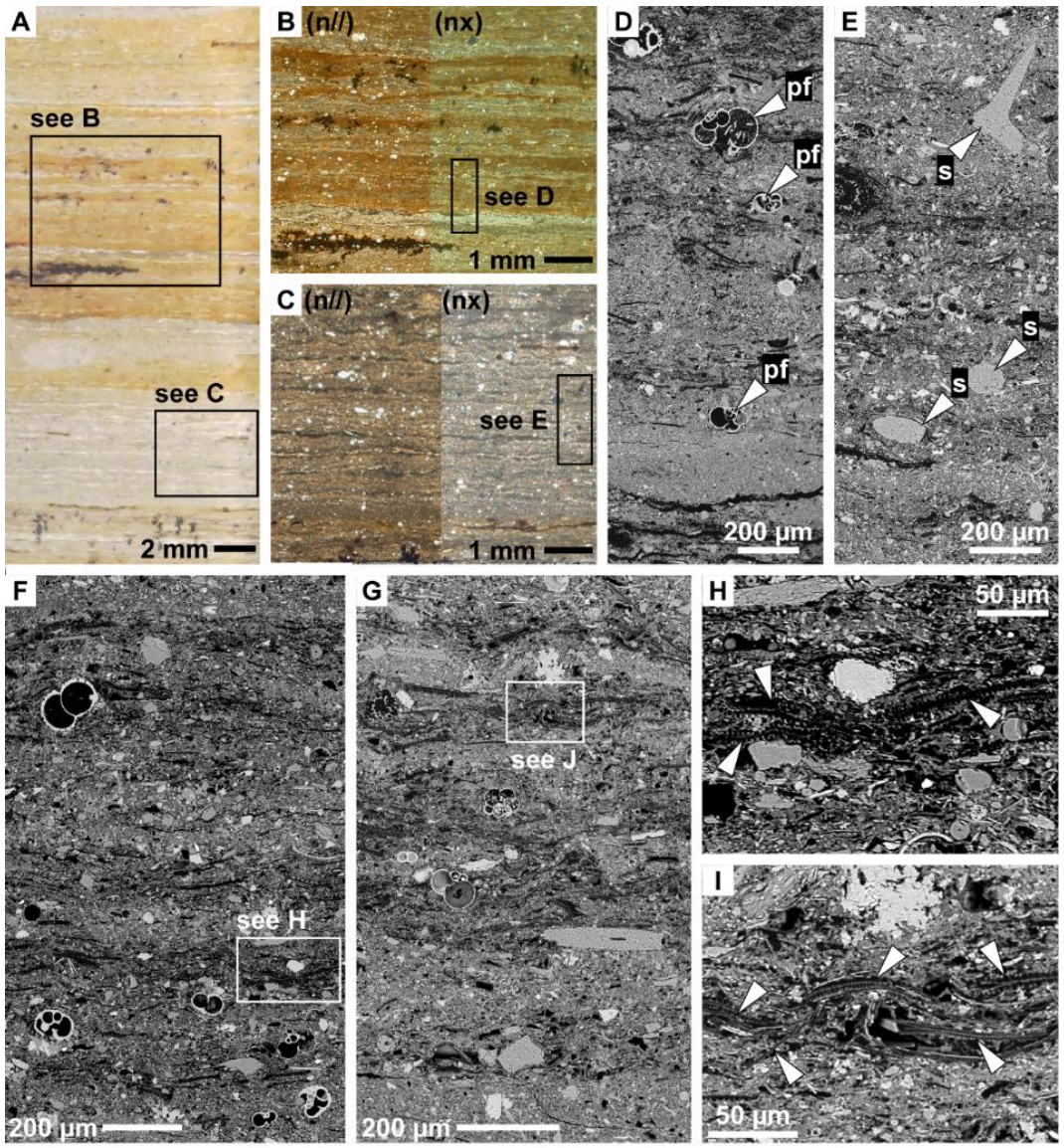

Figure 17. Diatomaceous mud laminae in polished thin section. A) RL micrograph. Type 1 laminated packet. Whitish colored, discontinuous razor-striped diatomaceous mud laminae alternating with grayish mixed terrigenous-biogenic laminae. In the upper half a reddish halo hampers the distinction of the two lamina types. B and C) TL micrographs. Details of A: the diatomaceousmud laminae are darker than the mixed terrigenous-biogenic laminae. D and E) BSEI micrographs. Details of B and C: the diatomaceous-mud laminae are dark; note the coarse biogenic components, such as planktonic foraminifers (pf) and sponge spicules (s). F and G) BSEI micrographs. Alternation of dark diatomaceous mud and bright mixed terrigenous-biogenic laminae. H and I) BSEI micrographs. Details of two diatomaceous mud laminae highlighted in F and G (white rectangles), respectively; arrowheads point to the valves of centric diatoms. RL: reflected light. TL: transmitted light.

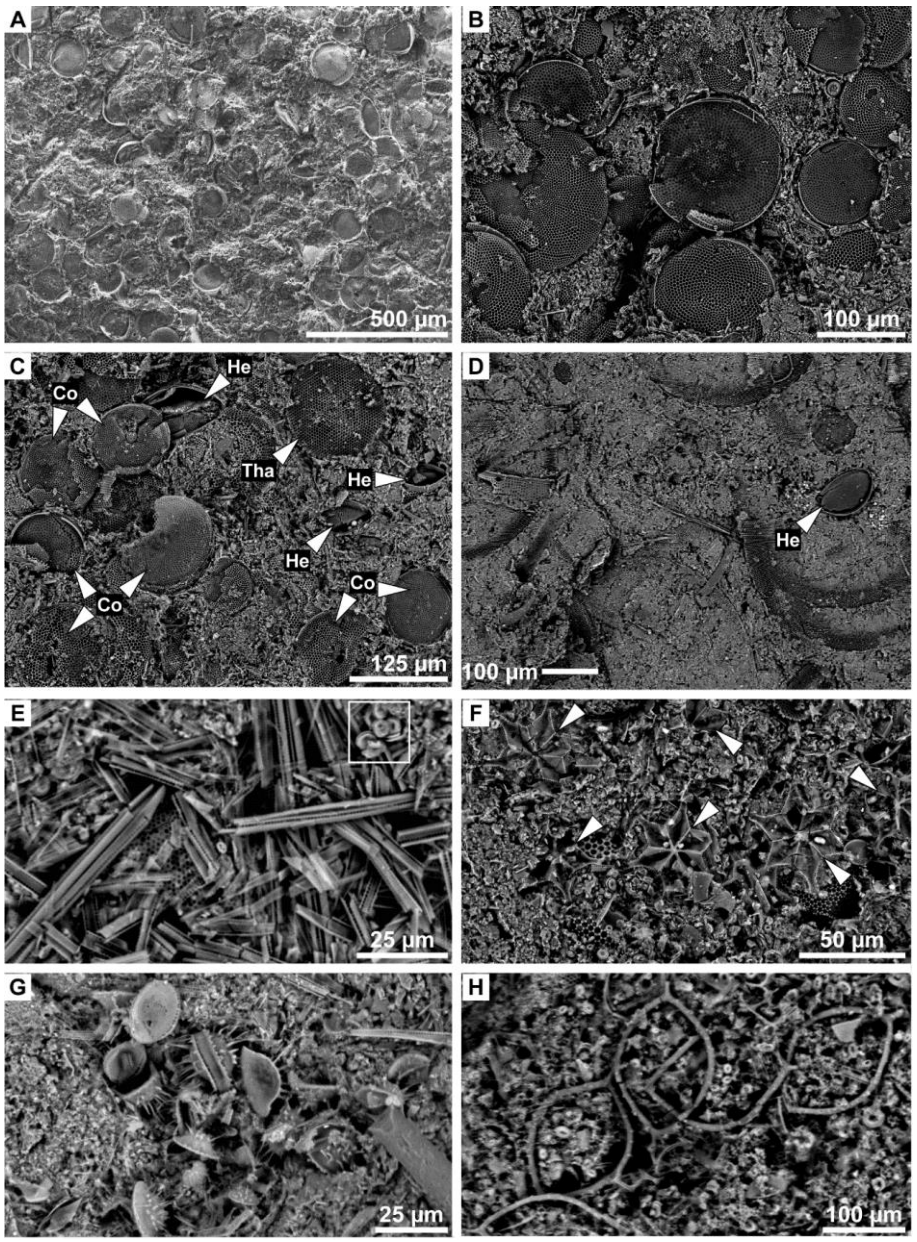

Figure 18. SEM topographic observation of diatomaceous mud laminae. A and B) Lamina surface covered by the valves of centric diatoms (*Coscinodiscus* spp.). C) Assemblage dominated by *Coscinodiscus* spp. (Co), with subordinated *Hemidiscus cuneiformis* (He) and a large thalassiosiroid (Tha); note the different degree of preservation of diatom valves. D) Very large centric frustules preserving only the marginal portion of the valve surface ('crescent moon' pattern); note a specimen of *H. cuneiformis* (He). E) Cluster of valves of *Thalassionema nitzschioides*; the square highlights a small cluster of coccoliths. F) Cluster of *Asterolampra acutiloba* (arrowheads), with only the central, star-shaped hyaline area preserved. G) *Chaetoceros* resting spores. H) Cluster of warm-water silicoflagellates (*Mesocena* sp.).

3.2.2. Diatom ooze laminae

These consist of razor- to chalk-striped laminae with good lateral continuity and moderate to good preservation of the lamina boundary (**Figs. 19A** to **D**). Overall, these laminae are dominated by frustules of Thalassionemataceae, forming uniform mats entrapping subordinated biogenic and lithogenic components (e.g., **Figs. 19E-F**). Observations of lamina surface confirm the considerable amount of closely entangled frustules of pennate diatoms, dominated by *Thalassionema nitzschioides*, (**Figs. 20A** to **C**). Thus, these laminae can be considered as almost monospecific diatom oozes. Grazing and dissolution of diatom frustules is evident (e.g., **Fig. 20D**), although at a more limited degree than in the other two lamina types. Inshore diatoms are absent to very rare, even though an accumulation of naviculoid diatoms has been recognized in the upper part of the section (e.g., **Fig. 20E**) where other pennate diatoms (e.g., *Denticulopsis* spp., *Nitzschia praereinholdii*, *Rouxia californica*) are also more represented, but always occur within the *Thalassionema*-rich oozes (e.g., **Figs. 20F** to **G**).

The subordinate components of these laminae consist of scattered frustules of *Coscinodiscus* spp., small thalassiosiroids and *Chaetoceros* resting spores (e.g., **Fig. 20H**), silicoflagellates (mainly *Stephanocha speculum*), isolated radiolarians (e.g., **Fig. 20I**), scarce calcareous nannofossils, ebridians and endoskeletal dinoflagellates, pelletal structures (see below) and scattered silt-sized grains.

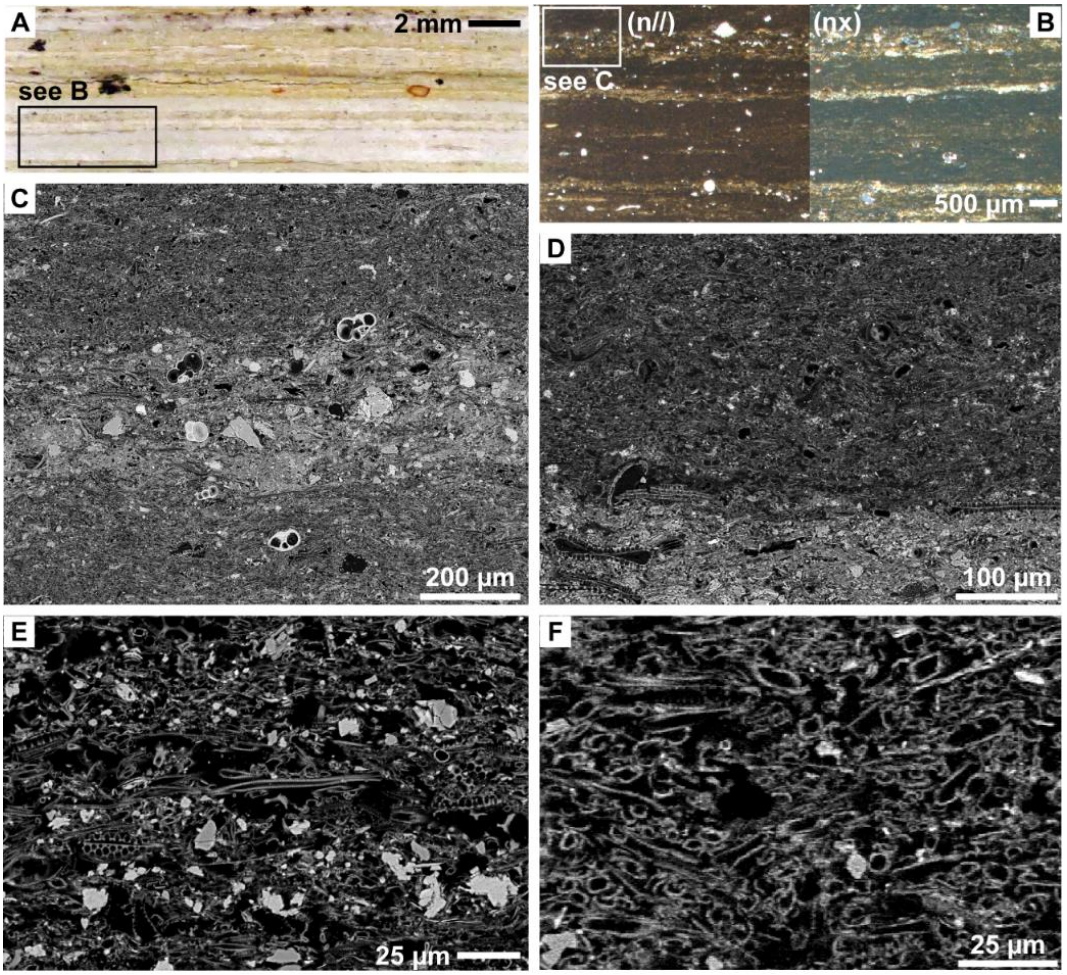

Figure 19. Diatom ooze laminae in polished thin section. A) RL micrograph. Type 2 laminated packet characterized by continuous, pin- to chalk-striped white diatom ooze laminae. B) TL micrograph. Detail of A: diatom ooze laminae are darker than the mixed terrigenous-biogenic laminae. C) BSEI micrograph. Detail of B: note the accumulation of diatom frustules and the stark grayscale contrast between the central, mixed terrigenous-biogenic lamina and the diatom ooze laminae above and below. D) BSEI micrograph. Sharp contact between a mixed terrigenous-biogenic lamina (below) and a diatom ooze lamina (above). E and F) BSEI micrographs. Almost monospecific composition of diatom ooze laminae, dominated by *Thalassionema nitzschioides*. RL: reflected light. TL: transmitted light. n//: parallel nicols; nx: crossed nicols

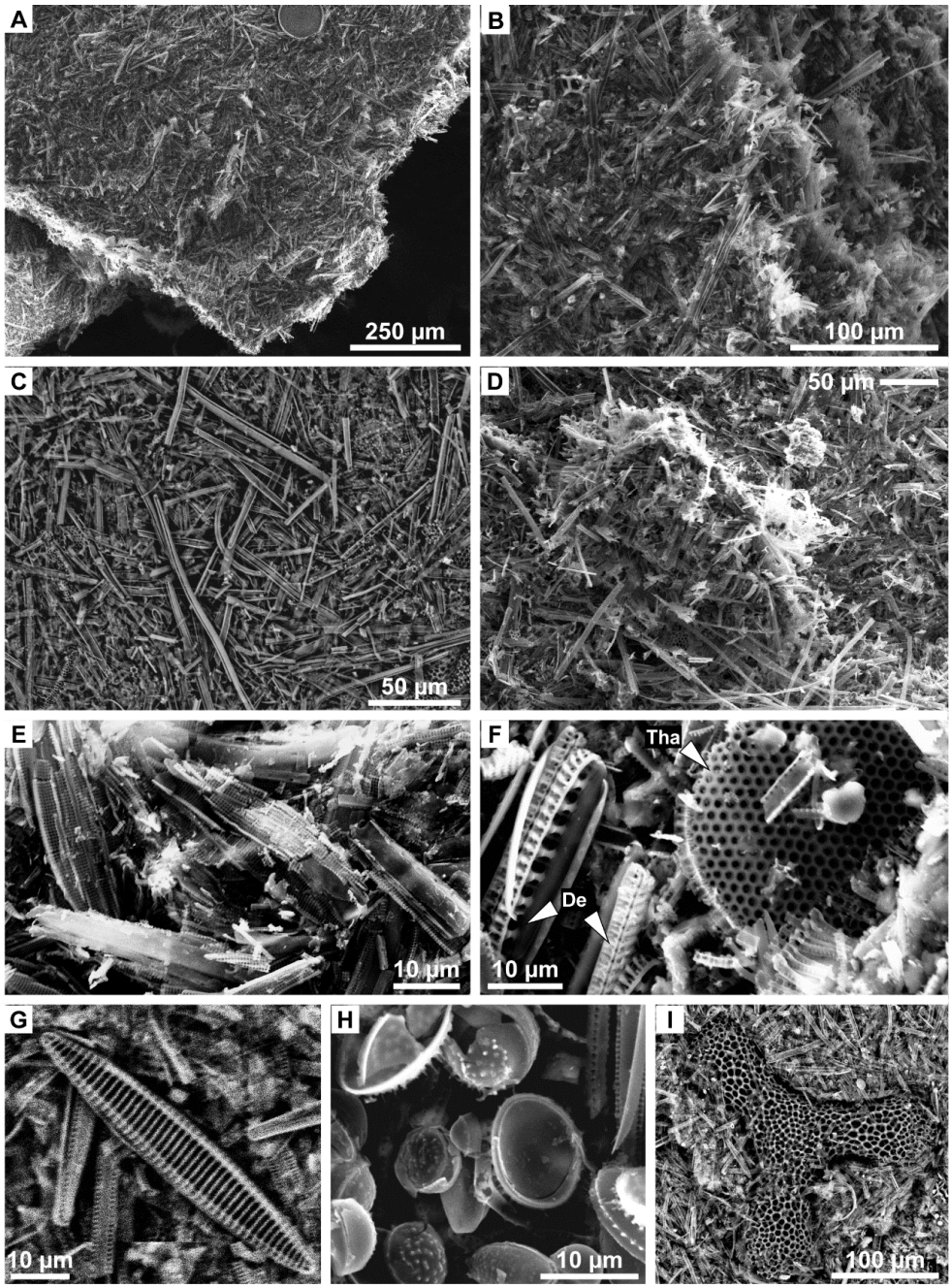

Figure 20. SEM topographic observation of diatom ooze laminae. A to C) Examples of different lamina surfaces; note the intricate meshwork deriving from the near-monospecific accumulation of needle-like frustules of *Thalassionema nitzschioides*. D) Cluster of macerated biogenic silica. E) Dense accumulation of naviculoid diatoms. F) *Denticulopsis* sp. (De) and *Thalassiosira* sp. (Tha). G) *Nitzschia praereinholdii*. H) *Chaetoceros* resting spores. I) Radiolarian (family Spongodiscidae).

Lamina types and subtypes		Diagnostic components	Mechanism of formation	Reference figures
Mixed terrigenous-biogenic		• Mixed clay-nannofossil-rich matrix • Silt-sized terrigenous particles • Inshore biogenic grains (diatoms, foraminifers)	• Influx of fine-grained lithogenic particles and coastal taxa • Background sedimentation dominated by calcareous nannoplankton • Basin shielded by coarse terrigenous influx	**Figs. 14-15**
Diatom-rich	*Diatomaceous mud*	• Nannofossil-rich matrix • Large centric diatoms (mostly *Coscinodiscus* spp.)	• Proliferation of deep chlorophyll maximum (DCM)-forming diatoms during water column stratification • Convective remixing of the water column • Sedimentation of DCM-forming diatoms (“fall dump”; Kemp et al., 2000)	**Figs. 17-18**
	Diatom ooze	• Meshwork of needle-like pennate diatoms (mostly *Thalassionema nitzschioides)*	• Proliferation of opportunistic diatoms during water column convective remixing • Exhaustion of nutrients in the upper water column • *En masse* sedimentation of opportunistic diatoms	**Figs. 19-20**

Table 6. Lamina types and subtypes, diagnostic components and genetic mechanisms.

3.3. Laminated packets

Two main types of laminated packets were distinguished (**Tab. 7**). Type 1 laminated packets (e.g., **Figs. 12B** and **17A**) mostly comprise low bimodality, mud-dominated, closely spaced suites of couplets that are composed of razor- to pin-striped mixed terrigenous-biogenic laminae alternating with razor-striped, diatom-rich (mainly diatomaceous mud) laminae (e.g., **Figs. 17D** to **G**). The diatom-rich laminae typically show a poor to moderate lateral continuity and a moderate preservation of lamina boundaries. Isolated, better preserved, razor- to pin-striped diatom ooze laminae may occur within these packets.

Type 2 laminated packets represent a very limited fraction of the laminated portion of the section (e.g., **Figs. 12B** and **19A**). They are composed of moderate to high bimodality, subequal- to diatom-dominated suites of couplets. These are closely to moderately spaced and characterized by pin- to chalk-striped terrigenous-biogenic laminae alternating with razor-striped or pin- to chalk-striped diatom ooze laminae, displaying a moderate to good lateral continuity and preservation of lamina boundaries (e.g., **Figs. 19B** to **D**). In the lower 10 cm of the studied section (**Fig. 12B**), a triplet has been observed. It is composed of a mixed terrigenous-biogenic lamina at the bottom, followed by a diatomaceous mud and a diatom ooze lamina (see Discussions).

3.4. Non-laminated intervals and burrows

Non-laminated intervals (**Fig. 12B; Tab. 7**) consist of homogeneous or graded layers ranging in thickness from >1.5 mm to a few cm and showing indistinct upper and lower contacts. In the homogeneous layers (**Fig. 21A**) the original laminae have been compromised by bioturbation. However, in some cases remnants of the original laminated fabric can still be discerned. Occasionally, lithogenic particles coated with Mn-Fe oxides (according to EDS analysis) occur as bright spots. Thin section and topographic observations confirm that the bulk composition of these layers is similar to that of the mixed terrigenous-biogenic laminae (**Figs. 21A-B**). The graded layers are composed of a mixture of clay- and silt-sized terrigenous grains, diatom valves and calcareous nannofossils, while the other biogenic components (e.g., foraminifers, sponge spicules) are very scarce to absent (**Figs. 21C** to **F**).

Burrows are unevenly distributed throughout the section, affecting both laminated packets and non-laminated intervals (**Fig. 12B**). The burrows are often characterized by amorphous blackish spots of Fe-Mn-oxides; transmitted light and BSEI observations highlighted their mixed clastic-biogenic composition.

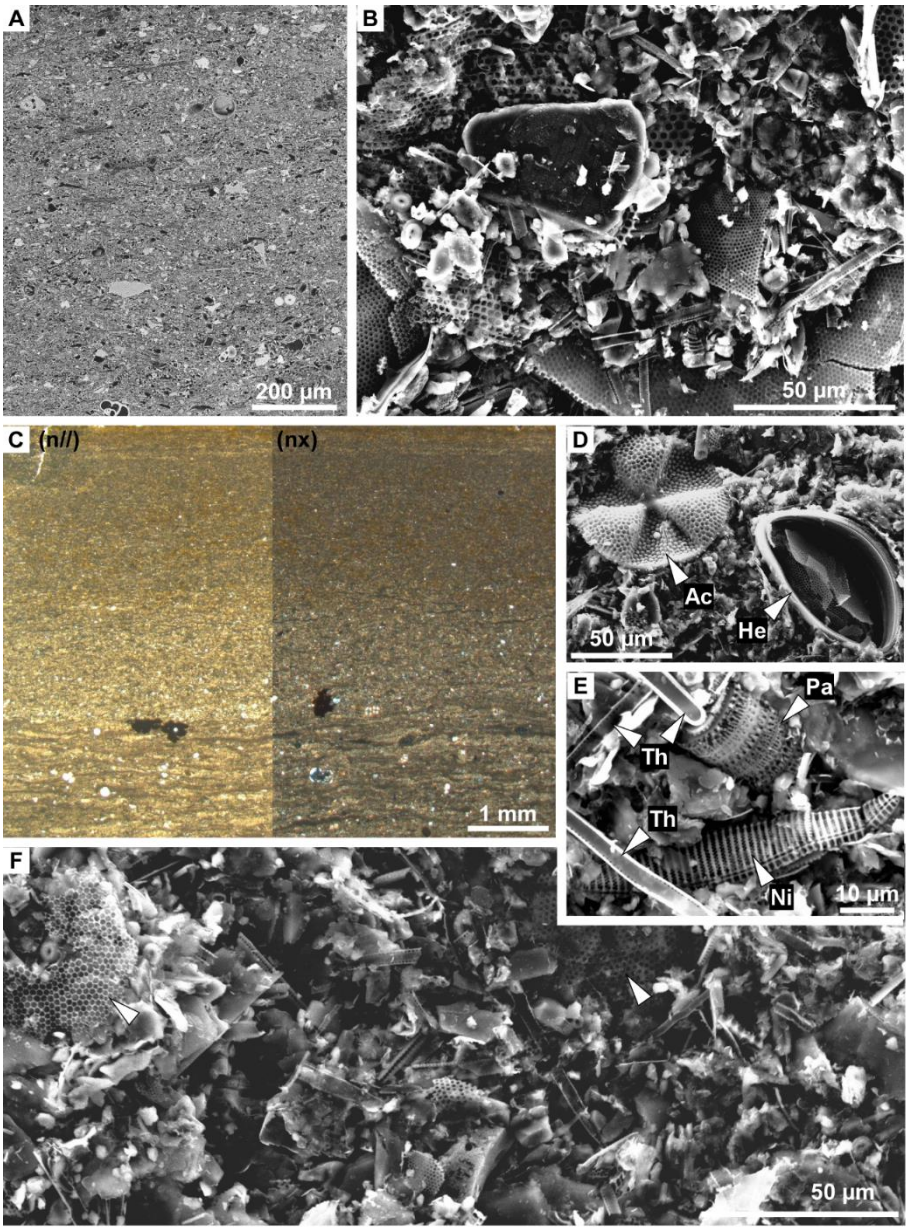

Figure 21. Non-laminated intervals in polished thin section and observed parallel to the bedding plane. A) BSEI micrograph. Homogeneous layer. B) SEI micrograph. Homogeneous layer; note the presence of terrigenous and skeletal debris. C) TL micrograph. Graded layer. D-E) SEI micrographs. Graded layer showing relatively well-preserved specimens of *Actinoptychus senarius* (Ac) and *Hemidiscus cuneiformis* (He), the neritic diatom *Paralia sulcata* (Pa), *Nitzschia praereinholdii* (Ni) and scattered specimens of *Thalassionema nitzschioides* (Th). F) SEI micrograph. Fragmented biogenic remains and clayey terrigenous particles in the upper part of a graded layer; note the presence of strongly etched diatom valves (arrowheads). TL: transmitted light. n//: parallel nicols; nx: crossed nicols.

3.5. Opal-rich aggregates and mixed pelletal structures

Opal-rich aggregates (**Tab. 7**) are shaped as short subovoidal pellets (**Figs. 22A-B**) and elongated, flattened or wavy strings (**Fig. 22C**) with a thickness in the range of some tens of micrometers and a major axis ranging from hundreds of micrometers to more than 1 mm. Only the thickest aggregates can be identified; they appear as whitish strings generally arranged parallel or slightly oblique to the bedding plane, well distinguishable from the surrounding matrix because of their sharp boundaries and color contrast. These features occur in the type 1 laminated packets or in the non-laminated intervals. Because of their high opal content, with transmitted light and under BSEI the aggregates appear dark, similar to the well-preserved diatom-rich laminae (**Figs. 22A** to **F**). When observed parallel to the bedding plane, the opal-rich aggregates show variable shapes, ranging from irregular to sub-circular (**Fig. 22G**). They are mostly composed of pristine valves of *Thalassionema nitzschioides* (**Figs. 22D** and **H-I**), although rare isolated aggregates of *Chaetoceros* resting spores and setae (**Figs. 22C, F** and **J-K**) and of silicoflagellates (*Stephanocha speculum*; **Figs. 22B, E** and **L-M**) have been also observed.

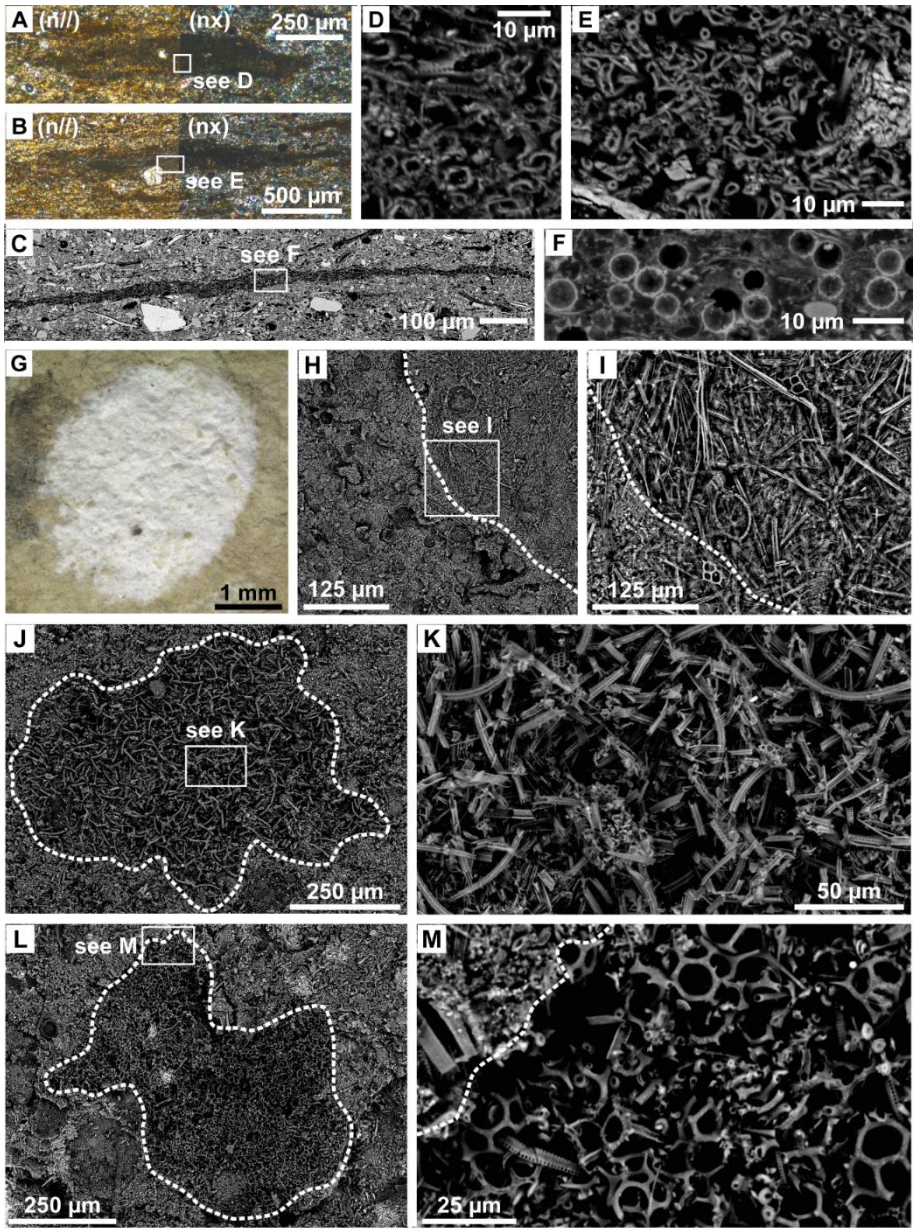

Figure 22. Opal-rich aggregates in polished thin section and observed parallel to the bedding plane. A and B) TL micrographs. Short, subovoidal pellets. C) BSEI micrograph. Flattened string. D to F) BSEI micrographs. Details of A, B and C, showing a dense accumulation of *Thalassionema nitzschioides* (D), silicoflagellates (E) and *Chaetoceros* resting spores (F). G) RL micrograph. Sub-circular aggregate observed; note the well-defined boundaries and the color contrast with the surrounding matrix. H and I) BSEI micrographs. Aggregate dominated by *T. nitzschioides*; note the compositional contrast with the surrounding matrix composed of clay and calcareous nannofossils. J and K) BSEI micrographs. Aggregate composed of *Chaetoceros* setae and scattered specimens of *T. nitzschioides*. L and M) BSEI micrographs. Silicoflagellate-rich aggregate composed of *Stephanocha speculum*. Dotted lines mark the aggregate boundaries. RL: reflected light. TL: transmitted light. n//: parallel nicols; nx: crossed nicols.

Mixed pelletal structures have a bright appearance in BSEI, due to the presence of comminuted lithogenic and biogenic particles, both siliceous and calcareous (**Fig. 23; Tab. 7**). The abundance of these types of pellets, apparently higher in the mixed terrigenous-biogenic laminae, is probably underestimated, since sediment compaction could have modified the original, subovoidal shape.

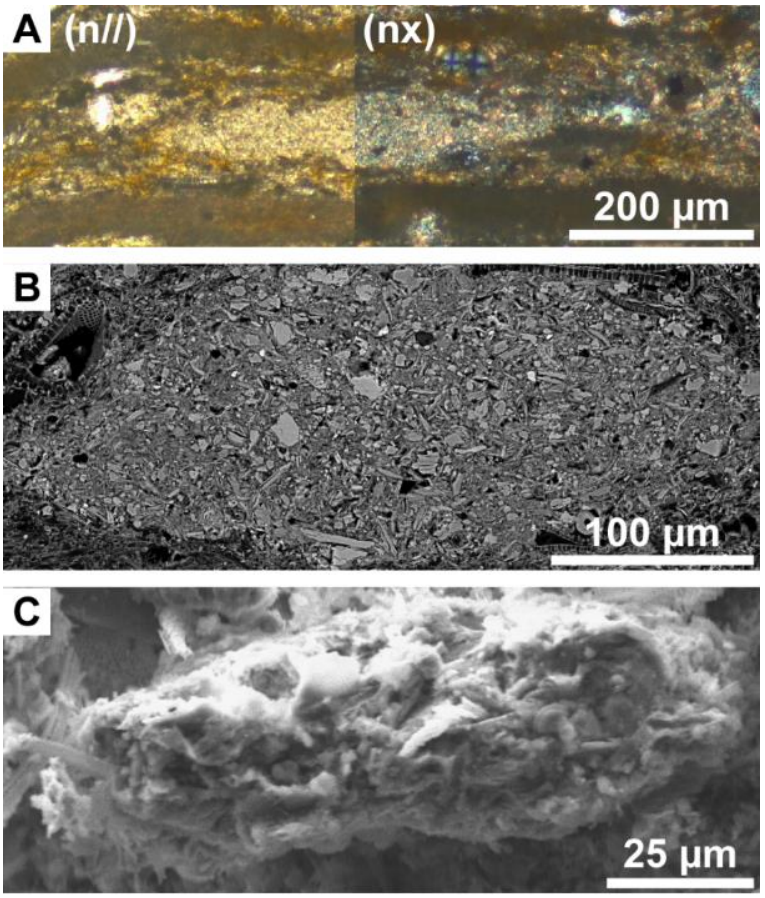

Figure 23. Mixed pelletal structures in polished thin section (A and B, TL and BSEI micrograph, respectively) and observed parallel to the bedding plane (C, SEI micrograph). TL: transmitted light. n//: parallel nicols; nx: crossed nicols.

Facies and subfacies		Description and occurrence	Interpretation	Reference figures
Laminated packets	*Type 1 laminated packets*	• Low bimodality • Mud-dominated • Couplets composed of mixed terrigenous-biogenic laminae alternating with discontinuous diatom-rich (mainly diatomaceous mud) laminae • Common	• Inefficient nutrient cycling • Weak seasonality, warm-humid climate • Slight convective remixing with limited reinjection of nutrients in the upper water column • Limited proliferation of ooze-forming diatoms	**Figs. 12B** and **17**
	Type 2 laminated packets	• Moderate to high bimodality • Subequal to diatom-dominated • Couplets composed of mixed terrigenous-biogenic laminae alternating with diatom ooze laminae • Triplet observed (see Fig. 24) • Rare	• Efficient nutrient cycling • Vigorous convective remixing with sustained reinjection of nutrients in the upper water column • Enhanced proliferation of ooze-forming diatoms	**Figs. 12B** and **19**
Non-laminated intervals	*Homogeneous layers*	• Structureless fabric • Common	• Pervasive bioturbation of former laminated packets • Bioturbation favored by scarcity of diatom-rich (especially diatom ooze) laminae	**Figs. 12B, 21A-B**
	Graded layers	• Normal grading • Rare	• Gravity flows possibly related to synsedimentary tectonic instability or to the rheological behaviour of the diatomaceous deposits	**Figs. 12B, 21C** to **F**
Burrows		• Common	• Bioturbation	**Fig. 12B**
Opal-rich aggregates		• Strings and pellets mostly composed of *Thalassionema nitzschioides* • Common	• Self-sedimentation of scattered colonies of siliceous phytoplankton	**Fig. 22**
Mixed pelletal structures		• Fecal pellets concentrated in the mixed terrigenous-biogenic laminae • Common	• Grazing in the water column and at the sediment-water interface	**Fig. 23**

Table 7. Main facies and sub-facies observed in the studied section.

4. Discussion

4.1. Origin of mixed terrigenous-biogenic laminae

The composition of these laminae (**Figs. 14-15**) reflects an increased rate of fine-grained terrigenous supply to a basin that was normally characterized by a background biogenic sedimentation dominated by calcareous nannoplankton and associated with a moderate biosiliceous production. The presence of mixed pelletal structures and the poor preservation of diatom valves (with the exception of the most robust taxa), indicates intense zooplankton and benthic grazing, resulting in the production of fecal pellets. The seafloor was sufficiently oxygenated to sustain benthic life, allowing processes of extensive bioturbation, as suggested by the random orientation of centric diatom frustules (e.g., **Fig. 14F**). Nevertheless, local anoxic niches formed, probably in response to a major concentration of organic matter, as witnessed by the presence of rare foraminifer tests and centric diatom frustules filled with framboidal pyrite (e.g., **Fig. 16**). The possible winnowing of the seafloor by (weak) bottom currents is indicated by clustered detrital and biogenic coarse particles (e.g., **Figs. 14H** to **J**).

The fine-grained terrigenous component and the abundance of calcareous nannofossils points to a relatively distal setting, partly shielded from the coarser

detrital influx. The angular shape of the silty particles suggests a brief transport from a nearby exposed area. Both the lithogenic and the coarsest biogenic particles with inshore affinity were likely transported via suspension and then settled from the water column (e.g., Chang et al., 1998).

The abundant spongolitic content of these laminae can be interpreted as being displaced from the shelf and re-deposited into a more distal and deeper setting (Sturani and Sampò, 1973). This interpretation is reinforced by the presence of sterraster microscleres of *Geodia* spp., representing an inner-shelf environment (Bonci et al., 1996).

The periodic input of terrigenous and inshore biogenic particles into the basin was caused by riverine discharge and/or eolian transport, reflecting wetter and drier conditions, respectively. The presence of geodiid remains (e.g., Bonci et al., 1996) and especially of the silicoflagellates of the *Dictyocha-Distephanopsis-Mesocena-Paramesocena* group points to a temperate-warm climate (e.g., Locker and Martini, 1989), which agrees with the interpretation of humid conditions during the deposition of these laminae (e.g., Rigual-Hernández et al., 2010).

4.2. Origin of diatomaceous mud laminae

The oligotypic assemblage of large centric diatoms that are characteristic of these laminae (**Figs. 18A** to **D**) can be primarily attributed to the selective grazing and/or dissolution of the less silicified opaline skeletons (e.g., Shemesh et al., 1989; Tanimura et al., 1990; Burckle et al., 1992). Grazing and dissolution are evidenced by the presence of comminuted opaline remains and scarcely-preserved diatom valves. Moreover, small-scale bioturbation that disrupted the lateral continuity of these laminae may have further obliterated the original assemblage due to mechanical breakage and preferential dissolution of the lightly silicified taxa. However, the overall composition of these laminae is too distinctive and recurrent, suggesting that the processes that modified the original bio- and taphocoenosis played a marginal role. Thus, this type of laminae can be attributed to the proliferation of 'giant' diatoms that are able to survive in the lower photic zone when the water column was stratified and typified by an oligotrophic upper layer, producing the so-called deep chlorophyll maximum (DCM). In modern oceans, the *en masse* sedimentation of these large taxa takes place when an abrupt, physical reconfiguration of the water column occurs (fall dump *sensu* Kemp et al., 2000). In contrast to the fast-growing, bloom-forming diatoms, this 'shade flora' is adapted to exploit the sub-photic layer of the water column (Sournia, 1982) and has a slower growth rate. The shade flora relies on the nutrient pool trapped below the pycnocline, on specific endosymbiotic diazotroph associations for its nitrogen demand and on the ability to control its buoyancy in order to migrate to the upper photic zone to photosynthesize (e.g., Kemp et al., 2000; Kemp et al., 2006; Kemp and Villareal,

2013). Members of the shade flora have been observed from the morphological and geochemical investigations of diatom-bearing and organic-rich sediments from different ages worldwide (e.g., Gombos, 1984; Pearce et al., 1998; Kemp et al., 1999; Pike, 2000; Burke et al., 2002; Bahk et al., 2003; Seeberg-Elverfeldt, 2004; Romero and Schmieder, 2006; Davies et al., 2009; Xiong et al., 2013; Gariboldi, 2015; Ohkouchi et al., 2015; Davies and Kemp, 2016; Kemp and Villareal, 2018), but were rarely considered as an additional controlling factor of the latest Miocene opaline accumulation in the Mediterranean (e.g., Pestrea et al., 2002; Pérez-Folgado et al., 2003). However, the few works that addressed the lamina-scale composition of the Mediterranean diatomaceous sediments by means of non-destructive SEM observations have already shown that the laminae are almost entirely dominated by large centric diatoms (e.g., Rouchy, 1982; Mansour et al., 1995).

The best known modern representatives of the DCM and fall dump process belong to the genera *Ethmodiscus*, *Coscinodiscus*, *Hemiaulus*, *Rhizosolenia* and *Thalassiothrix* (e.g., Villareal et al., 1999; Kemp et al., 2000), although increased interest about this mode of primary production provides continuous evidence of the non-ancillary role of other diatoms usually considered as solely bloom-forming taxa, including selected species of the family Chaetocerotaceae, recurrently present in the deep photic layer of the Mediterranean (e.g., Estrada, 1991; Siokou-Frangou et al., 2010; Crombet et al., 2011; Rigual-Hernández et al., 2013). *Thalassionema nitzschioides* also has been observed as a major component of the DCM in the

Mediterranean, as well as in the Celtic Sea (Hickman et al., 2009), providing further evidence of its opportunistic nature (discussed below; e.g., Siokou-Frangou et al., 2010). With respect to observations of characteristic taxa in the diatomaceous mud laminae, it is noteworthy that *Coscinodiscus radiatus* and *Hemidiscus cuneiformis* are common components of DCM patches that develop during summer water column stratification in the Northwestern Mediterranean (e.g., Estrada, 1991; Latasa et al., 1992). Therefore, the diatomaceous mud laminae can be interpreted as the product of the sedimentation of the 'shade flora' in response to the abrupt water column destabilization after a period of stratification. Since the examination of the nannofossil assemblage did not reveal the common occurrence of deep dwellers (excepted scattered *Discoaster* spp.), it is likely that when the water column was stratified the biomineralized phytoplankton was segregated into a community dominated by coccolithophores living in the oligotrophic surface waters, and a biosiliceous community represented by large centric diatoms inhabiting the more eutrophic subsurface waters. In this light, the limited occurrence and reduced preservation of the ubiquitous diatom *Thalassionema nitzschioides* (with the exception of the very well-preserved lensoidal aggregates discussed below) is consistent with nutrient-depleted conditions, and therefore with low rates of proliferation in the upper, oligotrophic water column, where this diatom was exposed to dissolution and grazing. Conversely, the occurrence of *Chaetoceros* resting spore aggregates within these laminae is consistent with the tendency of this taxon to live at the pycnocline during periods of water column stratification.

There is no evidence of the establishment of extensive bottom anoxia during the formation of this lamina type. Relatively low rates of primary production were unlikely to trigger a marked depletion of oxygen levels through the aerobic decomposition of organic matter. Limited primary production is also suggested by the overall thinness of these laminae, which were clearly affected by processes of microbioturbation. Benthic microbioturbators, however, were unable to completely obliterate the original taphocoenosis.

4.3. Origin of diatom ooze laminae

Diatom ooze laminae dominated by entangled and relatively well-preserved valves of *Thalassionema nitzschioides* (**Figs. 20A** to **C**) likely reflect bloom events followed by nutrient exhaustion and fast export of diatom aggregates to the seafloor, partially bypassing zooplankton grazing pressure (self-sedimentation *sensu* Grimm et al., 1997). Rapid transport can be attributed to diatom-related mucilage production, which increases the diatom sinking rates and protects the frustules from dissolution in the water column and at the sediment-water interface (Grimm et al., 1997). A further contribution to the preservation of these laminae could be related to their stiffening nature, which results from the rapid accumulation of the needle-like frustules of *T. nitzschioides*.

4.3.1. Possible triggers of the bloom events

Identifying the possible triggers responsible for the proliferation of *T. nitzschioides* is necessary for interpreting the processes underlying the formation of the diatom ooze laminae. While correlating the proliferation of *T. nitzschioides* to relatively eutrophic conditions in the upper water column is generally correct, the possible triggers responsible for this eutrophication are less obvious. The overabundance of *T. nitzschioides* in the upper Miocene diatomaceous sediments of the circum-mediterranean region has been often considered as indicative of strengthened oceanic circulation that promoted upwelling of cold, nutrient-rich and oxygen-depleted waters along the continental margins (e.g., Gaudant et al., 1996, 2006, 2010, 2015; Mansour and Saint Martin, 1999; Pestrea and Saint Martin, 2002; Saint Martin et al., 2003; El Ouahabi et al., 2007; Mansour et al., 2008). This interpretation is based on the assumption that the North Pacific basins, where upwelling actually exerted a major role on the latest Miocene diatomite accumulation (e.g., Barron and Baldauf, 1990) and currently governs the seasonal opaline production (e.g., Calvert, 1966), are the best analogues for interpreting the Mediterranean diatomaceous accumulation (e.g., Sturani and Sampò, 1973; McKenzie et al., 1979; Bennet, 1980; Moissette and Saint-Martin, 1992). In addition, *T. nitzschioides* is particularly abundant in Neogene (e.g., Barron and Keller, 1983) and Quaternary (e.g., Calvert, 1966) diatom-bearing sediments in the North Pacific, which is strongly influenced by upwelling. This

interpretation, however, has been re-evaluated by several authors who have considered some North Pacific species of *Chaetoceros* to be reliable indicators of coastal upwelling, while *T. nitzschioides* seems to preferentially exploit the less productive distal edges of upwelling plumes or even the gyres (e.g., Margalef, 1978; Sancetta, 1992; Tanimura, 1999; Lopes et al., 2006). Thus, some authors have cast doubt on the role that upwelling currents played in the accumulation of Mediterranean diatomaceous sediments enriched in *T. nitzschioides*, highlighting the broad spectrum of environmental conditions potentially exploitable by this cosmopolitan and opportunistic species (e.g., Rouchy et al., 1995; Pestrea et al., 2002). In the modern Mediterranean, rich assemblages of *T. nitzschioides* have been observed at the mouth of the Nile River (e.g., Halim et al., 1967; Aleem, 1972), and in other riverine-influenced settings, including the Northern Adriatic Sea (e.g., Bosak et al., 2009; Šupraha et al., 2011).

For the diatom ooze laminae observed in the present study, the reduction of clastic debris points to a delay between the interval of detrital input, represented by the mixed terrigenous-biogenic laminae, and the proliferation of *T. nitzschioides*. Therefore, the diatom ooze laminae could be attributed to a limited clastic input and a relatively well-remixed water column where nutrients that were previously trapped at depth were re-injected into the photic zone. In the Mediterranean such conditions do not necessarily coincide with upwelling, but mostly with the seasonal breakdown of the thermocline that occurs during the winter (convective remixing; e.g., Aleem

and Dowidar, 1967; Lakkis and Novel-Lakkis, 1981; Estrada, 1996; Rigual-Hernández et al., 2013).

The concentration of naviculoid diatoms within some of the diatom oozes (**Fig. 20E**) is also relevant. Naviculoid diatoms show a wide spectrum of ecological preferences, but they are mostly confined to shallow, coastal settings, where they generally live in the epipelon (e.g., Round et al., 1990). The observed valves are relatively well preserved, showing limited evidence of grazing and dissolution. If naviculoid diatoms were displaced *en masse* from the inshore area, the main cause may have been a sporadic riverine influx. This process is consistent with the reduced terrigenous content observed within the diatom ooze laminae and the good preservation of the valves.

4.3.2. Aggregation and sinking of diatoms

Today, colony-forming *T. nitzschioides* largely contributes to the formation of marine snow (e.g., Riebesell, 1991; Engel, 2002; Thornton, 2002). This process is mediated by the production of transparent exopolymer particles (TEP), a particular class of the extracellular polymeric substances (EPS), in response to nutrient-depleted conditions in the water column after a bloom episode (e.g., Passow et al., 1994; Passow, 2002a,b; Mari et al., 2017). Through the aggregation of lithogenic and biogenic particles suspended in the water column, the density of the mucilage would

have increased, as would its sinking rate through the so-called 'ballast effect' (e.g., Ittekot, 1993; Hamm, 2002; van der Jagt et al., 2018; Neumann et al., 2019; Rixen et al., 2017, 2019). Such a process reduces the zooplankton grazing pressure and the bacterially mediated degradation that normally affects isolated diatom cells during their slower descent in the water column, thus favoring the export and preservation of their opaline skeletons (e.g., Grimm et al., 1996, 1997; Moriceau et al., 2007). Once settled at the sediment-water interface, the cohesiveness of the marine snow, and therefore the potential preservation of the resulting lamina, is fostered by biostabilization processes involving EPS-rich substances and the benthic microbial communities (e.g., Westall and Rincé, 1994; Gerbersdorf and Wieprecht, 2015; Mejdandžic et al., 2015).

The pristine valves of *T. nitzschioides* within the diatom ooze laminae of Pecetto di Valenza (e.g., **Figs. 20A** to **C**) strongly point to their encasement in mucilage that limited dissolution during their descent to the seafloor and deposition at the sediment-water interface. The larger diatoms, foraminifers, radiolarians, sponge spicules and terrigenous debris, occasionally observed as minor components of these otherwise monospecific diatom-ooze laminae, may have played a significant role in ballasting the aggregates of *T. nitzschioides* that formed after the blooms, and favored their fast export toward the bottom and therefore the relatively good preservation of the opal. The role of zooplankton grazing was likely negligible in the deposition of these laminae.

4.3.3. Substrate nature vs oxygen levels: why was bioturbation inhibited?

A prominent feature of the diatoms of the family Thalassionemataceae (see Hallegraeff, 1986; Hasle, 2001) is their tendency to produce highly tensile mats composed of their densely interlocked, elongated frustules. Extraordinary examples of such mono- to oligotypic meshworks, dominated by *Thalassionema* spp. and *Thalassiothrix* spp., have been observed in the Southern Ocean (Grigorov et al., 2002), in the Northern (Dickens and Barron, 1997) and Equatorial Pacific (Sancetta, 1983; Kemp and Baldauf, 1993), and in the Northern Atlantic (Bodén and Backman, 1996; Shimada et al., 2008). Moreover, mats of *Thalassionema nitzschioides* and *Thalassiothrix longissima* have been observed in the Quaternary hemipelagic sediments of the Santa Barbara Basin (Bull and Kemp, 1995), Gulf of California (Pike and Kemp, 1999), Peruvian margin (Brodie and Kemp, 1994), and Baltic Sea (Burke et al., 2002), as well as in the Miocene Monterey Formation (Chang et al., 1998; Pike and Kemp, 1999), Pisco Formation (Gariboldi, 2015), and Gulf of Suez deposits (Rouchy et al., 1995). In the Mediterranean sediments, laminae almost entirely dominated by Thalassionemataceae have been reported in a few works concerning the upper Miocene diatomites (e.g., Rouchy, 1982; Mansour et al., 1995; Galán et al., 1993; Bellanca et al., 2001), and mid-Pliocene (Capozzi et al., 2006a, b) and Quaternary sapropels (e.g., Pearce, 1998).

Bioturbation seems to have marginally affected these mats, which are not exclusive to anoxic settings (e.g., Kemp and Baldauf, 1993; King et al., 1995). The reduced bioturbation may be explained by the high sedimentation rates of the mats, their fabric and/or their conspicuous thicknesses. In this way, benthic bioturbation was inhibited by mechanical (i.e., suffocation) rather than biochemical processes (i.e., oxygen consumption linked to the bacterial degradation of phytodetritus) (e.g., Kemp and Baldauf, 1993). It is noteworthy that Ploug et al. (1997) and Lehto et al. (2014) observed that anoxia development inside the phytodetritus-rich aggregates is a spatially limited transient phenomenon that is compositionally controlled and size-dependent. Along the Adriatic coasts, Penna et al. (1993) examined the mass occurrence of mucilaginous diatom aggregates, comprising *T. nitzschioides*, and did not see any evidence of severe oxygen depletion at the sediment-water interface due to the mucilage accumulation, with the exception of sites that were characterized by a marked stratification of the water column. Interestingly, the authors concluded that since no suboxia or anoxia occurred at the sediment-water interface, the mass mortality of mollusks observed after the deposition of the mucilaginous diatom-rich aggregates was related to the mechanical clogging of their filtration apparatus by accumulated organic material on the sea floor.

At Pecetto di Valenza, anoxic to suboxic seafloor conditions possibly occurred during the deposition of the diatom-ooze laminae. However, these conditions were likely ephemeral for at least two reasons: i) the recurrent macro- and

microbioturbations that partially affected these laminae in the studied section suggest frequently oxygenated conditions; and ii) pyrite framboids that form under sustained bacterial sulfate reduction are nearly absent, likely because of the low organic content of the laminae. To sum up, the inhibition of bioturbation in the diatom ooze laminae can be attributed to the tensile strength and cohesiveness of these laminae, rather than to oxygen depletion of bottom waters.

4.4. The annual sedimentary cycle

In the type 2 laminated packet observed in the lower 10 cm of the studied section (**Fig. 12B**), it was possible to identify a triplet composed of a terrigenous-biogenic lamina at the bottom, a diatomaceous mud lamina in the middle and a diatom ooze lamina at the top (**Fig. 24**). In other parts of the section, triplets were not observed but couplets, composed of only two out of three laminae mentioned above, were common.

According to the interpretation of each lamina type, the triplet should reflect the complete sequence of seasonal environmental fluctuations and depositional patterns over one year (**Fig. 25**). Specifically: i) the mixed terrigenous biogenic lamina is interpreted as the sedimentary product of the humid season, typified by increased terrigenous-inshore biogenic input into the basin (**Fig. 25A**); ii) the diatomaceous mud lamina reflects the subsquent thermal stratification of the water

column during the warm season, resulting in the formation of a DCM dominated by the shade flora in the deeper part of the water column (**Fig. 25B**); lamina deposition records water column remixing during the cold season and the consequent breakdown of the thermocline (**Fig. 25C**); and iii) the diatom ooze lamina records the proliferation of the bloom-forming diatoms under well-remixed conditions that occurred during the cold season, and their deposition once nutrients were consumed (**Fig. 25C**).

In the studied section, the triplet is approximately 300 μm thick, and consists of a ~150 μm-thick mixed terrigenous-biogenic lamina (lower MTB lamina in **Fig. 24**), a ~60 μm-thick diatomaceous mud lamina (DM in **Fig. 24**) and a ~100 μm-thick diatom ooze lamina (DO in **Fig. 24**). According to these values, the 'normal' annual sedimentation rate at Pecetto di Valenza was about 0.3 mm/year, which translates to 30 cm/kyr. Considering post-burial compaction, on average yielding ~60% of volume loss (Isaacs et al., 1983), a more realistic sedimentation rate would be ~50 cm/kyr. This is within the range of the sedimentation rates calculated by Ogniben (1957) for the Messinian diatomaceous deposits of Sicily, i.e. 10-50 cm/kyr. Conversely, the sedimentation rate calculated for the upper Miocene laminated diatomaceous mudstones of the Pisco Fm. (Peru) was ~250 cm/kyr (Gariboldi, 2015), i.e. from five to twenty-five times higher than in the Mediterranean. Although the data obtained from the evaluation of some tens of centimeters of sedimentary succession cannot be considered statistically significant (see Gariboldi, 2015), striking differences can already be seen, in terms of the paleoceanographic regimes

and related biological productivity, between the Mediterranean and other localities during the latest Miocene. The lack of a vigorous oceanic circulation in the semi-enclosed Mediterranean basin during the latest Miocene may have limited the redistribution of nutrients mostly provided by riverine runoff, precluding the possibility of sustained rates of biological productivity in a way similar to that observed in upwelling-influenced Pacific settings (e.g., Suess and von Huene, 1988).

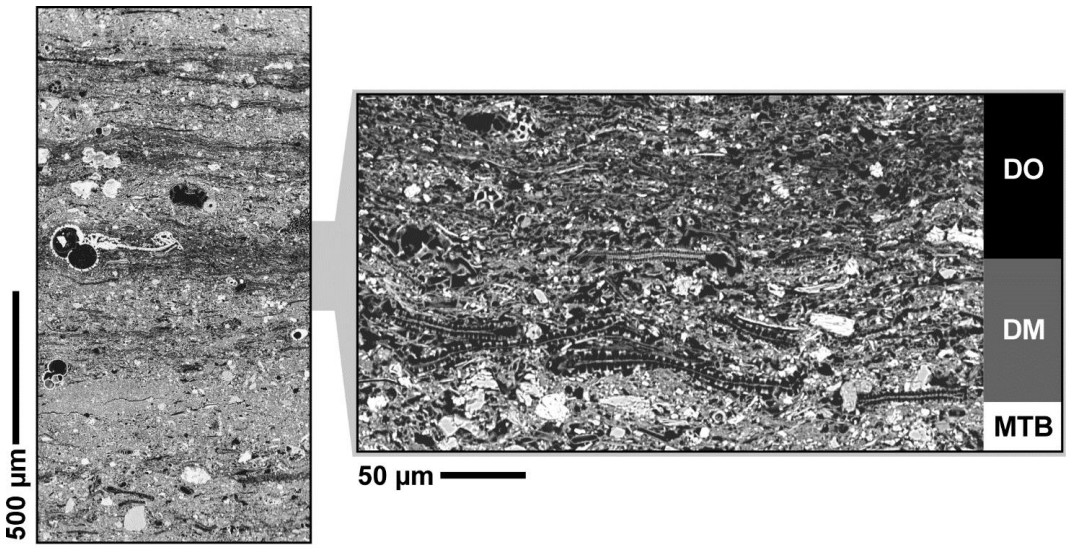

Figure 24. BSEI micrograph of the triplet identified in the lower part of the studied section (left; see Fig. 12B). The magnification on the right highlights the mixed terrigenous-biogenic lamina (MTB), the diatomaceous mud lamina (DM) and the diatom ooze lamina (DO); only the topmost part of the lower, mixed terrigenous-biogenic lamina is shown.

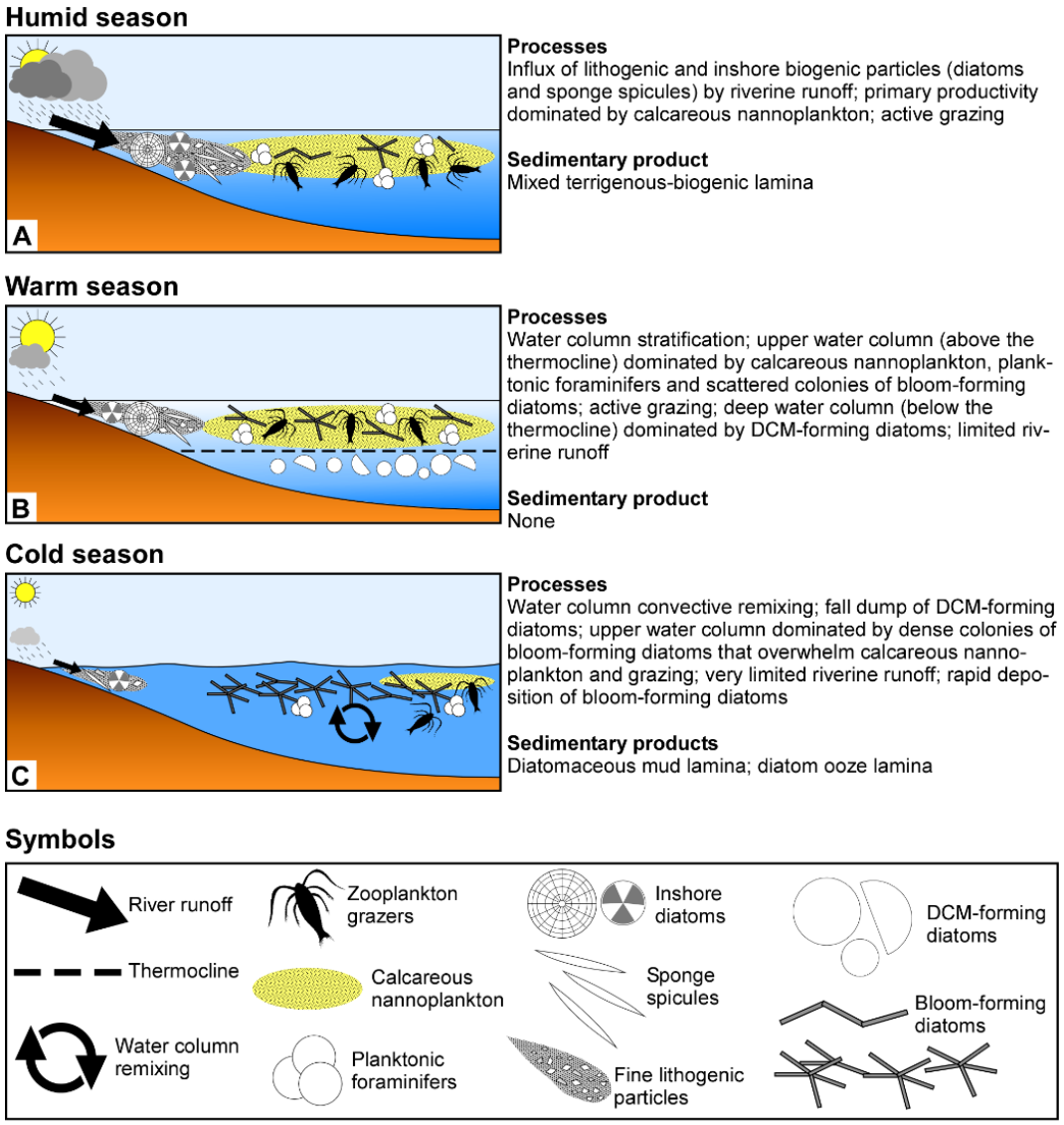

Figure 25. Interpretative sketch of the triplet reported in Fig. 24.

4.5. The modification of the annual sedimentary cycle

Since most of the laminated packets are represented by the alternation of mixed terrigenous-biogenic and diatomaceous mud laminae, with the occasional

intercalation of thick diatom ooze laminae or biosiliceous-rich aggregates (type 1 laminated packets; **Fig. 12B**, **Tab. 7**), it is possible to hypothesize that the annual sedimentary cycle underwent some modifications during the deposition of these laminated packets. The alteration of the normal pace of phytoplankton productivity was possibly linked to the reconfiguration of the hydrological cycles, in turn affecting the water column. It is noteworthy that the type 1 laminated packets may reflect the high-frequency variability of the water column within an overall warm and humid climate. Under such conditions, a vigorous water column remixing was probably prevented by thermal stratification and the stronger rainfall regime, which precluded the regular formation and deposition of extensive mats dominated by the Thalassionemataceae (e.g., Barron et al., 2013). Conversely, water column stratification favored the development of DCM species, regularly interrupted by slight water column perturbations. For these reasons, the annual sedimentary cycle most commonly comprised the first two steps of the annual sequence.

Where the diatom ooze laminae reach their major thickness but are not preceded by diatomaceous mud laminae within subequal to diatom-dominated (type 2) laminated packets (**Fig. 12B**, **Tab. 7**), the predominance of a drier and cooler climate may have precluded water column stratification.

4.6. Origin of non-laminated intervals and burrows

In the studied section, laminated packets are frequently interbedded with homogeneous layers. Such layers are commonly interpreted as the product of re-oxygenation events that allowed for the benthic bioturbation of laminated sediments that were deposited under otherwise anoxic conditions (e.g., Govean and Garrison, 1981; Ozalas et al., 1994) and/or of sediment reworking by bottom currents (Bennet, 1980).

However, the compostional similarities between the homogeneous layers and the terrigenous-biogenic laminae herein studied, may indicate that diatom productivity in the water column was weak. Such a scenario does not imply an abrupt increase in bottom water oxygen concentration with respect to the deposition of the laminated packets, but emphasizes the translation of weak diatom production in the water column to the accumulation of diatomaceous sediments that lack tensile strength (Pike and Kemp,1999). In this way bioturbation was not prevented by any physical obstacle, and the sediment could be reworked.

The graded beds can be unequivocally attributed to physical processes of sediment reworking, possibly related to gravity flows. Besides the synsedimentary tectonic activity (**Fig. 13F**), even the ongoing biosiliceous-terrigenous accumulation may have contributed to creating an unstable depositional environment. Once the highly porous, water-rich diatomaceous sediments are capped by low permeable

clayey deposits, the excess pore fluids would have accumulated at the interface between the two layers, increasing the shear stress and ultimately leading to failures (e.g., Urlaub et al., 2018).

Finally, the occurrence of various types of burrows produced by crustaceans and/or worms is another possible indication of the non-limiting nature of the oxygen levels, at least in the upper part of the sedimentary column.

4.7. Origin of opal-rich aggregates and mixed pelletal structures

Unfragmented diatom aggregates have been either interpreted as flocs derived from self-sedimentation processes (e.g., Grimm et al., 1997) or as fecal pellets of planktonic or benthic origin, in this latter case derived from the original diatom ooze (e.g., Brodie and Kemp, 1995; Bahk et al., 2000). In the present study, the pristine aggregates of *T. nitzschioides* can be interpreted as being derived from the self-sedimentation of scattered colonies that thrived in the upper portion of the water column during conditions that were unfavorable to their proliferation and thus prevented formation of continuous diatom ooze laminae. Bioturbation may have partially displaced the flocs, or locally interrupted the lateral continuity of the thinner flocs, but was ineffective in redistributing their content into the surrounding sediment because of the stiffened and cohesive nature of the aggregates (e.g., Chang and Grimm, 1999). The cohesiveness of the opal-rich aggregates could have been

fostered by the diatoms' increased production of TEP as a response to the nutrient-depleted environment that likely characterized the upper water column (e.g., Mari et al., 2017).

The mixed pelletal structures composed of crushed diatoms are clearly related to grazing processes, which may have occurred both in the water column and at the sediment-water interface, mostly during the formation of the mixed terrigenous-biogenic laminae.

4.8. The latest Miocene diatomaceous deposition in the Piedmont Basin: key-points and future directions

The latest Miocene opaline deposits outcropping in the Piedmont Basin record paleoceanographic events that occurred both before and during the Messinian salinity crisis (MSC). To date, only two pre-MSC sections (Pecetto di Valenza and Cappella Montei; Sturani and Sampò, 1973; Gaudant et al., 2010; Bonci et al., 1990, 1996; Bonci, 1995) and one syn-MSC section (Castagnito; Fourtanier et al, 1991) have been investigated in detail from a micropaleontological point of view, while only preliminary studies have been conducted on the other pre-MSC section of Mussotto (Sturani and Sampò, 1973) and the syn-MSC sections of Bric Santa Margherita, Cascina Dogliana and Cascina Botto (Irace, 2004). The microfossil assemblages document a shelf to slope depositional environment.

Thalassionemataceae are always very abundant throughout these sections (e.g., Fourtanier et al., 1991; Bonci, 1995; Irace, 2004; Gaudant et al., 2010), and a marked increase in the rhizosolenid diatoms was observed in the deposits that accumulated during the MSC (e.g., Fourtanier et al., 1991; Irace, 2004). The increasing abundance in rhizosolenioid diatoms deserves more attention, since it may underline a turnover in diatom communities adapted to stratified water conditions during the salinity crisis.

Diatoms and diatom molds have been also reported from other deposits of the Piedmont Basin, such as in the bottom-grown gypsum crystals (e.g., Dela Pierre et al., 2015; Carnevale et al., 2019) and the interbedded euxinic shales (Dela Pierre et al., 2014) from the Primary Lower Gypsum unit that represent the first phase of the MSC (Dela Pierre et al., 2011). The poor preservation of diatoms in the MSC organic-rich mudstones is particularly interesting in light of the ambiguity of the 'anoxic paradigm', i.e. the systematic link between the preservation of opaline laminated sediments and seafloor anoxia. Actually, a variety of processes occurring in organic-rich and oxygen-depleted conditions, such as pH fluctuations related to bacterial sulfate reduction, as well as reverse weathering, may promote biogenic silica dissolution (see **Chapter 3**). Increased rates of opaline preservation in the Piedmont Basin could have occurred only where oxygenated to transient anoxic bottom conditions were established, e.g., along the Monferrato structural high where the Pecetto di Valenza section is located. Conversely, in the deeper parts of the basin,

more extensive anoxic conditions, possibly linked to a persistent stratification of the water column, might have reduced the preservation of opal, resulting in the accumulation of organic-rich but opal-poor sediments.

The influence of upwelling in the Piedmont Basin during the late Miocene is rather questionable (see also Bonci et al., 1991). According to paleogeographic and paleoceanographic reconstructions (e.g., Dela Pierre et al., 2014), the Piedmont Basin was a sort of semi-isolated gulf, where the late Miocene diatomaceous accumulation took place during the progressive restriction of the connection between the Mediterranean and the Atlantic Ocean (e.g., Kouwenhoven et al., 1999), coupled to an ongoing increase in riverine runoff (e.g., Natalicchio et al., 2017, 2019; Sabino et al., 2020). These factors could have prevented upwelling conditions.

In sum, the late Miocene opal burst in the Piedmont Basin occurred under complex conditions that included: i) a variable but high nutrient availability, attributable to the occurrence of fluvial discharge rather than to the establishment of upwelling phenomena; ii) the significant role of the shade flora in controlling biosiliceous accumulation both before and after the onset of the Messinian salinity crisis; and iii) the possible obliteration of the opaline signal due to diagenetic processes that took place in slightly anoxic settings.

5. Conclusions

The morphological investigation of the Pecetto di Valenza diatomaceous sediments suggests that the initial stages of diatomaceous deposition in the northernmost offshoot of the Mediterranean basin during the Messinian was controlled by the interplay between riverine runoff and two different styles of primary production, characterized by slow-growing and rapidly reproducing diatoms that were able to thrive under stratified and well-remixed water column settings, respectively. At the beginning of the diatomaceous accumulation, the basin was shielded from coarser terrigenous influx, but was influenced by the deposition of clayey and silty particles. The clastic influx was associated with input into the basin of the remains of coastal diatoms and sponges that thrived in the shallower area of the basin. Riverine runoff played a central role in fertilizing the water column. The nutrients, mostly derived from the weathering of the uplifting Alpine range (see **Chapter 3**), were trapped below the pycnocline during the warm season and subsequently reinjected into the surface through convective remixing of the water column during the cold season. The complete product of these processes is an annual triplet composed of a mixed terrigenous-biogenic lamina, a diatomaceous mud lamina and a diatom ooze lamina. However, only one triplet was recorded, since the annual sedimentary cycle was modified by climatic or sedimentary perturbations, as explained previously.

No evidence for intensified upwelling and bottom water anoxia formation was observed in the studied section. The annual rate of biosiliceous productivity, based on the calculated sedimentation rate of 50 cm/kyr, was maintained at a level that was much lower than those recorded in an active upwelling area, e.g., along the eastern Pacific. The lack of persistent bottom anoxia is clearly demonstrated by the slight but pervasive microbioturbation that was only inhibited during the deposition of the diatom ooze laminae. Such a pattern suggests that bioturbation was suppressed by physical (tensile-strength meshworks), rather than by chemical (oxygen depletion) factors.

Future research addressing the late Miocene diatom-bearing sediments from the Mediterranean area should consider the extensive application of non-destructive, SEM-based approaches. In addition, quantitative geochemical investigations of redox sensitive elements (e.g., Chang et al., 2015), may help to solve the question of the role of oxygen concentration on the preservation of opaline laminated sediments. A more comprehensive dataset could provide new insights on two of the most peculiar sedimentary events of the Miocene epoch, i.e. the global increase in biosiliceous productivity and the Mediterranean Messinian salinity crisis.

CHAPTER 3 - THE MESSINIAN DIATOMITE DEPOSITION IN THE MEDITERRANEAN REGION AND ITS RELATIONSHIPS TO THE GLOBAL SILICA CYCLE‡

Since Neogene diatomaceous deposition studies began, there has been vivid interest and debate on the processes responsible for the enhanced availability of the silica exploited by diatoms and other silica-secreting microorganisms (e.g., Bramlette, 1946). The aim of this chapter is to summarize and update the current state of knowledge about the processes that may have fostered the biogeochemical cycle of silica during the Neogene, proposing an alternative (or at least a complimentary) point of view on the deep causes at the origin of the Mediterranean "opal burst".

1. The Mediterranean diatomite deposition and the late Neogene global biogenic bloom

Following the closure of the Tethyan Seaway about 19 Ma (e.g., Harzhauser et al., 2007) the Mediterranean was transformed into a semi-enclosed appendix of the Atlantic Ocean. Here, diatomite accumulation has occurred since around 7.8 Ma

‡ This chapter is based on Pellegrino, L., Dela Pierre, F., Natalicchio, M. and Carnevale, G. (2018). The Messinian diatomite deposition in the Mediterranean region and its relationships to the global silica cycle. Earth-Science Reviews 178, 154-176.

(Krijgsman et al., 2000; Köhler et al., 2010), but the main phase of the Mediterranean opal burst took place diachronously in the early Messinian, between 7 and 6 Ma, forming the well-known 'Tripoli' unit (Hilgen and Krijgsman, 1999). This unit exhibits a well-defined lithological cyclicity, recorded at both the macro- and microscale. The former (**Fig. 26A**) is expressed by dm- to m-thick lithological cycles consisting of diatom-rich layers rhythmically interbedded with calcareous marls and sapropels, and is believed to reflect precessionally-controlled dry-wet climate fluctuations influencing the hydrological budget of the Mediterranean marginal basins (e.g., Hilgen and Krijgsman, 1999; Modestou et al., 2017). The microscale cyclicity (**Fig. 26B**) is instead evidenced by the alternation of mm-thick biogenic and lithogenic laminae, and is related to short-term (seasonal, annual), climatically-driven variations in the terrigenous supply (e.g., Rouchy, 1982).

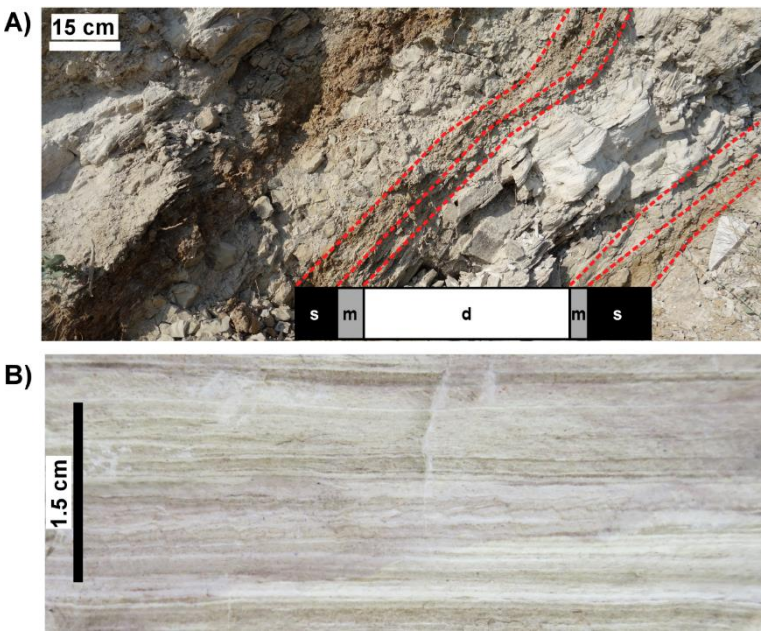

Figure 26. Cyclical patterns of diatomaceous deposits, at different scales. A) Macroscale cyclicity: brownish layers correspond to sapropels (s), grayish layers to marls (m) and the thick whitish layer to diatomite (d) (Serra Pirciata section, Caltanissetta Basin). B) Microscale cyclicity: greyish-brownish laminae are detrital-rich, whitish laminae are diatom-rich (Capo di Fiume section, Abruzzo).

These cyclic diatomaceous deposits are found in a variety of uplifted marginal basins that originated in different geodynamic settings along the southern rim of the Mediterranean (Southern Iberian Peninsula, Northern Africa, Sicily, Ionian Islands, Crete, Gavdos, Cyprus) and in the Apennine range (**Fig. 27A**). The offshore occurrence of the lower Messinian diatomites is instead uncertain, due to the paucity of data beneath the abyssal evaporites. A deep perspective is solely provided by two DSDP-ODP sites (Cita et al., 1978; Pierre and Rouchy, 1990), but this record is too scanty to support a broader distribution of the Messinian diatomaceous facies throughout the entire Mediterranean.

In Spain, opal-cristobalite (opal-CT) layers that originated from the diagenetic transformation of diatomites are found in the Sorbas and Nijar pull-apart basins within the lower Abad Member (Turre Fm.), whose base is dated at 7.2 Ma. They are overlain by a cyclic diatomaceous succession deposited between 6.7 and 6 Ma (upper Abad Member), represented by the quadripartite cycle of sapropel-marl-diatomite-marl (Vázquez et al., 2000; Krijgsman et al., 2001; Sierro et al., 2001, 2003; Pérez-Folgado et al., 2003). In Morocco (Boudinar and Melilla-Nador post-orogenic basins), diatomites deposited between 6.73 and 6.11 Ma (Saint Martin et al., 2003; van Assen et al., 2006; El Ouahabi et al., 2007) are rhythmically interbedded with marly, clayey and tephra layers. In Algeria, the alternation of diatomites, scattered ash layers and diatomaceous, calcareous, sandy, clayey or organic-rich marls are reported from the Chelif and Oran wedge-top basins, forming the so called Beida Stage (Anderson, 1933, 1936; Perrodon, 1957; Baudrimont and

Degiovanni, 1974; Rouchy, 1982; Gersonde and Schrader, 1984; Mansour et al., 1995, 2008; Mansour and Saint-Martin, 1999; Arab et al., 2015). This succession is one of the thickest (175 m on average) and best exposed outcrops in the Mediterranean region; although detailed astrochronological dating is still missing, its age is comparable with that of Moroccan deposits from Melilla-Nador, i.e. between 6.7 and 6.1 Ma (Mansour and Saint Martin, 1999; Cornée et al., 2004). On the Italian Peninsula, scattered outcrops of lower Messinian diatomites interbedded with silty and sandy turbiditic layers are reported from the Piedmont Basin (Pecetto di Valenza and Mussotto d'Alba), at the junction between the Alps and Apennines (Sturani and Sampò, 1973). In the Northern Apennine, diatomitic layers are reported from the main foredeep basins (Mondaino and Montefiore Conca), where they are interbedded with bituminous marls, organic-rich mudstones, siltstones and turbiditic sandstones (Selli, 1954; Savelli and Wezel, 1978; Arcaleni et al., 1995; Coward et al., 1999), and from a hinterland basin developed along the Tyrrhenian margin of the chain (Fine Valley), where diatomites alternate with silty and sandy marls (Bradley and Landini, 1984; Bossio et al., 1998; Benvenuti et al., 2014). Similar successions are reported from the Southern Apennine foredeep and wedge-top basins, near Monte dei Frentani (Ciaranfi et al., 1980), at Capo di Fiume (Carnevale, 2004b) and in the Apulia foreland ramp (Matano et al., 2005; Matano, 2007). The Tripoli Fm. is found in the Calabrian wedge-top basins, near Rossano and Crotone (Roda, 1964; Barone et al., 2008; Zecchin et al., 2013), and diatomites regularly interbedded with sapropels have been also reported near Catanzaro (Cianflone and Dominici, 2011).

In Sicily, cyclic sequences mostly composed of sapropel-diatomite-marl triplets were deposited between 7 and 6 Ma (Tripoli Fm.) in the Caltanissetta foredeep basin and in the Castelvetrano and Ciminna wedge-top basins (Gersonde and Schrader, 1984; Pedley and Grasso, 1993; Hilgen and Krijgsman, 1999; Roveri et al., 2008). Thin successions of nearly pure "papershale" diatomites are reported from the Iblean foreland, associated with diatremes (Suiting and Schmincke, 2010). In the Ionian Islands, lower Messinian biosiliceous levels with diatoms and silicoflagellates are reported from Zakynthos and Corfu (Rouchy, 1982; Frydas and Keupp, 2015). In Crete, scanty silicoflagellate-bearing opaline deposits characterize the lower Messinian succession of the Heraklion graben (Frydas, 2004). Cyclic diatomaceous deposits dated between 6.8 and 6 Ma and characterized by sapropel-diatomite-marl triplets have been described from Gavdos (Metochia section; Pérez-Folgado et al., 2003; Drinia et al., 2007). The major biosiliceous event in Cyprus is dated between 6.5 and 6.1 Ma (Orszag-Sperber et al., 2009). Diatomites interbedded with marls, sapropels and carbonate beds (Pakhna Fm.) occur in the Polemi, Pissouri and Psematismenos basins, around the Troodos Massif (Rouchy, 1982; Orszag-Sperber et al., 2009; Manzi et al., 2016) and in the Mesaoria basin, close to the Kyrenia Range (Manzi et al., 2016; Varol and Atalar, 2016). In Turkey, lower Messinian biosiliceous facies, primarily composed of sponge spicules, are found in the Adana basin (Faranda et al., 2013).

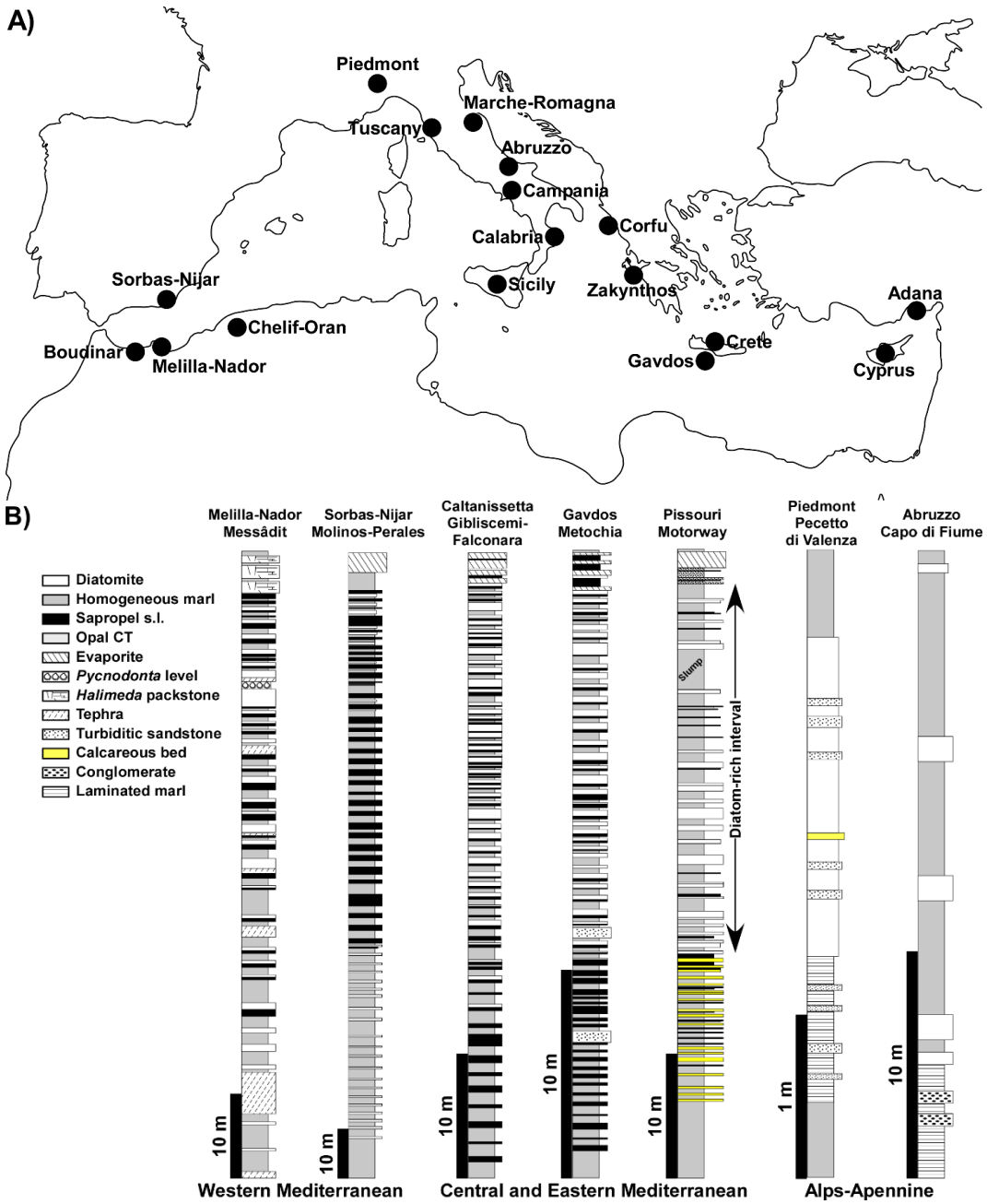

Figure 27. A) Distribution of lower Messinian marine biosiliceous (mainly diatom-rich) deposits in the Mediterranean. B) Main stratigraphic architectures of the lower Messinian Mediterranean diatomite successions. See text for a detailed discussion and references.

Outside the Mediterranean, the last 15 Ma constitute a period of remarkable intensification of opaline deposition in the global oceans (Renaudie, 2016), associated with the evolutionary diversification of diatoms (Lazarus et al., 2014). In this regard, it is interesting to note the global occurrence of extensive pelagic oozes, starting at about 15 Ma, composed of mat forming giant diatoms of the genera *Coscinodiscus*, *Ethmodiscus*, *Rhizosolenia*, *Stephanopyxis* and *Thalassiothrix*, which are adapted to exploit stratified waters usually occurring in correspondence with oceanic fronts or in response to the establishment of a seasonal pycnocline induced by freshwater inflows in land-locked basins (Kemp and Baldauf, 1993; Smetacek, 2000; Kemp et al., 2006). This highly-silicified "shade-flora" (Sournia, 1982) may support an enormous subsurface primary production at the Deep Chlorophyll Maximum, rivaling or even outcompeting diatom taxa inhabiting the surface layer (Kemp et al., 2006). The expansion of the cryosphere after the Mid-Miocene Climatic Optimum favored the development of the North Atlantic Deep Waters, the strengthening of the Antarctic Bottom Waters and the establishment of the Atlantic anti-estuarine circulation, which promoted the collapse of the Atlantic opaline productivity and the relative silica-enrichment of the Indian and Pacific oceans (Cortese et al., 2004).

A subsequent peak in the global biosiliceous production took place broadly between 7 and 4.5 Ma and is commonly referred to as the late Miocene-early Pliocene biogenic bloom (Cortese et al., 2004; **Fig. 28**).

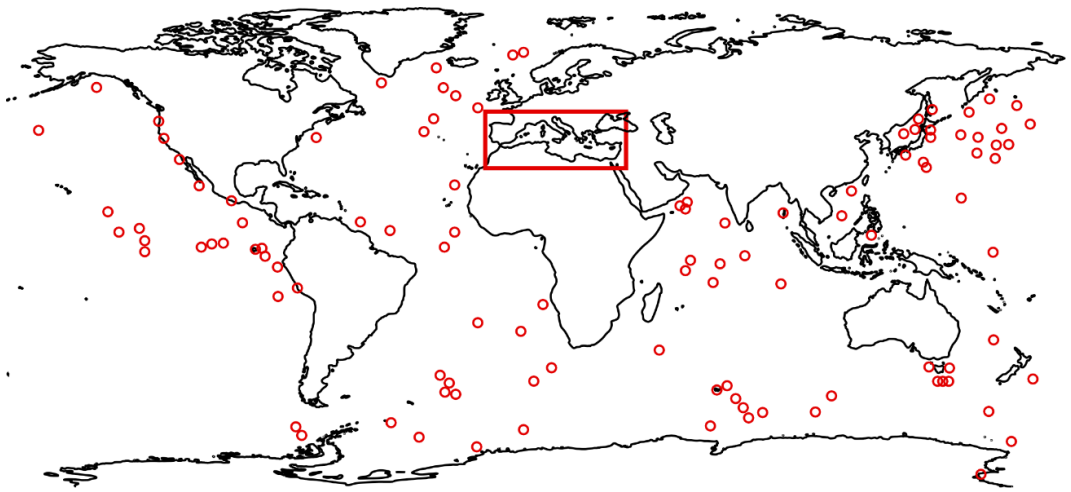

Figure 28. Global distribution of Upper Miocene and Lower Pliocene oceanic diatom-bearing deposits (circles). The rectangle indicates the Mediterranean basin. Modified from Renaudie (2016).

The late Neogene opal burst was associated with the world-wide enhancement of carbonate, phosphate and barium accumulation rates, to the vertical extension of the oxygen minimum zones (Diester-Haass et al., 2002, 2004), and to the considerable abundance, biodiversity and increase in body size of many groups of large predatory marine vertebrates, including fishes (e.g., Santini et al., 2013; Santini and Sorenson, 2013; Schwarzhans and Aguilera, 2013), marine mammals (e.g., Pyenson and Vermeij, 2016) and seabirds (Warheit, 2002; Norris et al., 2013). These data support a scenario of dramatic boost of oceanic productivity dominated by diatoms, fueling the whole trophic web (Berger, 2007). Originally recorded in the equatorial Indo-Pacific ocean and reported as a product of the nutrient redistribution between basins (Farrell et al., 1995), the world-wide extension of the late Miocene-early Pliocene biogenic bloom suggests that it was rather related to an overall increase of nutrient supply from lands to oceans (Filippelli and Delaney, 1994;

Filippelli, 1997; Hermoyian and Owen, 2001; Diester-Haass et al., 2002, 2004, 2005; Jianru et al., 2002; Cortese et al., 2004; Guptha et al., 2007; Lyle and Baldauf, 2015; Zhang et al., 2016).

2. Geobiosphere interactions on continents: a neglected link to the silica cycle

The bioavailability of dissolved silica (orthosilicic acid, H_4SiO_4; hereafter DSi) controls the diatom life-history in modern oceans (Sullivan and Volcani, 1981; Egge and Aksnes, 1992; Martin-Jézéquell et al., 2000, 2003; Ragueneau et al., 2000) and has triggered the evolutionary rise of diatoms as prominent primary producers in the geological past, especially during the last 40 Ma (Falkowski et al., 2004; Cermeño et al., 2015).

The current content of silicon in the modern oceans has been estimated to be around 97,000 Tmol Si, with an average residence time of about 10,000 years. Therefore, from a deep time perspective, the oceans are dependent on land-derived DSi, which is mainly supplied by river runoff (~7.3 ± 2 Tmol Si yr^{-1}). Nevertheless, the continental silica cycle is not completely understood and quantified as in the oceans, where about 240 ± 40 Tmol Si yr^{-1} are sequestered by diatoms in the upper (photic) water column to produce their siliceous tests (frustules), and ~6.3 ± 3.6 Tmol Si yr^{-1} are exported to the ocean floor through sinking of diatom frustules (Tréguer and De La Rocha, 2013).

On land, the ultimate source of DSi is the weathering of silicate rocks, which is based on the following reaction:

$$CaSiO_3 + 2H_2O + CO_2 \rightarrow Ca^{2+} + \mathbf{DSi} + CO_3^-$$

Silicate weathering is primarily the product of the interaction between tectonics and climate (**Fig. 29**). Tectonic uplift increases the surface of fresh rock exposed to meteoric agents and the deepening of fluvial erosion. On the other hand, elevated mountain ranges exposed to insolation promote the seasonal formation of wide atmospheric low-pressure zones, with consequent intensification of monsoonal rainfalls, in turn increasing the riverine erosion and the oceanward transport of weathered materials and dissolved nutrients (Ruddiman, 1997). A direct product of tectonics is volcanism, which may favor silica eutrophication of aquatic basins through the input of volcanic ashes (Taliaferro, 1933). Furthermore, the combined effect of plate tectonics and orbital variability controls the growth of the cryosphere; the consequent eustatic fluctuations expose subaerially the continental shelves and lower the riverine base level, playing a fundamental role in the transfer of terrestrial silicates toward the oceans (Hay and Southam, 1977).

Biogenic silica (hereafter BSi) is a fundamental component of the terrestrial silica cycle, but its importance has been overlooked for a long time (Street-Perrott and Barker, 2008). Vascular plants are weathering-agents of primary silicates and clays, able to enhance the extraction of DSi from the substratum and to convert it

into BSi in the form of phytoliths, which are released to the soil after plant senescence and herbivore digestion (Cooke and Leishman, 2011). Although the original role of plant silicification is still a matter of debate among evolutionary biologists (Coughenour, 1985), phytoliths have a structural, physiological and defensive role against a great variety of abiotic and biotic stresses (Raven, 1983; McNaughton et al., 1985; Richmond and Sussman, 2003; Ma and Yamaji, 2006; Cooke and Leishman, 2011). The high dissolution rates of the BSi particulate, which is more rapidly convertible into DSi than lithogenic silica (Fraysse et al., 2006; Guntzer et al., 2012), make a crucial contribution to the export of DSi from continents to oceans from terrestrial vegetation (Alexandre et al., 1997; Derry et al., 2005; Fulweiler and Nixon, 2005; Pokrovsky et al., 2005; Gérard et al., 2008; Struyf and Conley, 2009; Struyf et al., 2010; Ran et al., 2015). According to Struyf and Conley (2012), terrestrial plants are huge silica filters able to store ~60-200 Tmol Si yr^{-1} in their living tissues. Such values are comparable to the annual production of BSi in the oceans (see above). Nevertheless, the underground store of BSi, derived from the ongoing accumulation of phytoliths in the soil, may be even more than 400 times greater than its aboveground counterpart (Blecker et al., 2006). Considering the vast soil-plant pool of fast dissolvable BSi, it is therefore necessary to take into account the evolution of terrestrial ecosystems and plant communities through time, in order to properly interpret the history of oceanic opaline productivity (Conley and Carey, 2015; Trembath-Reichert et al., 2015).

Grass-dominated ecosystems, which presently cover ~40% of the Earth's landmass surface (White et al., 2000) and are dominated by plants with high silicon requirements (up to 10% of their dry weight) and high turnover rates (Hodson et al., 2005; Linder and Rudall, 2005; Ma and Yamaji, 2006), are considerably active ecosystems in the so-called "*terrestrial silica pump*" (Blecker et al., 2006; Carey and Fulweiler, 2012; Conley and Carey, 2015; Osterrieth et al., 2015; **Fig. 29**). In grasslands, two additional components significantly contribute to the continental silica cycle: grazers and fires. Grazers, both vertebrates and invertebrates, and fires act as "*ecological engineers*" through a selective pressure triggering favorable feedbacks for grassland stability and the expansion of grasses. Due to their low metabolic requirement, grasses are more adaptable than trees or woody shrubs to highly-stressed environments (Rice and Parenti, 1978; Batmanian and Haridasan, 1985; Abrams et al., 1986; McNaughton et al., 1988; Milchunas et al., 1988; Ojima et al., 1989; Day and Detling, 1990; Wallace, 1990; Holland et al., 1992; Singh, 1993; Frank et al., 1998; Higgins et al., 2000; Bond et al., 2003a,b; Bond and Keeley, 2005). As a defensive response to grazing and fire, grasses tend to accumulate more phytoliths, enhancing the DSi extraction (Cid et al., 1989; Massey et al., 2007; Melzer et al., 2010). Phytoliths present in grazers' feces are greater than 15 times more susceptible to dissolution than those derived from the senescence of plant tissues in the litter, due to physical and chemical digestive processes removing the organic film that envelopes phytoliths (Vandervenne et al., 2013). Remarkably, grazers are mobile and dependent on waterways, therefore they can further facilitate

the silica input to rivers. Moreover, it should be taken into account that land mammal mobility preceeding the late Pleistocene-early Holocene extinction events was much greater than that of today, representing a key factor in the past land-to-sea nutrient mobilization (Doughty et al., 2016). Fires act similarly to grazers, degrading the organic envelope of phytoliths, enhancing their solubility and their long-distance dispersion through ashes, which are rapidly mobilized by winds during dry periods, or by rivers during flooding events (Folger et al., 1967; Locker and Martini, 1986; LaClau et al., 2002; Pisaric, 2002; Vermeire et al., 2005; Pierson et al., 2011; Unzué-Belmonte et al., 2016).

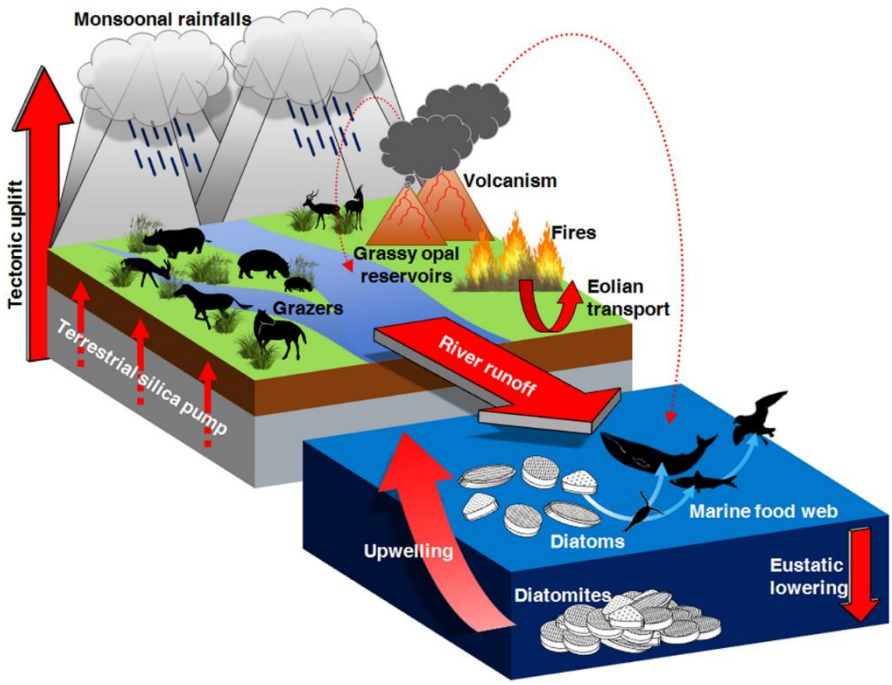

Figure 29. Diagrammatic representation of the relationships between the terrestrial silica cycle and diatomite deposition in the oceans.

3. The global geobiosphere contribution to late Neogene silica fluxes

The analysis of the late Neogene geo-paleontological global record reveals an intriguing coincidence between the intensification of tectonic processes, climate changes and terrestrial biotic turnovers, overall favorable to the strengthening of continental silica release to the ocean, and the latest Miocene opaline deposition (Kidder and Erwin, 2001; Falkowski et al., 2004; Kidder and Gierlowski-Kordesch, 2005; Cermeño et al., 2015).

Tectonic processes were particularly intense during the middle and late Miocene (Potter and Szatmari, 2009, 2015), and were responsible for the remarkable events of mountain uplift, closure and opening of oceanic gateways, acceleration of ocean spreading rates and increase of terrigenous fluxes to oceans. The two most cited and debated late Miocene geologic events were the uplift of the Tibetan-Himalayan sector at about 8 Ma (Harrison et al., 1992; Molnar et al., 1993; Zhisheng et al., 2001; Molnar, 2005; Zheng et al., 2003, 2006; Yang et al., 2016) and the roughly contemporaneous uplift of the Andean range, the latter associated with widespread volcanism (Garzione et al., 2008). These processes largely affected the global atmospheric circulation patterns, resulting in the reinforcement of monsoonal regimes, river runoff, continental erosion and nutrient cycling (Raymo et al., 1988; Rea, 1992; Molnar et al., 1993; Filippelli, 1997; Burckle, 1989; An et al., 2001; Garzione et al., 2008). Similar coeval processes involved other sectors, such as Africa and western Eurasia (Potter and Szatmari, 2009, 2015 and references herein).

Such events occurred in a global context of considerable sea-level lowering (Haq et al., 1987; Abreu and Anderson, 1998; Rai and Maurya, 2009) able to enhance the erosional processes primarily driven by tectonic uplift.

During the middle and late Miocene a remarkable displacement of the forest cover occurred associated with a global expansion of grassy biomes (Jacobs et al., 1999; Strömberg, 2011; Pound, 2012), likely induced by a long-term (~40 Ma) trend of cooling and aridification resulting from the progressive establishment of a marked seasonality and wide rain shadows in continental interiors. The growth of ice caps during the middle-late Miocene (Zachos et al., 2001) and the widespread Neogene tectonics (Rea et al., 1998; Dettman et al., 2001; Zhisheng et al., 2001; Guo et al., 2004; Sepulchre et al., 2006; Kohn and Fremd, 2008), actively contributed to such an ecological transition.

The emergence of C_4 photosynthesis was a powerful physiological innovation which also contributed to enhance this turnover. Originally proposed as an ecological response to a supposed global pCO_2 drawdown (Cerling et al., 1997; Ehleringer et al., 1997), the C_4 revolution is currently considered a consequence of enhanced seasonality, water stress and recurrence of fire, all conditions that characterized the latest Miocene landscapes (Pagani et al., 1999; Bond et al., 2005; Keeley and Rundel, 2005; Beerling and Osborne, 2006; Tipple and Pagani, 2007; Osborne, 2008; Scheiter et al., 2012; Hoetzel et al., 2013; Bond, 2015). However, C_3 grasslands remained common at higher latitudes and altitudes and continued to persist and to be grazed upon in wetter patches of tropical-subtropical regions

dominated by C_4 grasses and sedges (Edwards et al., 2010; Strömberg, 2011). Actually, it is possible to affirm that "*fully open grasslands, whether C_3 or C_4, were likely a late Miocene-Pliocene phenomenon*" (Strömberg, 2011). However, as far as the differences between the silica content of C_3 and C_4 grasses are concerned, the available data are rather scanty and contradictory (e.g. Kaufman et al., 1985; McInerney et al., 2011), with just a few studies stating that C_4 grasses accumulate more phytoliths than C_3 grasses (Merceron et al., 2005; Ségalen et al., 2007; Bouchenak-Khelladi et al., 2009). The question is complicated by the fact that grass opal content is not simply the direct product of the evolutionary history of the grass taxa, but represents an ecological response to grazing and fire (see above). Therefore, it is reasonable to hypothesize that the global rise of grassy open habitats, not their specific C_3-C_4 grass composition (apparently not influential in terms of phytolith production), represents the crucial biotic event that enhanced the terrestrial silica pump in the latest Miocene.

The grassland spread had a significant influence on terrestrial animal communities, especially among mammals (Janis, 1993), but also among birds (Fuchs et al., 2015) and insects (Voje et al., 2009). The Miocene-Pliocene herbivore record clearly shows a marked adaptation to cursorial movements, and to the improvement of the chewing of abrasive particles like phytoliths and grit (i.e. hypsodonty and hypselodonty), thereby providing a clear indication of the broad occurrence of grass-dominated open habitats subjected to periodical drought (Damuth and Fortelius, 2001; Hummell et al., 2010; Liu et al., 2012; Kaiser et al., 2013; Retallack, 2013).

The expansion of grass-dominated "flammable ecosystems" provided the fuel for the increase in the fire regime around 7 Ma, as suggested by the global charcoal record (Bond, 2015).

Finally, the increased dust accumulation recorded in many oceanic and terrestrial sectors during the latest Miocene (Diester-Haass et al., 2006) suggests the global intensification of the eolian transport, likely favored by the reduction of the dense arboreal cover and by the strengthening of monsoonal winds. Winds may have provided a significant contribution to the continental silica flux, blowing phytolith-rich dusts removed from grassland top soils during arid periods.

Summarizing this long discussion, the integrative analysis of the available data indicates that the late Miocene-early Pliocene opaline peak was broadly coeval to the global rise of C_3 and C_4 grasslands populated by grazers, affected by fire and wind, and to an active geodynamic context and low global eustatic level (**Fig. 30)**. In some sectors of the Pacific margin of North and South America, reinforced upwelling triggered by global cooling helped diatom proliferation (Suto et al., 2012), but the amount of silica supplied by continents was evidently enough to ensure opaline production also in typical oligotrophic contexts (Kemp and Baldauf, 1993).

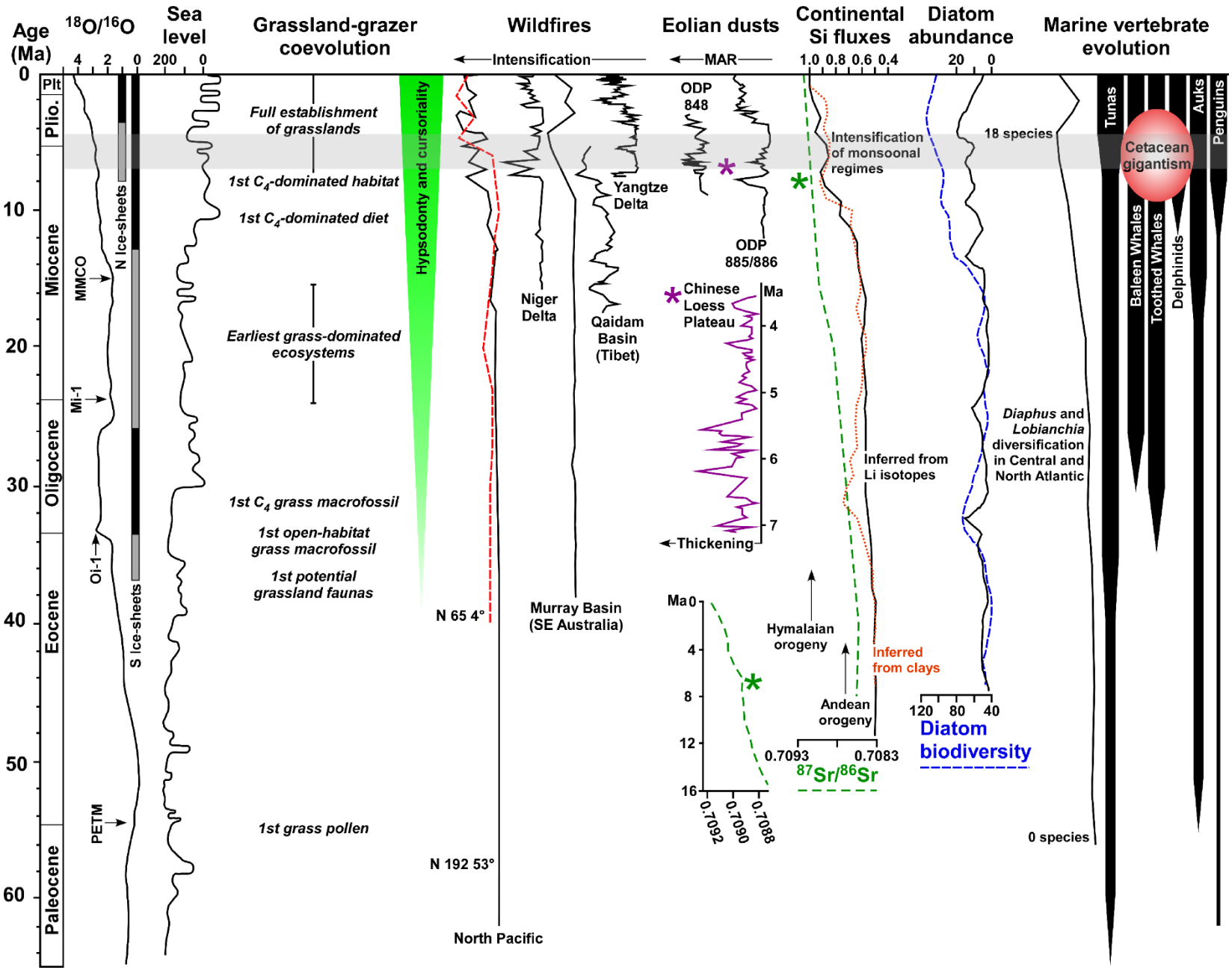
Age (Ma)
$^{18}O/^{16}O$
Sea level
Grassland-grazer coevolution
Wildfires
Eolian dusts
Continental Si fluxes
Diatom abundance
Marine vertebrate evolution
Intensification
MAR
Plt
Plio.
Miocene
Oligocene
Eocene
Paleocene
MMCO
Mi-1
Oi-1
PETM
N Ice-sheets
S Ice-sheets
Full establishment of grasslands
1st C_4-dominated habitat
1st C_4-dominated diet
Earliest grass-dominated ecosystems
1st C_4 grass macrofossil
1st open-habitat grass macrofossil
1st potential grassland faunas
1st grass pollen
Hypsodonty and cursoriality
N 65 4°
N 192 53°
North Pacific
Niger Delta
Yangtze Delta
Qaidam Basin (Tibet)
Murray Basin (SE Australia)
ODP 848
ODP 885/886
Chinese Loess Plateau
Ma
Thickening
Hymalaian orogeny
Andean orogeny
Inferred from clays
Inferred from Li isotopes
$^{87}Sr/^{86}Sr$
Intensification of monsoonal regimes
18 species
0 species
Diatom biodiversity
Diaphus and Lobianchia diversification in Central and North Atlantic
Tunas
Baleen Whales
Toothed Whales
Delphinids
Auks
Penguins
Cetacean gigantism

◄**Figure 30**. Proxies of the global intensification of silica cycle during the Cenozoic. $^{18}O/^{16}O$ (‰) – Zachos et al. (2001); Sea level (m) – Haq et al., 1987; Grassland-grazer coevolution – Jacobs et al. (1999), Strömberg (2011); Wildfires (charcoal record) – Bond (2015), Miao et al. (2016); Eolian dusts – Rea et al. (1998), Diester-Haass et al. (2006); $^{87}Sr/^{86}Sr$ (‰) – Filippelli (1997), Potter and Szatmari (2015); Continental Si fluxes (relative to present) – Cermeño et al. (2015); Diatom abundance (% median/smear slide) and biodiversity (% to modern) – Lazarus et al. (2014), Renaudie (2016); Marine vertebrate evolution – Norris et al. (2013), Schwarzhans and Aguilera (2013), Pyenson and Vermeij (2016), Mayr et al. (2017). The temporal extension of the late Miocene-early Pliocene opaline peak is roughly indicated by the gray horizontal bar. PETM –Paleocene-Eocene Thermal Maximum; Oi-1 – 1st Oligocene oxygen isotope event; Mi-1 – 1st Miocene oxygen isotope event; MMCO – Middle Miocene Climatic Optimum.

4. The Messinian silica-enrichment of the Mediterranean

The origin of lower Messinian diatomites in the Mediterranean has been traditionally interpreted as the record of the early stages of restriction of the Atlantic connection initiated at around 7.2 Ma and possibly resulting from the combined effect of tectonic uplift and glacio-eustatic fluctuations (Kouwenhoven et al., 1999; Krijgsman et al., 1999). According to this interpretation, such conditions may have promoted a sluggish deep water circulation and the increase of bottom anoxia characterized by weak benthic activity, which therefore favored the preservation of diatom tests and opaline deposits (e.g., Parea and Ricci Lucchi, 1972; Sturani and Sampò, 1973; Sturani, 1976). In addition, nutrient retention favored by the weakening of the deep water outflow from the Mediterranean stimulated a considerable diatom productivity. However, as prophetically noted by Ogniben (1955, 1957), the remarkable world-wide occurrence of the Upper Miocene opaline deposits suggests that besides the Mediterranean regional context, other global-scale controlling factors must be taken into account. For instance, a reinforced upwelling

regime bringing deep, nutrient-rich waters toward the photic zone, has been proposed as the main triggering factor of diatom productivity (e.g., Perrodon, 1957; Sturani and Sampò, 1973; McKenzie et al., 1979; Moissette and Saint Martin, 1992), mostly based on the relative abundance of the diatom *Thalassionema nitzschioides* and the foraminifer *Globigerina bulloides* in a few lower Messinian diatomites (but see Pestrea et al., 2002). Nevertheless, the widespread occurrence of giant mat-forming diatoms like *Coscinodiscus* spp. and members of the family Rhizosoleniaceae as well as of neogloboquadrinid foraminifers, points to the periodic stratification of the basin (Kemp et al., 2000; Kemp and Villareal, 2013) likely associated with conspicuous freshwater inputs. Moreover, the progressive attenuation of the upwelling currents and the increased influence of river runoff have been highlighted in many studies focusing on the factors stimulating the deposition of lower Messinian diatomaceous successions, especially in the central and eastern Mediterranean domains (e.g., van der Zwaan, 1979; Suc et al., 1995; Bellanca et al., 2001; Blanc-Valleron et al., 2002; Londeix et al., 2007; Pérez-Folgado et al., 2003), but also in the westernmost settings (e.g. Moissette and Saint Martin, 1992; Mansour et al., 1995; van Assen et al., 2006). Therefore, the role of upwelling currents in the Mediterranean during the early Messinian should be framed within a context of considerable river runoff (Gladstone et al., 2007; Simon et al., 2017).

In any case, even admitting a marked influence of riverine contribution, the ultimate sources of the DSi delivered to the Mediterranean basin remain unclear.

The lack of effort dedicated to this topic is surprising, particularly if considered from the perspective of a land-locked sea surrounded by vast drainage systems (Gladstone et al., 2007) and suffering the initial stages of ongoing isolation from the oceanic domain (Kouwenhoven et al., 1999; Krijgsman et al., 1999). In such a regional context, the rapid exhaustion of silicon and its efficient burial rate after each event of frustule settling reduced the residence times of this element in the water column (Laruelle et al., 2009), likely resulting in a growing demand from diatom communities of crucial importance to maintain their ecological supremacy over non-siliceous phytoplankton (see above). Consequently, a cyclical injection of DSi was crucial to support the proliferation of diatoms and their preservation in the sedimentary record. Therefore, the assessment of both oceanic and terrestrial sources of DSi, as well as of the tectonic and eustatic processes that may have favored its basinward release and the possible role of volcanism, is needed to explain the latest Miocene silica enrichment in the Mediterranean.

4.1. The role of the Atlantic inflow

As mentioned above, the Atlantic Ocean experienced a dramatic decrease in opaline accumulation since about 15 Ma. A partial recovery occurred during the late Miocene-early Pliocene, although the Indo-Pacific domain continued to represent the main opal sink and the Antarctic opal belt started to develop at that time (e.g., Gombos, 1984; Diester-Haass et al., 2002; Diekmann et al., 2003; Cortese et al.,

2004; Renaudie, 2016). Intriguingly, the Amazon drainage system and its effective runoff toward the Atlantic Ocean, started around 9 Ma becoming fully established at 6.8 Ma because of the intensification of the Andean uplift in a context of global lowstand (Hoorn et al., 2010, 2017; Latrubesse et al., 2010). The Amazon river drained extensive grassy areas, which developed from 9 Ma on soils derived from the Andean dismantling (Hoorn et al., 2010, 2017; Latrubesse et al., 2010). On the other side of the Atlantic, fire-inception in grass-dominated habitats is observed in the pollen and charcoal records from the Niger delta since the Tortonian-Messinian boundary (Morley and Richards, 1993). The pollen record of ODP Site 1081 (offshore Namibia) highlights an abrupt increase of grasses at 6.8 Ma and a peak in charred cuticles between 7.1 and 5.8 Ma (Hoetzel et al., 2013). Therefore, both the western and eastern Atlantic continental margins were prone to the release of DSi during the late Neogene. Under this perspective, the Mediterranean was the easternmost *locus* of the Atlantic opaline accumulation, and may have sequestered significant amounts of DSi during the late Neogene phase of silica-enrichment of the Atlantic waters.

However, the reduction of the connections between the Atlantic Ocean and the Mediterranean Sea, started at about 7.2 Ma because of the tectonic uplift of the Rifian and Betic gateways (Kouvenhowen et al., 1999; Capella et al., 2016), may have severely limited the budget of DSi entering the Mediterranean Sea. In this context, considering a Messinian anti-estuarine thermohaline circulation pattern similar to the modern one (Kouvenhowen and van der Zwaan, 2006; but see Martín

and Braga, 1994), the possible oceanic DSi inputs were limited to the surface Atlantic inflow, which in terms of DSi concentration and transport is rivaled by the present Mediterranean riverine discharge (Ribera d'Alcalà et al., 2003). Therefore, although an Atlantic contribution is not *a-priori* excludable, the main controlling factor of the Mediterranean silica-enrichment actually was the continental supply from the surrounding regions.

4.2. The terrestrial sources of silica

The late Miocene runoff in the Mediterranean basin was at least three times greater than that of today and was strongly controlled by the African rivers, particularly in the central and eastern parts of the basin (Gladstone et al., 2007). The intensification of the African runoff was most likely related to the rearrangements of atmospheric circulation patterns, in turn promoted by the combination of the orbital variability, i.e. the precessionally-controlled northward shift of the Intertropical Convergence Zone, as well as by the late Miocene geodynamics (Griffin, 2002; Marzocchi et al., 2015). The tectonic uplift of Himalaya-Tibet (~8-7 Ma) and Ethiopian (~10-6 Ma) plateaus triggered the enhancement of the coupled Asian-African monsoonal system and the rejuvenation of the inner African watersheds (Sepulchre et al., 2006; Gani and Gani, 2007; Köhler, 2008; Marzocchi et al., 2015). At the same time, but especially between 7.5 and 4.6 Ma, the Eonile, Sahabi, Gabes and Libyan basins began to supply the central and eastern Mediterranean with large

amounts of continental waters derived from boosted seasonal rainfalls (Zeit Wet Phase *sensu* Griffin, 2002). These basins covered vast regions of the African continental interiors, characterized by the expansion of grass-dominated open biomes during the late Neogene.

In the sectors immediately surrounding the Mediterranean, a general trend of cooling and seasonal aridification occurred from 8-7 Ma until 5.9 Ma, promoting a sharp decrease in the sea surface temperature (from 28 to 19°C), which reached its lowest values at 7.2 Ma (Tzanova et al., 2015; Böhme et al., 2017). The onset of Sahara desertification around 7 Ma (Schuster et al., 2006; Klaver et al., 2015; Böhme et al., 2017) is one of the most impressive results of the late Tortonian-early Messinian perimediterranean climate deterioration. Most likely, the resulting expansion of open habitats and the consequent strenghtening of the eolian transport were able to induce a further increase of DSi concentration into the Mediterranean.

4.2.1. The inner African opal reservoirs

The progressive expansion of savannah habitats with a significant C_4 component in central Africa about 7 Ma is documented by the mammal assemblages (dominated by high-crowned bovids), mesowear and isotope ratios of dental remains of Toros-Menalla, Tchad (Vignaud et al., 2002; Ségalen et al., 2007; Blondel et al., 2010). Another evidence of the presence of the latest Miocene grassland expansion in Central Africa is the high abundance of smectite in the clay fraction of Lake Chad,

deriving from the leaching of vertisols surrounding the lake and developed under a grassy cover (Moussa et al., 2016). The hydrographical and paleoecological continuity between Tchad and Libya during the Messinian is suggested by the co-occurrence of remains of the wetland anthrachotheriid *Lybicosaurus petrocchii,* in coeval strata at Toros-Menalla and Sahabi (Lihoreau et al., 2006), as well as by similar ichthyofaunas (e.g., Stewart, 2001).

The analysis of the pollen content of the DSDP 231 core from the Gulf of Aden documents a peak in grass fraction around 10.5 Ma, suggesting an early radiation of grass-dominated ecosystems in eastern Africa, followed by two subsequent stages of expansion at about 7 Ma and 5.5 Ma (Bonnefille, 2010). Although the East African grass pollen increase at ~7 Ma was associated with an isolated tree pollen peak, likely indicative of a very short humid phase, the early Messinian grassy burst occurred during an overall decrease of the forest cover, attesting the rise of full open landscapes during this period. The early Messinian phase of grassland spread in Eastern Africa coincided with the increase of biodiversity and hypsodonty values in herbivorous mammals, particularly bovids, as well as with shifts toward a C_4-rich diet (Cerling et al., 1997; Bibi et al., 2009; Bibi, 2011; Bobe, 2011; Stromberg, 2011). At about 6 Ma, the East African grasslands collapsed, and a dramatic expansion of arid shrublands occurred (Bonnefille, 2010).

4.2.2. The perimediterranean grassy biomes

The reconstruction of the perimediterranean Messinian biomes provided by Favre et al. (2007), shows the presence of a mainly C_3-dominated grassy cover (Cerling et al., 1997; Senut et al., 2009; but see Böhme et al., 2017) along the actively drained southern margin of the Mediterranean (Gladstone et al., 2007), from the Iberian Peninsula to the Nile delta, including the emerging Apennine chain, Southern Greece and western Anatolia. According to Fortelius et al. (2006), high hypsodont herbivores well adapted to exploit the grass-dominated ecosystems surrounding the Mediterranean, were widespread at about 7-5 Ma.

More specifically, the North African fossil record reveals a clear trend toward more open habitats during the late Miocene (Fauquette et al., 2006; Favre et al., 2007). In Morocco, herbaceous taxa mainly represented by Poaceae and Asteraceae are abundant in the Tortonian-Messinian pollen record from the Rifian Corridor (Bachiri-Taoufiq et al., 2008). In Algeria, the lower Messinian deposits of Chelif Basin indicate a similar scenario, with extensive grassy lowlands behind the littoral zone (Chikhi, 1992). The abundant carbonized plant remains recovered in the Beida Stage of the Chelif Basin, suggest the presence of grassy environments affected by fires in the proximity of the basin. Anderson (1936) reported that "*Imprints of small blades of fresh- or brackish-water monocotyledons are fairly common*" and "*The blades of sedges or grasses are of types that grew either in fresh or, at most, brackish water and are probably not far from their original habitat*", Based on the vertebrate

assemblage of the Sahabi Formation, Boaz et al. (2008) inferred a wooded savannah punctuated by wetlands in northern Libya around 7 Ma. Compared to North Africa, Calabria and Sicily probably experienced more arid conditions (Suc et al., 1995; Fauquette et al., 2006). Nevertheless, as previously reported, their faunal assemblages suggest similar savannah-like ecological settings (Ferretti et al., 2003; Rook et al., 2006; Gramigna et al., 2008; Marra et al., 2011). The palynological record of offshore Egypt (site Naf 1) corroborates a scenario where grassy open habitats with different composition (steppe-like on the western side, savannah-like on the eastern side, according to Fauquette et al., 2006) formed a more or less continuous belt along perimediterranean North Africa during the Messinian.

In western Eurasia, the presence of open habitats dominated by Poaceae and other herbaceous taxa is well documented in the Iberian Peninsula since the Early Miocene, and an important increase of southern and eastern steppes in this region is recorded during the Tortonian and Messinian (Jimenez-Moreno et al., 2010; Casas-Gallego, 2015). On the Italian Peninsula, Neogene open vegetation is poorly represented in the northern regions (Bertini and Martinetto, 2008), but abundant grasses are documented in the early Messinian Apennine localities such as Gabbro and Velona (Berger, 1957; Trevisan, 1967; Bradley and Landini, 1984; Ghetti et al., 2002; Favre et al., 2007), suggesting a N-S aridity gradient. A synoptic overview of the terrestrial paleoecological transitions in Greece was provided by Ioakim et al. (2005), who reported a regional trend toward more open biomes in northern, central and southern basins during the late Miocene (10-7 Ma), as well as a N-S gradient

similar to that recorded in Spanish and Italian localities. Recently, Böhme et al. (2017) have inferred a savannah biome with a significant C_4 grassy component, increasing from the late Tortonian to the early Messinian, at Pikermi and Pirgos. This is only partially consistent with the phytolith and pollen record of Anatolia and surrounding areas, which suggests the presence of mostly C_3- (rather than C_4-) dominated savannah settings since the early Miocene, and their subsequent expansion at about 9 Ma (Strömberg et al., 2007, 2011; Biltekin, 2010; Kayseri-Özer et al., 2017).

In the mammalian communities, two main events occurred in the late Miocene, the so-called Vallesian Crisis and the rise of Pikermian mammals. The Vallesian event occurred around 9.7 Ma and consisted of the extinction of many european forest-adapted taxa (e.g., tapirids, cervids, hominoids, false saber-tooth cats and bear dogs, flying squirrels; Agustí et al., 2013). The Pikermian faunas, characterized by hypsodont savannah-adapted equids and bovids, originated in the sub-Paratethyan region around 13 Ma and dispersed westward, reaching their climax around ~8-7 Ma (Eronen et al., 2009; Böhme et al., 2017). Since the earliest Messinian, they were substituted by more dry-adapted mammalian guilds (post-Pikermian faunas *sensu* Böhme et al., 2017), until their final disappearance around the Miocene-Pliocene boundary, most likely due to the return of more humid and forested conditions unfavorable to the presence of large assemblages of grazers in western Eurasia (Fortelius et al., 2014).

4.3. Tectonics and eustasy during diatomaceous deposition

The Mediterranean diatomaceous deposition between 7 and 6 Ma occurred in a context of recurrent eustatic fluctuations (McKenzie et al., 1979; Thunell et al., 1987; Pomar and Ward, 1994; Kouvenhowen et al., 1999; Pedley et al., 2007; Orszag-Sperber et al., 2009) and active geodynamics (see below). Tectonics and eustasy may have enhanced the release of continental DSi through the steepening and expansion of hydrographic networks and the exposure of continental margins. In any case, it is necessary to take into account that diatomites originated in the distal sectors of the sedimentary basins mostly reached by nepheloid plumes triggered by riverine transport or shelf instability, and therefore by the finest, dissolution-prone and more distal detrital fraction deriving from the continental dismantling, able to support diatom productivity without the dilution of the opaline tests due to the detrital fraction, thereby promoting the preservation of pristine biogenic sediments (e.g., Sturani and Sampò, 1973).

4.3.1. Betics-Rif

Diatomite deposition in the Betic Cordillera during the late Tortonian-early Messinian coincides with important events of uplift, basin shallowing and restriction, siliciclastic deposition and subsidence (Krijgsman et al., 2001; Sierro et al., 2001; Braga et al., 2003; Jolivet et al., 2006), which are related to the tectonic inversion of

the Algero-Balearic basin (Giaconia et al., 2015). Clear markers of synsedimentary tectonic processes are small-scale deformations and the emplacement of turbiditic layers and slumps recorded in the Sorbas-Nijar basins (Krijgsman et al., 2001; Sierro et al., 2001, 2003; Braga et al., 2003; Pérez-Folgado et al., 2003; Flores et al., 2005). The closure of the Betic Corridor started with the continentalization of the Granada and Guadix basins about 7.3 Ma and was terminated at 6.8 Ma (Jolivet et al., 2006). The mammalian record suggests land bridges were formed by the interplay between tectonic and eustasy, which sporadically connected the Iberian Peninsula and North Africa ~250.000 years before the onset of the salinity crisis (Agustí et al., 2006; Gibert et al., 2013).

In the Rif area, Krijgsman et al. (1999) interpreted the shallowing of the Taza-Guercif basin at around 7.2 Ma as the result of regional tectonic uplift and global sea level lowering. This process was responsible for the progressive restriction of the Rifian Corridor, which terminated at about 6 Ma. Conversely, the sectors surrounding the eastern Rifian area, characterized by diatomaceous deposition (e.g., Boudinar and Melilla-Nador), were mainly affected by extensional tectonics (Azdimousa et al., 2006). Moreover, the Arbaa Taourirt basin records a sedimentological transition, from marls to shallow marine conglomerates and sandstones in the early Messinian, while the nearby Boudinar basin shallowed at 6.5 Ma (Achalhi et al., 2017).

4.3.2. Atlas-Tell

Toward the easternmost regions of northwestern Africa (Algeria, Tunisia), the Neogene uplift was less intense in a general setting primarily characterized by extensional tectonics (Frizon de Lamotte et al., 2009). Diatomaceous deposition in the Chelif Basin occurred during its maximum widening, in a local context dominated by a moderate tectonic uplift (Neurdin-Trescartes, 1995). However, synsedimentary tectonic activity is recorded in the Algerian diatomitic successions by the local occurrence of slumps (Perrodon, 1957; Rouchy, 1982), and the emergence of the Algerian coastline between Algiers and Chenoua Massifs, which started in the middle Miocene and apparently increased since the late Miocene (Authemayou et al., 2016).

4.3.3. Alps-Apennine

The extensive late Miocene erosion of the Alpine belt started at about 5.5 Ma (Willett, 2010), and was preceded by the rapid exhumation of the external crystalline massifs (Mt. Blanc, Aiguilles Rouges, Aar-Gotthard and Argentera) between 10 and 5 Ma (Bigot-Cormier et al., 2000, 2006; Carrapa et al., 2004; Glotzbach et al., 2008, 2010; Valla et al., 2012). The enhanced dismantling of Ligurian Alps occurred around 7 Ma, in response to relative sea-level lowering (Foeken et al., 2003).

According to Wölfler et al. (2016), the exhumation of many sectors of the eastern Alps occurred during the Messinian.

In the Piedmont Basin (PB), the terrigenous contribution during the diatomaceous deposition is attested by the recurrence of turbiditic siltstones and sandstones and by the presence of plant remains within the Pecetto di Valenza succession (Sturani and Sampò, 1973; Pavia, 1989; Gaudant et al., 2010). The major source of detrital supply to the PB during the middle-late Miocene was most likely the Argentera Massif, at least until 7.12 Ma (Carrapa et al., 2004). A huge slump recorded in the Pollenzo section of the PB provides evidence of the remarkable synsedimentary tectonic activity during the early Messinian in this area (Dela Pierre et al., 2011).

The Apennines uplift rate intensified since the late Miocene, in response to the opening of the Tyrrhenian Basin between 8.6 and 7.8 Ma (Duermeijer et al., 1998) and the related eastward migration of the chain system. In the Northern Apennines, the Peri-Adriatic foredeep basin originated in an active compressional setting that led to the deposition of turbidites sourced by the erosion of the Alps (i.e. Marnoso-Arenacea Fm.; Ricci Lucchi, 1986), and organic-rich shales. The latter are coeval to the Tripoli Formation deposited in the marginal settings, and are associated with enhanced denudation processes favored by the uplift of the surrounding sectors (Coward et al., 1999; van der Meulen et al., 1999; Roveri et al., 2001; Hüsing et al., 2009) and by the development of sill-restricted basins (Savelli and Wezel, 1978). The diatomites outcropping in Emilia Romagna, Marche and Tuscany are

characterized by important markers of synsedimentary tectonics (e.g., Sarti et al., 1995), riverine incision (Savelli and Wezel, 1978; Arcaleni et al., 1995) and terrestrial supply (Savelli and Wezel, 1978; Bradley and Landini, 1984). Erosional surfaces, unconformities and synorogenic turbiditic deposits, confirm the active denudation of Central Apennines during the late Tortonian-early Messinian (Centamore and Rossi, 2009; Vezzani et al., 2010). Diatomites from the Capo di Fiume section are characterized by recurrent markers of synsedimentary tectonics and terrigenous supply, such as intrastratal microfractured zones, slumps, speckled beds, fillites and other remains of continental origin (Carnevale, 2004b). In the Southern Apennines, active compressional tectonics gave rise to the formation of wedge-top basins and to the deposition of synorogenic sediments during the late Tortonian-early Messinian (Vezzani et al., 2010). During the Messinian, the forearc Crotone basin was characterized by "*the highest accumulation rates of the whole Late Neogene-Quaternary*" and by *"alternating pulse of subsidence and uplift"* (Massari et al., 2010). The sediment supply to the Crotone and Rossano basins was supported by the erosion of the Sila Massif, along the Ionian flank of the Calabrian Arc, since the late Tortonian (Barone et al., 2008).

4.3.4. Sicily

A series of E-W striking wedge-top basins developed during the late Tortonian-early Messinian in Sicily, in response to the southward migration of the

fold and thrust Apennine-Maghrebides belt (Pedley and Grasso, 1993; Rosenbaum et al., 2002; Roveri et al., 2008). These basins were filled with siliciclastic (Terravecchia Fm.) and pelagic sediments (Licata Fm.), which are overlain by the diatomaceous Tripoli Fm. (Butler et al., 1995). The diatomitic deposits exhibit variation of thickness and sedimentation rate, which point to a strong synsedimentary tectonic activity (Suc et al., 1995; Pedley and Maniscalco, 1999), further confirmed by the recurrence of slumps (Richter-Bernburg, 1973; Bellanca et al., 2001). The Iblean foreland of SE Sicily, records a late Tortonian-early Messinian tectonic quiescence (Pedley et al., 2007), although manifold volcanic events occurred in this area, where thin diatomitic layers are associated with diatremes, since about 7 Ma (Schmincke et al., 1997).

4.3.5. Greek Islands

Following the late Miocene collision between the Apulian platform and western Greece, the latter experienced a shortening phase that promoted the progressive uplift of the Ionian Islands, especially in the mid-Pliocene (van Hinsbergen et al., 2006). The partial emergence of Zakynthos Island started, however, during the early Messinian and is attested by terrigenous layers, rich in terrestrial plant remains, which accumulated in Laganas Bay (Papanikolau and Dermitzakis, 1981; Rouchy, 1982), and Corfu was also partly uplifted and eroded during the Messinian (van Hinsbergen et al., 2006).

The increased denudation of the Aegean uplifted area led to the first stage of sapropel deposition at Gavdos around 10 Ma (Schenau et al., 1999), while a change in the source of terrigenous supply occurred about 8.2 Ma, in this case with a considerable contribution from North African rivers (Köhler et al., 2008). A strong tectonic control on the lower Messinian succession of Metochia is inferred by Drinia et al. (2007), who also reported reworked benthic foraminiferans (*Elphidium* spp. and *Asteriginata planorbis*) most likely derived from erosional processes involving the shallower area of the basin.

4.3.6. Cyprus and western Anatolia

Extensional tectonics affected Cyprus during the late Miocene-early Pliocene, although evidence of an incipient emersion and erosion of the Troodos Massif are recorded in the upper Tortonian-lower Messinian sediments bordering this ophiolitic complex (Orszag-Sperber et al., 2009; Manzi et al., 2016). In the Polemi basin, markers of synsedimentary tectonics (slumps, angular unconformities) and terrigenous supply (plant remains) are recorded in many sections (Merle et al., 2002; Orszag-Sperber et al., 2009). The Pissouri basin was certainly affected by synsedimentary tectonics, at least during the last phases of diatomaceous deposition, as revealed by the presence of slumps (Krijgsman et al., 2002; Merle et al., 2002). The Tokhni section of the Psematismenos basin recorded an increase in detrital grains from 6.5 Ma, suggesting the intensification of riverine supply, probably linked

to the tectonically-induced shallowing of the basin (Orszag-Sperber et al., 2009; Gennari et al., 2017). The Kyrenia range was actively uplifted in the late Miocene (Rouchy, 1982; Harrison et al., 2004; McCay and Robertson, 2013; Varol and Atalar, 2016).

The late Miocene uplift of the Taurides range, along the southern margin of the Central Anatolian plateau, started between 8-7 and 5.45 Ma (Cosentino et al., 2012; Schildgen et al., 2012), and its dismantling resulted in the massive accumulation of terrigenous deposits in the Adana basin (Faranda et al., 2013).

4.4. The role of volcanism

A causal relationship between Mediterranean volcanism and the deposition of Messinian diatomites was proposed by Anderson (1933, 1936) and Ogniben (1955, 1957), on the basis of the seminal work of Taliaferro (1933). Nevertheless, such a relationship is weakly supported by stratigraphic evidence, particularly by the lack of a systematic association between the diatomitic and ash layers. In the interval comprised between 7 and 6 Ma only a few volcanic events are documented in the perimediterranean region (see Potter and Szatmari, 2015). Volcanism mainly affected the southwestern Mediterranean area (Savelli et al., 2002; Doblas et al., 2007) and the Hoggar region in Southern Algeria (Azzouni-Sekkal et al., 2007). Only in the Melilla-Nador and Chelif basins and locally in Sicily (Ogniben, 1955, Suiting and Schmincke, 2010) and in a few sectors of the Southern Apennine (Matano,

2007), does the occurrence of several ash layers interbedded with diatomites support the hypothesis of a volcanic origin of DSi, but most likely at a very local scale (Courme and Lauriat-Rage, 1998; Saint Martin et al., 2003; van Assen et al., 2006). In the northernmost Mediterranean sector involved in the diatomaceous deposition (Piedmont Basin), no volcanic activity has been documented during the Messinian (Sturani and Sampò, 1973). The age for eastern Mediterranean volcanism was substantially out-of-phase with the early Messinian marine diatomite deposition, with only very minor events occurring between 7 and 6 Ma, in Thrace and western Anatolia (Fytikas et al., 1984; Agostini et al., 2007).

4.5. A general model to interpret the Mediterranean opal burst

The above review of the current state of knowledge on the lower Messinian Mediterranean opaline event strongly suggests that diatomites may represent the sedimentary expression of the complex interplay between ecological turnover on land and predisposing conditions in the basins, rather than the simple byproduct of basin restriction preluding the onset of the Messinian salinity crisis.

Even if the restriction of the Atlantic communication at ~7.2 Ma (Kouvenhowen and van der Zwaan, 2006) may have promoted nutrient retention in the Mediterranean, in the absence of a continuous supply of DSi diatoms would have been quickly replaced by other groups of microplaktonic organisms able to flourish under silica-limited conditions (see above) and the deposition of diatomaceous

sediments in the circum-mediterranean marginal basins would have been severely limited. On the contrary, the extension, thickness, and excellent preservation of the lower Messinian diatomites, are indicative of an overabundance of DSi in Mediterranean waters, able to promote diatom productivity and the preservation of their opaline remains within the sedimentary archive. DSi was supplied by river runoff and, most likely, by the enhanced eolian transport of phytoliths from continental sectors surrounding the Mediterranean peripheral basins, particularly from the African inlands. The onset of diatomaceous deposition is remarkably coeval with the expansion of the East African grassy biomes at about 7 Ma and with the rise of grass-dominated ecosystems in the western and central regions of the continent (Morley and Richards, 1993; Bonnefille, 2010). On the other hand, the demise of Mediterranean diatomites at about 6 Ma coincided with the abrupt decline of grasslands and the maximum expansion of arid shrublands in East Africa (Bonnefille, 2010). These intriguing time relationships strongly support a causal linkage between terrestrial turnovers and marine opaline production in the Mediterranean during the latest Miocene (**Fig. 31**). It is reasonable to hypothesize that the general trend of aridification that occurred in Eastern Africa during the early Messinian stage of grassland expansion, acted as a further catalyst for silica mobilization. At least initially, both deforestation and desertification may have strongly favored the Mediterranean silica enrichment, promoting the opening of the African grassy opal sinks and making them more susceptible to release their huge siliceous reservoirs through stronger fluvial and eolian erosion. On the contrary, the

extreme drought affecting the East African landscapes at ~6 Ma reduced the extension of quickly dissolvable terrestrial opal reservoirs and promoted the expansion of opal-poor biomes or dusty environments, mostly composed of inert lithogenic silica scarcely exploitable by diatoms. As a consequence, the DSi budget of the Mediterranean dropped, severely limiting the development of the diatomaceous facies. Intriguingly, the decrease of the Eonile discharge after ~7 Ma, in response to the Sahara desertification (Klaver et al., 2015), is consistent with these interpretations.

Although the crucial factor for the silica enrichment of the Mediterranean was the African inland contribution, the local DSi-supply from circum-mediterranean regions was also relevant and may explain the temporal and spatial distribution of diatomite deposits and their variable thickness. The distribution of grass-dominated open biomes (Favre et al., 2007) and hypsodont mammals (Fortelius et al., 2006) in the Mediterranean region during the Messinian was associated with the main sites of diatomite deposition. The increases in cooling, aridity and habitat opening that occurred during the early Messinian in the Mediterranean region (Tzanova et al., 2015; Böhme et al., 2017), may have acted as further positive feedback mechanism for terrestrial silica mobilization, promoting concentrated seasonal rainfalls and strong winds able to remove the opal-rich topsoil layers of the perimediterranean grass-dominated habitats, similarly to what happened in Eastern Africa around 7-6 Ma.

Diatomaceous deposition occurred in basins widely affected by late Miocene geodynamics and sea-level fluctations. These basins were regularly eutrophied by the highest bioavailable portion of the terrigenous supply, and only marginally affected by the negative effects of the river discharge, for example the surface water turbidity that could inhibit the proliferation of phytoplankton or excessively dilute the biogenic fraction of the sediments. Only in these terms, is it possible to consider such settings as "starved" (*sensu* Butler and Grasso, 1993). Moreover, tectonic and eustatic re-arrangements affected the physiography of marginal basins (e.g., bathymetry and development of sills) and the accommodation space, influencing, for example, the thickness of diatomitic successions. At a regional scale, the Sicily Channel may have limited the connections between western and eastern sectors of the Mediterranean, amplifying the difference between their hydrologic regimes (Gladstone et al., 2007; Pérez-Folgado et al., 2003), well before the onset of the Messinian salinity crisis (Jolivet et al., 2006). Paleocurrents may have played a critical role in the redistribution of DSi within the Mediterranean peripheral basins. This may explain why the diatomaceous event at the two extremities of the Mediterranean, Algeria and Cyprus, occurred with different magnitudes, producing more extensive and thicker deposits in the Algerian localities. This is apparently surprising considering the proximity of many eastern basins to the main North African river mouths, where certainly large concentrations of DSi and other nutrients were introduced. Nevertheless, if an anti-estuarine circulation was active during the early Messinian (Kouvenhowen and van der Zwaan, 2006), the eastern

Mediterranean nutrient budget was partly transferred toward the westernmost domains through the Levantine Intermediate Waters. In this regard, the reconstructions of paleocurrents in the Chelif Basin provided by Neurdin-Trescartes (1995) suggest a relevant E to W paleoflow. Therefore, the Algerian basins may have profited from a favorable interplay between localized (herbaceous biomes, volcanism) and more distal sources of DSi.

Volcanic ashes, very scattered within the (westernmost) early Messinian diatomaceous successions of the Mediterranean, possibly played a local role as sources of readily exploitable silica for diatom communities. However, the cyclical occurrence of the diatomitic layers within the early Messinian successions suggests a periodical increase of silica levels in the basin, hardly compatible with discontinuous volcanic eruptions.

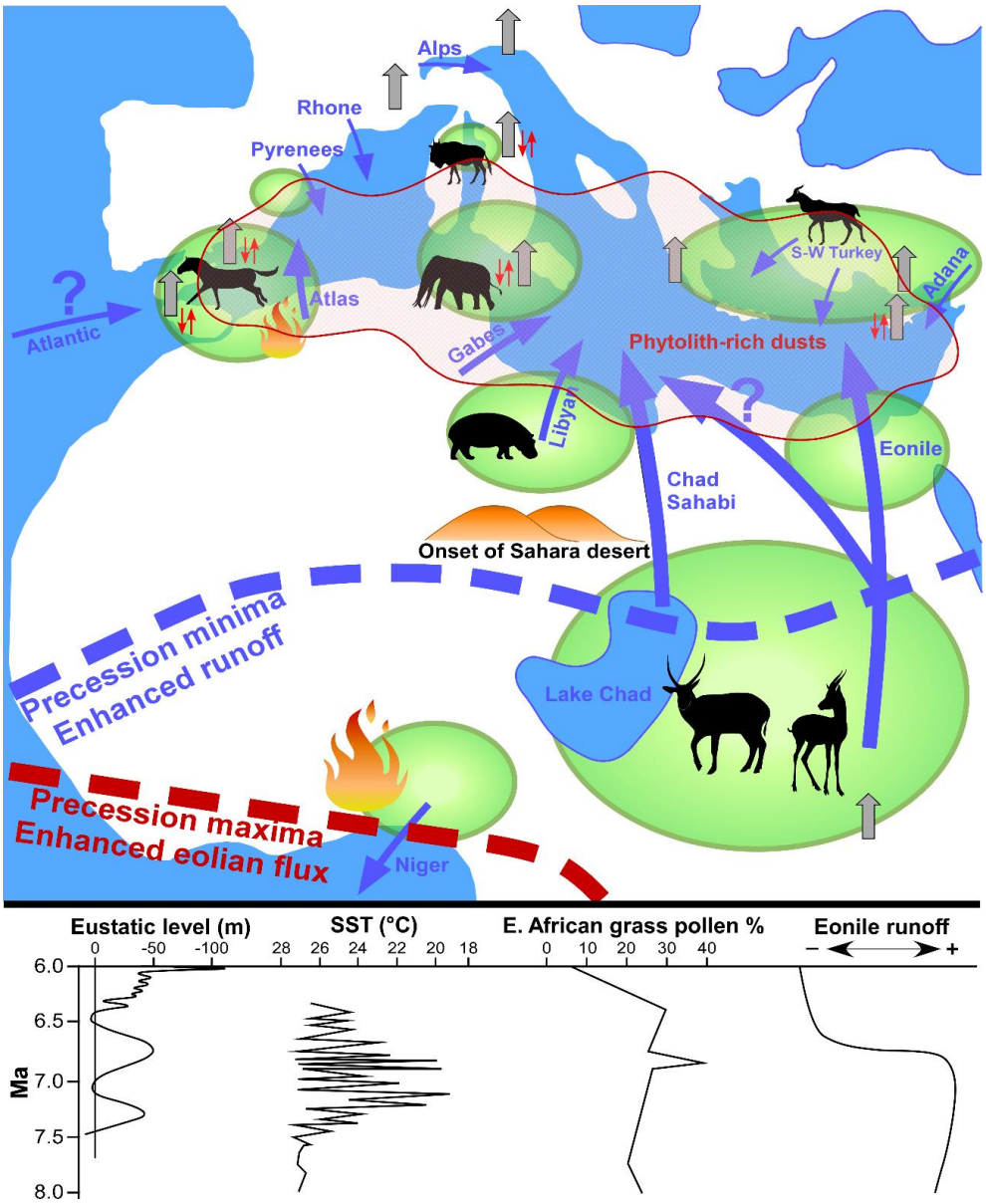

Figure 31. A simplified model to interpret the Mediterranean silica-enrichment during the early Messinian, in the light of the African and perimediterranean abiotic and biotic events. Tectonics and eustasy promoted the mobilization of the local opal reservoirs. Moreover, the intensification of monsoonal rainfalls during the northward migration of the Inter Tropical Convergence Zone (ITCZ) favored the DSi-rich runoff from grassy African interiors and perimediterranean regions, affected by aridification; the southward shift of the ITCZ promoted water stress, reduced runoff and increased eolian transport of phytoliths. Green circles represent the main grassy areas. Gray arrows indicate tectonic uplift. Red arrows indicate eustatic fluctuations in the main areas where diatomite deposition occurred. Eustatic level – Pedley et al. (2007); SST (Sea Surface Temperature) – Tzanova et al. (2015); East African grass pollen – Bonnefille (2010); Eonile runoff (inferred from DSDP sites 375-376) – Klaver et al. (2015). The blue question mark refers to the possible Eonile flow toward the Gulf of Sirt during the early Messinian, proposed by Carmignani et al. (2009).

5. Sapropel-diatomite couplet and laminated fabric: an interpretation

The most striking feature of the lower Messinian diatomitic successions is their rhythmic interbedding with organic rich layers (sapropels), arranged in cyclical successions that are extremely heterogeneous throughout the Mediterranean (**Fig. 27B**) and whose interpretation still represents a matter of intense debate (e.g., Nijenhuis, 1999; Pérez-Folgado et al., 2003). Moreover, diatomites are often characterized by a fairly laminated style that has been typically interpreted as evidence of anoxic conditions at the ocean bottom (e.g., Sturani and Sampò, 1973; Savelli and Wezel, 1978; Ciaranfi et al., 1980; Rouchy, 1982; Mansour et al., 1995).

However, an improved knowledge of diatom ecology and life cycles reveals that an alternative explanation can be proposed to properly interpret the context of diatomite accumulation. Many diatoms are able to constitute robust, rapidly sinking flocs and mats via chemical or physical aggregation (Smetacek, 1985; Alldredge and Gottschalk, 1989; Alldredge et al., 1993; Kemp and Baldauf, 1993; Passow et al., 1994, 2001; Bodén and Backman, 1996; Grimm et al., 1997; Pike and Kemp, 1999; Passow, 2002a,b; Prieto et al., 2002; Engel, 2004). Such aggregates efficiently bypass zooplankton grazing, and once deposited on the seafloor form resistant, impenetrable structures which hamper both benthic and infaunal activity, promoting the excellent preservation of seasonal laminae and their associated biological

content, also in well-oxygenated environments (Kemp, 1996; Brand et al., 2004; Esperante et al., 2015).

Oxygen-poor environments favor the preservation of diatom coating, composed of polysaccharides, amino acids and glycoproteins that protect frustules from dissolution in DSi-undersaturated waters (Lewin, 1961; Hecky et al., 1973). Bacteria, through their enzymatic activity, are the main degrading agents of such organic envelopes (Patrick and Holding, 1985; Bidle and Azam, 1999, 2001; Bidle et al., 2003; Roubeix et al., 2008; Passow et al., 2001). Assuming anaerobic bacteria as being "*relatively inefficient in decomposing organic matter*" (Kaplan and Rittenberg, 1963), anoxic conditions have been considered for a long time as a pre-requisite for diatomite preservation (see Sturani and Sampò, 1973). However, recent studies revealed that oxygen-depleted conditions may increase, rather than mitigate, BSi dissolution, especially in the long term (e.g., White et al., 1992; Li, 1995; Schieber, 1996; Schulz et al., 1996; Souchu et al., 1998; Wallman et al., 2008; Villnäss et al., 2012; Abe et al., 2014; Ekeroth et al., 2016a,b; Lehtimäki et al., 2016; Petranich et al., 2018). The reasons behind the enhanced degradation of BSi under conditions of oxygen depletion and organic matter enrichment are not fully clarified, but they could be due to a shift in the composition of the microbial assemblages able to decompose the organic coating of diatoms (e.g., Lehtimäki et al., 2016). Peculiar bacterial communities may proliferate much easier in hypoxic waters, because of the drastic reduction of bacteriovores (e.g., ciliates) (Cole et al., 1993). The analysis of bacterial communities of Mediterranean sapropels and hypoxic settings in the Gulf

of Finland provided by Süß et al. (2004) and Sinkko et al. (2013), highlights the presence of Proteobacteria, Actinobacteria and Bacteroidetes, which are involved in BSi-dissolution (Bidle et al., 2003). Once the organic coating has been removed, frustule degradation can be caused by the modulation of pH, because opal, and more generally silicates, are prone to dissolution in alkaline environments (Brehm et al., 2005; Ehrlich et al., 2010). It is well known that the degradation of organic matter via sulfate-reducing bacteria, which are ubiquitous in oxygen-depleted waters (Muyzer and Stams, 2008), may promote an increase of pore water pH that can induce the dissolution of diatom frustules and the consequent remobilization of DSi. The possible linkage between enhanced anoxigenic bacterial activity and the Si biogeochemical cycle during the early Messinian diatomite accumulation may explain the regular occurrence of well-developed sapropels interbedded with diatomites, which is believed to reflect orbitally (precession) driven humid-arid climate fluctuations (e.g., Hilgen and Krijgsman, 1999; Modestou et al., 2017); other processes potentially involved in the dissolution of BSi under anoxic and organic-rich conditions comprise the reverse weathering, which involves metal hydroxides, dissolved cations and HCO_3^- and led to the formation of authigenic clays (e.g., Wallmann et al., 2008).

The presence of sapropels attests that many Mediterranean basins, from Algeria to Cyprus, were affected by prolonged periods of water stratification and anoxia. According to Hilgen and Krijgsman (1999), such conditions were favored during humid periods of marked runoff promoted by monsoonal rainfalls at times of

precession minima. Therefore, it is reasonable to assume that huge amounts of DSi derived by the leaching of grassland soils were massively supplied to the Mediterranean during sapropel formation. Conversely, diatomite deposition occurred during drier periods with increased mixing of the water column, which were probably more accentuated in the western domain (Filippelli et al., 2003; Pérez-Folgado et al., 2003) than in the central and eastern ones (Hilgen and Krijgsman, 1999; Pérez-Folgado et al., 2003). Such differences were possibly due to the complex interplay between physio- and hydrographic features of the basins (e.g., Pérez-Folgado et al., 2003). An overall reduction of continental runoff is expected during the earliest stage of an arid phase, with a consequent reduction of DSi-rich waters supply to the Mediterranean.

To reconcile such a complex scenario with the previous assumptions, the intervention of stratification-adapted and heavily silicified giant diatoms, solenioid diatoms, *Thalassiothrix* spp. and *Coscinodiscus* spp. (Kemp et al., 2000), during the deposition of lower Messinian sapropels, can be proposed. In the modern oceans, such taxa produce oligo- or mono-specific laminae after the seasonal breakdown of thermocline and nutricline, when the destabilization of the water column promotes their massive settling (fall dump *sensu* Kemp et al., 2000). These slow-growing diatoms are abundantly represented in the lower Messinian diatomite successions of the Mediterranean and have been reported in Morocco (El Ouahabi et al., 2007), Algeria (Rouchy et al., 1982; Mansour et al., 1995, 2008), Spain (Saint Martin et al., 2001), Apennine (Sturani and Sampò, 1973; Ciaranfi et al., 1980; Carnevale, 2004b;

Fig. 32), Sicily (Gaudant et al., 1996; Bellanca et al., 2001; Blanc-Valleron et al., 2002; Pestrea and Saint Martin, 2002), Gavdos (Pérez-Folgado et al., 2003) and Cyprus (Pestrea et al., 2002). However, the possible role of these taxa in the Messinian sapropel deposition has been underestimated or denied (e.g., Filippelli et al., 2003), although their contribution to Pliocene and Pleistocene sapropel deposition has been confirmed by several studies (e.g., Consolaro et al., 2013 and references therein; Kemp and Villareal, 2013 and reference therein). This is primarily due to the very poor preservation of diatom tests in Mediterranean sapropelitic muds (Pearce et al., 1998). The lack of diatom remains in sediments should not be considered as evidence of their absence in the water column. Molecular fossil data revealed that mat-forming diatoms contributed to the deposition of many organic-rich and BSi-free muds from the Late Cretaceous onwards (Köster et al., 1998; Schwark et al., 2009; McKirdy et al., 2010, 2013; Kemp and Villareal, 2013). Unfortunately, an accurate analysis of molecular fossils in the lower Messinian sapropels is still not available. Some scattered, but intriguing physical evidence of their presence was recorded in the lower Messinian successions of Gibellina (Sicily) and Cyprus, where Pestrea and Saint Martin (2002) and Pestrea et al. (2002) recorded an explosion of Rhizosoleniaceae abundance in the organic-rich layers. Furthermore, Dela Pierre et al. (2014) identified abundant ghosts of giant mat-forming diatoms derived by frustule dissolution in anoxic Messinian mudstones from the Piedmont Basin.

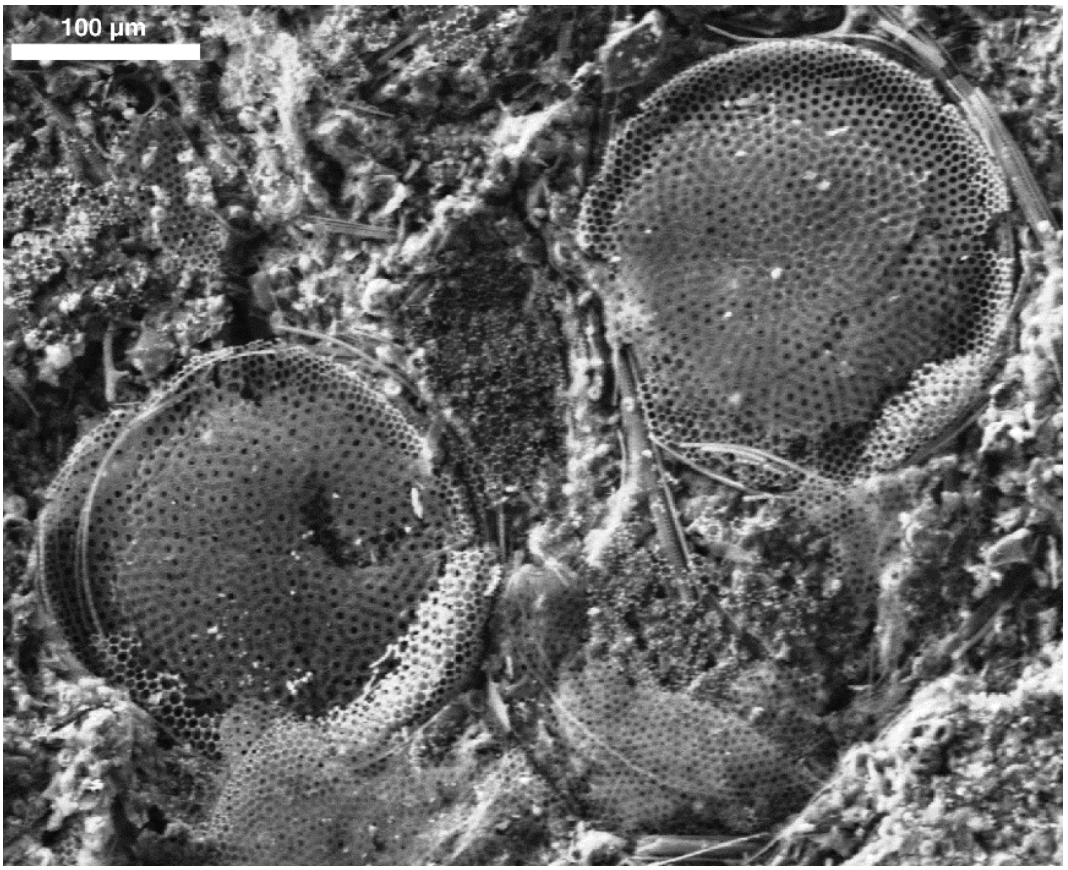

Figure 32. Concentration of *Coscinodiscus* sp. giant frustules in a diatomitic lamina from the Pecetto di Valenza section (Piedmont Basin). Note the variable degrees of dissolution affecting diatoms tests.

During humid periods of enhanced monsoonal runoff at precession minima (**Fig. 33A**), severe water stratification may have favored the proliferation of giant, highly-silicified mat-forming diatoms, which slowly consumed the enormous budget of DSi provided by rivers. Through their settling, such diatoms yielded a periodical source of degradable organic matter to the bottom of the ocean, which was then progressively metabolized by sulfate reducing bacteria. Such conditions promoted the increase of bottom pH, frustule dissolution and the consequent release of DSi, which remained trapped in the lower layers of the stratified Mediterranean waters.

During the subsequent onset of a cooler and arid climate (**Fig. 33B**), characterized by a strong mixing of the water column, the DSi-rich waters were transported toward the surface, where a broader spectrum of diatoms could proliferate.

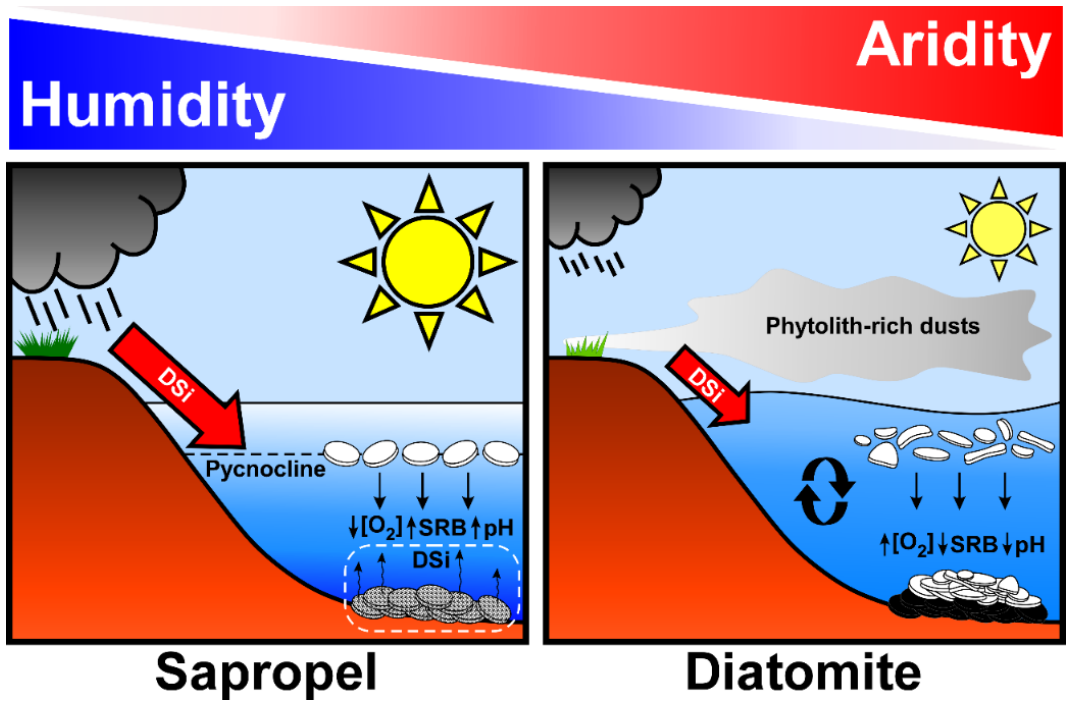

Figure 33. A simplified Si-based model explaining the regular occurrence of sapropels and diatomites in the early Messinian successions of the Mediterranean. A) Sapropel formation. During humid phases (precession minima, insolation maxima), a strong runoff provided huge amount of DSi to the basins and promoted water column stratification favoring the proliferation of oligospecific, highly silicified subsurface diatom assemblages (shade flora). Upon reaching the seafloor, the diatom frustules were dissolved due to the activity of sulfate reducing bacteria (SRB) which increased pH of the pore waters. B) Diatomite formation. During arid phases the reduction of river runoff and the mixing of the water column favored the reinjection of recycled DSi (previously trapped below the pycnocline) in the photic layer. Phytolith-rich dust further contributed to the silica saturation of the water column. Diversified diatom assemblages, adapted to exploit the silica-rich surface waters, proliferated and their frustules were further deposited on well-oxygenated sea bottom. The suppression of sulfate reducing bacteria favored the preservation of diatom frustules (see text for details).

A further contribution to the silica budget during the drier phases was most likely provided by the wind-driven injection of BSi, through the direct transport of

easily dissolvable phytoliths to the basins. Diatomite deposition occurred under progressively more oxygenated waters, which prevented the activity of anaerobic bacteria and the dissolution of frustules. Therefore, the preservation of laminated *fabric* was ostensibly promoted by the aggregation strategies of diatoms depending on their particular life-history, and not necessarily on the emergence of anoxic conditions. Diatomite accumulation proceeded until the complete exhaustion of DSi.

6. Summary and conclusions

Considered from a deep time perspective, the interplay between abiotic and biotic weathering of terrestrial silicates controls the release of DSi from land to ocean. The late Miocene-early Pliocene opaline peak around 7-4.5 Ma was a global event most likely promoted by the synergistic effect of vast tectonic readjustments (uplift and volcanism), climatic reconfigurations (strong aridity and monsoonal rainfalls) and biological turnovers (full expansion of grass-dominated ecosystems), able to promote a substantial increase of the oceanic pools of silica through riverine and eolian mobilization of the quickly-dissolvable terrestrial opal reservoirs.

The Mediterranean, a land-locked sea actively fed by rivers, represents a virtually unstudied system for unravelling the complex relationships between the terrestrial sources of silica and the marine biosiliceous production in the geological past. The early Messinian diatomitic deposition in the Mediterranean at about 7-6 Ma was the product of synergistic geobiosphere events that occurred on a global

scale, and their consequence on a semi-enclosed basin. Even if the Atlantic contribution cannot be ruled out, the main contribution to the Mediterranean silica enrichment was most likely provided by the African interiors and the perimediterranean regions, both affected by active tectonics and characterized by an extensive grassy cover in the early Messinian. The increasing aridity trend involving these regions around 7-6 Ma, may have acted as a catalyst for silica mobilization toward the Mediterranean, promoting the further expansion of grassy biomes and the erosion of their opal-rich topsoils, through concentrated seasonal rainfalls and a strong eolian transport. Volcanic ashes, typically considered as a fundamental source of DSi, were overall scanty and mainly localized in the westernmost domains of the Mediterranean, likely representing only an extremely limited local contribution to the early Messinian silica-enrichment of the Mediterranean.

The lower Messinian Mediterranean diatomite deposits share a fine lamination and are commonly alternated with sapropels, i.e. organic-rich sediments formed under stratified waters promoted by intensive runoff during the Northern Hemisphere summer perihelion. Although typically interpreted as the byproduct of oxygen-depleted conditions, the laminated *fabric* of diatomites may be efficiently preserved also in well-oxygented settings, through the formation of compacted flocs and mats able to hamper benthic activity. Recent advancements in the knowledge of silica biogeochemistry in anoxic settings suggest a possible linkage between the recurrence of sapropels, the recycling of DSi and the following episodes of diatomite deposition. The proliferation of giant, mat-forming diatoms during prolonged

periods of water stratification may have sequestered the huge amounts of silica provided by increased runoff. Anoxic conditions, promoting the growth of sulfate reducing bacteria able to increase the pH of bottom waters, may have completely dissolved the settled frustules. The resulting DSi was therefore trapped below the photic zone and subsequently re-injected during drier periods of stronger mixing of the water column, promoting the proliferation of a broader spectrum of diatoms and their preservation in oxygenated settings. Most likely, the drier periods of silica re-injection were also characterized by a reinforced eolian regime, able to considerably increase the amount of phytoliths dispersed toward the Mediterranean basins, and promoting a further spike of silica concentration favorable to the preservation of diatomites.

Although other triggering factors (e.g. peculiar physiography of each sub-basin, paleocurrents, sources and distribution of other nutrients such as N, P and Fe) should also be taken into account to more properly interpret the diachronic onset and demise of the lower Messinian diatomite deposition in the Mediterranean, as well as their specific stratigraphic architectures, a first attempt has been provided herein in order to better frame this event under a terrestrial silica perspective, suggesting a possible linkage with the latest Miocene global intensification of the oceanic opaline production.

CONCLUSIONS AND FUTURE RESEARCH PERSPECTIVES

Summarizing, the research presented herein provides the following results: i) the improvement of the micropaleontological dataset of the upper Miocene diatom-bearing section of Pecetto di Valenza, especially for what concerns the biosiliceous assemblages of this overlooked but potentially very relevant locality for our understanding of the Messinian events in the northernmost Mediterranean region; the comparative interpretation of the response of silica-secreting and calcareous biota to the dominant paleoceanographic processes triggered by precessionally-driven climate changes; ii) a detailed analysis of the sedimentology of the Pecetto di Valenza section, with the definition of the role of diatom ecological groups in the formation of different types of laminae and the reconstruction of an annual depositional cycle; iii) an updated 'state of the art' concerning the Messinian diatomaceous deposition in the Mediterranean area and its possible linkages with coeval global paleoceanographic and continental events.

Overall, the obtained dataset suggests that caution is needed in linking the diatomaceous deposition that occurred in the Mediterranean area during the latest Miocene to the enhancement of upwelling and/or to the establishment of anoxic conditions at the seafloor. Rather than a regional-scale intensification of upwelling, a more realistic model based on the interplay between riverine runoff, water column stratification and convective remixing, in a general context characterized by a

significant increase of silica availability triggered by abiotic and biotic continental processes, can be proposed. Moreover, since the morphological analysis did not reveal any unquestionable evidence of anoxia (such as for example widespread occurrence of framboidal pyrite or the complete absence of macro- and microbioturbations), the possible role of physical barriers able to limit the benthic bioturbation of diatomaceous sediments should always be considered before attributing the presence of laminations to oxygen depletion on the seafloor.

However, further researches based on high-resolution and non-destructive micropaleontological and sedimentological investigations, possibly supported by geochemical and biomarker studies, are needed in order to expand each of the above mentioned points.

For what concerns the Pecetto di Valenza section, both the Mn-rich and the upper diatomaceous layer deserve future investigations focused at understanding the processes that occurred immediately before and after the onset of the diatomaceous deposition, herein just hinted and tentatively interpreted. In particular, the Mn-rich layer should be better characterized throughout the analysis of redox sensitive elements. Moreover, useful information about the seafloor conditions may derive from the taphonomic studies of macrofossils.

Comparisons with other sections are urgently needed in order to highlight differences and similarities between the various upper Miocene diatomaceous deposits located at different latitudes in the Mediterranean area. In this regard, it is worth noting the potential relevance of the Messinian sections of Capo di Fiume

(Abruzzo) and Serra Pirciata (Sicily), whose micropaleontological and sedimentological characterization is already in progress.

The Capo di Fiume section (Abruzzo; **Fig. 34**) exhibits five lithological cycles consisting in the meter-thick alternation of lithified diatomaceous sediments, recording strike evidences of synsedimentary tectonic instability, and organic-rich mudstones (Carnevale, 2004b). It represents an excellent case study for understanding the role of diagenetic processes (involving silica, phosphorus and organic matter) and tectonic activity on the diatomaceous and sapropelitic deposition in the Central Apennine area.

The Serra Pirciata section (Sicily) is located in the Caltanissetta Basin and consists of 25 cycles made up of a meter-thick alternation of sapropels, marls and diatomites (e.g., Bellanca et al., 2001; **Figs. 26A** and **35**). Even if this section has been intensively studied, until now no detailed lamina-scale observations have been provided.

Intriguingly, in both the Capo di Fiume and Serra Pirciata sections, preliminary micropaleontological investigations highlighted an impressive occurrence of large centric diatoms (**Fig. 34E-F, 35**). This feature might further confirm the relevant role of the subsurface primary production during the Messinian diatomaceous accumulation in the Mediterranean area.

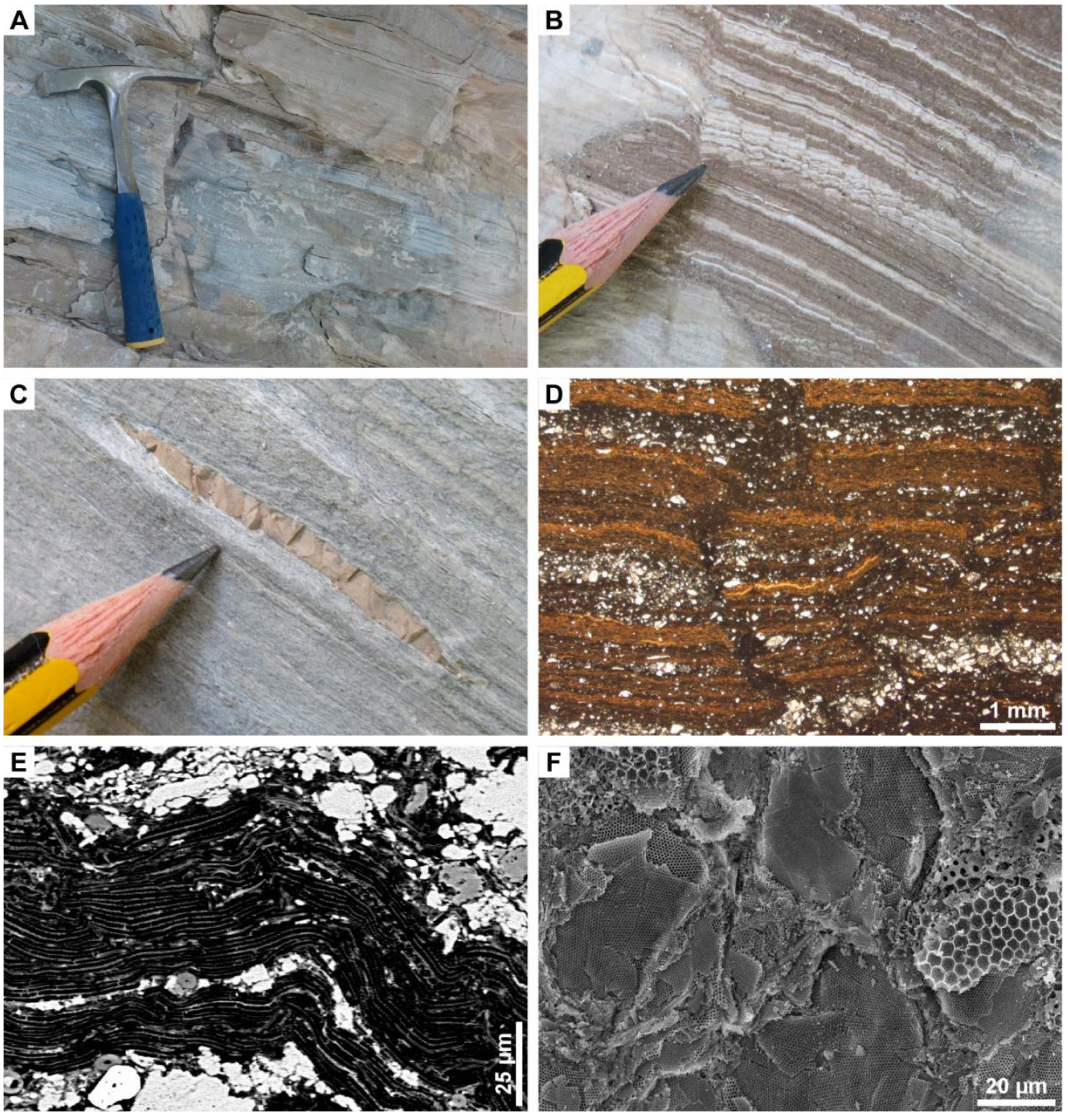

Figure 34. Capo di Fiume section (Abruzzo). A) A diatomaceous interval. B) Normal faults affecting a laminated packet consisting of an alternation of diatom-rich (whitish) and terrigenous laminae (brown). C) Phosphate nodule. D) LM micrograph (parallel nicols) of diatom-rich and terrigenous laminae; the diatom-rich laminae are orange because of the presence of phosphates; note the presence of a prominent water escape structure interrupting the lateral continuity of the laminae. E-F) BSE and SE micrographs of a diatom-rich lamina entirely composed of centric diatoms, observed in polished thin section and parallel to the bedding plane, respectively.

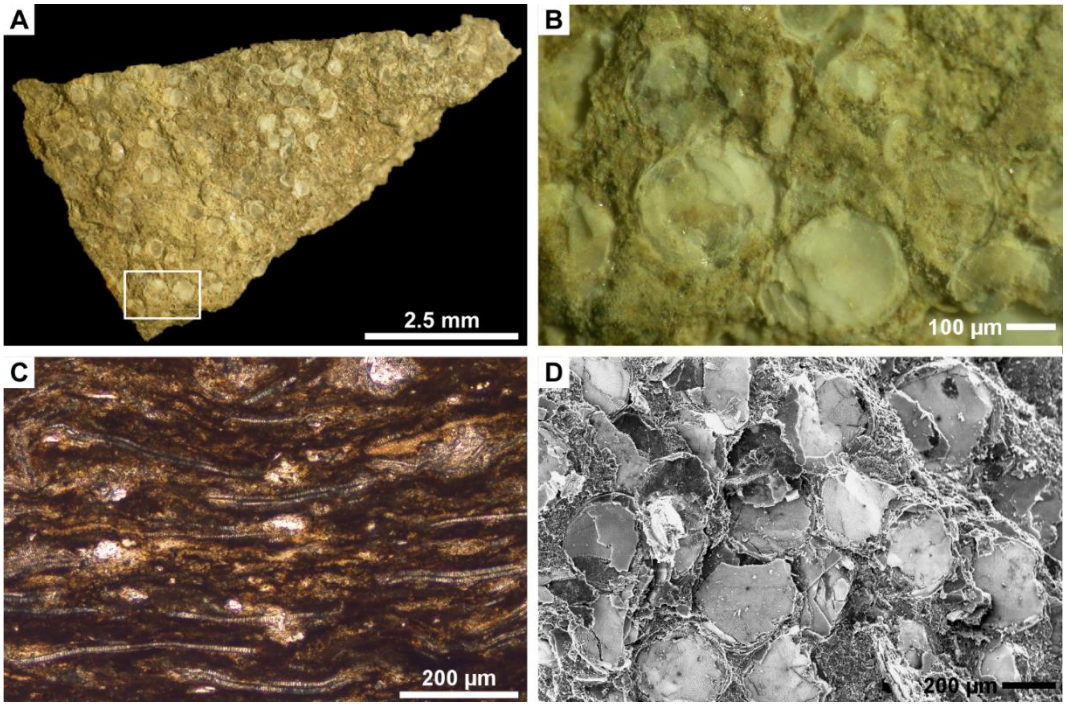

Figure 35. Serra Pirciata section (Sicily). RL (A-B), LM (parallel nicols; C) and SE (D) micrographs of a cm-thick layer characterized by the impressive accumulation of large centric diatoms.

Finally, the study of Si-isotopes, as well as other land-derived elements (e.g., Sutton et al., 2018; Modestou et al., 2019) and biomarkers (e.g., Sabino et al., 2020), may significantly improve the interpretation of the role of continental processes in providing limiting factors able to boost the proliferation of diatoms in the Mediterranean during the late Miocene.

REFERENCES

Abe, K., Nakagawa, N., Abo, K., Tsujino, M., 2014. Dissolution of silica accompanied by oxygen consumption in the bottom layer of Japan's central Seto Inland Sea in summer. J. Oceanogr. 70 (3), 267-276.

Abrams, M.D., Knapp, A.K., Hulbert, L.C., 1986. A ten-year record of aboveground biomass in a Kansas tallgrass prairie: effects of fire and topographic position. Am. J. Bot. 73 (10), 1509-1515.

Abreu, V.S., Anderson, J.B., 1998. Glacial eustasy during the Cenozoic: sequence stratigraphic implications. AAPG Bull. 82 (7), 1385-1400.

Achalhi, M., Münch, P., Cornée, J.J., Azdimousa, A., Melinte-Dobrinescu, M., Quillévéré, F., Drinia, H., Fauquette, S., Jiménez-Moreno, G., Merzeraud, G., 2016. The late Miocene Mediterranean-Atlantic connections through the North Rifian Corridor: New insights from the Boudinar and Arbaa Taourirt basins (northeastern Rif, Morocco). Palaeogeogr. Palaeoclimatol. Palaeoecol. 459, 131-152.

Agostini, S., Doglioni, C., Innocenti, F., Manetti, P., Tonarini, S., Savaşçin, M.Y., 2007. The transition from subduction-related to intraplate Neogene magmatism in the Western Anatolia and Aegean area. Geol. Soc. Spec. Pap. 418, 1-15.

Agustí, J., Cabrera, L., Garcés, M., 2013. The Vallesian Mammal Turnover: A Late Miocene record of decoupled land-ocean evolution. Geobios, 46 (1), 151-157.

Agustí, J., Garcés, M., Krijgsman, W., 2006. Evidence for African–Iberian exchanges during the Messinian in the Spanish mammalian record. Palaeogeogr. Palaeoclimatol. Palaeoecol. 238 (1), 5-14.

Aleem, A.A., 1972. Effect of river outflow management on marine life. Mar. Biol. 15, 200-208.

Aleem, A.A., Dowidar, N., 1967. Phytoplankton production in relation to nutrients along the Egyptian Mediterranean Coast. Stud. Trop. Oceanogr. 5, 305-322.

Alexandre, A., Meunier, J.D., Colin, F., Koud, F., 1997. Plant impact on the biogeochemical cycle of silicon and related weathering processes. Geochim. Cosmochim. Acta 61 (3), 677-682.

Alldredge, A.L., Gotschalk, C.C., 1989. Direct observations of the mass flocculation of diatom blooms: characteristics, settling velocities and formation of diatom aggregates. Deep-Sea Res. 36 (2), 159-171.

Alldredge, A.L., Passow, U., Logan, B.E., 1993. The abundance and significance of a class of large, transparent organic particles in the ocean. Deep-Sea Res. Pt. I 40, 1131-1140.

Altenbach, A.V., Pflaumann, U., Schiebel, R., Thies, A., Timm, S., Trauth, M., 1999. Scaling percentages and distributional patterns of benthic foraminifera with flux rates of organic carbon. J. Foraminiferal Res. 29 (3), 173-185.

Alve, E., 1994. Opportunistic features of the foraminifer *Stainforthia fusiformis* (Williamson): evidence from Frierfjord, Norway. J. Micropaleontol. 13 (1), 13-24.

An, Z., Kutzbach, J.E., Prell, W.L., Porter, S.C., 2001. Evolution of Asian monsoons and phased uplift of the Himalaya-Tibet plateau since late Miocene times. Nature 411, 62-66.

Anderson, R.v.V., 1933. The Diatomaceous and Fish-Bearing Beida Stage of Algeria. J. Geol. 41 (7), 673-698.

Anderson, R.v.V., 1936. Beida Stage. In: Anderson, R.v.V. (Ed.), Geology in the coastal Atlas of western Algeria. Geol. Soc. Am. Mem. 4, 169-187.

Arab, M., Bracene, R., Roure, F., Zazoun, R.S., Mahdjoub, Y., Badji, R., 2015. Source rocks and related petroleum systems of the Chelif Basin, (western Tellian domain, north Algeria). Mar. Pet. Geol. 64, 363-385.

Arcaleni, M., Casabianca, D., De Donatis, M., Galeazzi, M., Mazzoli, S., Tamburini, F., Tiberi, P., 1995. Schema geologico delle dorsali di Montefiore Conca-Monte Colbordolo, di Ginestreto e di Gabicce-Pesaro (Note illustrative). St. Geol. Cam., Vol. Spec. 1, 11-17.

Authemayou, C., Pedoja, K., Heddar, A., Molliex, S., Boudiaf, A., Ghaleb, B., Van Vliet Lanoe, B., Delcaillau, B., Djellit, H., Yelles, K., Nexer, M., 2015. Coastal uplift west of Algiers (Algeria): pre- and post-Messinian sequences of marine terraces and rasas and their associated drainage pattern. Int. J. Earth Sci. 106 (1), 19-41.

Azdimousa, A., Poupeau, G., Rezqui, H., Asebriy, L., Bourgois, J., Aït Brahim, L., 2006. Géodynamique des bordures méridionales de la mer d'Alboran;

application de la stratigraphie séquentielle dans le bassin néogène de Boudinar (Rif oriental, Maroc). Bull. Inst. Scient., Rabat, sect. Sci. Terre 28, 9-18.

Azzouni-Sekkal, A., Bonin, B., Benhallou, A., Yahiaoui, R., Liégeois, J.P., 2007. Cenozoic alkaline volcanism of the Atakor massif, Hoggar, Algeria. In: Beccaluva, L., Bianchini, G., Wilson, M. (Eds), Cenozoic Volcanism in the Mediterranean Area. Geol. Soc. Spec. Pap. 418, 321-340.

Bachiri Taoufiq, N., Barhoun, N., Suc, J.P., 2008. Les environnements continentaux du corridor rifain (Maroc) au Miocène supérieur d'après la palynologie. Geodiversitas 30 (1), 41-58.

Bahk, J.J., Yoon, H.I., Kim, Y., Kang, C.Y., Bae, S.H., 2003. Microfabric analysis of laminated diatom ooze (Holocene) from the eastern Bransfield Strait, Antarctic Peninsula. Geosci. J. 7 (2), 135-142.

Balch, W. M. 2004. Re-evaluation of the physiological ecology of coccolithophores, in: Coccolithophores: from molecular processes to global impact, edited by: Thierstein, H. R. and Young, J. R., Springer, Berlin, 165–190, 2004.

Baldauf, J.G., Barron, J.A., 1990. Evolution of Biosiliceous Sedimentation Patterns – Eocene through Quaternary: Paleoceanographic Response to Polar Cooling. In: Bleil, U., Thiede, J. (Eds.), Geological History of the Polar Oceans: Arctic Versus Antarctic, Kluwer Academic Publishers, pp. 575-607.

Barone, M., Dominici, R., Muto, F., Critelli, S., 2008. Detrital modes in a late Miocene wedge-top basin, northeastern Calabria, Italy: compositional record of wedge-top partitioning. J. Sediment. Res. 78 (10), 693-711.

Barron, J.A., Baldauf, J.G., 1990. Development of Biosiliceous Sedimentation in the North Pacific during the Miocene and Early Pliocene. In: Pacific Neogene Events – Their Timing, Nature and Interrelationship (Ed R. Tsuchi), 43-63.

Barron, J.A., Bukry, D., Field, D.B., Finney, B., 2013. Response of diatoms and silicoflagellates to climate change and warming in the California Current during the past 250 years and the recent rise of the toxic diatom *Pseudo-nitzschia australis*. Quatern. Int. 310, 140-154.

Barron, J.A., Keller, G., 1983. Paleotemperature oscillations in the Middle and Late Miocene of the northeastern Pacific. Micropaleontology 29 (2), 150-181.

Batmanian, G.J., Haridasan, M., 1985. Primary production and accumulation of nutrients by the ground layer community of cerrado vegetation of central Brazil. Plant and Soil 88, 437-440.

Baudrimont, R., Degiovanni, C., 1974. Les diatomees marines du Miocene Superieur de l'Oranais (Algerie) et leur contexte geologique. Bull. Soc. Hist. nat. Afr. Nord. 65 (1-2), 35-66.

Bellanca, A., Caruso, A., Ferruzza, G., Neri, R., Rouchy, J.M., Sprovieri, M., Blanc-Valleron, M.M., 2001. Transition from marine to hypersaline conditions in the Messinian Tripoli Formation from the marginal areas of the central Sicilian Basin. Sed. Geol. 140, 87-105.

Bennet, G., 1980. The sedimentology, diagenesis and palaeo-oceanography of diatomites from the Miocene of Sicily. PhD Thesis, Durham University, 223 pp.

Benvenuti, M., Del Conte, S., Scarselli, N., Dominici, S., 2014. Hinterland basin development and infilling through tectonic and eustatic processes: latest Messinian-Gelasian Valdels Basin, Northern Apennines, Italy. Basin Res. 26, 387-402.

Berger, W., 1957. Untersuchungen an der obermiozänen (sarmatischen) Flora von Gabbro (Monti Livornesi) in der Toskana. Ein Beitrag zur Auswertung tertiärer Blattfloren für die Klima- und Florengeschichte. Palaeont. it. 51 (21), 1-96.

Berger, W.H., 2007. Cenozoic cooling, Antarctic nutrient pump, and the evolution of whales. Deep-Sea Res. Pt. II 54, 2399-2421.

Bertini, A., Martinetto, E., 2008. Messinian to Zanclean vegetation and climate of Northern and Central Italy. Boll. Soc. Pal. It. 47 (2), 105-121.

Bibi, F., 2011. Mio-Pliocene faunal exchanges and African biogeography: the record of fossil bovids. PLoS One 6 (2), e16688.

Bibi, F., Bukhsianidze, M., Gentry, A.W., Geraads, D., Kostopoulos, D. S., Vrba, E.S., 2009. The fossil record and evolution of Bovidae: state of the field. Palaeont. Electron. 12 (3), 1-11.

Bidle, K.D., Azam, F., 1999. Accelerated dissolution of diatom silica by marine bacterial assemblages. Nature 397, 508-512.

Bidle, K.D., Azam, F., 2001. Bacterial control of silicon regeneration from diatom detritus: significance of bacterial ectohydrolases and species identity. Limnol. Oceanogr. 46 (7), 1606-1623.

Bidle, K.D., Brzezinski, M.A., Long, R.A., Jones, J.L., Azam, F., 2003. Diminished efficiency in the oceanic silica pump caused by bacteria-mediated silica dissolution. Limnol. Oceanogr. 48 (5), 1855-1868.

Bigi, G., Cosentino, D., Parotto, M., Sartori, R., Scandone, P., 1990. Structural Model of Italy: Geodinamic Project. Consiglio Nazionale delle Ricerche, S.EL.CA, scale 1:500,000, sheet 1.

Bigot-Cormier, F., Poupeau, G., Sosson, M., 2000. Dénudations différentielles du massif cristallin externe alpin de l'Argentera (Sud-Est de la France) révélées par thermochronologie traces de fission (apatites, zircons). C. R. Acad. Sci. IIA 330 (5), 363-370.

Bigot-Cormier, F., Sosson, M., Poupeau, G., Stéphan, J.F., Labrin, E., 2006. The denudation history of the Argentera Alpine External Crystalline Massif (Western Alps, France-Italy): an overview from the analysis of fission tracks in apatites and zircons. Geodin. Acta 19 (6), 455-473.

Biltekin, D., 2010. Vegetation and climate of north anatolian and north aegean region since 7 Ma according to pollen analysis. Earth Sciences. Université Claude Bernard - Lyon I.

Blanc-Valleron, M.M., Pierre, C., Caulet, J.P., Caruso, A., Rouchy, J.M., Cespuglio, G., Sprovieri, R., Pestrea, S., Di Stefano, S., 2002. Sedimentary, stable isotope and micropaleontological records of paleoceanographic change in the Messinian Tripoli Formation (Sicily, Italy). Palaeo. Palaeo. Palaeo., 185 (3-4), 255-286.

Blecker, S.W., McCulley, R.L., Chadwick, O.A., Kelly, E.F., 2006. Biologic cycling of silica across a grassland bioclimosequence. Glob. Biogeochem. Cycles 20 (3), 1-11.

Blondel, C., Merceron, G., Andossa, L., Taisso, M.H., Vignaud, P., Brunet, M., 2010. Dental mesowear analysis of the late Miocene Bovidae from Toros-Menalla (Chad) and early hominid habitats in Central Africa. Palaeogeogr. Palaeoclimatol. Palaeoecol. 292 (1), 184-191.

Boaz, N.T., El-Arnauti, A., Agustí, J., Bernor, R.L., Pavlakis, P., Rook, L., 2008. Temporal, Lithostratigraphic, and Biochronologic Setting of the Sahabi Formation, North-Central Libya. Geology of East Libya 3, 959-972.

Bobe, R., 2011. Fossil Mammals and Paleoenvironments in the Omo-Turkana Basin. Evol. Anthropol. 20 (6), 254-263.

Bodén, P., Backman, J., 1996. A laminated sediment sequence from the northern North Atlantic Ocean and its climatic record. Geology 24 (6), 507-510.

Böhme, M., Spassov, N., Ebner, M., Geraads, D., Hristova, L., Kirscher, U., Kötter, S., Linnemann, U., Prieto, J., Roussiakis, S., Theodorou, G., Uhlig, G., Winklhofer, M., 2017. Messinian age and savannah environment of the possible hominin *Graecopithecus* from Europe. PloS One 12 (5), e0177347.

Bonci, M.C., 1995. L'associazione a Diatomee del Miocene superiore di Cappella Montei (Alessandria). Boll. Soc. Pal. It. 34 (2), 163-191.

Bonci, M.C., Clari, P., Ferrero Mortara, E., Ghibaudo, G., Pirini, C., Ricci, B., Valleri, G. and Violanti, D, 1990. The diatomites of Marmorito (Western Monferrato, Northern Italy). Mem. Sci. Geol. 67, 189-226.

Bonci, M.C., Fanucci, F., Pirini Radrizzani, C., Rizzi, A., Tedeschi, D., 1991. I livelli diatomitici della successione miocenica di Cappella Montei (area di Serravalle Scrivia, Bacino di Alessandria). Boll. Soc. Pal. It. 30 (3), 381-301.

Bonci, M.C., Magnino, G., Pirini Radrizzani, C., Pronzato, R., 1996. Finding of *Geodia* (Demospongiae) sterrasters in the Late Miocene of Cappella Montei (Alessandria) and comparison with living forms. Boll. Soc. Pal. It. 35 (3), 245-256.

Bond, W.J., 2015. Fires in the Cenozoic: a late flowering of flammable ecosystems. Front. Plant Sci. 5, 1-11.

Bond, W.J., Keeley, J.E., 2005. Fire as a global 'herbivore': the ecology and evolution of flammable ecosystems. Trends Ecol. Evol. 20 (7), 387-394.

Bond, W.J., Midgley, G.F., Woodward, F.I., 2003a. What controls South African vegetation – climate or fire? S. Afr. J. Bot. 69 (1), 79-91.

Bond, W.J., Midgley, G.F., Woodward, F.I., 2003b. The importance of low atmospheric CO2 and fire in promoting the spread of grasslands and savannas. Glob. Change Biol. 9, 973-982.

Bonnefille, R., 2010. Cenozoic vegetation, climate changes and hominid evolution in tropical Africa. Glob. Planet. Change 72 (4), 390-411.

Bosak, S., Burić, Z., Djakovac, T., Viličić, D., 2009. Seasonal distribution of plankton diatoms in Lim Bay, northeastern Adriatic Sea. Acta Bot. Croat. 68 (2), 351-365.

Bosak, S., Godrijan, J., Šilović, T., 2016. Dynamics of the marine planktonic diatom family Chaetocerotaceae in a Mediterranean coastal zone. Estuar. Coast. Shelf Sci. 180, 69-81.

Bossio, A., Foresi, L.M., Liotta, D., Mazzanti, R., Mazzei, R., Salvatorini, G., Squarci, P., 1999. Riordino delle conoscenze sul Bacino Neogenico del Tora-Fine (Toscana, Italia). Atti Soc. Tosc. Sci. Nat. Pisa 106, 1-16.

Bouchenak-Khelladi, Y., Verboom, G.A., Hodkinson, T.R., Salamin, N., Fracois, O., Chonghaile, G.N., Savolainen, V., 2009. The origins and diversification of C_4 grasses and savanna-adapted ungulates. Glob. Change Biol. 15, 2397-2417.

Bown, P.R., Young, J.R., 1998. Techniques. In: Bown, P.R. (Ed.), Calcareous Nannofossil Biostratigraphy. Chapman and Hall, London, 132–199.

Bradley, F., Landini, W., 1984. I fossili del «Tripoli» Messiniano del Gabbro (Livorno). Palaeont. It. 73, 1-33.

Braga, J.C., Martín, J.M., Quesada, C., 2003. Patterns and average rates of late Neogene-Recent uplift of the Betic Cordillera, SE Spain. Geomorphology 50, 3-26.

Bramlette, M.N., 1946. The Monterey Formation of California and the origin of its siliceous rocks. USGS Professional Papers 212, 57 pp.

Brand, L.E., 1994. Physiological ecology of marine coccolithophores. In: Winter, A., Siesser, A. (Eds.), Coccolithophores. Cambridge University Press, Cambridge, 39– 49.

Brand, L.R., Esperante, R., Chadwick, A.V., Poma Porras, O., Alomía, M., 2004. Fossil whale preservation implies high diatom accumulation rate in the Miocene-Pliocene Pisco Formation of Peru. Geology 32 (2), 165-168.

Brehm, U., Gorbushina, A., Mottershead, D., 2005. The role of microorganisms and biofilms in the breakdown and dissolution of quartz and glass. Palaeogeogr. Palaeoclimatol. Palaeoecol. 219 (1), 117-129.

Brodie, I., Kemp, A.E.S., 1994. Variation in biogenic and detrital fluxes and formation of laminae in late Quaternary sediments from the Peruvian coastal upwelling zone. Mar. Geol. 116, 385-398.

Brodie, I., Kemp, A.E.S., 1995. Pelletal structures in Peruvian upwelling sediments. J. Geol. Soc. London 152, 141-150.

Bukry, D., 1974. Coccoliths as paleosalinity indicators-Evidence from the Black Sea. In: Degens, E.T., Ross, D.A. (Eds.), The Black Sea-Geology, chemistry, and biology: American Association of Petroleum Geologists Memoirs 2, 353-363.

Bull, D., Kemp, A.E.S., 1995. Composition and origins of Late Quaternary and Holocene sediments from the Santa Barbara Basin, California. In: Proc. Ocean Drill. Progr. Sci. Res. (Eds J.P. Kennett, J.G. Baldauf and M. Lyle) 146 (Pt. 2), 77-87.

Burckle, L.H., 1978. Diatom biostratigraphy of Unit 2 (Tripoli) of the neostratotype Messinian. Riv. Ital. Paleont. Strat. 84, 1037-1050.

Burckle, L.H., 1989. Distribution of diatoms in sediments of the northern Indian Ocean: Relationship to physical oceanography. Mar. Micropaleontol. 15 (1-2), 53-65.

Burckle, L.H., Sturz, A., Emanuele, G., 1992. Dissolution and preservation of diatoms in the Sea of Japan and the effect on sediment thanatocoenosis. In: Proc. Ocean Drill. Progr. Sci. Res. (Eds K.A. Pisciotto, J.C. Jr. Ingle, M.T. von Breymann, J. Barron et al.) 127/128 (Pt. 1), 309-316.

Burke, I.T., Grigorov, I., Kemp, A.E.S., 2002. Microfabric study of diatomaceous and lithogenic deposition in laminated sediments from the Gotland Deep, Baltic Sea. Mar. Geol. 183, 89-105.

Butler, R.W.H., Grasso, M., 1993. Tectonic controls on base-level variations and depositional sequences within thrust-top and foredeep basins: examples from the Neogene thrust belt of central Sicily. Basin Res. 5, 137-151.

Butler, R.W.H., Lickorish, W.H., Grasso, M., Pedley, H.M., Ramberti, L., 1995. Tectonics and sequence stratigraphy in Messinian basins, Sicily: constraints on the initiation and termination of the Mediterranean salinity crisis. Geol. Soc. Am. Bull. 107 (4), 425-439.

Cachao, M., Moita, M.T., 2000. *Coccolithus pelagicus*, a productivity proxy related to moderate fronts off Western Iberia. Marine Micropaleontology 39, 131–155.

Calvert, S.E., 1966. Origin of diatom-rich, varved sediments from the Gulf of California. J. Geol. 74 (5), Pt. I, 546-565.

Capella, W., Matenco, L., Dmitrieva, E., Roest, W.M.J., Hessels, S., Hssain, M., Chakor-Alami, A., Sierro, F.J., Krijgsman, W., 2016. Thick-skinned tectonics closing the Rifian Corridor. Tectonophysics 710-711, 249-265.

Capozzi, R., Dinelli, E., Negri, A., Picotti, V., 2006a. Productivity-generated annual laminae in mid-Pliocene sapropels deposited during precessionally forced periods of warmer Mediterranean climate. Palaeo. Palaeo. Palaeo. 235, 208-222.

Capozzi, R., Negri, A., Picotti, V., Dinelli, E., Giunta, S., Morigi, C., Scotti, P., Lombi, G., Marangoni, F., 2006b. Mid-Pliocene warm climate and annual primary productivity peaks recorded in sapropel deposition. Clim. Res. 31, 137-144.

Carmignani, L., Salvini, R., Bonciani, F., 2009. Did the Nile flow to the Gulf of Sirt during the late Miocene? Boll. Soc. Geol. It. 128 (2), 403-408.

Carnevale, G., 2004a. New species of sand lance (Teleostei, Ammodytidae) from the Miocene of Algeria. Geodiversitas 26 (2), 297-307.

Carnevale, G., 2004b. Tafonomia, paleoecologia e paleobiogeografia delle ittiofaune mioceniche dell'Italia centrale. Tesi di Dottorato XV Ciclo, Università di Pisa, 368 pp.

Carnevale, G., 2004c. The first fossil ribbonfish (Teleostei, Lampridiformes, Trachipteridae). Geol. Mag. 141, 573-582.

Carnevale, G., 2006a. A new snake mackerel from the Miocene of Algeria. Palaeontology 49 (2), 391-403.

Carnevale, G., 2006b. Morphology and biology of the Miocene butterflyfish *Chaetodon ficheuri* (Teleostei: Chaetodontidae). Zool. J. Linn. Soc. 146, 251-267.

Carnevale, G., 2007. New gadiform fishes (Teleostei, Gadiformes) from the Miocene of Algeria. J. Afr. Earth Sci. 47, 95-111.

Carnevale, G., Bannikov, A.F., 2006. Description of a new stromateoid fish from the Miocene of St. Eugène, Algeria. Acta Palaeont. Pol. 51 (3), 489-497.

Carnevale, G., Gennari, R., Lozar, F., Natalicchio, M., Pellegrino, L., Dela Pierre, F., 2019. Living in a deep desiccated Mediterranean Sea: An overview of the Italian fossil record of the Messinian salinity crisis. Boll. Soc. Pal. It. 58 (1), 109-140.

Carnevale, G., Pietsch, T.W., 2006. Filling the gap: a fossil frogfish, genus *Antennarius* (Teleostei: Lophiiformes: Antennariidae), from the Miocene of Algeria. J. Zool. London 270, 448-457.

Carnevale, G., Tyler, J.C., 2010. Review of the fossil pufferfish genus *Archaeotetraodon* (Teleostei, Tetraodontidae), with description of three new taxa from the Miocene of Italy. Geobios 43 (3), 283-304.

Carrapa, B., Wijbrans, J., Bertotti, G., 2004. Detecting provenance variations and cooling patterns within the western Alpine orogen through $^{40}Ar/^{39}Ar$

geochronology on detrital sediments: The Tertiary Piedmont Basin, northwest Italy. Geol. Soc. Spec. Pap. 378, 69-102.

Casas-Gallego, M., Lassaletta, L., Barrón, E., Bruch, A.A., Montoya, P., 2015. Vegetation and climate in the eastern Iberian Peninsula during the pre-evaporitic Messinian (late Miocene). Palynological data from the Upper Turolian of Venta del Moro (Spain). Rev. Palaeobot. Palynol. 215, 85-99.

Catalano, R., Di Stefano, E., Sprovieri, R., Lena, G., Valenti, V., 2016. The barren Messinian Tripoli in Sicily and its palaeoenvironmental evolution: suggestions on the exploration potential. Pet. Geosci. 22, 322-332.

Centamore, E., Rossi, D., 2009. Neogene-Quaternary tectonics and sedimentation in the Central Apennines. Boll. Soc. Geol. It. 128 (1), 73-88.

Cerling, T.E., Harris, J.M., MacFadden, B.J., Leakey, M.G., Quade, J., Eisenmann, V., Ehleringer, J.R., 1997. Global vegetation change through the Miocene/Pliocene boundary. Nature 389, 153-158.

Cermeño, P., 2016. The geological story of marine diatoms and the last generation of fossil fuels. Persp. Phycol. 3 (2), 53-60.

Cermeño, P., Falkowski, P.G., Romero, O.E., Schaller, M.F., Vallina, S.M., 2015. Continental erosion and the Cenozoic rise of marine diatoms. Proc. Natl. Acad. Sci. USA 112 (14), 1-6.

Chang, A.S., Grimm, K.A., 1999. Speckled beds: Distinctive gravity-flow deposits in finely laminated diatomaceous sediments, Miocene Monterey Formation, California. J. Sed. Res. 69 (1), 122-134.

Chang, A.S., Grimm, K.A., White, L.D., 1998. Diatomaceous sediments from the Miocene Monterey Formation, California: A lamina-scale investigation of biological, ecological, and sedimentary processes. Palaios 13, 439-458.

Chang, A.S., Pichevin, L., Pedersen, T.F., Gray, V., Ganeshram, R., 2015. New insights into productivity and redox-controlled trace element (Ag, Cd, Re, and Mo) accumulation in a 55 kyr long sediment record from Guaymas Basin, Gulf of California. Paleoceanography 30, 77-94.

Chikhi, H., 1992. Une palynoflore méditerranéenne à subtropicale au Messinien pré-évaporitique en Algérie. Géol. Médit. 19 (1), 19-30.

Cianflone, G., Dominici, R., 2011. Physical stratigraphy of the upper Miocene sedimentary succession in the northeastern Catanzaro Through (Central Calabria, Italy). Rend. Online Soc. Geol. It. 17, 63-9.

Ciaranfi, N., Dazzaro, L., Pieri, P., Rapisardi, L., 1980. I depositi del Miocene superiore al confine molisano-abruzzese. Boll. Soc. Geol. It. 99, 103-118.

Cid, M.S., Detling, J.K., Brizuela, M.A., Whicker, A.D., 1989. Patterns in grass silicification: response to grazing history and defoliation. Oecologia 80 (2), 268-271.

Cita, M. B., Colalongo, M. L., d'Onofrio, S., Iaccarino, S., Salvatorini, G., 1978. Biostratigraphy of Miocene deep-sea sediments (Sites 372 and 375), with special reference to the Messinian/pre-Messinian interval. Init. Rep. DSDP, 42 (1), 671-685.

Cole, J.J., Pace, M.L., Caraco, N.F., Steinhart, G.S., 1993. Bacterial biomass and cell size distributions in lakes: more and larger cells in anoxic waters. Limnol. Oceanogr. 38 (8), 1627-1632.

Colmenero-Hidalgo, E., Flores, J.A., Sierro, F.J., Barcena, M.A., Lowemark, L., Schőnfeld, J., Grimalt, J., 2004. Ocean surface water response to short-term climate changes revealed by coccolithophores from the Gulf of Cadiz (NE Atlantic) and Alboran Sea (W Mediterranean). Palaeogeogr. Palaeoclimatol. Palaeoecol. 205, 317– 336.

Colombero, S., Angelone, C., Bonelli, E., Carnevale, G., Cavallo, O., Delfino, M., Giuntelli, P., Mazza, P.P.A., Pavia, G., Pavia, M., Repetto, G. (2014). The Messinian vertebrate assemblages of Verduno (NW Italy): another brick for a latest Miocene bridge across the Mediterranean. N. Jb. Geol. Paläont., Abh. 273 (3), 287-324.

Conley, D.J., Carey, J.C., 2015. Biogeochemistry: Silica cycling over geologic time. Nat. Geosci. 8 (6), 431-432.

Consolaro, C., Macrì, P., Massari, F., Speranza, F., Fornaciari, E., 2013. A major change in the sedimentation regime in the Crotone Basin (Southern Italy) around 3.7-3.6 Ma. Palaeogeogr. Palaeoclim. Palaeoecol. 392, 398-410.

Cooke, J., Leishman, M.R., 2011. Is plant ecology more siliceous than we realise? Trends Plant Sci. 16 (2), 61-68.

Cornée, J.J., Saint Martin, J.P., Conesa, G., Münch, P., André, J.P., Saint Martin, S., Roger, S., 2004. Correlations and sequence stratigraphic model for Messinian

carbonate platforms of the western and central Mediterranean. Int. J. Earth Sci. 93, 621-633.

Cortese, G., Gersonde, R., Hillenbrand, C.D., Kuhn, G., 2004. Opal sedimentation shifts in the World Ocean over the last 15 Ma. Earth Planet. Sci. Lett. 224, 509-527.

Cosentino, D., Schildgen, T.F., Cipollari, P., Faranda, C., Gliozzi, E., Hudáčková, N., Lucifora, S., Strecker, M.R., 2012. Late Miocene surface uplift of the southern margin of the Central Anatolian Plateau, Central Taurides, Turkey. Geol. Soc. Am. Bull. 124 (1-2), 133-145.

Coughenour, M.B., 1985. Graminoid Responses to Grazing by Large Herbivores: Adaptations, Exaptations, and Interacting. Ann. Miss. Bot. Gard. 72 (4), 852-863.

Courme, M. D., Lauriat-Rage, A., 1998. Le Miocène supérieur à l'ouest du Gourougou (bassin de Melilla-Nador, Maroc): analyse biostratigraphique de formations sédimentaires associées à du volcanisme acide, et paléoenvironnement. Géol. Médit. 25 (2), 75-103.

Coward, M.P., De Donatis, M., Mazzoli, S., Paltrinieri, W., Wezel, F.C., 1999. Frontal part of the northern Apennines fold and thrust belt in the Romagna-Marche area (Italy): Shallow and deep structural styles. Tectonics 18 (3), 559-574.

Cramp, A., O'Sullivan, G., 1999. Neogene sapropels in the Mediterranean: a review. Mar. Geol. 153 (1), 11-28.

Crombet, Y., Leblanc, K., Quéguiner, B., Moutin, T., Rimmelin, P., Ras, J., Claustre, H., Leblond, N., Oriol, L., Pujo-Pay, M., 2011. Deep silicon maxima in the stratified oligotrophic Mediterranean Sea. Biogeosciences 8, 459-475.

Crosta, X., Pichon, J.J., Labracherie, M., 1997. Distribution of *Chaetoceros* resting spores in modern peri-Antarctic sediments. Mar. Micropaleontol. 29 (3-4), 283-299.

Crudeli, D., Young, J.R., Erba, E., Geisen, M., Ziveri, P., de Lange, G.J., P. Slomp, C.P., 2006. Associations from the Mediterranean (Holocene–late Pleistocene): Evaluation of carbonate diagenesis and palaeoecological–palaeocenographic implications. Palaeogeography, Palaeoclimatology, Palaeoecology 237, 191-224.

Damuth, J., Fortelius, M., 2001. Reconstructing mean annual precipitation, based on mammalian dental morphology and local species richness. In: Agustí, J., Oms, O. (Eds.), EEDEN Plenary Workshop on Late Miocene to Early Pliocene Environments and Ecosystems, pp. 23-24.

Davies, A., Kemp, A.E.S., 2016. Late Cretaceous seasonal palaeoclimatology and diatom palaeoecology from laminated sediments. Cret. Res. 65, 82-111.

Davies, A., Kemp, A.E.S., Pike, J., 2009. Late Cretaceous seasonal ocean variability from the Arctic. Nature 460, 254-259.

Day, T.A., Detling, J.K., 1990. Grassland patch dynamics and herbivore grazing preference following urine deposition. Ecology 71, 180-188.

de Visser, J.P., 1992. Clay mineral stratigraphy of Miocene to recent marine sediments in the central Mediterranean. Geol. Ultr. 75, 1-243.

Dela Pierre, F., Bernardi, E., Cavagna, S., Clari, P., Gennari, R., Irace, A., Lozar, F., Lugli, S., Manzi, V., Natalicchio, M., Roveri, M., Violanti, D., 2011. The record of the Messinian salinity crisis in the Tertiary Piedmont Basin (NW Italy): The Alba section revisited. Palaeo. Palaeo. Palaeo. 310 (3-4), 238-255.

Dela Pierre, F., Clari, P., Natalicchio, M., Ferrando, S., Giustetto, R., Lozar, F., Lugli, S., Manzi, V., Roveri, M., Violanti, D., 2014. Flocculent layers and bacterial mats in the mudstone interbeds of the Primary Lower Gypsum unit (Tertiary Piedmont basin, NW Italy): Archives of palaeoenvironmental changes during the Messinian salinity crisis. Mar. Geol. 355, 71-87.

Dela Pierre, F., Natalicchio, M., Ferrando, S., Giustetto, R., Birgel, D., Carnevale, G., Gier, S., Lozar, F., Marabello, D., Peckmann, J., 2015. Are the large filamentous microfossils preserved in Messinian gypsum colorless sulfide-oxidizing bacteria? Geology 43, 855-858.

Dela Pierre, F., Natalicchio, M., Lozar, F., Bonetto, S., Carnevale, G., Cavagna, S., Colombero, S., Sabino, M., Violanti, D., 2016. The northernmost record of the Messinian salinity crisis (Piedmont basin, Italy). Geol. Field Trips 8 (2.1), 58 pp.

Derry, L.A., Kurtz, A.C., Ziegler, K., Chadwick, O.A., 2005. Biological control of terrestrial silica cycling and export fluxes to watersheds. Nature 433, 728-730.

Dettman, D.L., Kohn, M.J., Quade, J., Ryerson, F.J., Ojha, T.P., Hamidullah, S., 2001. Seasonal stable isotope evidence for a strong Asian monsoon throughout the past 10.7 m.y. Geology 29 (1), 31-34.

Dickens, G.R., Barron, J.A., 1997. A rapidly deposited pennate diatom ooze in Upper Miocene-Lower Pliocene sediment beneath the North Pacific polar front. Mar. Micropaleontol. 31, 177-182.

Dickens, G.R., Owen, R.M., 1999. The Latest Miocene-Early Pliocene biogenic bloom: a revised Indian Ocean perspective. Mar. Geol. 161, 75-91.

Diekmann, B., Fälker, M., Kuhn, G., 2003. Environmental history of the south-eastern South Atlantic since the Middle Miocene: evidence from the sedimentological records of ODP Sites 1088 and 1092. Sedimentology 50, 511-529.

Diester-Haas, L., Billups, K., Emeis, K.C., 2006. Late Miocene carbon isotope records and marine biological productivity: Was there a (dusty) link? Paleoceanography 21 (4), 1-18.

Diester-Haass, L., Billups, K., Emeis, K.C., 2005. In search of the late Miocene-early Pliocene “biogenic bloom” in the Atlantic Ocean (Ocean Drilling Program Sites 982, 925, and 1088). Paleoceanography 20 (4), 1-13.

Diester-Haass, L., Meyers, P.A., Bickert, T., 2004. Carbonate crash and biogenic bloom in the late Miocene: Evidence from ODP Sites 1085, 1086, and 1087 in the Cape Basin, southeast Atlantic Ocean. Paleoceanography 19 (1), 1-19.

Diester-Haass, L., Meyers, P.A., Vidal, L., 2002. The late Miocene onset of high productivity in the Benguela Current upwelling system as part of a global pattern. Mar. Geol. 180 (1–4), 87–103.

Doblas, M., López-Ruiz, J., Cebriá, 2007. Cenozoic evolution of the Alboran Domain: A review of the tectonomagmatic models. In: Beccaluva, L., Bianchini, G., Wilson, M. (Eds.), Cenozoic Volcanism in the Mediterranean Area. Geol. Soc. Spec. Pap. 418, pp. 303-320.

Dougthy, C.E., Roman, J., Faurby, S., Wolf, A., Haque, A., Bakker, E.S., Malhi, Y., Dunning Jr. J.B., Svenning, J.C., 2016. Global nutrient transport in a world of giants. Proc. Natl. Acad. Sci. USA 113 (4), 868-873.

Drinia, H., Antonarakou, A., Tsaparas, N., Kontakiotis, G., 2007. Paleoenvironmental conditions preceding the Messinian Salinity Crisis: A case study from Gavdos Island. Geobios 40, 251-265.

Duermeijer, C.E., Van Vugt, N., Langereis, C.G., Meulenkamp, J.E., Zachariasse, W.J., 1998. A major late Tortonian rotation phase in the Crotone basin using AMS as tectonic tilt correction and timing of the opening of the Tyrrhenian basin. Tectonophysics 287 (1), 233-249.

Edwards, E.J., Osborne, C.P., Strömberg, C.A.E., Smith, S.A., 2010. The origins of C_4 grasslands: integrating evolutionary and ecosystem science. Science 328, 587-591.

Egge, J.K., Aksnes, D.L., 1992. Silicate as regulating nutrient in phytoplankton competition. Mar. Ecol. Prog. Ser. 83, 281-289.

Ehleringer, J.R., Cerling, T.E., Helliker, B.R., 1997. C_4 photosynthesis, atmospheric CO_2, and climate. Oecologia, 112 (3), 285-299.

Ehrlich, H., Demadis, K.D., Pokrovsky, O.S., Koutsoukos, P.G., 2010. Modern views on desilicification: biosilica and abiotic silica dissolution in natural and artificial environments. Chem. Rev. 110 (8), 4656-4689.

Ekeroth, N., Blomqvist, S., Hall, P.O., 2016_b. Nutrient fluxes from reduced Baltic Sea sediment: effects of oxygenation and macrobenthos. Mar. Ecol. Prog. Ser. 544, 77-92.

Ekeroth, N., Kononets, M., Walve, J., Blomqvist, S., Hall, P.O., 2016_a. Effects of oxygen on recycling of biogenic elements from sediments of a stratified coastal Baltic Sea basin. J. Mar. Syst. 154, 206-219.

El Ouahabi, F.Z., Saint Martin, S., Saint Martin, J.P., Moussa, A.B., Conesa, G., 2007. Les assemblages de diatomées du basin messinien de Boudinar (Maroc nord-oriental). Rev. Micropal. 50, 149-167.

Engel, A., 2002. Direct relationship between CO_2 uptake and transparent exopolymer particles production in natural phytoplankton. J. Plankton Res. 24 (1), 49-53.

Engel, A., 2004. Distribution of transparent exopolymer particles (TEP) in the northeast Atlantic Ocean and their potential significance for aggregation processes. Deep-Sea Res. Pt. I 51 (1), 83-92.

Eronen, J.T., Ataabadi, M.M., Micheels, A., Karme, A., Bernor, R.L., Fortelius, M., 2009. Distribution history and climatic controls of the Late Miocene Pikermian chronofauna. Proc. Natl. Acad. Sci. USA 106 (29), 11867-11871.

Esperante, R., Brand, L.R., Chadwick, A.V., Poma, O., 2015. Taphonomy and paleoenvironmental conditions of deposition of fossil whales in the diatomaceous sediments of the Miocene/Pliocene Pisco Formation, southern Peru—A new fossil-lagerstätte. Palaeogeogr. Palaeoclimatol. Palaeoecol. 417 (1), 337-370.

Estrada, M., 1991. Phytoplankton assemblages across a NW Mediterranean front: changes from winter mixing to spring stratification. Oecol. Aquat. 10, 157-185.

Estrada, M., 1996. Primary production in the northwestern Mediterranean. Sci. Mar. 60, 55-64.

Eynaud, F., Cronin, T.M., Smith, S.A., Zaragosi, J., Mavel, J., Mary, Y., Mas, V., Pujol, C., 2009. Morphological variability of the planktonic foraminifer *Neogloboquadrina pachyderma* from ACEX cores: implications for Late Pleistocene circulation in the Arctic Ocean. Micropaleontology 55 (2-3), 101-116.

Falkowski, P.G., Katz, M.E., Knoll, A.H., Quigg., A., Raven J.A., Schofield, O., Taylor, F.J.R., 2004. The Evolution of Modern Eukaryotic Phytoplankton. Science 305, 354-360.

Faranda, C., Gliozzi, E., Cipollari, P., Grossi, F., Darbaş, G., Gürbüz, K., Nazik, A., Gennari, R., Cosentino, D., 2013. Messinian paleoenvironmental changes in the easternmost Mediterranean Basin: Adana Basin, southern Turkey. Turk. J. Earth Sci. 22, 1-25.

Farrell, J.W., Raffi, I., Janecek, T.R., Murray, D.W., Levitan, M., Dadey, K.A., Emeis, K.C., Lyle, M., Flores, J.A., Hovan, S., 1995. Late Neogene sedimentation patterns in the Eastern Equatorial Pacifc Ocean. In: Pisias, N.G., Mayer, L.A., Janecek, T.R., Palmer-Julson, A., van Andel, T.H. (Eds.), Proc. Ocean Drill. Progr. Sci. Res. 138, 717-756.

Fauquette, S., Suc, J.P., Bertini, A., Popescu, S.M., Warny, S., Taoufiq, N.B., Perez Villa, M.J., Chikhi, H., Feddi, N., Subally, D., Clauzon, G., Ferrier, J., 2006. How did climate force the Messinian salinity crisis? Quantified climatic conditions from pollen records in the Mediterranean region. Palaeogeogr. Palaeoclimatol. Palaeoecol. 238 (1-4), 281-301.

Favre, E., François, L., Fluteau, F., Cheddadi, R., Thévenod, L., Suc, J.P., 2007. Messinian vegetation maps of the Mediterranean region using models and interpolated pollen data. Geobios 40, 433-443.

Ferretti, M.P., Rook, L., Torre, D., 2003. Stegotetrabelodon *(Proboscidea, Elephantidae)* from the late Miocene of southern Italy. J. Vert. Pal. 23 (3), 659-666.

Filippelli, G.M., 1997. Intensification of the Asian monsoon and a chemical weathering event in the late Miocene-early Pliocene: Implications for late Neogene climate change. Geology 25 (1), 27-30.

Filippelli, G.M., Delaney, L.M., 1994. The oceanic phosphorus cycle and continental weathering during the Neogene. Paleoceanography 9 (5), 643-652.

Filippelli, G.M., Sierro, F.J., Flores, J.A., Vázquez, A., Utrilla, R., Pérez-Folgado, M., Latimer, J.C., 2003. A sediment-nutrient-oxygen feedback responsible for productivity variations in Late Miocene sapropel sequences of the western Mediterranean. Palaeogeogr. Palaeoclimatol. Palaeoecol. 190, 335-348.

Flores, J.A., Sierro, F.J., Filippelli, G.M., Bárcena, M.A., Pérez-Folgado, M., Vázquez, A., Utrilla, R., 2005. Surface water dynamics and phytoplankton communities during deposition of cyclic late Messinian sapropel sequences in the western Mediterranean. Mar. Micropaleontol. 56, 50-79.

Foeken, J.P.T., Dunai, T.J., Bertotti, G., Andriessen, P.A.M., 2003. Late Miocene to present exhumation in the Ligurian Alps (southwest Alps) with evidence for accelerated denudation during the Messinian salinity crisis. Geology 31 (9), 797-800.

Folger, D.W., Burckle, L.H., Heezen, B.C., 1967. Opal Phytoliths in a North Atlantic Dust Fall. Science 155, 1243-1244.

Fortelius, M., Eronen, J., Liu, L., Pushkina, D., Tesakov, A., Vislobokova, I., Zhang, Z., 2006. Late Miocene and Pliocene large land mammals and climatic changes in Eurasia. Palaeogeogr. Palaeoclimatol. Palaeoecol. 238 (1-4), 219-227.

Fortelius, M., Eronen, J.T., Kaya, F., Tang, H., Raia, P., Puolamäki, K., 2014. Evolution of Neogene Mammals in Eurasia: Environmental Forcing and Biotic Interactions. Ann. Rev. Earth Planet. Sci. 42, 579-604.

Fourtanier, E., Gaudant, J., Cavallo, O., 1991. La diatomite de Castagnito (Piémont): une nouvelle preuve de l'existence d'oscillations modérées du niveau marin pendant le Messinien évaporitique. Boll. Soc. Pal. It. 30 (1), 79-95.

Frank, D.A., McNaughton, S.J., Tracy, B.F., 1998. The Ecology of the Earth's Grazing Ecosystems. BioScience 48 (7), 513-521.

Fraysse, F., Pokrovsky, O.S., Schott, J., Meunier, J.D., 2009. Surface chemistry and reactivity of plant phytoliths in aqueous solutions. Chem. Geol. 258, 197-206.

Frigerio, C., Bonadeo, L., Zerboni, A., Livio, F., Ferrario, M.F., Fioraso, G., Irace, A., Brunamonte, F., Michetti, A.M., 2017. First evidence for Late Pleistocene to Holocene earthquake surface faulting in the Eastern Monferrato Arc (Northern Italy): Geology, pedostratigraphy and structural study of the Pecetto di Valenza site. Quatern. Int. 451, 143-164.

Frizon de Lamotte, D., Leturmy, P., Missenarda, Y., Khomsi, S., Ruiz, G., Saddiqi, O., Guillocheau, F., Michard, A., 2009. Mesozoic and Cenozoic vertical movements in the Atlas system (Algeria, Morocco, Tunisia): An overview. Tectonophysics 475 (1), 9-28.

Frydas, D., 2004. Calcareous and siliceous phytoplankton stratigraphy of Neogene marine sediments in central Crete (Greece). Rev. Micropal.. 47 (2), 87-102.

Frydas, D., Keupp, H., 2015. Late Cenozoic silicoflagellates from Zakynthos and Aegina Islands, Greece, and their comparison to CG Ehrenberg's microgeological collection. Ann. Paleontol. 101 (1), 43–53.

Fuchs, J., Johnson, J.A., Mindell, D.P., 2015. Rapid diversification of falcons (Aves: Falconidae) due to expansion of open habitats in the Late Miocene. Mol. Phylogen. Evol. 82, 166-182.

Fulweiler, R.W., Nixon, S.W., 2005. Terrestrial vegetation and the seasonal cycle of dissolved silica in a southern New England coastal river. Biogeochemistry 74, 115-130.

Fytikas, M., Innocenti, F., Manetti, P., Peccerillo, A., Mazzuoli, R., Villari, L., 1984. Tertiary to Quaternary evolution of volcanism in the Aegean region. Geol. Soc. London Spec. Publ. 17 (1), 687-699.

Galán, E., González, I., Mayoral, E., Miras, A., 1993. Properties and applications of diatomitic materials from SW Spain. Appl. Clay. Sci. 8 (1), 1-18.

Gani, N.D.S., Gani, M.R., 2007. Blue Nile incision on the Ethiopian Plateau: Pulsed plateau growth, Pliocene uplift, and hominin evolution. GSA today 17 (9), 4-11.

García-Bernal, V., Paz, O., Cermeño, P., 2017. Changes in the Si/P weathering ratio and their effect on the selection of coccolithophores and diatoms. Biogeosciences Discuss. 1-19.

Gariboldi, K., 2015. Fossil diatom (Bacillariophyceae) association from the Mio-Pliocene laminated sediments of the Pisco Formation (East Pisco Basin, Peru): relations with the preservation of marine vertebrates in the fossil fecord and investigations on the influence of volcanic activity on primary production. Ph.D. thesis, Pisa University, 164 pp.

Garzione, C.N., Hoke, G.D., Libarkin, J.C., Withers, S., MacFadden, B., Eiler, J., Ghosh, P., Mulch, A., 2008. Rise of the Andes. Science 320, 1304-1307.

Gaudant, J., 2008. L'ichtyofaune messinienne du bassin de Sorbas (Almería, Espagne) et ses rapport avec l'environnement sédimentaire. Revista Española de Paleontología 23 (2), 211-223.

Gaudant, J., Caulet, J.P., Di Geronimo, I., Di Stefano, A., Fourtanier, E., Romeo, M., Venec-Peyre, M.T., 1996. Analyse séquentielle d'un nouveau gisement de poisons fossils du Messinien marin diatomitique: Masseria il Salto près de Caltagirone (Province de Catane, Sicile). Géol. Médit. 23 (2), 117-153.

Gaudant, J., Courme-Rault, M.D., Fornaciari, E., Fourtanier, E., 2010. The Upper Miocene fossil fish locality of Pecetto di Valenza (Piedmont, Italy): a multidisciplinary approach. Boll. Soc. Pal. It. 49 (3), 203–225.

Gaudant, J., Soria, J.M., Fierro, I., Saint Martin, S., 2015. The Upper Miocene fish fauna of the Fortuna Basin, as observed in the surroundings of Abanilla (Murcia province, Spain). Spanish J. Paleont. 30 (1), 65-78.

Gaudant, J., Tsaparas, N., Antonarakou, A., Drinia, H., Saint Martin, S., Dermitzakis, M.D., 2006. A new marine fish fauna from the pre-evaporitic Messinian of Gavdos Island (Greece). C.R. Palevol 5, 795-802.

Gennari, R., Lozar, F., Turco, E., Dela Pierre, F., Manzi, V., Natalicchio, M., Lugli, S., Roveri, M., Schreiber, C., Taviani, M., 2018. Integrated stratigraphy and paleoceanographic evolution of the pre-evaporitic phase of the Messinian

salinity crisis in the Eastern Mediterranean as recorded in the Tokhni section (Cyprus island). News. Strat. 50, 1-23.

Gérard, F., Mayer, K.U., Hodson, M.J., Ranger, J., 2008. Modelling the biogeochemical cycle of silicon in soils: application to a temperate forest ecosystem. Geochim. Cosmochim. Acta 72 (3), 741-758.

Gerbersdorf, S.U., Wieprecht, S., 2015. Biostabilization of cohesive sediments: revisiting the role of abiotic conditions, physiology and diversity of microbes, polymeric secretion, and biofilm architecture. Geobiology 13, 68-97.

Gersonde, R., Schrader, H., 1984. Marine planktic diatom correlation of lower Messinian deposits in the western Mediterranean. Mar. Micropaleontol. 9 (2), 93-110.

Ghetti, P., Anadón, P., Bertini, A., Esu, D., Gliozzi, E., Rook, L., Soulié-Märsche, I., 2002. The Early Messinian Velona basin (Siena, central Italy): paleoenvironmental and paleobiogeographical reconstructions. Palaeogeogr. Palaeoclimatol. Palaeoecol. 187 (1-2), 1-33.

Giaconia, F., Booth-Rea, G., Ranero, C.R., Gràcia, E., Bartolome, R., Calahorrano, A., Lo Iacono, C., Vendrell, M.G., Cameselle, A.L., Costa, S., Gómez de la Peña, L., Martínez-Loriente, S., Perea, H., Viñas, M., 2015. Compressional tectonic inversion of the Algero-Balearic basin: Latemost Miocene to present oblique convergence at the Palomares margin (Western Mediterranean). Tectonics 34 (7), 1516-1543.

Gibbs, S., Shackleton, N., Young, J.R., 2004. Orbitally forced climate signals in mid-Pliocene nannofossil assemblages. Marine Micropaleontology 51, 39-56.

Gibert, L., Scott, G.R., Montoya, P., Ruiz-Sánchez, F.J., Morales, J., Luque, L., Abella, J., Lería, M., 2013. Evidence for an African-Iberian mammal dispersal during the pre-evaporitic Messinian. Geology 41 (6), 691-694.

Giraudeau et al., 1992; Distribution of Recent nannofossils beneath the Benguela system: southwest African continental margin. Marine Geology, 108, 219-237.

Gladstone, R., Flecker, R., Valdes, P., Lunt, D., Marwick, P., 2007. The Mediterranean hydrologic budget from a Late Miocene global climate simulation. Palaeogeogr. Palaeoclimatol. Palaeoecol. 251, 254-267.

Glotzbach, C., Reinecker, J., Danišík, M., Rahn, M., Frisch, W., Spiegel, C., 2008. Neogene exhumation history of the Mont Blanc massif, western Alps. Tectonics 27 (4), 1-17.

Glotzbach, C., Reinecker, J., Danišík, M., Rahn, M., Frisch, W., Spiegel, C., 2010. Thermal history of the central Gotthard and Aar massifs, European Alps: Evidence for steady state, long-term exhumation. J. Geophys. Res. Earth Surf. 115 (F3), 1-24.

Gombos, A.M., 1984. Late Neogene diatoms and diatom oozes in the Central South-Atlantic. In: Init. Rep. DSDP (Eds K.J. Hsü, J.L. LaBrecque and K.A. Pisciotto) 73, 487-494.

González-Regalado, M.L., Romero, V., Abad, M., Tosquella, J., Izquierdo, T., Gómez, P., Clement, M.J., Toscano, A., Rodríguez Vidal, J., Cáceres, L.M.,

Muñoz, J.M., Prudencio, M.I., Dias, M.I., Marques, R., García, E.X.M., Carretero, M.I., Ruiz, F., Monge, G., 2019. Late Tortonian-middle Messinian palaeoenvironmental changes in the western Betic Strait (SW Spain). Ameghiniana 56 (4), 336-360.

Govean, F.M., Garrison, R.E., 1981. Significance of laminated and massive diatomites in the upper part of the Monterey Formation, California. In: The Monterey Formation and Related Siliceous Rocks of California (Eds R.E. Garrison, R.G. Douglas, K.E. Pisciotto, C.M. Isaacs and J.C. Ingle), 181-198.

Gramigna, P., Guido, A., Mastandrea, A., Russo, F., 2008. The paleontological site of Cessaniti: a window on a coastal marine environment of seven million years ago (Southern Calabria, Italy). Geol. Rom. 41, 25-34.

Griffin, D.L., 2002. Aridity and humidity: two aspects of the late Miocene climate of North Africa and the Mediterranean. Palaeogeogr. Palaeoclimatol. Palaeoecol. 182, 65-91.

Grigorov, I., Pearce, R., Kemp, A.E.S., 2002. Southern Ocean laminated diatom ooze: mat deposits and potential for palaeo-flux studies, ODP leg 177, Site 1093. Deep-Sea Res. Pt. II 49 (16), 3391-3407.

Grimm, K.A., Lange, C.B., Gill, A.S., 1997. Self-sedimentation of phytoplankton blooms in the geologic record. Sed. Geol. 110 (3-4), 151-161.

Grimm, K.A., Lange, K.B., Gill, A.S., 1996. Biological forcing of hemipelagic sedimentary laminae: Evidence from ODP site 893, Santa Barbara Basin, California. J. Sed. Res. 66 (3), 613-624.

Guntzer, F., Keller, C., Meunier, J.D., 2012. Benefits of plant silicon for crops: a review. Agron. Sustain. Dev. 32, 201-213.

Guo, Z., Peng, S., Hao, Q., Biscaye, P.E., An, Z., Liu, T., 2004. Late Miocene–Pliocene development of Asian aridification as recorded in the Red-Earth Formation in northern China. Glob. Planet. Change 41 (3-4), 135-145.

Guptha, M.V.S., Banerjee, R., Mergulhao, L.P., Banerjee, P., Parthiban, G., Tewari, M., 2007. Early Pliocene paleoceanography of the Vityaz Fracture Zone, Central Indian Ridge. Acta Geol. Sinica 81, 614-621.

Halim, Y., Guergues, S.K., Saleh, H., 1967. Hydrographic conditions and plankton in the south east Mediterranean during the last normal Nile flood (1964). Int. Revue ges. Hydrobiol. 52 (3), 401-425.

Hallegraeff, G.M., 1986. Taxonomy and morphology of the marine plankton diatoms *Thalassionema* and *Thalassiothrix*. Diatom Res. 1 (1), 57-80.

Hamm, C.E., 2002. Interactive aggregation and sedimentation of diatoms and clay-sized lithogenic material. Limnol. Oceanogr. 47 (6), 1790-1795.

Haq, B.U., Hardenbol, J., Vail, P.R., 1987. Chronology of fluctuating sea levels since the Triassic. Science 235, 1156-1167.

Harrison, R.W., Newell, W.L., Batıhanlı, H., Panayides, I., McGeehin, J.P., Mahan, S.A., Őzhűr, A., Tsiolakis, E., Necdet, M., 2004. Tectonic framework and Late Cenozoic tectonic history of the northern part of Cyprus: implications for earthquake hazards and regional tectonics. J. Asian Earth. Sci. 23 (2), 191-210.

Harrison, T.M., Copeland, P., Kidd, W.S.F., Yin, A., 1992. Raising Tibet. Science 255, 1663-1670.

Harzhauser, M., Kroh, A., Mandic, O., Piller, W.E., Göhlich, U., Reuter, M., Berning, B., 2007. Biogeographic responses to geodynamics: A key study all around the Oligo-Miocene Tethyan Seaway. Zool. Anz. 246, 241-256.

Hasle, G.R., 2001. The marine, planktonic diatom family Thalassionemataceae: morphology, taxonomy and distribution. Diatom Res. 16 (1), 1-82.

Hasle, G.R., Syvertsen, E.E., 1997. Marine diatoms. In: Tomas, C.R. (Ed.), Identifying Marine Phytoplankton, 5-385.

Hay, W.W., Southam, J.R. (1977). Modulation of marine sedimentation by the continental shelves. In: Andersen, N.R., Malahoff, A. (Eds.) The fate of fossil fuel CO_2 in the oceans. Plenum Press, New York, pp. 569-604.

Hecky, R.E., Mopper, K., Kilham, P., Degens, E.T., 1973. The amino acid and sugar composition of diatom cell-walls. Mar. Biol. 19 (4), 323-331.

Hermoyian, C.S., Owen, R.M., 2001. Late Miocene-early Pliocene biogenic bloom: Evidence from low-productivity regions of the Indian and Atlantic Oceans. Paleoceanography 16 (1), 95-100.

Hickman, A.E., Holligan, P.M., Moore, C.M., Sharples, J., Krivtsov, V., Palmer, M.R., 2009. Distribution and chromatic adaptation of phytoplankton within a shelf sea thermocline. Limnol. Oceanogr. 54 (2), 525-536.

Higgins, S.I., Bond, W.J., Trollope, W.S.W., 2000. Fire, resprouting and variability: a recipe for grass-tree coexistence in savanna. J. Ecol. 88, 213-229.

Hilgen, F.J., Krijgsman, W., 1999. Cyclostratigraphy and astrochronology of the Tripoli diatomite formation (pre-evaporite Messinian, Sicily, Italy). Terra Nova 11, 16–22.

Hinrichs, K.U., Boetius, A., 2002. The anaerobic oxidation of methane: new insights in microbial ecology and biogeochemistry. In: Wefer, G., Billet., D., Hebbeln, D., Jorgensen, B.B., Schlüter, M., Weering, T.C.E.V. (Eds.), Ocean margin systems, Springer Berlin Heidelberg, pp. 457-477.

Hodson, M.J., White, P.J., Mead, A., Broadley, M.R., 2005. Phylogenetic Variation in the Silicon Composition of Plants. Ann. Bot. 96, 1027-1046.

Hoetzel, S., Dupont, L., Schefuß, E., Rommerskirchen, F., Wefer, G., 2013. The role of fire in Miocene to Pliocene C_4 grassland and ecosystem evolution. Nat. Geosci. 6, 1027-1030.

Holland, E.A., Parton, W.J., Detling, J.K., Coppock, D.L., 1992. Physiological responses of plant populations to herbivory and their consequences for ecosystem nutrient flow. Am. Nat. 140 (4), 685-706.

Hoorn, C., Bogotá-A, G.R., Romero-Baez, M., Lammertsma, E.I., Flantua, S.G.A., Dantas, E.L., Dino, R., do Carmo, D.A., Chemale Jr., F., 2017. The Amazon at sea: Onset and stages of the Amazon River from a marine record, with special reference to Neogene plant turnover in the drainage basin. Glob. Planet. Change 153, 51-65.

Hoorn, C., Wesselingh, F.P., ter Steege, H., Bermudez, M.A., Mora, A., Sevinik, J., Sanmartín, I., Sanchez-Meseguer, A., Anderson, C.L., Figueiredo, J.P.,

Jaramillo, C., Riff, D., Negri, F.R., Hooghiemstra, H., Lundberg, J., Stadler, T., Särkinen, T., Antonelli, A., 2010. Amazonia Through Time: Andean Uplift, Climate Change, Landscape Evolution, and Biodiversity. Science 330, 927-931.

Hummel, J., Findeisen, E., Südekum, K.H., Ruf, I., Kaiser, T.M., Bucher, M., Clauss, M., Codron, D., 2010. Another one bites the dust: faecal silica levels in large herbivores correlate with high-crowned teeth. Proc. R. Soc. B 278, 1742-1747.

Hüsing, S.K., Kuiper, K.F., Link, W., Hilgen, F.J., Krijgsman, W., 2009. The upper Tortonian–lower Messinian at Monte dei Corvi (Northern Apennines, Italy): completing a Mediterranean reference section for the Tortonian stage. Earth Planet. Sci. Lett. 282 (1), 140-157.

Iliopoulos, G., Roussiakis, S., Fassoulas, C., 2012. First occurrence of carnivore footprint with hyaenid affinities from the Late Miocene of Crete (Greece). Palaeobiodivers. Palaeoenviron. 92 (2), 265-271.

Incarbona, A., Jonkers, L., Ferraro, S., Sprovieri, R., Tranchida, G., 2019. Sea surface temperatures and paleoenvironmental variability in the Central Mediterranean during historical times reconstructed using planktonic foraminifera. Paleoceanogr. Paleocl. 34 (3), 394-408.

Ioakim, C., Rondoyanni, T., Mettos, A., 2005. The Miocene Basins of Greece (Eastern Mediterranean) from a palaeoclimatic perspective. Rev. Paleobiol. 24 (2), 735-748.

Irace, A., 2004. Il Messiniano piemontese: nuovi dati da due aree campione. Ph.D. thesis, University of Torino, 167 pp.

Isaacs C.M., Pisciotto K.A., Garrison R.E., 1983. Facies and diagenesis of the Miocene Monterey Formation, California: a summary. Developments in Sedimentology 36, 247-282.

Ittekot, V., 1993. The abiotically driven biological pump in the ocean and short-term fluctuations in atmospheric CO_2 contents. Global Planet. Change 8, 17-25.

Jacobs, B.F., Kingston, J.D., Jacobs, L.L., 1999. The Origin of Grass-Dominated Ecosystems. Ann. Miss. Bot. Gard. 86 (2), 590-643.

Janis, C.M., 1993. Tertiary Mammal Evolution in the Context of Changing Climates, Vegetation, and Tectonic Events. Ann. Rev. Ecol. Evol. Syst. 24, 467-500.

Jianru, L., Rujian, W., Baohua, L., 2002. Variations of opal accumulation rates and paleoproductivity over the past 12 Ma at ODP Site 1143, southern South China Sea. Chin. Sci. Bull. 47 (7), 596-598.

Jiménez-Moreno, G., Fauquette, S., Suc, J.P., 2010. Miocene to Pliocene vegetation reconstruction and climate estimates in the Iberian Peninsula from pollen data. Rev. Paleobot. Palynol. 162, 403-415.

Jolivet, L., Augier, R., Robin, C., Suc, J.P., Rouchy, J.M., 2006. Lithospheric-scale geodynamic context of the Messinian salinity crisis. Sed. Geol. 188, 9-33.

Jonkers, H.A., 1984. Pliocene benthonic foraminifera from homogeneous and laminated marls on Crete. Utrecht Microapleontological Bulletins 31, 79 pp.

Jordan, R.W., Stickley, C.E., 2010. Diatoms as indicators of paleoceanographic events. In: Smol, J.P., Stoermer, E.F. (Eds.), The Diatoms. Applications for the Environmental and Earth Sciences (2nd edition), Cambridge University Press, pp. 424-453.

Jorissen, F.J., Barmawidjaja, D.M., Puskaric, S., van der Zwaan, G.J., 1992. Vertical distribution of benthic foraminifera in the northern Adriatic Sea: the relation with the organic flux. Mar. Micropaleontol. 19, 131-146.

Jorissen, F.J., de Stigter, H.C., Widmark, J.G.V., 1995. A conceptual model explaining benthic foraminiferal microhabitats. Mar. Micropaleontol. 26, 3-15.

Jurskschat, T., Fenner, J., Fischer, R., Michalzik, D., 2000. Environmental changes in pre-evaporitic Late Miocene time in the Lorca Basin (SE Spain): diatom results. In: Climates: Past and Present (Ed M.B. Hart), Geol. Soc. London Spec. Publ. 181, 65-78.

Kaiser, T.M., Müller, D.W., Fortelius, M., Schulz, E., Codron, D., Clauss, M., 2013. Hypsodonty and tooth facet development in relation to diet and habitat in herbivorous ungulates: implications for understanding tooth wear. Mammal Rev. 43 (1), 34-46.

Kallel, N., Duplessy, J.C., Labeyrie, L., Fontugne, M., Paterne, M., Montacer, M., 2000. Mediterranean pluvial periods and sapropel formation over the last 200.000 years. Palaeo. Palaeo. Palaeo. 157 (1-2), 45-58.

Kaplan, I.R., Rittenberg, S., 1963. Basin sedimentation and diagenesis. The Sea 3, 583-619.

Karakitsios, V., Roveri, M., Lugli, S., Manzi, V., Gennari, R., Antonarakou, A., Triantaphyllou, M., Agiadi, K., Kontakiotis, G., Kafousia, N., De Rafelis, M., 2016. A record of the Messinian salinity crisis in the eastern Ionian tectonically active domain (Greece, eastern Mediterranean). Basin Research 28 (1), 1-31.

Kato, Y., 2019. Late Miocene to Pliocene fossil chrysophyte cysts from ODP Site 689 and DSDP Site 513, the Atlantic sector of the Southern Ocean. In: Jordan, R.W., Yokoyama, J. (Eds.), Chrysophytes – Taxonomy, biodiversity and palaeoecology. Nowa Hedwigia 148, 131-156.

Kaufman, P.B., Dayanandan, P., Franklin, C.I., Takeoka, Y., 1985. Structure and function of silica bodies in the epidermal system of grass shoots. Ann. Bot. 55 (4), 487-507.

Kayseri-Özer, M., Karadenizli, L., Akgün, F., Oyal, N., Saraç, G., Şen, Ş., Tunoğlu, C., Tuncer, A., 2017. Palaeoclimatic and palaeonvironmental interpretations of the Late Oligocene, Late Miocene-Early Pliocene in the Çankırı-Çorum Basin. Palaeogeogr. Palaeoclimatol. Palaeoecol. 467, 16-36.

Keeley, J.E., Rundel, P.W., 2005. Fire and the Miocene expansion of C_4 grasslands. Ecol. Lett. 8 (7), 683-690.

Kemp, A.E., 1996. Laminated sediments as palaeo-indicators. In: Kemp, A.E. (Ed.), Palaeoclimatology and Palaeoceanography from Laminated Sediments, Geol. Soc. London Spec. Publ. 116 (1), 7-12.

Kemp, A.E.S., Baldauf, J.G., 1993. Vast Neogene laminated diatom mat deposits from the eastern equatorial Pacific Ocean. Nature 362, 141-144.

Kemp, A.E.S., Pearce, R.B., Grigorov, I., Rance, J., Lange, C.B., Quilty, P., Salter, I., 2006. Production of giant marine diatoms and their export at oceanic frontal zones: Implications for Si and C flux from stratified oceans. Glob. Biogeochem. Cycles 20, 1-13.

Kemp, A.E.S., Pearce, R.B., Koizumi, I., Pike, J., Rance, S.J., 1999. The role of mat-forming diatoms in the formation of Mediterranean sapropels. Nature 398, 57-61.

Kemp, A.E.S., Pike, J., Pearce, R.B., Lange, C.B., 2000. The "Fall dump" – a new perspective on the role of a "shade flora" in the annual cycle of diatom production and export flux. Deep-Sea Res. Pt. II 47 (9), 2129-2154.

Kemp, A.E.S., Villareal, T.A., 2013. High diatom production and export in stratified waters–A potential negative feedback to global warming. Prog. Oceanogr. 119, 4-23.

Kemp, A.E.S., Villareal, T.A., 2018. The case of the diatoms and the muddled mandalas: time to recognize diatom adaptations to stratified waters. Progr. Oceanogr. 167, 138-149.

Kidder, D.L., Erwin, D.H., 2001. Secular distribution of biogenic silica through the Phanerozoic: comparison of silica-replaced fossils and bedded cherts at the series level. J. Geol. 109 (4), 509-522.

Kidder, D.L., Gierlowski-Kordesch, E.H., 2005. Impact of grassland radiation on the nonmarine silica cycle and Miocene diatomite. Palaios 20, 198-206.

King, S.C., Kemp, A.E.S., Murray, J.W., 1995. Benthic foraminifer assemblages in Neogene laminated diatom ooze deposits in the Eastern Equatorial Pacific Ocean (Site 844). In: Proc. Ocean Drill. Progr. Sci. Res. (Eds N.G. Pisias, L.A. Mayer, T.R. Janecek, A. Palmer-Julson and T.H. van Andel) 138, 665-673.

Klaver, M., Djuly, T., de Graaf, S., Sakes, A., Wijbrans, J., Davies, G., Vroon, P., 2015. Temporal and spatial variations in provenance of Eastern Mediterranean Sea sediments: Implications for Aegean and Aeolian arc volcanism. Geochim. Cosmochim. Acta 153, 149-168.

Köhler, C.M., 2008. Proxy based reconstructions of late Miocene climatic and tectonic driven changes in the Eastern Mediterranean. University of Bremen, 86 pp.

Köhler, C.M., Heslop, D., Krijgsman, W., Dekkers, M.J., 2010. Late Miocene paleoenvironmental changes in North Africa and the Mediterranean recorded by geochemical proxies (Monte Gibliscemi section, Italy). Palaeogeogr. Palaeoclimatol. Palaeoecol. 285 (1), 66-73.

Köhler, C.M., Heslop., D., Dekkers, M.J., Krijgsman, W., van Hinsbergen, D.J.J., von Dobeneck, T., 2008. Tracking provenance changes during the late Miocene in the Eastern Mediterranean Metochia section using geochemical and environmental magnetic proxies. Geochem. Geophys. Geosyst. 9 (12), 1-14.

Kohn, M.J., Fremd, T.J., 2008. Miocene tectonics and climate forcing of biodiversity, western United States. Geology 36 (10), 783-786.

Koizumi, I., Yamamoto, H., 2018. Diatom ooze and diatomite-diatomaceous sediments in and around the North Pacific Ocean. JAMSTEC Rep. Res. Dev. 27, 26-46.

Korhola, A., Smol, J.P., 2001. Ebridians. In: Smol, J.P., Birks, H.J.B., Last, W.M. (Eds.), Tracking Environmental Change Using Lake Sediments. Volume 3: Terrestrial, Algal, and Siliceous Indicators, 225-234.

Köster, J., Rospondek, M., Schouten, S., Kotarba, M., Zubrzycki, A., Sinninghe Damsté, J.S., 1998. Biomarker geochemistry of a foreland basin: the Oligocene Menilite Formation in the Flysch Carpathians of Southeast Poland. Org. Geochem. 29 (1-3), 649-669.

Kouwenhoven, T.J., 2000. Survival under stress: benthic foraminiferal patterns and Cenozoic biotic crises. Geologica Ultraiectina 186, 206 pp.

Kouwenhoven, T.J., Seidenkrantz, M.S., van der Zwaan, G.J., 1999. Deep-water changes: the near-synchronous disappearance of a group of benthic foraminifera from the Late Miocene Mediterranean. Palaeo. Palaeo. Palaeo. 152 (3-4), 259-281.

Kouwenhoven, T.J., van der Zwaan, G.J., 2006. A reconstruction of late Miocene Mediterranean circulation patterns using benthic foraminifera. Palaeogeogr. Palaeoclimatol. Palaeoecol. 238 (1), 373-385.

Krijgsman, W., 2002. The Mediterranean: mare nostrum of earth sciences. Earth Planet. Sci. Lett. 205 (1), 1-12.

Krijgsman, W., Blanc-Valleron, M.M., Flecker, R., Hilgen, F.J., Kouwenhoven, T.J., Merle, D., Orszag-Sperber, F., Rouchy, J.M., 2002. The onset of the Messinian salinity crisis in the Eastern Mediterranean (Pissouri Basin, Cyprus). Earth Planet. Sci. Lett. 194 (3-4), 15 299-310.

Krijgsman, W., Fortuin, A.R., Hilgen, F.J., Sierro, F.J., 2001. Astrochronology for the Messinian Sorbas basin (SE Spain) and orbital (precessional) forcing for evaporite cyclicity. Sed. Geol. 140, 43-60.

Krijgsman, W., Garcés, M., Agustí, J., Raffi, I., Taberner, C., Zachariasse, W.J., 2000. The 'Tortonian salinity crisis' of eastern Betics (Spain). Earth Planet. Sci. Lett. 181, 497-511.

Krijgsman, W., Hilgen, F.J., Raffi, I., Sierro, F.J., Wilson, D.S., 1999. Chronology, causes and progression of the Messinian salinity crisis. Nature 400, 652-655.

Krijgsman, W., Langereis, C.G., Zachariasse, W.J., Boccaletti, M., Moratti, G., Gelati, R., Iaccarino, S., Papani, G., Villa, G., 1999. Late Neogene evolution of the Taza–Guercif Basin (Rifian Corridor, Morocco) and implications for the Messinian salinity crisis. Mar. Geol. 153 (1-4), 147-160.

Krinsley, D.H., Pye, K., Boggs, S., Tovey, N.K., 1998. Backscattered Scanning Electron Microscopy and Image Analysis of Sediments and Sedimentary Rocks. Cambridge University Press, 193 pp.

LaClau, J.P., Sama-Poumba, W., Nzila, J.D.D., Bouillet, J.P., Ranger, J., 2002. Biomass and nutrient dynamics in a littoral savanna subjected to annual fires in Congo. Acta Oecol. 23, 41-50.

Lakkis, S., Novel-Lakkis, V., 1981. Composition, annual cycle and species diversity of the phytoplankton in Lebanese coastal water. J. Plankton Res. 3 (1), 123-136.

Langer, M.R., 1993. Epiphytic foraminifera. Mar. Micropaleontol. 20, 235-265.

Laruelle, G.G., Roubeix, V., Sferratore, A., Brodherr, B., Ciuffa, D., Conley, D.J., Dürr, H.H., Garnier, J., Lancelot, C., Le Thi Phuong, Q., J.D., Meunier, Meybeck, M., Michalopoulos, P., Moriceau, B., Ni Longphuirt, S., Loucaides, S., Papush, L., Presti, M., Ragueneau, O., Regnier, P., Saccone, L., Slomp, C.P., Spiteri, C., Van Cappellen, P., 2009. Anthropogenic perturbations of the silicon cycle at the global scale: Key role of the land-ocean transition. Glob. Biogeochem. Cycles 23, 1-17.

Latasa, M., Estrada, M., Delgado, M., 1992. Plankton-pigment relationships in the Northwestern Mediterranean during stratification. Mar. Ecol. Prog. Ser. 88, 61-73.

Latrubesse, E.M., Cozzuol, M., da Silva-Caminha, S.A.F., Rigsby, C.A., Absy, M.L., Jaramillo, C., 2010. The Late Miocene paleogeography of the Amazon Basin and the evolution of the Amazon River system. Earth-Sci. Rev. 99, 99-124.

Lazarus, D., Barron, J., Renaudie, J., Diver, P., Türke, A., 2014. Cenozoic Planktonic Marine Diatom Diversity and Correlation to Climate Change. PLoS One 9 (1), e84857.

Lehtimäki, M., Sinkko, H., Tallberg, P., 2016. The role of oxygen conditions in the microbial dissolution of biogenic silica under brackish conditions. Biogeochemistry 129 (3), 355-371.

Lehto, N., Glud, R.N., á Norði, G., Zhang, H., Davison, W., 2014. Anoxic microniches in marine sediments induced by aggregate settlement: biogeochemical dynamics and implications. Biogeochemistry 119, 307-327.

Leinen, M., 1979. Biogenic silica accumulation in the central equatorial Pacific and its implications for Cenozoic paleoceanography: summary. Geol. Soc. Am. Bull. 90, 801-803.

Lewin, J.C., 1961. The dissolution of silica from diatom walls. Geochim. Cosmochim. Acta 21 (3-4), 182-198.

Li, J., 1995. A study of the effect of organic matter on silica diagenesis using a geochemical modeling code. Graduate Student Theses, Dissertations & Professional Papers, 7508, 62 pp.

Lihoreau, F., Boisserie, J.R., Viriot, L., Coppens, Y., Likius, A., Mackaye, H.T., Tafforeau, P., Vignaud, P., Brunet, M., 2006. Anthracothere dental anatomy reveals a late Miocene Chado-Libyan bioprovince. Proc. Natl. Acad. Sci. USA 103 (23), 8763-8767.

Linder, H.P., Rudall, P.J., 2005. Evolutionary History of Poales. Ann. Rev. Ecol. Evol. Syst. 36, 107-124.

Lirer, F., Foresi, L.M., Iaccarino, S.M., Salvatorini, G., Turco, E., Cosentino, C., Sierro, F.J., Caruso, A., 2019. Mediterranean Neogene planktonic foraminifer biozonation and biochronology. Earth-Sci. Rev. 196, 1-36.

Liu, L., Puolamäki, K., Eronen, J.T., Ataabadi, M.M., Hernesniemi, E., Fortelius, M., 2012. Dental functional traits of mammals resolve productivity in terrestrial ecosystems past and present. Proc. R. Soc. B 279 (1739), 2793-2799.

Locker, S., Martini, E., 1986. Phytoliths from the Southwest Pacific, Site 591. Init. Rep. DSDP 90, 1079-1084.

Locker, S., Martini, E., 1989. Cenozoic silicoflagellates, ebridians and actiniscidians from the Vøring Plateaeu (ODP Leg 104). Proc. ODP Sci. Results (Eds O. Eldholm, J. Thiede, E. Taylor et al.) 104, 543-585.

Londeix, L., Benzakour, M., Suc, J.P., Turon, J.L., 2007. Messinian palaeoenvironments and hydrology in Sicily (Italy): The dinoflagellate cyst record. Geobios 40 (3), 233-250.

Lopes, C., Mix, A.C., Abrantes, F., 2006. Diatoms in northeast Pacific surface sediments as paleoceanographic proxies. Mar. Micropaleontol. 60, 45-65.

Lozar, F., Violanti, D., Bernardi, E., Dela Pierre, F., Natalicchio, M., 2018. Identifying the onset of the Messinian salinity crisis: a reassessment of the biochronostratigraphic tools (Piedmont Basin, NW Italy). Newsletters on Stratigraphy, 51 (1), 11-31.

Lozar, F., Violanti, D., Dela Pierre, F., Bernardi, E., Cavagna, S., Clari, P., Irace, A., Martinetto, E., Trenkwalder, S., 2010. Calcareous nannofossils and

Foraminifers herald the Messinian salinity crisis: the Pollenzo section (Alba, Cuneo; NW Italy). Geobios 43, 21–32.

Lyle, M., Baldauf, J., 2015. Biogenic sediment regimes in the Neogene equatorial Pacific, IODP Site U1338: Burial, production, and diatom community. Palaeo. Palaeo. Palaeo. 433, 106-128.

Ma, J.F., Yamaji, N., 2006. Silicon uptake and accumulation in higher plants. Trends Plant Sci. 11 (8), 392-397.

Malinverno, E., Cerino, F., Karatsolis, B.T., Ravani, A., Dimiza, M., Psarra, S., Gogou, A., Triantaphyllou, M.V., 2019. Silicoflagellates in the eastern mediterranean and Black Seas: seasonality, distribution and sedimentary record. Deep-Sea Res. Pt. II 164, 122-134.

Mancini, A.M., Gennari, R., Ziveri, P., Mortyn, P.G., Stolwijk, D.J., Lozar, F., *submitted*. Calcareous nannofossil and foraminiferal trace element records in the Sorbas Basin: a new piece of the Messinian Salinity Crisis onset puzzle.

Mansour, B., Bessedik, M., Saint Martin, J.P., Belkebir, L., 2008. Signification paléoécologique des assemblages de diatomées du Messinien du Dahra sud-occidental (bassin du Chélif, Algérie nord-occidentale). Geodiversitas 30 (1), 117-139.

Mansour, B., Moissette, P., Noël, D., Rouchy, J.M., 1995. L'enregistrement par les associations de diatomées des environnements messiniens: l'exemple de la coupe de Sig (Bassin du Chélif-Algérie). Geobios 28 (3), 261-279.

Mansour, B., Saint Martin, J.P., 1999. Conditions de depôt des diatomites messiniennes en contexte de plateforme carbonatée d'après l'etude des assemblages de diatomées: Exemple du Djebel Murdjadjo (Algérie). Geobios 32 (3), 395-408.

Manzi, V., Gennari, R., Hilgen, F., Krijgsman, W., Lugli, S., Roveri, M., Sierro, F.J., 2013. Age refinement of the Messinian salinity crisis onset in the Mediterranean. Terra Nova 25 (4), 1-8.

Manzi, V., Lugli, S., Roveri, M., Dela Pierre, F., Gennari, R., Lozar, F., Natalicchio, M., Schreiber, C., Taviani, M., Turco, E., 2016. The Messinian Salinity Crisis in Cyprus: a further step toward a new stratigraphic framework for Eastern Mediterranean. Basin Res. 28, 207-236.

Mari, X., Passow, U., Migon, C., Burd, A.B., Legendre, L., 2017. Transparent exopolymer particles: Effects on carbon cycling in the ocean. Prog. Oceanogr. 151, 13-37.

Marra, A.C., Solounias, N., Carone, G., Rook, L., 2011. Palaeogeographic significance of the giraffid remains (Mammalia, Arctiodactyla) from Cessaniti (Late Miocene, Southern Italy). Geobios 44 (2), 189-197.

Martín, J.M., Braga, J.C., 1994. Messinian events in the Sorbas Basin in southeastern Spain and their implications in the recent history of the Mediterranean. Sed. Geol. 90, 257-268.

Martin-Jézéquel, V., Hildebrand, M., Brzezinski, M.A., 2000. Silicon metabolism in diatoms: implications for growth. J. Phycol. 36, 821-840.

Martin-Jézéquel, V., Lopez, P.J., 2003. Silicon – a central metabolite for diatom growth and morphogenesis. In: Müller, W.E.G. (Ed.), Silicon Biomineralization, Prog. Mol. Subcell. Biol. 33, 99-124.

Marzocchi, A., Lunt, D.J., Flecker, R., Bradshaw, C.D., Farnsworth, A., Hilgen, F.J., 2015. Orbital control on late Miocene climate and the North African monsoon: insight from an ensemble of sub-precessional simulations. Clim. Past 11 (10), 1271-1295.

Massari, F., Prosser, G., Capraro, L., Fornaciari, E., Consolaro, C., 2010. A revision of the stratigraphy and geology of the south-western part of the Crotone Basin (South Italy). It. J. Geosci. 129 (3), 353-384.

Massey, F.P., Ennos, A.R., Hartley, S.E., 2007. Herbivore specific induction of silica-based plant defences. Oecologia 152 (4), 677-683.

Matano, F., 2007. The 'Evaporiti di Monte Castello' deposits of the Messinian Southern Apennines foreland basin (Irpinia-Daunia Mountains, Southern Italy): stratigraphic evolution and geological context. In: Schreiber, B.C., Lugli, S., Babel, M. (Eds.), Evaporites Through Space and Time, Geol. Soc. London Spec. Publ. 285, pp. 191-218.

Matano, F., Barbieri, M., Di Nocera, S., Torre, M., 2005. Stratigraphy and strontium geochemistry of Messinian evaporite-bearing successions of the southern Apennines foredeep, Italy: implications for the Mediterranean "salinity crisis" and regional palaeogeography. Palaeogeogr. Palaeoclimatol. Palaeoecol. 217 (1-2), 87-114.

Mayr, G., De Pietri, V.L., Scofield, R.P., 2017. A new fossil from the mid-Paleocene of New Zealand reveals an unexpected diversity of world's oldest penguins. Sci. Nat. 104 (9).

McCay, G.A., Robertson, A.H.F., 2013. Upper Miocene–Pleistocene deformation of the Girne (Kyrenia) Range and Dar Dere (Ovgos) lineaments, northern Cyprus: role in collision and tectonic escape in the easternmost Mediterranean region. Geol. Soc. London Spec. Publ. 372 (1), 421-445.

McInerney, F.A., Strömberg, C.A., White, J.W., 2011. The Neogene transition from C_3 to C_4 grasslands in North America: stable carbon isotope ratios of fossil phytoliths. Paleobiology 37 (1), 23-49.

McKenzie, J.A., Jenkyns, H.C., Bennet, G.G., 1979. Stable isotope study of the cyclic diatomite-claystones from the Tripoli formation, Sicily: a prelude to the Messinian salinity crisis. Palaeo. Palaeo. Palaeo. 29, 125-141.

McKirdy, D.M., Spiro, B., Kim, A.W., Brenchley, A.J., Hepplewhite, C.J., Mazzoleni, A. G., 2013. Environmental significance of mid-to late Holocene sapropels in Old Man Lake, Coorong coastal plain, South Australia: an isotopic, biomarker and palaeoecological perspective. Org. Geochem. 58, 13-26.

McKirdy, D.M., Thorpe, C.S., Haynes, D.E., Grice, K., Krull, E.S., Halverson, G.P., Webster, L.J., 2010. The biogeochemical evolution of the Coorong during the mid-to late Holocene: An elemental, isotopic and biomarker perspective. Org. Geochem. 41 (2), 96-110.

McNaughton, S.J., 1985. Ecology of a Grazing Ecosystem: The Serengeti. Ecol. Monogr. 55 (3), 259-294.

McNaughton, S.J., Ruess, R.W., Seagle, S.W., 1988. Large Mammals and Process Dynamics in African Ecosystems. BioScience 38 (11), 794-800.

Mejdandžić, M., Ivanković, T., Pfannkuchen, M., Godrijan, J., Pfannkuchen, D.M., Hrenović, J., Ljubešić, Z., 2015. Colonization of diatoms and bacteria on artificial substrates in the northeastern coastal Adriatic Sea. Acta Bot. Croat. 74 (2), 1-16.

Melki, T., Kallel, N., Fontugne, M., 2010. The nature of transitions from dry to wet condition during sapropel events in the Eastern Mediterranean Sea. Palaeo. Palaeo. Palaeo. 291 (3-4), 267-285.

Melzer, S.E., Knapp, A.K., Kirkman, K.P., Smith, M.D., Blair, J.M., Kelly, E.F., 2010. Fire and grazing impacts on silica production and storage in grass dominated ecosystems. Biogeochemistry 97 (2-3), 263-278.

Merceron, G., De Bonis, L., Viriot, L., Blondel, C., 2005. Dental microwear of fossil bovids from northern Greece: paleoenvironmental conditions in the eastern Mediterranean during the Messinian. Palaeogeogr. Palaeoclimatol. Palaeoecol. 217 (3), 173-185.

Merle, D., Lauriat-Rage, A., Gaudant, J., Pestrea, S., Courme-Rault, M.D., Zorn, I., Blanc-Valleron, M.M., Rouchy, J.M., Orszag-Sperber, F., Krijgsman, W., 2002. Les paléopeuplements marins du Messinien pré-évaporitique de Pissouri

(Chypre, Méditerranée orientale): aspects paléoécologiques précédant la crise de salinité messinienne. Geodiversitas 24 (3), 669-689.

Miao, Y., Fang, X., Song, C., Yan, X., Zhang, P., Meng, Q., Li, F., Wu, F., Yang, S., Kang, S., Wang, Y., 2016. Late Cenozoic fire enhancement response to aridification in mid-latitude Asia: Evidence from microcharcoal records. Quat. Sci. Rev. 139, 53-66.

Milchunas, D.G., Sala, O.E., Lauenroth, W.K., 1988. A Generalized Model of the Effects of Grazing by Large Herbivores on Grassland Community Structure. Am. Nat. 132 (1), 87-106.

Modestou, S.E., Gutjahr, M., van der Schee, M., Ellam, R.M., Flecker, R., 2019. Precessional cyclicity of seawater Pb isotopes in the late Miocene Mediterranean. Paleoceanography and Paleoclimatology 34, 1-22.

Modestou, S.E., Simon, D., Gutjahr, M., Marzocchi, A., Kouwenhoven, T.J., Ellam, R.M., Flecker, R., 2017. Precessional variability of $^{87}Sr/^{86}Sr$ in the late Miocene Sorbas Basin: An interdisciplinary study of drivers of interbasin exchange. Paleoceanography 32, 1-22.

Moissette, P., Saint Martin, J.P., 1992. Upwelling and benthic communities in the Messinian of western Mediterranean. Paleont. Evol. 24-25, 245-254.

Molnar, P., 2005. Mio-Pliocene Growth of the Tibetan Plateau and Evolution of the East Asian Climate. Palaeontol. Electron. 8 (1), 1-23.

Molnar, P., England, P., Martinod, J., 1993. Mantle dynamics, uplift of the Tibetan Plateau, and the Indian monsoon. Rev. Geophys. 31 (4), 357-396.

Moriceau, B., Garvey, M., Ragueneau, O., Passow, U., 2007. Evidence for reduced biogenic silica dissolution rates in diatom aggregates. Mar. Ecol. Prog. Ser. 333, 129-142.

Morley, R., Richards, K., 1993. Gramineae cuticle: a key indicator of Late Cenozoic climatic change in the Niger Delta. Rev. Paleobot. Palynol. 77, 119-127.

Mosca, P., Polino, R., Rogledi, S., Rossi, M., 2010. New data for the kinematic interpretation of the Alps-Apennines junction (Northwestern Italy). Int. J. Earth Sci. 99 (4), 833-849.

Moussa., A., Novello, A., Lebatard, A.E., Decarreae, A., Fontaine, C., Barboni, D., Sylvestre, F., Bourlès, D.L., Paillès, C., Buchet, G., Duringer, P., Ghienne, J.F., Maley, J., Mazur, J.C., Roquin, C., Schuster, M., Vignaud, P., Brunet, M., 2016. Lake Chad sedimentation and environments during the late Miocene and Pliocene: New evidence from mineralogy and chemistry of the Bol core sediments. J. Afr. Earth Sci. 118, 192-204.

Murray, J., 2006. Ecology and applications of benthic foraminifera. Palaeo. Palaeo. Palaeo. 95, 1-426.

Muyzer, G., Stams, A.J., 2008. The ecology and biotechnology of sulphate-reducing bacteria. Nature Rev. Microbiol. 6 (6), 441-454.

Natalicchio, M., Birgel, D., Peckmann, J., Lozar, F., Carnevale, G., Liu, X., Hinrichs, K.U., Dela Pierre, F., 2017. An archaeal biomarker record of paleoenvironmental change across the onset of the Messinian salinity crisis in

the absence of evaporites (Piedmont Basin, Italy). Org. Geochem. 113, 242-253.

Natalicchio, M., Dela Pierre, F., Birgel, D., Brumsack, H., Carnevale, G., Gennari, R., Gier, S., Lozar, F., Pellegrino, L., Sabino, M., Schnetger, B., Peckmann, J., 2019. Paleoenvironmental change in a precession-paced succession across the onset of the Messinian salinity crisis: Insight from element geochemistry and molecular fossils. Palaeo. Palaeo. Palaeo. 518, 45-61.

Negri, A., Morigi, C., Giunta, S., 2003. Are productivity and stratification important to sapropel deposition? Microfossil evidence from late Pliocene insolation cycle 180 at Vrica, Calabria. Palaeogeogr. Palaeoclimatol. Palaeoecol. 190, 243– 255.

Negri, A., Capotondi, L., Keller, J., 1999a. Calcareous nannofossils, planktic foraminifers and oxygen isotopes in the late Quaternary sapropels of the Ionian Sea. Marine Geology 157, 84–99.

Negri, A., Giunta, S., Hilgen, F., Krijgsman, W., Vai, G.B., 1999b. Calcareous nannofossil biostratigraphy of the M. del Casino section (northern Apennines, Italy) and palaeoceanographic conditions at times of Late Miocene sapropel formation. Marine Micropalaeontology 36 (1), 13-30.

Negri, A., Villa, G., 2000. Calcareous nannofossil biostratigraphy, biochronology and palaeoecology at the Tortonian/Messinian boundary of the Faneromeni section (Crete). Palaeogeography, Palaeoclimatology, Palaeoecology 156 (3-4), 195-209.

Nelson, D.M., Tréguer, P., Brzezinski, M.A., Leynaert, A., Quéguiner, B., 1995. Production and dissolution of biogenic silica in the ocean: revised global estimates, comparison with regional data and relationship to biogenic sedimentation. Glob. Biogeochem. Cycles 9 (3), 359-372.

Neumann, A., Hass., H.C., Möbius, J., Naderipour, C., 2019. Ballasted flocs capture pelagic primary production and alter the local sediment characteristics in the coastal German Bight (North Sea). Geosciences 9, 344, 1-14.

Neurdin-Trescartes, J., 1995. Paléogeographie du Bassin du Chélif (Algérie) au Miocène. Causes et conséquences. Géol. Médit. 22 (2), 61-71.

Nijenhuis, I.A., 1999. Geochemistry of eastern Mediterranean sedimentary cycles. On the origin of Miocene to Pleistocene sapropels, laminites and diatomites. Geol. Ultra. 167, 170 pp.

Nomaki, H., Heinz, P., Nakatsuka, T., Shimanaga, M., Kitazato, H., 2005. Species-specific ingestion of organic carbon by deep-sea benthic foraminifera and meiobenthos: in situ tracer experiments. Limnol. Oceanogr. 50 (1), 134-146.

Nomaki, H., Heinz, P., Nakatsuka, T., Shimanaga, M., Ohkouchi, N., Ogawa, N.O., Kogure, K., Ikemoto, E., Kitazato, H., 2006. Different ingestion patterns of ^{13}C-labeled bacteria and algae by deep-sea benthic foraminifera. Mar. Ecol. Prog. Ser. 310, 95-108.

Norris, R.D., Kirtland Turner, S., Hull, P.M., Ridgwell, A., 2013. Marine Ecosystem Responses to Cenozoic Global Change. Science 341, 492-498. http://dx.doi.org/10.1126/science.1240543

O'Brien, N., 1996. Shale lamination and sedimentary processes. In: Palaeoclimatology and Palaeoceanography from Laminated Sediments (Ed A.E.S. Kemp), Geol. Soc. London Spec. Publ. 116, 23-36.

Ogniben, L., 1955. Relazioni fra tripoli delia Serie Solfifera siciliana e vulcanismo. Boll. Serv. Geol. It. 77, 23-31.

Ogniben, L., 1957. Tripoli. In: Ogniben, L. (Ed.), Petrografia della serie solfifera siciliana e considerazioni geologiche relative. Servizio geologico d'Italia, Libreria dello Stato, Roma, pp. 17-55.

Ohkouchi, N., Kuroda, J., Taira, A., 2015. The origin of Cretaceous black shales: a change in the surface ocean ecosystem and its triggers. Proc. Jpn. Acad. Ser. B 91 (7), 273-291.

Ojima, D.S., Parton, W.J., Schimel, D.S., Owensby, C.E., 1989. Simulated Impacts of Annual Burning on Prairie Ecosystems. In: Collins, S.L., Wallace, L.L. (Eds.), Fire in North American Tallgrass Prairies, University of Oklahoma Press, 118-132.

Onodera, J., Watanabe, E., Nishino, S., Harada, N., 2015. Distribution and vertical fluxes of silicoflagellates, ebridians, and the endoskeletal dinoflagellate *Actiniscus* in the western Arctic Ocean. Polar Biology 39, 327-341.

Orszag-Sperber, F., Caruso, A., Blanc-Valleron, M.M., Merle, D., Rouchy, J.M., 2009. The onset of the Messinian salinity crisis: Insights from Cyprus sections. Sed. Geol. 217, 52-64.

Osborne, C.P., 2008. Atmosphere, ecology and evolution: what drove the Miocene expansion of C_4 grasslands? J. Ecol. 96 (1), 35-45.

Osborne, C.P., Beerling, D.J., 2006. Nature's green revolution: the remarkable evolutionary rise of C_4 plants. Phil. Trans. R. Soc. B. 361, 173-194.

Osterrieth, M., Borrelli, N., Alvarez, M.F., Honaine, M.F., 2015. Silica biogeochemical cycle in temperate ecosystems of the Pampean Plain, Argentina. J. South Am. Earth Sci. 63, 172-179.

Ozalas, K., Savrda, C.E., Fullerton, R.R. Jr, 1994. Bioturbated oxygenation-event beds in siliceous facies: Monterey Formation (Miocene), California. Palaeo. Palaeo. Palaeo. 112, 63-83.

Pagani, M., Freeman, K.H., Arthur, M.A., 1999. Late Miocene Atmospheric CO_2 Concentrations and the Expansion of C_4 Grasses. Science 285, 876-879.

Papanikolaou, D.J., Dermitzakis, M.D., 1981. The Aegean arc during Burdigalian and Messinian: a comparison. Riv. Ital. Paleont. S. 87 (1), 83-92.

Parea, G.C., Ricci Lucchi, F., 1972. Resedimented evaporites in periadratic trough (upper Miocene, Italy). Isr. J. Earth Sci. 21 (3-4), 125-141.

Passow, U., 2002a. Production of transparent exopolymer particles (TEP) by phyto- and bacterioplankton. Mar. Ecol. Prog. Ser. 236, 1-12.

Passow, U., 2002b. Transparent exopolymer particles (TEP) in aquatic environments. Progr. Oceanogr. 55, 287-333.

Passow, U., Alldredge, A.L., Logan, B.E., 1994. The role of particulate carbohydrate exudates in the flocculation of diatom blooms. Deep-Sea Res. Pt. I 41 (2), 335-357.

Passow, U., Shipe, R.F., Murray, A., Pak, D.K., Brzezinski, M.A., Alldredge, A.L., 2001. The origin of transparent exopolymer particles (TEP) and their role in the sedimentation of particulate matter. Cont. Shelf Res. 21 (4), 327-346.

Patrick, S., Holding, A.J., 1985. The effect of bacteria on the solubilization of silica in diatom frustules. J. Appl. Microbiol. 59 (1), 7-16.

Pavia, G., 1989. Il giacimento a pesci messiniani di Pecetto di Valenza (Alessandria). Boll. Soc. Piem. Archeol. Belle Arti 43, 15-21.

Pearce, R.B., Kemp, A.E.S., Koizumi, I., Pike, J., Cramp, A., Rowland, S.J., 1998. A lamina-scale, SEM-based study of a Late Quaternary diatom-ooze sapropel from the Mediterranean Ridge, Site 971. In: Robertson, A.H.F., Emeis, K.C., Ricvhter, C., Camerlenghi, A. (Eds.), Proc. Ocean Drill. Prog. Sci. Results 160, pp. 349-363.

Pedley, H.M., Grasso, M., 1993. Controls on faunal and sediment cyclicity within the Tripoli and Calcare di Base basins (Late Miocene) of central Sicily. Palaeogeogr. Palaeoclimatol. Palaeoecol. 105 (3-4), 337-360.

Pedley, M., Grasso, M., Maniscalco, R., Esu, D., 2007. The Monte Carrubba Formation (Messinian, Sicily) and its correlatives: New light on basin-wide processes controlling sediment and biota distributions during the

Palaeomediterranean–Mediterranean transition. Palaeogeogr. Palaeoclimatol. Palaeoecol. 253 (3), 363-384.

Pedley, M., Maniscalco, R., 1999. Lithofacies and faunal succession (faunal phase analysis) as a tool in unravelling climatic and tectonic signals in marginal basins; Messinian (Miocene), Sicily. J. Geol. Soc. London 156 (4), 855-863.

Penna, N., Rinaldi, A., Montanari, G., Di Paolo, A., Penna, A., 1993. Mucilaginous masses in the Adriatic Sea in the summer of 1989. Wat. Res. 27, 12, 1767-1771.

Pérez-Folgado, M., Sierro, F.J., Bárcena, M.A., Flores, J.A., Vázquez, A., Utrilla, R., Hilgen, F.J., Krijgsman, W., Filippelli, G.M., 2003. Western versus eastern Mediterranean paleoceanographic response to astronomical forcing: a high-resolution microplankton study of precession-controlled sedimentary cycles during the Messinian. Palaeo. Palaeo. Palaeo. 190, 317-334.

Perrodon, A., 1957. Étude géologique des bassins néogènes de l'Algérie occidentale. Serv. Cart. Géol. Algérie 12, 1-328.

Pestrea, S., Blanc-Valleron, M.M., Rouchy, J.M., 2002. Les assemblages de diatomées des niveaux infra-gypseux du Messinien de Méditerranée (Espagne, Sicile, Chypre). Geodiversitas, 24 (3), 543-583.

Pestrea, S., Saint Martin, J.P., 2002. La microflore de diatomées du Messinien de Gibellina (Sicile occidentale, Italie). Geodiversitas 24 (3), 585-610.

Petranich, E., Covelli, S., Acquavita, A., De Vittor, C., Faganelli, J., Contin, M., 2018. Benthic nutrient cycling at the sediment-water interface in a lagoon fish faming system (northern Adriatic Sea, Italy). Sci. Total Environ. 644, 137-149.

Piana, F., 2000. Structural Setting of Western Monferrato (Alps-Apennines Junction Zone, NW Italy). Tectonics 19 (5), 943-960.

Pierre, C., Rouchy, J. M., 1990. Sedimentary and diagenetic evolution of Messinian evaporites in the Tyrrhenian Sea (ODP Leg 107, Sites 652, 653, and 654): petrographic, mineralogical, and stable isotope records. In: Kastens, K.A., Mascle, J., et al. (Eds.), Proc. Ocean Drill. Progr. Sci. Res. 107, 187-210.

Pierson, F.B., Williams, C.J., Hardegree, S.P., Weltz, M.A., Stone, J.J., Clark, P.E., 2011. Fire, Plant Invasion, and Erosion Events on Western Rangelands. Rangeland Ecol. Man. 64 (5), 439-449.

Pike, J., 2000. Data report: backscattered electron imagery analysis of Early Pliocene laminated *Ethmodiscus* ooze, Site 1010. In: Proc. Ocean Drill. Prog. Sci. Res. (Eds M. Lyle, I. Koizumi, C. Richter, T.C. Jr Moore) 167, 207-212.

Pike, J., Bernhard, J.M., Moreton, S.G., Butler, I.B., 2001. Microbioirrigation of marine sediments in dysoxic environments: Implications for early sediment fabric formation and diagenetic processes. Geology 29 (10), 923-926.

Pike, J., Kemp, A.E.S., 1996. Records of seasonal flux in Holocene laminated sediments, Gulf of California. In: Palaeoclimatology and Palaeoceanography from Laminated Sediments (Ed A.E.S. Kemp), Geol. Soc. London Spec. Publ. 116, 157-169.

Pike, J., Kemp, A.E.S., 1999. Diatom mats in Gulf of California sediments: Implications for the paleoenvironmental interpretation of laminated sediments and silica burial. Geology 27 (4), 311-314.

Pilskaln, C.H., Pike, J., 2001. Formation of Holocene sedimentary laminae in the Black Sea and the role of the benthic flocculent layer. Paleoceanography 16 (1), 1-19.

Pisaric, M.F.J., 2002. Long-distance transport of terrestrial plant material by convection resulting from forest fires. J. Paleolimn. 28, 349-354.

Ploug, H., Kühl, M., Buchholz-Cleven, B., Jørgensen, B.B., 1997. Anoxic aggregates – an ephemeral phenomenon in the pelagic environment? Aquat. Microb. Ecol. 13, 285-294.

Pokrovsky, O.S., Schott, J., Kudryavtzev, D.I., Dupré, B., 2005. Basalt weathering in Central Siberia under permafrost conditions. Geochim. Cosmochim. Acta 69 (24), 5659–5680.

Pomar, L., Ward, W.C., 1994. Response of a late Miocene Mediterranean reef platform to high-frequency eustasy. Geology 22 (2), 131-134.

Potter, P.E., Szatmari, P., 2009. Global Miocene tectonics and the modern world. Earth-Sci. Rev. 96, 279-295.

Potter, P.E., Szatmari, P., 2015. The global Middle and Late Miocene and the deep earth: Model for earlier orogenies. Mar. Pet. Geol. 68, 178-191.

Pound, M.J., 2012. Middle to Late Miocene terrestrial biota and climate. Ph.D. thesis, University of Leeds, 416 pp.

Prieto, L., Ruiz, J., Echevarría, F., García, C.M., Bartual, A., Gálvez, J.A., Corzo, A., Macías, D., 2002. Scales and processes in the aggregation of diatom blooms: high time resolution and wide size range records. Deep-Sea Res. Pt. I 49, 1233-1253.

Pyenson, N. D., Vermeij, G. J., 2016. The rise of ocean giants: maximum body size in Cenozoic marine mammals as an indicator for productivity in the Pacific and Atlantic Oceans. Biol. Lett. 12 (7), 20160186.

Ragueneau, O., Tréguer, P., Leynaert, A., Anderson, R.F., Brzezinski, M.A., DeMaster, D.J., Dugdale, R.C., Dymond, J., François, R., Heinze, C., Maier-Reimer, E., Martin-Jézéquel, V., Nelson, D.M., Quéguiner, B., 2000. A review of the Si cycle in the modern ocean: recent progress and missing gaps in the application of biogenic opal as a paleoproductivity proxy. Glob. Planet. Change 26 (4), 317-365.

Rai, A.K., Maurya, A.S., 2009. Effect of Miocene paleoceanographic changes on the benthic foraminiferal diversity at ODP site 754A (southeastern Indian Ocean). Indian J. Mar. Sci. 38 (4), 423-431.

Rai, J, 2006. Late Miocene siliceous endoskeletal dinoflagellates from the Sawai Bay Formation, Neill Island, Andaman Sea, India. Journal of Micropalaeontology 25, 37-44.

Ran, X., Che, H., Zang, J., Yu, Y., Liu, S., Zheng, L., 2015. Variability in the composition and export of silica in the Huanghe River Basin. Sci. China Earth. Sci. 58 (11), 2078-2089.

Raven, J.A., 1983. The transport and function of silicon in plants. Biol. Rev. 58, 179-207.

Raymo, M.E., Ruddiman, W.F., Froelich, P.N., 1988. Influence of late Cenozoic mountain building on ocean geochemical cycles. Geology 16, 649-653.

Rea, D.K., 1992. Delivery of Himalayan sediment to the northern Indian Ocean and its relation to global climate, sea level, uplift, and seawater strontium. In: Duncan, R.A., Rea, D.K., Kidd, R.B., von Rad, U., Weissel, J.K. (Eds.), Synthesis of Results from Scientific Drilling in the Indian Ocean, Geophys. Monogr. Ser. 70, pp. 387-402.

Rea, D.K., Snoeckx, H., Joseph, L.H., 1998. Late Cenozoic eolian deposition in the North Pacific: Asian drying, Tibetan uplift, and cooling of the northern hemisphere. Paleoceanography 13 (3), 215-224.

Renaudie, J., 2016. Quantifying the Cenozoic marine diatom deposition history: links to the C and Si cycles. Biogeosciences, 13, 6003-6014.

Retallack, G.J., 1990. Soils of the past – An introduction to paleopedology. Unwin Hyman Ltd, 520 pp.

Retallack, G.J., 2013. Global cooling by grassland soils of the geological past and near future. Ann. Rev. Earth. Planet. Sci. 41, 69-86.

Ribera d'Alcalà, M., Civitarese, G., Conversano, F., Lavezza, R., 2003. Nutrient ratios and fluxes hint at overlooked processes in the Mediterranean Sea. J. Geophys. Res. Atmos. 108 (C9), 7.1-7.16.

Ricci Lucchi, F., 1986. The foreland basin system of the Northern Apennines and related clastic wedges: a preliminary outline. G. Geol. 48 (3), 165-185.

Rice, E.L., Parenti, R.L., 1978. Causes of Decreases in Productivity in Undisturbed Tall Grass Prairie. Am. J. Bot. 65 (10), 1091-1097.

Richmond, K.E.R., Sussman, M., 2003. Got silicon? The non-essential beneficial plant nutrient. Curr. Opin. Plant Biol. 6, 268-272.

Richter-Bernburg, G., 1973. Facies and paleogeography of the messinian evaporates in Sicily. In: Drooger, C.W. (Ed.), Messinian events in the Mediterranean, Geodynamic Scientific Report No. 7 on the colloquium held in Utrecht, March 2-4, 1973, pp. 124-141.

Riebesell, U., 1991. Particle aggregation during a diatom bloom. II. Biological aspects. Mar. Ecol. Prog. Ser. 69, 281-291.

Rigual-Hernández, A., Bárcena, M.A., Sierro, F.J., Flores, J.A., Hernández-Almeida, I., Sanchez-Vidal, A., Palanques, A., Heussner, S., 2010. Seasonal to interannual variability and geographic distribution of the silicoflagellate fluxes in the Western Mediterranean. Mar. Micropaleontol. 77, 46-57.

Rigual-Hernández, A.S., Bárcena, M.A., Jordan, R.W., Sierro, F.J., Flores, J.A., Meier, K.J.S., Beaufort, L., Heussner, S., 2013. Diatom fluxes in the NW Mediterranean: evidence from a 12-year sediment trap record and surficial sediments. J. Plankton Res. 35 (5), 1109-1125.

Rigual-Hernández, A.S., Sierro, F.J., Bárcena, M.A., Flores, J.A., Heussner, S., 2012. Seasonal and interannual changes of planktic foraminiferal fluxes in the

Gulf of Lions (NW Mediterranean) and their implications for paleoceanographic studies: two 12-year sediment trap records. Deep-Sea Research Pt. I: Oceanographic Research Papers 66, 26-40.

Rixen, T., Gaye, B., Emeis, K.C., Ramaswamy, V., 2017. The ballast effect in the Indian Ocean. Biogeosciences Discuss., 1-45.

Rixen, T., Gaye, B., Emeis, K.C., Ramaswamy, V., 2019. The ballast effect of lithogenic matter and its influences on the carbon fluxes in the Indian Ocean. Biogeosciences 16, 485-503.

Robertson, A.H.F., Necdet, M., Raffi, I., Chen, G., 2019. Early Messinian manganese deposition in NE Cyprus related to cyclical redox changes in a silled hemipelagic basin prior to the Mediterranean salinity Crisis. Sediment. Geol. 385, 126-148.

Roda, C., 1964. Distribuzione e facies dei sedimenti neogenici nel Bacino Crotonese. Geol. Rom. 3, 319-366.

Romero, O., Schmieder, F., 2006. Occurrence of thick *Ethmodiscus* oozes associated with a terminal Mid-Pleistocene Transition event in the oligotrophic subtropical South Atlantic. Palaeo. Palaeo. Palaeo. 235, 321-329.

Rook, L., Gallai, G., Torre, D., 2006. Lands and endemic mammals in the Late Miocene of Italy: Constrains for paleogeographic outlines of Tyrrhenian area. Palaeogeogr. Palaeoclimatol. Palaeoecol. 238 (1), 263-269.

Rosenbaum, G., Lister, G. S., Duboz, C., 2002. Reconstruction of the tectonic evolution of the western Mediterranean since the Oligocene. J. Virt. Expl. 8, 107-130.

Rossi, M., 2017. Outcrop and seismic expression of stratigraphic patterns driven by accommodation and sediment supply turnarounds: Implications on the meaning and variability of unconformities in syn-orogenic basins. Mar. Petroleum Geol. 87, 112-127.

Rossi, M., Craig, J., 2016. A new perspective on sequence stratigraphy of syn-orogenic basins: Insights from the Tertiary Piedmont Basin (Italy) and implications for play concepts and reservoir heterogeneity. In: Bowman, M., Smyth, H.R., Good, T.R., Passey, S.R., Hirst, J.P.P., Jordan, C.J. (Eds.) The Value of Outcrop Studies in Reducing Subsurface Uncertainty and Risk in Hydrocarbon Exploration and Production, Geol. Soc. London Spec. Publ. 436 (1), 93-133.

Roubeix, V., Becquevort, S., Lancelot, C., 2008. Influence of bacteria and salinity on diatom biogenic silica dissolution in estuarine systems. Biogeochemistry 88 (1), 47-62.

Rouchy, J.M., 1982. La genèse des évaporites messiniennes de Méditerranée. Mém. Mus. Nat. Hist. Nat. Sér. C, Sci. Terre, 267 pp.

Rouchy, J.M., Noël, D., Wali, A.M.A., Aref, M.A.M., 1995. Evaporitic and biosiliceous cyclic sedimentation in the Miocene of the Gulf of Suez – depositional and diagenetic aspects. Sed. Geol. 94, 277-297.

Round, F.E., 1984. Structure of the cells, cell division and colony formation in the diatoms *Isthmia enervis* Ehr. And *I. nervosa* Kütz. Ann. Bot., 53 (4), 457-468.

Round, F.E., Crawford, R.M., Mann, D.G., 1990. The diatoms – Biology & Morphology of the Genera. Cambridge University Press, 747 pp.

Roveri, M., Bassetti, M.A., Lucchi, F.R., 2001. The Mediterranean Messinian salinity crisis: an Apennine foredeep perspective. Sed. Geol. 140 (3), 201-214.

Roveri, M., Lugli, S., Manzi, V., Gennari, R., 2008. Large-scale mass wasting processes in the Messinian Ciminna Basin (northern Sicily). Geoacta 7, 45-62.

Ruddiman, W.F., Raymo, M.E., Prell, W.L., Kutzbach, J.E., 1997. The Uplift-Climate Connection: A Synthesis. In: Ruddiman, W.F. (ed.) Tectonic Uplift and Climate Change. Springer US, pp. 471-515.

Sabino, M., Schefuß, E., Natalicchio, M., Dela Pierre, F., Birgel, D., Bortels, D., Schnetger, B., Peckmann., J., 2020. Climatic and hydrologic variability in the northern Mediterranean across the onset of the Messinian salinity crisis. Palaeo., Palaeo., Palaeo. 545, 109632.

Saint Martin, J.P., Pestrea, S., Conesa, G., 2001. Les assemblages de diatomées des niveaux infra-gypseux du basin messinian de Sorbas (Espagne). Cryptog. Algol. 22 (1), 127-149.

Saint Martin, S., Conesa, G., Saint Martin, J.P., 2003. Les assemblages de diatomées du Messinien dans le basin de Melilla-Nador (Rif Nord-Oriental Maroc). Rev. Micropal. 46, 161-190.

Sancetta, C., 1992. Comparison of phytoplankton in sediment trap time series and surface sediments along a productivity gradient. Paleoceanography 7 (2), 183–194.

Sancetta, C.A., 1983. Biostratigraphic and paleoceanographic events in the Eastern Equatorial Pacific: results of Deep-Sea Drilling Project Leg 69. In: Cann, J.R., Langseth, M.G., Honnorez, J., Von Herzen R.P., White, S.M., et al. (Eds.), Init. Repts. DSDP 69, 311-320.

Santini, F., Carnevale, G., Sorenson, L., 2013. First molecular scombrid timetree (Percomorpha: Scombridae) shows recent radiation of tunas following invasion of pelagic habitat. It. J. Zool. 80 (2), 210-221.

Santini, F., Sorenson, L., 2013. First molecular timetree of billfishes (Istiophoriformes: Acanthomorpha) shows a Late Miocene radiation of marlins and allies. It. J. Zool. 80 (4), 481-489.

Sarti, G., 1995. Controllo tettonico ed eustatico sulla deposizione delle unità del Miocene superiore della Val di Fine (Toscana, Pisa). St. Geol. Cam., Vol. Spec. 1, 581-582.

Savelli, C., 2002. Time-space distribution of magmatic activity in the western Mediterranean and peripheral orogens during the past 30 Ma (a stimulus to geodynamic considerations). J. Geodyn. 34 (1), 99-126.

Savelli, D., Wezel, F.C., 1978. Schema geologico del Messiniano del Pesarese. Boll. Soc. Geol. It. 97 (1-2), 165-188.

Scheiter, S., Higgins, S.I., Osborne, C.P., Bradshaw, C., Lunt, D., Ripley, B.S., Taylor, L.L., Beerling, D.J., 2012. Fire and fire-adapted vegetation promoted C_4 expansion in the late Miocene. New Phytol. 195, 653-666.

Schenau, S.J., Antonarakou, A., Hilgen, F.J., Lourens, L.J., Nijenhuis, I.A., Van der Weijden, C.H., Zachariasse, W.J., 1999. Organic-rich layers in the Metochia section (Gavdos, Greece): evidence for a single mechanism of sapropel formation during the past 10 My. Mar. Geol. 153 (1), 117-135.

Schieber, J., 1996. Early diagenetic silica deposition in algal cysts and spores: a source of sand in black shales? J. Sed. Res. 66 (1), 175-183.

Schildgen, T.F., Cosentino, D., Bookhagen, B., Niedermann, S., Yıldırım, C., Echtler, H., Wittmann, H., Strecker, M.R., 2012. Multi-phased uplift of the southern margin of the Central Anatolian plateau, Turkey: A record of tectonic and upper mantle processes. Earth Planet. Sci. Lett. 317-318, 85-95.

Schimmelmann, A., Lange, C.B., Schieber, J., Francus, P., Ojala, A.E.K., Zolitschka, B., 2016. Varves in marine sediments: A review. Earth-Sci. Rev. 159, 215-246.

Schmincke, H.U., Behncke, B., Grasso, M., Raffi, S., 1997. Evolution of the northwestern Iblean Mountains, Sicily: uplift, Pliocene/Pleistocene seal-level changes, paleoenvironment, and volcanism. Geol. Rundsch. 86 (3), 637-669.

Schulz, H., Von Rad, U., Von Stackelberg, U., 1996. Laminated sediments from the oxygen-minimum zone of the northeastern Arabian Sea. In: Palaeoclimatology and Palaeoceanography from Laminated Sediments (Ed A.E.S. Kemp), Geol. Soc. London Spec. Publ. 116, 185-207.

Schuster, M., Duringer, P., Ghienne, J. F., Vignaud, P., Mackaye, H.T., Likius, A., Brunet, M., 2006. The age of the Sahara desert. Science 311 (5762), 821-821.

Schwark, L., Ferretti, A., Papazzoni, C.A., Trevisani, E., 2009. Organic geochemistry and paleoenvironment of the early Eocene "Pesciara di Bolca" Konservat-Lagerstätte, Italy. Palaeogeogr. Palaeoclimatol. Palaeoecol. 273 (3), 272-285.

Schwarzhans, W., Aguilera, O., 2013. Otoliths of the Myctophidae from the Neogene of tropical America. Palaeo Ichthyologica 13, 83-150.

Seeberg-Elverfeldt, 2004. Laminated diatomaceous sediments of the Red Sea, their composition and significance as recorders of abrupt changes in productivity and circulation during the Late Quaternary. Ph.D. thesis, University of Bremen, 122 pp.

Ségalen, L., Lee-Thorp, J.A., Cerling, T., 2007. Timing of C_4 grass expansion across sub-Saharian Africa. J. Hum. Evol. 53 (5), 549-559.

Selli, R., 1954. Il Bacino del Metauro. Descrizione geologica, risorse minerarie, idrogeologia. G. Geol. 24, 293 pp.

Senut, B., Pickford, M., Ségalen, L., 2009. Neogene desertification of Africa. C. R. Geosci. 341, 591-602.

Sepulchre, P., Ramstein, G., Fluteau, F., Sschuster, M., Tiercelin, J.J., Brunet, M., 2006. Tectonic Uplift and Eastern Africa Aridification. Science 313 (5792), 1419-1423.

Shemesh, A., Burckle, L.H., Froelich, P.N., 1989. Dissolution and preservation of Antarctic diatoms and the effect on sediment thanatocoenoses. Quat. Res. 31 (2), 288-308.

Shimada, C., Sato, T., Toyoshima, S., Yamasaki, M., Tanimura, Y., 2008. Paleoecological significance of laminated diatomaceous oozes during the middle-to-late Pleistocene, North Atlantic Ocean (IODP Site U1304). Mar. Micropaleontol. 69, 139-150.

Shukla, S.K., Mohan, R., 2012. The contribution of diatoms to worldwide oil crude deposits. In: Gordon, R., Seckbach, J. (Eds.), The Science of Algal Fuels: Phycology, Geology, Biophotonics, Genomics and Nanotechnology, Springer, Netherlands, pp. 355-382.

Sierro, F.J., Flores, J.A., Francés, G., Vazquez, A., Utrilla, R., Zamarreño, I., Erlenkeuser, H., Barcena, M.A., 2003. Orbitally-controlled oscillations in planktic communities and cyclic changes in western Mediterranean hydrography during the Messinian. Palaeo. Palaeo. Palaeo. 190, 289-316.

Sierro, F.J., Hilgen, F.J., Krijgsman, W., Flores, J.A., 2001. The Abad composite (SE Spain): a Messinian reference section for the Mediterranean and the APTS. Palaeo. Palaeo. Palaeo 168, 141-169.

Silva, A., Palma, S., Moita, M.T., 2008. Coccolithophores in the upwelling waters of Portugal: four years of weekly distribution in Lisbon bay. Continental Shelf Research 28, 2601–2613.

Simon, D., Marzocchi, A., Flecker, R., Lunt, D.J., Hilgen, F.J., Meijer, P.Th., 2017. Quantifying the Mediterranean freshwater budget throughout the late Miocene: New implications for sapropel formation and the Messinian Salinity Crisis. Earth Planet. Sci. Lett. 472, 25-37.

Singh, R.S., 1993. Effect of winter fire on primary productivity and nutrient concentration of a dry tropical savanna. Vegetatio 106 (1), 63-71.

Sinkko, H., Lukkari, K., Sihvonen, L.M., Sivonen, K., Leivuori, M., Rantanen, M., Paulin, L., Lyra, C., 2013. Bacteria Contribute to Sediment Nutrient Release and Reflect Progressed Eutrophication-Driven Hypoxia in an Organic-Rich Continental Sea. PloS One 8 (6), e67061, 1-14.

Siokou-Frangou, I., Christaki, U., Mazzocchi, M.G., Montresor, M., Ribera d'Alcalá, M., Vaqué, D., Zingone, A., 2010. Plankton in the open Mediterranean Sea: a review. Biogeosciences 7, 1543-1586.

Smetacek, V., 2000. The giant diatom dump. Nature 406 (6796), 574-575.

Smetacek, V.S., 1985. Role of sinking in diatom life-history cycles: ecological, evolutionary and geological significance. Mar. Biol. 84 (3), 239-251.

Smrzka, D., Kraemer, S.M., Zwicker, J., Birgel, D., Fischer, D., Kasten, S., Goedert, J.L., Peckmann, J., 2015. Constraining silica diagenesis in methane-seep deposits. Palaeogeogr. Palaeoclimatol. Palaeoecol. 420, 13-26.

Souchu, P., Gasc, A., Collos, Y., Vaquer, A., Tournier, H., Bibent, B. and Deslous-Paoli, J.M., 1998. Biogeochemical aspects of bottom anoxia in a Mediterranean lagoon (Thau, France). Mar. Ecol. Prog. Ser. 164, 135-146.

Sournia, A., 1982. Is there a shade flora in the marine plankton? J. Plank. Res. 4 (2), 391-399.

Steininger, F.F., Rögl, F., 1984. Paleogeography and palinspastic reconstruction of the Neogene of the Mediterranean and Paratethys. In: Dixon, J.E., Robertson, A.H.F. (Eds.), The Geological Evolution of the Eastern Mediterranean, pp. 659-668.

Stewart, K.M., 2001. The freshwater fish of Neogene Africa (Miocene-Pleistocene): systematics and biogeography. Fish and Fisheries 2 (3), 177-230.

Street-Perrott, F.A., Barker, P.A., 2008. Biogenic silica: a neglected component of the coupled global continental biogeochemical cycles of carbon and silicon. Earth Surf. Process. Landf. 33 (9), 1436-1457.

Strömberg, C.A.E., 2011. Evolution of grasses and grassland ecosystems. Ann. Rev. Earth Planet. Sci. 39 (1), 517-544.

Strömberg, C.A.E., Werdelin, L., Friis, E.M., Saraç, G., 2007. The spread of grass-dominated habitats in Turkey and surrounding areas during the Cenozoic: Phytolith evidence. Palaeogeogr. Palaeoclimatol. Palaeoecol. 250 (1-4), 18-49.

Struyf, E., Conley, D.J., 2009. Silica: an essential nutrient in wetland biogeochemistry. Front. Ecol. Environ. 7 (2), 88-94.

Struyf, E., Conley, D.J., 2012. Emerging understanding of the ecosystem silica filter. Biogeochemistry 107 (1), 9-18.

Struyf, E., Smis, A., Van Damme, S., Garnier, J., Govers, G., Van Wesemael, B., Conley, D.J., Batelaan, O., Frot, E., Clymans, W., Vandervenne, F., Lancelot,

C., Goos, P., Meire, P., 2010. Historical land use change has lowered terrestrial silica mobilization. Nature Communications 1 (8):129, 1-7.

Sturani, C., 1976. Messinian facies in the Piedmont Basin. Mem. Soc. Geol. It. 16, 11-25.

Sturani, C., Sampò, M., 1973. Il Messiniano inferiore in facies diatomitica nel Bacino Terziario Piemontese. Mem. Soc. Geol. It. 12, 335-358.

Suc, J.P., Violanti, D., Londeix, L., Poumot, C., Robert, C., Clauzon, G., Gautier, F., Turon, J.L., Ferrier, J., Chikhi, H., Cambon, G., 1995. Evolution of the Messinian Mediterranean environments: the Tripoli Formation at Capodarso (Sicily, Italy). Rev. Paleobot. Palynol. 87 (1), 51-79.

Suess, E., von Huene, R., 1988. Ocean Drilling Program Leg 112, Peru continental margin: Part 2, Sedimentary history and diagenesis in a coastal upwelling environment. Geology 16 (10), 939-943.

Suiting, I., Schmincke, H.U., 2010. Iblean diatremes 2: shallow marine volcanism in the Central Mediterranean at the onset of the Messinian Salinity Crisis (Iblean Mountains, SE-Sicily) – a multidisciplinary approach. Int. J. Earth Sci. 99 (8), 1917-1940.

Sullivan, C.W., Volcani, B.E., 1981. Silicon in the Cellular Metabolism of Diatoms. In: Simpson, T.L., Volcani, B.E. (Eds.), Silicon and Siliceous Structures in Biological Systems, Springer-Verlag New York, pp. 15-42.

Šupraha, L., Bosak, S., Ljubešić, Z., Olujić, G., Horvat, L., Viličić, D., 2011. The phytoplankton composition and spatial distribution in the north-eastern Adriatic Channel in autumn 2008. Acta Adriat. 52 (1), 29-44.

Süß, J., Engelen, B., Cypionka, H., Sass, H., 2004. Quantitative analysis of bacterial communities from Mediterranean sapropels based on cultivation-dependent methods. FEMS Microbiol. Ecol. 51 (1), 109-121.

Suto, I., Kawamura, K., Hagimoto, S., Teraishi, A., Tanaka, Y., 2012. Changes in upwelling mechanisms drove the evolution of marine organisms. Palaeogeogr. Palaeoclimatol. Palaeoecol. 339-341, 39-51.

Sutton, J.N., André, L., Cardinal, D., Conley, D.J., de Souza, G.F., Dean, J., Dodd, J., Ehlert, C., Ellwood, M.J., Frings, P.J., Grasse, P., Hendry, K., Leng, M.J., Michalopoulos, P., Panizzo, V.N., Swann, G.E.A., 2018. A review of the stable isotope bio-geochemistry of the global Silicon cycle and its associated trace elements. Front. Earch Sci. 5-112, 1-24.

Takata, H., Itaki, T., Ikehara, K., Khim, B.K., 2018. Correlation between faunal transitions of benthic foraminifera and ballasting of particulate organic carbon by siliceous plankton during the Holocene off San-in district, southwestern Japan. The Holocene 28 (3), 444-454.

Takata, H., Kim, H.J., Asahi, H., Thomas, E., Yoo, C.M., Chi, S.B., Khim, B.K., 2019. Central Equatorial Pacific benthic foraminifera during the mid-Brunhes dissolution interval. Ballasting of particulate organic matter by biogenic silica and carbonate. Quat. Sci. 2010, 64-79.

Takahashi, K., 1991. Silicoflagellates and *Actiniscus*: vertical fluxes at Pacific and Atlantic sediment trap stations. Ocean Biocoenosis, Series 2, 1-35.

Taliaferro, N.L., 1933. The relation of volcanism to diatomaceous and associated siliceous sediments. University of California Press, Bull. Dep. Geol. Sci. 23 (1), 1-55.

Tanimura, Y., 1999. Varieties of a single cosmopolitan diatom species associated with surface water masses in the North Pacific. Mar. Micropaleontol. 37, 199-218.

Tanimura, Y., Fukuchi, M., Watanabe, K., Moriwaki, K., 1990. Diatoms in Water Column and Sea-ice in Lützow-Holm Bay, Antarctica, and their Preservation in the Underlying Sediments. Bull. Natn. Sci. Mus. Tokyo, Ser. C 16 (1), 15-39.

Thomas, E., 1980. Details of *Uvigerina* development in the Cretan Mio-Pliocene. Utrecht Micropaleontological Bulletins 23, 168 pp.

Thornton, D.C.O., 2002. Diatom aggregation in the sea: mechanisms and ecological implications. Eur. J. Phycol. 37, 149-161.

Tipple, B.J., Pagani, M., 2007. The early origins of terrestrial C_4 photosynthesis. Annu. Rev. Earth Planet. Sci. 35 (1), 435-461.

Tréguer, P., De La Rocha, 2013. The World Ocean Silica Cycle. Ann. Rev. Mar. Sci. 5, 477-501. http://dx.doi.org/10.1146/annurev-marine-121211-172346

Trembath-Reichert, E., Wilson, J.P., McGlynn, S.E., Fischer, W.W., 2015. Four hundred million years of silica biomineralization in land plants. Proc. Natl. Acad. Sci USA 112 (17), 5449-5454.

Trevisan, L., 1967. Pollini fossili del Miocene superiore nei tripoli del Gabbro (Toscana). Palaeont. It. 62, 1-73.

Tzanova, A., Herbert, T.D., Peterson, L., 2015. Cooling Mediterranean Sea surface temperatures during the Late Miocene provide a climate context for evolutionary transitions in Africa and Eurasia. Earth Planet. Sci. Lett. 419, 71-80.

Unzué-Belmonte, D., Struyf, E., Clymans, W., Tischer, A., Potthast, K., Bremer, M., Meire, P., Schaller, J., 2016. Fire enhances solubility of biogenic silica. Sci. Total Environ. 572, 1289-1296.

Urlaub, M., Geersen, J., Krastel, S., Schwenk, T., 2018. Diatom-ooze: Crucial for the generation of submarine mega-slides? Geology 46 (4), 331-334.

Valla, P.G., Beek, P.A., Shuster, D.L., Braun, J., Herman, F., Tassan-Got, L., Gautheron, C., 2012. Late Neogene exhumation and relief development of the Aar and Aiguilles Rouges massifs (Swiss Alps) from low-temperature thermochronology modeling and $^{4}He/^{3}He$ thermochronometry. J. Geophys. Res. Earth Surf. 117 (F1), 1-23.

van Assen, E., Kuiper, K.F., Barhoun, N., Krijgsman, W., Sierro, F.G., 2006. Messinian astrochronology of the Melilla Basin: Stepwise restriction of the

Mediterranean-Atlantic connection through Morocco. Palaeogeogr. Palaeoclimatol. Palaeoecol. 238, 15-31.

van der Jagt, H., Friese, C., Stuut, J.B.W., Fischer, G., Iversen, M.H. (2018) The ballasting effect of Saharan dust deposition on aggregate dynamics and carbon export: Aggregation, settling, and scavenging potential of marine snow. Limnol. Oceanogr. 63(3), 1386-1394.

Van der Meulen, M.J., Kouwenhoven, T.J., van der Zwaan, G.J., Meulenkamp, J.E., Wortel, M.J. R., 1999. Late Miocene uplift in the Romagnan Apennines and the detachment of subducted lithosphere. Tectonophysics 315 (1-4), 319-335.

van der Zwaan, G.J., 1979. The pre-evaporite late Miocene environment of the Mediterranean; stable isotopes of planktonic foraminifera from section Falconara, Sicily. K. Ned. Akad. Wetensch. 82, 487-502.

Van Gorsel, J.T., Troelstra, S.R., 1980. Late Neogene climate changes and the Messinian salinity crisis. Géol. Médit. 7 (1), 127-134.

Van Hinsbergen, D.V., Van der Meer, D.G., Zachariasse, W.J., Meulenkamp, J.E., 2006. Deformation of western Greece during Neogene clockwise rotation and collision with Apulia. Int. J. Earth Sci. 95 (3), 463-490.

Vandervenne, F.I., Barão, A.L., Schoelynck, J., Smis, A., Ryken, N., Van Damme, S., Meire, P., Struyf, E., 2013. Grazers: biocatalysts of terrestrial silica cycling. Proc. R. Soc. B 280, 1-9.

Varol, B., Atalar, C., 2016. Messinian evaporites in the Mesaoria Basin, North Cyprus: facies and environmental interpretations. Carbon. Evap., 1-17.

Vázquez, A., Utrilla, R., Zamarreño, I., Sierro, F.J., Flores, J.A., Francés, G., Bárcena, M.A., 2000. Precession-related sapropelites of the Messinian Sorbas Basin (South Spain): paleoenvironmental significance. Palaeogeogr. Palaeoclimatol. Palaeoecol. 158 (3-4), 353-370.

Vermeire, L.T., Wester, D.B., Mitchell, R.B., Fuhlendorf, S.D., 2005. Fire and Grazing Effects on Wind Erosion, Soil Water Content, and Soil Temperature. J. Environ. Qual. 34 (5), 1559-1565.

Vezzani, L., Festa, A., Ghisetti, F.C., 2010. Geology and Tectonic Evolution of the Central-Southern Apennines, Italy. Geol. Soc. Spec. Pap. 469, 1-58.

Vignaud, P., Duringer, P., Mackaye, H.T., Likius, A., Blondel, C., Boisserie, J.R., de Bonis, L., Eisenmann, V., Etienne, M.E., Geraads, D., Guy, F., Lehmann, T., Lihoreaeu, F., Lopez-Martinez, N., Mourer-Chauviré, C., Otero, O., Rage, J.C., Schuster, M., Viriot, L., Zazzo, A., Brunet, M., 2002. Geology and palaeontology of the Upper Miocene Toros-Menalla hominid locality, Chad. Nature 418 (6894), 152-155.

Villareal, T.A., Joseph, L., Brzezinski, M.A., Shipe, R.F., Lipschultz, F., Altabet, M., 1999. Biological and chemical characteristics of the giant diatom *Ethmodiscus* (Bacillariophyceae) in the Central North Pacific gyre. J. Phycol. 35, 896-902.

Villnäs, A., Norkko, J., Lukkari, K., Hewitt, J., Norkko, A., 2012. Consequences of increasing hypoxic disturbance on benthic communities and ecosystem functioning. PLoS One 7 (10), e44920, 1-12.

Violanti, D., 1996. Paleoautoecological analysis of *Bulimina echinata* (Messinian, Mediterranean area). Boll. Soc. Paleont. Ital., Spec. Vol. 3, 243-253.

Violanti, D., Lozar, F., Dela Pierre, F., Natalicchio, M., Bernardi, E., Clari, P., Cavagna, S., 2013. Stress tolerant microfossils of a Messinian succession from the northern Mediterranean basin (Pollenzo section, Piedmont, Northwestern Italy). Bollettino della Società Paleontologica Italiana 52 (1), 45-54.

Voje, K.L., Hemp, C., Flagstad, Ø., Sætre, G.P., Stenseth, N.C., 2009. Climatic change as an engine for speciation in flightless Orthoptera species inhabiting African mountains. Mol. Ecol. 18 (1), 93-108.

Wade, B.S., Bown P.R., 2006. Calcareous nannofossils in extreme environments: The Messinian Salinity Crisis, Polemi Basin, Cyprus. Palaeogeography, Palaeoclimatology, Palaeoecology 233, 271-286.

Wallace, L.L., 1990. Comparative Photosynthetic Responses of Big Bluestem to Clipping versus Grazing. J. Range. Manage. 43 (1), 58-61.

Wallman, K., Aloisi, G., Haeckel, M., Tishchenko, P., Pavlova, G., Greinert, J., Kutterolf, S. Eisenhauer, A., 2008. Silicate weathering in anoxic marine sediments. Geochim. Cosmochim. Acta 72, 3067-3090.

Warheit, K.I., 2001. The Seabird Fossil Record and the Role of Paleontology in Understanding Seabird Community Structure. In: Schreiber, E.A., Burger, J. (Eds.), Biology of Marine Birds, CRC Press, pp. 17-55.

Wei, W., Wise, S.W., Jr., 1990. Biogeographic gradients of middle Eocene – Oligocene calcareous nannoplankton in the South Atlantic Ocean. Palaeogeography Palaeoclimatology Palaeoecology 79, 29–61.

Westall, F., Rincé, Y., 1994. Biofilms, microbial mats and microbe-particle interactions: electron microscope observations from diatomaceous sediments. Sedimentology 41, 147-162.

White, L.D., Garrison, R.E., Barron, J.A., 1992. Miocene intensification of upwelling along the California margin as recorded in siliceous facies of the Monterey Formation and offshore DSDP sites. In: Upwelling systems: Evolution Since the Early Miocene (Eds C.P. Summerhayes, W.L. Prell and K.C. Emeis), Geol. Soc. Spec. Publ. 64, 429-442.

White, R., Murray, S., Rohweder, M., 2000. Pilot analysis of global ecosystems: Grassland ecosystems. World Resources Institute, 81 pp.

Willett, S.D., 2010. Late Neogene erosion of the Alps: a climate driver? Ann. Rev. Earth Planet. Sci. 38, 411-437.

Wölfler, A., Kurz, W., Fritz, H., Glotzbach, C., Danišík, 2016. Late Miocene increasing exhumation rates in the eastern part of the Alps – implications from low temperature thermochronology. Terra Nova 28 (5), 297-305.

Xiong, Z., Li, T., Crosta, X., Algeo, T., Chang, F., Zhai, B., 2013. Potential role of giant marine diatoms in sequestration of atmospheric CO2 during the Last Glacial Maximum: $\delta^{13}C$ evidence from laminated *Ethmodiscus rex* mats in tropical West Pacific. Global Planet. Change 108, 1-14.

Yang, Y., Fang, X., Galy, A., Jin, Z., Wu, F., Yang, R., Zhang, W., Zan, J., Liu, X., Gao, S., 2016. Plateau uplift forcing climate change around 8.6 Ma on the northeastern Tibetan Plateau: evidence from an integrated sedimentary Sr record. Palaeogeogr. Palaeoclimatol. Palaeoecol. 461, 418-431.

Zachos, J., Pagani, M., Sloan, L., Thomas, E., Billups, K., 2001. Trends, rhythms, and aberrations in global climate 65 Ma to present. Science 292 (5517), 686-693.

Zecchin, M., Civile, D., Caffau, M., Muto, F., Di Stefano, A., Maniscalco, R., Critelli, S., 2013. The Messinian succession of the Crotone Basin (southern Italy) I: stratigraphic architecture reconstructed by seismic and well data. Mar. Pet. Geol. 48, 455-473.

Zhang, L., Chen, M., Xiang, R., Zhang, L., Lu, J., 2016. Productivity and continental denudation history from the South China Sea since the late Miocene. Mar. Micropaleontol. 72, 76-85.

Zheng, D., Zhang, P., Wan, J., Li, C., Cao, J., 2003. Late Cenozoic deformation subsequence in northeastern margin of Tibet: detrital AFT records from Linxia Basin. Sci. China Earth Sci. (Series D) 46, 266-275.

Zheng, D., Zhang, P.Z., Wan, J., Yuan, D., Li, C., Yin, G., Zhang, G., Wang, Z., Min, W., Chen, J., 2006. Rapid exhumation at ~8 Ma on the Liupan Shan thrust fault from apatite fission-track thermochronology: implications for growth of the northeastern Tibetan Plateau margin. Earth Planet. Sci. Lett. 248 (1-2), 198-208.

Zhisheng, A., Kutzbach, J.E., Prell, W.L., Porter, S.C., 2001. Evolution of Asian monsoons and phased uplift of the Himalaya–Tibetan plateau since Late Miocene times. Nature 411 (6833), 62-66.

Zhou, X., Lyu, X., Liu, C., Liu, Z., Li, Q., Jin, X., Zhang, H., Dadd, K., 2019. Depositional mechanisms for upper Miocene sediments in the South China Sea central basin: Evidence from calcareous nannofossils. Mar. Micropaleontol. 151, 101768.

Ziveri, P., Baumann, K.-H., Böckel, B., Bollmann, J., Young, J.R., 2004. Present day coccolithophore biogeography of the Atlantic Ocean. In: Thierstein, H.R., Young, J.R. (Eds.), Coccolithophores: From Molecular Processes to Global Impact. Springer Verlag, pp. 529–562.

Zorn, I., 1997. Holoplanktonic gastropods from the Early Messinian of the Heraklion Basin (Crete, Greece). Contr. Tert. Quatern. Geol., 34 (1-2), 31-45.

ACKNOWLEDGEMENTS

It is rather trivial to start by thanking a supervisor… Therefore, I hope this does not sound too much formal to you. Few years ago you gave me an idea that has gradually become my obsession. We are still very far from a solution and much more work is needed, but I love this adventure. Frankly speaking, thanks a lot Giorgio!

I warmly thank all the "Torino Messinian Crew", and especially Cecco: you cannot imagine how much I learnt from you. Marcello, Francesca, Rocco, Mathia, Federico and Alan: thanks a lot for your fundamental support and our never ending discussions!

I wish to thank also Luca Martire and Luca Barale: for your availability and your valuable suggestions and teachings.

I am grateful to all my colleagues and friends met during these three years, in particular to Matteo, Nicolò and Francesca. We shared ups and downs, and you reminded me that there is a social life out there… For this and many other things, thank you guys!

Simona, Linda, Marco, Carmelo, Vittorio, Giorgio, Emilia and Michele: thanks a lot for your concrete support and the funny moments shared together.

I am in debt to Karen Gariboldi: you taught me "how to do" when I was just at the beginning of my experience. Thank you Karen!

I also thank Annalaura Pistarino, for allowing me to work on the MRSN collections.

A special thanks to Kenta aka "Hoover" and Kazuki, two hard workers from whom I learnt a lot. I miss our long SEM sessions, coffee breaks, lunches and hilarious gags, and I will never forget your kindness and your help.

Alex, Viktor and Shurik: dear Russian friends, you gave me a chance to grow both scientifically and humanely. I really miss you and that remote corner of paradise in the middle of nowhere.

I thank virtually all those curious from Pecetto di Valenza who occasionally stopped to ask me what I was doing along that dusty road called 'Strada Molina', maybe offering me some water or a cold beer. In particular Luciano, Patty, Andrea Bortoloni and Flavio Destefanis.

This work is dedicated to three extraordinary persons: my girlfriend Silvia, my father Claudio and a friendly, wise hermit who once told me "*stay in the game!*".